UNIVERSIDAD D CÓRDOBA

Programa de doctorado

Ingeniería Agraria, Alimentaria, Forestal y de Desarrollo Rural Sostenible

Título de la tesis

Pea genetic breeding to enhance rust resistance in Mediterranean environments

---

Mejora genética del guisante por resistencia a roya en ambientes Mediterráneos

Autor

Salvador Osuna Caballero

Directores

Dr. Diego Rubiales

Dr. Nicolas Rispail

Córdoba, enero 2024

CSIC
CONSEJO SUPERIOR DE INVESTIGACIONES CIENTÍFICAS

INSTITUTO DE AGRICULTURA SOSTENIBLE IAS

TITULO: *Pea genetic breeding to enhance rust resistance in Mediterranean environments*

AUTOR: *Salvador Osuna Caballero*

Campus de Rabanales
Ctra. Nacional IV, Km. 396 A
14071 Córdoba

https://www.uco.es/ucopress/index.php/es/
ucopress@uco.es

Mención Internacional

La presente Tesis cumple con los requisitos establecidos por la Universidad de Córdoba para la obtención del Título de Doctor con Mención Internacional:

- Realización de una estancia mínima de 3 meses fuera de España. El doctorando ha realizado una estancia internacional de 3 meses (2 de diciembre del 2021-7 de marzo, 2022) en el Consejo para la Investigación de Agricultura y Economía (CREA – Consiglio per la ricerca in agricoltura e l'analisi dell'economia agraria) bajo la supervisión del Dr. Nelson Nazzicari.
- La Tesis Doctoral se ha redactado y se presentará en inglés.
- Informe previo, acreditado oficialmente, de dos doctores/as expertos y con experiencia investigadora acreditada pertenecientes a alguna institución de educación superior o instituto de investigación distinto de España:
  - Dr. Khazaei Hamid (Natural Resources Institute, Finlandia)
  - Dr. Amero Emeran (Kafrelsheikh University, Egipto)
- Un doctor/a perteneciente a alguna institución de educación superior o centro de investigación no española, y distinto del responsable de la estancia de investigación, formará parte del tribunal evaluador de la tesis.
  - Dr. Maria Carlota Vaz Patto (ITQB NOVA, Portugal)

El doctorando:

Firmado por OSUNA CABALLERO SALVADOR - ***1417** el día 26/01/2024 con un certificado

Fdo: Salvador Osuna Caballero

INFORME RAZONADO DE LAS/LOS DIRECTORAS/ES DE LA TESIS

Este documento se presentará junto con el depósito de la tesis en https://moodle.uco.es/ctp3/

DOCTORANDA/O

Salvador Osuna Caballero

TÍTULO DE LA TESIS:

Pea genetic breeding to enhance rust resistance in Mediterranean environments

INFORME RAZONADO DE LAS/LOS DIRECTORAS/ES DE LA TESIS
(se hará mención a la evolución y desarrollo de la tesis, así como a trabajos y publicaciones derivados de la misma)

Por la presente informamos que la tesis ha sido culminada con éxito en el marco de un contrato predoctoral del doctorando en el Instituto de Agricultura Sostenible, concedido por la Agencia Estatal de Investigación asociado al proyecto AGL2017-82907-R, que después fue continuado con el proyecto PID2020-114668RB-I00. La parte experimental de la tesis y análisis, interpretación y discusión de los resultados han culminado con éxito. Ello ha dado lugar a dos artículos JIF ya publicados y a dos enviados y otro en fase avanzada de redacción en todos los cuales el doctorando es primer autor. El contrato predoctoral finalizó el 31 de agosto de 2023, pero lo que estimamos que la tesis puede ser defendida en la modalidad "clásica" solicitando mención internacional.

Indicios de calidad de la tesis:

- Osuna-Caballero S, Rispail N, Barilli E, Rubiales D, 2022. Identification and characterization of novel sources of resistance to rust (Uromyces pisi) in Pisum spp. Plants 11:2268, Q1.

- Osuna-Caballero S, Olivoto T, Jiménez-Vaquero MA, Rubiales D, Rispail N, 2023. RGB image-based method for phenotyping rust disease progress in pea leaves using R. Plant Methods 19:86, Q1

- otros tres articulos aun no aceptados

Por todo ello, se autoriza la presentación de la tesis doctoral.

Córdoba, a 24 de enero de 2024

Las/los directoras/es

Firmado por RUBIALES OLMEDO DIEGO - ***9499** el día 24/01/2024 con un certificado emitido por AC FNMT Usuarios

RISPAIL RISPAIL NICOLAS MARCEL HENRI - X6272788K

Digitally signed by RISPAIL RISPAIL NICOLAS MARCEL HENRI - X6272788K
Date: 2024.01.24 22:34:20 +01'00'

Fdo.:Diego Rubiales Nicolas Rispail

INFORME RAZONADO DE LA/EL TUTORA/OR

Este documento se presentará junto con el depósito de la tesis en https://moodle.uco.es/ctp3/

DOCTORANDA/O

Salvador Osuna Caballero

TÍTULO DE LA TESIS:

Pea genetic breeding to enhance rust resistance in Mediterranean environments

INFORME RAZONADO DE LA TUTORA/OR
(Ratificando el informe favorable del director. Sólo cuando el director no pertenezca a la Universidad de Córdoba)

Por la presente suscribo el informe emitido por los directores de la tesis. El trabajo ha dado lugar a dos artículos JIF ya publicados y a dos enviados y un quinto en fase avanzada de redacción en todos los cuales el doctorando es primer autor. El doctorando realizó una estancia de tres meses en Italia, debidamente autorizada. Por tanto, estimamos que la tesis puede ser defendida en la modalidad "clásica" solicitando mención internacional.

Indicios de calidad de la tesis:
- Osuna-Caballero S, Rispail N, Barilli E, Rubiales D, 2022. Identification and characterization of novel sources of resistance to rust (Uromyces pisi) in Pisum spp. Plants 11:2268, Q1.
- Osuna-Caballero S, Olivoto T, Jiménez-Vaquero MA, Rubiales D, Rispail N, 2023. RGB image-based method for phenotyping rust disease progress in pea leaves using R. Plant Methods 19:86, Q1

Por todo ello, se autoriza la presentación de la tesis doctoral.

Córdoba, a 25 de Enero de 2024

La/el Tutor/a

MUÑOZ DIEZ MARIA DE LA CONCEPCION - 77320961K

Firmado digitalmente por MUÑOZ DIEZ MARIA DE LA CONCEPCION - 77320961K
Fecha: 2024.01.25 11:26:39 +01'00'

Fdo.:Concepción Muñoz Díez

"Everything else can wait, agriculture can't."

Norman Borlaug

Agradecimientos / Acknowledgment

Llegó el momento de escribir estos párrafos previos al depósito de la tesis. Algo muy parecido a "cuando se junta el hambre con las ganas de comer".

A Diego Rubiales, el investigador y científico más brillante que conozco dentro de esta bonita área de conocimiento que compartimos. Tu pasión, dedicación y esfuerzo por la mejora vegetal y el campo son contagiosas. Gracias por haber confiado en mí durante todos estos años, en los que también ha habido altibajos, pero siempre has sabido sacar lo mejor de mí y espero que en esta tesis se haya visto reflejado mi compromiso. Además del trabajo también me llevo las agradables charlas, de las que siempre he salido aprendiendo, y buenos momentos que hemos compartido.

A Nicolas Rispail, muchas gracias por tu apoyo desde el primer momento, aun cuando hacía mi máster. Sin ti no hubiera logrado llegar hasta aquí. Gracias por haberme guiado con tus acertados consejos. Me llevo con afecto todas nuestras charlas y reuniones, que han sido clases magistrales para poder hacer un buen trabajo tanto en el laboratorio como con los análisis de datos y la escritura. Gracias también por haber tenido siempre en cuenta mi opinión y haber visto y sabido valorar mis aptitudes dentro de esta bonita carrera científica que pretendo continuar.

Gracias a Eleonora Barilli por enseñarme a inocular y evaluar roya en guisante. ¡No hubiera sido posible construir la casa sin unos buenos cimientos! También tengo que darte las gracias por los buenos ratos y risas durante las siembras, comidas y todos los eventos compartidos. Tampoco me puedo olvidar de María José Cobos, gracias por compartir tu cariño y paciencia por el campo y toda la ayuda que me has dado estos años. ¡Siempre dando la cara por nosotros en el laboratorio y frente a las injusticias que, en ocasiones, sufrimos los doctorandos! Gracias también a Ángel Villegas, otro del equipo "senior" que siempre ha estado dispuesto a ayudar con lo que sea a los novatos.

Al resto de compañeros, tanto actuales como antiguos, y amigos del laboratorio 7, con los que he tenido el placer de trabajar, compartir espacios, aprender y discutir (si, de las discusiones también se aprende). Gracias a Fran Agudo y Wohor Zakaria, con quienes empecé este camino al mismo tiempo. Juntos nos hemos apoyado, resuelto dudas y pasado buenos ratos. ¡Gracias a todo eso ya estamos en la recta final! Gracias a Manuel Alejandro, por tu ayuda con los ensayos, tu dedicación, tus contagiosas

ganas de aprender y mejorar y ¡por los buenos momentos (a.k.a. cervezas) que hemos echado y espero que sigamos echando! Gracias al mejor equipo en formación que se juntó en este grupo de investigación, en especial a María Córdoba, a Carmen Ruiz, a Sara Rodríguez, a Marina Anagnosti, a Yaiza y a Ángela. También gracias al fantástico dúo de grandes post-docs (y mejores fontaneros) Mario González y Pierluigi Reveglia, por todos vuestros consejos, dudas resueltas y perspectivas aportadas. También tengo que daros las gracias, Pedro Luna y Antonio Nadal, por todo lo que me habéis ayudado con las campañas del campo. El trabajo más tedioso y que más pasa desapercibido cuando todas esas horas de trabajo únicamente se plasman en unas líneas de "paper" pero ¡sin duda el más fundamental para que todo esto cobre sentido!

Gracias también al resto de líneas de investigación que forman nuestro grupo. En especial a Elena, Gracia y Fran, por tener siempre el laboratorio abierto y ayudarme a resolver todas las dudas tanto teóricas como prácticas que he ido teniendo durante esta etapa.

Grazie al Dr. Paolo Annicchiarico e al Dr. Nelson Nazzicari per avermi ospitato durante i tre mesi della mia permanenza in Italia. Grazie mille per tutto quello che mi avete insegnato sulla bioinformatica, i modelli e l'analisi dei dati. Tutta la conoscenza che mi avete trasmesso è raccolta in questo documento, quindi senza di voi non avrei potuto raggiungere questo traguardo. Grazie anche a Margherida, Barbara, Fillipo e Daniele per le chiacchierate e i bei momenti passati a Lodi!!

No todo el mundo tiene la suerte, o la desgracia, de trabajar con horarios tan inciertos como los de un doctorando de ciencias aplicadas. Hay gente que pasa buena parte de su vida entrando a las 8 y saliendo a las 15. Sin experimentar la adrenalina que se siente al entrar a las 8, pensar que vas a salir a las 18 y, finalmente, salir a las 21 porque nada o casi nada ha ido como esperabas. Esto sí que es vivir al límite (literalmente). Por suerte, y esto si que es una suerte, tienes personas al lado que están igual de ~~jodidas~~ entusiasmadas que tú, con idénticos problemas, similares intereses y las mismas ganas de cerveza (o vino, en Córdoba depende de la fecha). Esto hace que por simple afinidad en el IAS se hayan forjado amistades que espero que duren y perduren. Sin más, estas líneas son para dar las gracias a los amigos y a las amigas que he hecho en el IAS, con los que he tenido el placer de compartir todo tipo de eventos dentro y fuera de Córdoba, experiencias, abrazos, risas y también

lágrimas. No hubiera sido lo mismo sin vosotros ni sin los recuerdos tan bonitos que hemos formado juntos. Todo esto culmina con haber conocido a la mejor persona que uno pudiera imaginar. Gracias Martina, por haber caminado conmigo durante esta etapa. Gracias por estar ahí siempre, gracias por tu cariño, tu honestidad y por ser la mejor compañera de viaje. A este paso el mundo se nos va a quedar pequeño, pero ya se nos ocurrirá algo, contigo cualquier reto sea grande o pequeño es una aventura que estoy impaciente por comenzar.

También tengo que dar las gracias a mis amigos de Lucena, los de toda la vida. Siempre es una alegría volver a casa, tomar aire fresco (y no tan fresco), retomar el contacto con tus raíces y continuar con las pilas cargadas. Gracias a mi MermeTeam.

Gracias a mi familia. En especial a mis padres, cuyo trabajo es el más desagradecido del mundo. Mis logros son los vuestros, pues sin vuestro apoyo incondicional, recursos, cariño y amor no hubiera podido llegar hasta aquí. Gracias por haberme convertido en lo que soy y en todo lo que soy capaz de hacer. Gracias a mis hermanos Lidia y Carlos y en especial a mi hermano Antonio, cuya ayuda con la informática se ha visto reflejada en este trabajo. Gracias a mis tías Soledad y Teresa y mis abuelos Juana y Salvador, el cariño que me inculcasteis por la naturaleza se ve manifestado en esta tesis doctoral y en mi día a día.

A todos y a todas, gracias.

Contents

List of Figures

List of Tables

List of Additional files

Abbreviations

a*	values relative to the green–magenta opponent colours in the CIELAB colour space
ABA	Abscisic Acid
ABI	Abscisic Acid Insensitive
AMMI	Additive Main Effects and Multiplicative Interaction
ANOVA	Analysis of Variance
ARP	Actin-Related Protein
ATP	Adenosine Triphosphate
AUDPC	Area Under Disease Progress Curve
b*	values which represent the blue–yellow opponent colours in the CIELAB colour space
BCAs	Biological Control Agents
BIC	Bayesian Information Criterion
BL	Bayesian Lasso
BLINK	Bayesian information and Linkage disequilibrium iteratively Nested Keyway
BLUE	Best Linear unbiased Estimation
BLUP	Best Linear unbiased Prediction
BV	Breeding Value
bZIP	basic Leucine Zipper Domain
CC	Controlled Conditions
ccc	the Lin's concordance correlation coefficient
CDF3	Cycling DOF factor 3
CDPK	Calcium-Dependent Protein Kinase
CER	Eceriferum-like enzyme
CIELAB	three-dimensional colour space defined by the International Commission on Illumination
COPI	Coat Protein Complex I
COPII	Coat Protein Complex II

CRISPR	Clustered Regularly Interspaced Short Palindromic Repeats
CS	Colony Size
CV	Cross-Validation
CV%	Coefficient of Variation %
CV_e	error Coefficient of Variance
CV_g	genotypic Coefficient of Variance
CV_i	genotype by environment interaction Coefficient of Variance
dai	days after inoculation
DArT	Diversity Array Technology
Dim1	Dimension 1
Dim2	Dimension 2
DNA	Deoxyribonucleic Acid
dpi	days post inoculation
DRP	Dynamin-Related Protein
DS	Disease Severity
ER	Endoplasmic Reticulum
FAI-BLUP	Factor Analysis and Ideotype-design index
FDR	False Discovery Rate
FRAC	Fungicide Resistance Action Committee
GBLUP	Genomic Best Linear Unbiased Prediction
GBS	Genotyping-by-Sequencing
GEBV	Genomic Estimated Breeding Values
GEI	Genotype by Environment Interaction
GLAI	Green Leaf Area Index
GRAS	GAI-RGA- and -SCR transcription factor
GRM	Genomic Relationship Matrix
GS	Genomic Selection
GWAS	Genome Wide Association Study
GxE	Genotype by Environment
H^2	Heritability

HAD	Haloacid dehalogenase-like hydrolase
HI	primary colours Hue Index
HMC	Haustorial Mother Cell
HR	Hypersensitive Response
HSFB3	Heat Stress Transcription Factor B-3
IF	Infection frequency
IT	Infection type
KEGG	Kyoto Encyclopaedia of Genes and Genomes
L*	values referred as perceptual lightness in the CIELAB colour space
LM	Linear Model
LMM	Linear Mixed Model
LN	Linn-Binn superiority measures
LP_{50}	Latency Period
LRR	Leucine-Rich Repeat
LRT	Likelihood Ratio Test for genotype effect
MAF	Minor Allele Frequency
MAH	Mid-chain Alkane Hydroxylase
MAS	Marker-Assisted Selection
MDPr	Monocyclic Disease Progress rate
MegaENV	Mega Environment
MET	Multi- Environment Trial
MGIDI	Multi-trait Genotype-Ideotipe Distance index
MLM	Mixed Minear Model
mRNA	messenger Ribonucleic Acid
*Mt*N	*Medicago truncatula* NODULIN
MxE	Marker by Environment
MYB	myeloblastosis
NBS	Nucleotide Binding Site domain
NGRDI	Normalized Green Red Difference Index
NLP9	Nodule inception-like 9 protein

P450	Cytochrome 450
PCA	Principal Component Analysis
PCs	Principal Components
PP	Protein Phosphatase
PR	Partial Resistance
PR	Partial Resistance
PS	Pustule Size
PVE	Phenotypic Variance Explained
QoIs	Quinoline Outside Inhibitors
Q-Q	Quantile-Quantile
QTL	Quantitative Trait Loci
r	rate
r_{ab}	Predictive ability
r_{ac}	Predictive accuracy
RAPD	Random Amplified Polymorphic DNA
RCBD	Randomized Complete Block Design
REML	Restricted Maximum Likelihood
r_g	Genetic Correlation
RG	rhamnogalacturonan
RGB	Red – Green - Blue
RMSE	Root-Mean-Square Error
RNA	Ribonucleic Acid
RNAi	Ribonucleic Acid interference
r_p	Phenotypic Correlation
rrBLUP	ridge regression BLUP
SAD	Standard Area Diagram
SAR	Systemic Acquired Response
SCAR	Sequence-Characterized Amplified Region
SDH	Succinate Ddehydrogenase
SE	Standard Error

SF	Splicing Factor
sgRNA	single-guided Ribonucleic Acid sequence
SH	Smith-Hazel index
SNP	Single Nucleotide Polymorphism
SVD	Singular Value Decomposition
syn.	synonim
TCA	Tricarboxylic Acid Cycle
TFs	Transcription Factors
TILLING	Targeting Induced Local Lesions IN Genomes
TIR	*Toll* Interleukin Receptor
TZF9	Tandem Zinc Finger 9
UAV	Unmanned aerial vehicle
UpCo-01	*Uromyces pisi* Cordoba isolate 2001
UpKeS-05	*Uromyces pisi* Kafr-El-Sheik isolate 2005
WAT	Walls Are Thin
WGS	Whole-Genome sequency
λ	genomic inflation
ρ_c	Lin's concordance correlation coefficient

Summary

Rust diseases are a significant concern in legume production worldwide, causing substantial losses, particularly in developing countries that rely on grain legumes as a staple food and a key protein source. Fungal species from the genera *Uromyces*, *Phakopsora*, and *Puccinia* are the main causative agents. They contribute to yield losses of up to 100% in susceptible cultivars and are emerging as a substantial threat to global food security. Therefore, developing durable resistance to rusts has become a critical goal in plant breeding, along with efforts to improve cultural practices and disease management. This doctoral thesis begins by specifically focusing on recent advances in understanding and improving genetic resistance to rust in various leguminous crops, as they share common infection and resistance strategies that are approachable from a plant breeding perspective. Key topics covered in the first chapter include: i) the diversity and host range of rust species affecting legumes; ii) disease management strategies ranging from cultural practices to chemical control; iii) available detection methods to identify new sources of resistance; iv) the genetic basis of resistance, encompassing both major resistance genes and quantitative trait loci; v) insights into genetic regulation and effector molecules that lead to interactions between legumes and rust; and vi) emerging genomics-assisted breeding techniques that can accelerate the development of durable resistance to rust in legumes. Overall, the first chapter of this doctoral thesis highlights the progress made to date and the remaining challenges in the sustainable management of rusts in various leguminous crops through integrated approaches that encompass pathogen biology, advanced phenotyping, genetic resistance, and molecular breeding.

Pea (*Pisum sativum* L.) is a temperate zone grain legume that is extensively cultivated. It ranks as the second most cultivated legume in the world and the first in Europe, including both dry and green peas. Its use extends to food and feed and represents a versatile and economical protein source, offering benefits to human health. Pea rust has become a major concern globally, causing losses between 30-50% under suitable climatic conditions for the fungus. Depending on the region, pea rust has been reported to be caused by *Uromyces viciae-fabae* (Pers. de Bary) in tropical and subtropical zones, or by *U. pisi* (Pers.) (Wint.) in more temperate areas. To date, only moderate levels of partial resistance against *U. pisi* have been identified in peas, urging an expansion of available resistance levels for breeding. In the second chapter of this doctoral thesis, we describe the response to *U. pisi* in 320 *Pisum* spp. accessions, including cultivated peas and wild relatives, under both field and controlled conditions. Significant variations in the response to *U. pisi* infection were observed for most traits among the pea samples, in both field and controlled conditions, allowing for the detection of genotypes with partial resistance. Simultaneous multi-trait indices were applied to the datasets, enabling the

identification of partial resistance, particularly in the samples JI224, BGE004710, JI198, JI199, CGN10205, and CGN10206. Macroscopic observations were complemented by histological observations of the nine most resistant accessions and compared to three intermediate and three susceptible ones. This study confirmed that the reduction in infection of the resistant accessions was associated with smaller rust colonies due to a decrease in the number of haustoria and hyphal tips per colony. Furthermore, a late-acting hypersensitive response was identified for the first time in a pea sample (PI273209). The findings obtained in the second chapter demonstrate that screening pea collections remains a necessary method in the search for complete resistance against *U. pisi*. Additionally, the wide phenotypic diversity contained in the studied collection will be useful for further association analysis and breeding perspectives.

Therefore, rust is a harmful disease that affects vital crops, including peas, and the identification of highly resistant genotypes remains a challenge, as concluded in the second chapter. Accurate measurement of infection levels in large germplasm collections is crucial for finding new sources of resistance. Current evaluation methods are based on the visual estimation of disease severity and infection type under field or controlled conditions. While they identify some sources of resistance, they are prone to errors and time-consuming. An image analysis system proves useful, as it provides an affordable and user-friendly way to quickly count and measure rust-induced pustules in pea samples. In the third chapter of this doctoral thesis, an automated image analysis process was developed to accurately calculate the parameters of rust disease progression under controlled conditions, ensuring reliable data collection. This work was carried out using R to create a highly efficient and automated image-based method for evaluating rust on pea leaves. The optimization and validation of the method involved testing different segmentation indices and image resolutions on 600 pea leaflets with rust symptoms. The approach allows for the automatic estimation of parameters such as the number of pustules, the size of the pustules, leaf area, and the percentage of pustule coverage. It reconstructs time-series data for each leaf and integrates daily estimates into the disease progression parameters, including the latency period and the area under the disease progression curve. In this chapter, significant variation in disease responses among genotypes was observed using visual ratings and image-based analysis. Among the evaluated segmentation indices, the Normalized Green-Red Difference Index (NGRDI) proved to be the fastest, analysing 600 leaflets with 60% resolution in 62 seconds using parallel processing. The Lin's Concordance Correlation Coefficient between visual and image-based pustule counts showed an accuracy greater than 0.98 at full resolution. While a lower resolution slightly reduced accuracy, the differences were statistically insignificant for most disease progression parameters, significantly reducing processing time and storage space. NGRDI was optimal at all times, providing highly accurate estimates with minimal cumulative error. This work

proposes a new image-based method to monitor pea rust disease on detached leaves, using RGB spectral index segmentation and pixel value thresholding, to improve resolution and accuracy compared to traditional evaluations. This allows for the rapid analysis of hundreds of images with accuracy comparable to visual methods and superior to other image-based approaches. This method evaluates the progression of rust in peas, eliminating evaluator-induced errors in traditional methods. Implementing this new approach to evaluate large germplasm collections will enhance our understanding of plant-pathogen interactions and aid in the future breeding of new pea cultivars with greater resistance to rust.

In the fourth chapter, it is highlighted that, despite some efforts to assess the natural variation in pea resistance, its efficient exploitation in plant breeding is limited due to the scarcity of identified resistance loci and the unknown nature of their responsible genes. To overcome this knowledge gap, a comprehensive genome-wide association study (GWAS) on pea rust, caused by *Uromyces pisi*, was conducted to discover genetic loci associated with resistance. This utilized the datasets produced in the previous two chapters. Thus, using a diverse collection of 320 pea accessions and the phenotypic responses to two rust isolates using traditional methods and advanced image-based phenotyping, the association studies were carried out. We detected 95 significant trait marker associations using a set of 26,045 polymorphic DArT-seq markers. Our in-silico analysis identified 62 candidate genes supposedly involved in rust resistance, grouped into different functional categories, such as gene expression regulation, vesicle trafficking, cell wall biosynthesis, and hormonal signalling. This research conducted in the fifth chapter highlights the potential of GWAS to identify sources of resistance, molecular markers associated with resistance, and candidate genes against pea rust, offering new targets for precision breeding. By integrating our findings with current breeding programs, we can facilitate the development of pea varieties with greater rust resistance, contributing to sustainable agricultural practices and food security. This study lays the groundwork for future functional genomic analyses and the application of genomic selection approaches to improve disease resistance in peas.

In the fifth and final chapter, the same phenotypic and genotypic datasets were used for a marker-assisted selection (MAS) approach different from GWAS: Genomic Selection (GS). Genomic prediction or selection has become an indispensable tool in modern plant breeding, particularly for complex traits such as resistance to rust in peas, which are strongly influenced by environmental factors. In this chapter, the effectiveness of GS to predict rust resistance was evaluated, using the panel of 320 pea accessions and 26,045 Silico-DArT markers. We compared the predictive abilities of various GS models, including the Best Linear Unbiased Genomic Prediction (GBLUP), and explored the impact of incorporating marker × environment (MxE) interactions as a covariate in the GBLUP model. The analysis encompassed both data generated in the field and under controlled conditions. We assessed the predictive

accuracy of different cross-validation strategies and compared the efficiency of using single traits versus a multi-trait index approach, specifically FAI-BLUP, which combines traits from controlled conditions. The GBLUP model, particularly when modified to include MxE interactions, consistently outperformed other models, demonstrating its suitability for traits affected by complex genotype-environment interactions. Specifically, the best predictive ability (0.635) was achieved using the FAI-BLUP approach within the Bayesian Lasso (BL) model. The inclusion of MxE interactions significantly improved prediction accuracy in various environments in the GBLUP models, although it did not notably improve predictions for non-phenotyped lines. These findings highlight the variability of predictive capabilities due to genotype by environment interactions (GEI) and the effectiveness of multi-trait approaches in addressing such complexities. Overall, our study illustrates the potential of GS, especially when employing a multi-trait index like FAI-BLUP and considering MxE interactions, in pea breeding programs focused on rust resistance. This approach provides a solid framework to tackle the challenges of GEI, making GS an asset in the quest for improved rust resistance in peas.

Resumen

Las royas son una preocupación importante en la producción de leguminosas en todo el mundo y causan pérdidas sustanciales, particularmente en los países en desarrollo que dependen de las leguminosas como alimento básico y fuente clave de proteínas. Las especies de hongos de los géneros *Uromyces*, *Phakopsora* y *Puccinia* son los principales agentes causantes. Contribuyen a pérdidas de rendimiento de hasta el 100% en cultivares susceptibles y están surgiendo como una amenaza sustancial para la seguridad alimentaria mundial. Por lo tanto, desarrollar una resistencia duradera a las royas se ha convertido en un objetivo crítico en el fitomejoramiento, junto con los esfuerzos para mejorar las prácticas culturales y el manejo de enfermedades. Esta tesis doctoral comienza centrándose específicamente en los avances recientes en la comprensión y mejora de la resistencia genética a la roya en varios cultivos de leguminosas, ya que comparten estrategias comunes de infección y resistencia que son accesibles desde una perspectiva de fitomejoramiento. Los temas clave cubiertos en el primer capítulo incluyen: i) la diversidad y la gama de huéspedes de especies de roya que afectan a las leguminosas; ii) estrategias de manejo de enfermedades que van desde prácticas culturales hasta control químico; iii) métodos de detección disponibles para identificar nuevas fuentes de resistencia; iv) la base genética de la resistencia, que abarca tanto los principales genes de resistencia como los loci de rasgos cuantitativos (QTL); v) conocimientos sobre la regulación genética y las moléculas efectoras que conducen a interacciones entre las leguminosas y la roya; y vi) nuevas técnicas de mejoramiento asistidas por genómica que pueden acelerar el desarrollo de una resistencia duradera a la roya en las leguminosas. En general, el primer capítulo de esta tesis doctoral destaca los avances realizados hasta la fecha y los desafíos pendientes en el manejo sostenible de las royas en diversos cultivos de leguminosas a través de enfoques integrados que abarcan la biología de patógenos, el fenotipado avanzado, la resistencia genética y el mejoramiento molecular.

El guisante (*Pisum sativum* L.) es una leguminosa de grano de zona templada que se cultiva extensivamente. Se sitúa como la segunda leguminosa más cultivada en el mundo y la primera en Europa, incluyendo tanto los guisantes secos como los verdes. Su uso se extiende a los alimentos y piensos y representa una fuente de proteínas versátil y económica, que ofrece beneficios para la salud humana. La roya del guisante se ha convertido en una gran preocupación a nivel mundial, provocando pérdidas de entre el 30 y el 50 % en condiciones climáticas adecuadas para el hongo. Dependiendo de la región, se ha informado que la roya del guisante es causada por *Uromyces viciae-fabae* (Pers. de Bary) en zonas tropicales y subtropicales, o por *U. pisi* (Pers.) (Wint.) en áreas más templadas. Hasta la fecha, sólo se han identificado niveles moderados de resistencia parcial contra *U. pisi* en los guisantes, lo que insta a ampliar los niveles de resistencia disponibles para el mejoramiento. En el segundo

capítulo de esta tesis doctoral describimos la respuesta a *U. pisi* en 320 *Pisum* spp. accesiones, incluidos guisantes cultivados y parientes silvestres, tanto en condiciones de campo como controladas. Se observaron variaciones significativas en la respuesta a la infección por *U. pisi* para la mayoría de los rasgos entre las muestras de guisantes, tanto en condiciones de campo como controladas, lo que permitió la detección de genotipos con resistencia parcial. Se aplicaron índices de multi-rasgos simultáneos a los conjuntos de datos, lo que permitió la identificación de resistencia parcial, particularmente en las entradas JI224, BGE004710, JI198, JI199, CGN10205 y CGN10206. Las observaciones macroscópicas se complementaron con observaciones histológicas de las nueve accesiones más resistentes y se compararon con tres intermedias y tres susceptibles. Este estudio confirmó que la reducción en la infección de las accesiones resistentes se asoció con colonias de roya más pequeñas debido a una disminución en el número de haustorios y puntas de hifas por colonia. Además, se identificó por primera vez una respuesta hipersensible de acción tardía en una muestra de guisantes (PI273209). Los hallazgos obtenidos en el segundo capítulo demuestran que el cribado de colecciones de guisantes sigue siendo un método necesario en la búsqueda de una resistencia completa contra *U. pisi*. Además, la amplia diversidad fenotípica contenida en la colección estudiada será útil para análisis de asociación adicionales y perspectivas de mejoramiento.

Así pues, la roya es una enfermedad dañina que afecta a cultivos vitales, incluidos los guisantes, y la identificación de genotipos altamente resistentes sigue siendo un desafío, como se concluye en el segundo capítulo. La medición precisa de los niveles de infección en grandes colecciones de germoplasma es crucial para encontrar nuevas fuentes de resistencia. Los métodos de evaluación actuales se basan en la estimación visual de la gravedad de la enfermedad y el tipo de infección en condiciones de campo o controladas. Si bien identifican algunas fuentes de resistencia, son propensos a cometer errores y requieren mucho tiempo. Un sistema de análisis de imágenes resulta útil, ya que proporciona una forma asequible y fácil de usar para contar y medir rápidamente las pústulas inducidas por la roya en accesiones de guisantes. En el tercer capítulo de esta tesis doctoral, se desarrolló un proceso automatizado de análisis de imágenes para calcular con precisión los parámetros de la progresión de la roya en condiciones controladas, garantizando una recopilación de datos confiable. Este trabajo se llevó a cabo utilizando R para crear un método basado en imágenes altamente eficiente y automatizado para evaluar la roya en las hojas de guisantes. La optimización y validación del método implicó probar diferentes índices de segmentación y resoluciones de imagen en 600 folíolos de guisantes con síntomas de roya. Este método permite la estimación automática de parámetros como el número de pústulas, el tamaño de las pústulas, el área foliar y el porcentaje de cobertura de las pústulas. Es capaz de reconstruir datos de series temporales para cada hoja e integra estimaciones diarias en los parámetros de progresión de la enfermedad, incluido el período de latencia y el área bajo la curva de

progresión de la enfermedad. En este capítulo, se observó una variación significativa en las respuestas a las enfermedades entre genotipos mediante clasificaciones visuales y análisis basados en imágenes. Entre los índices de segmentación evaluados, el Índice Normalizado de Diferencia Verde-Rojo (NGRDI) demostró ser el más rápido, analizando 600 muestras con una resolución del 60% en 62 segundos utilizando procesamiento paralelo de la GPU. El coeficiente de correlación de concordancia de Lin entre los recuentos de pústulas visuales y basados en imágenes mostró una precisión superior a 0,98 a resolución completa. Si bien una resolución más baja redujo ligeramente la precisión, las diferencias fueron estadísticamente insignificantes para la mayoría de los parámetros de progresión de la enfermedad, lo que redujo significativamente el tiempo de procesamiento y el espacio de almacenamiento. NGRDI fue el índice de segmentación óptimo en todo momento, proporcionando estimaciones muy precisas con un error acumulativo mínimo. Este trabajo propone un nuevo método basado en imágenes para monitorear la enfermedad de la roya del guisante en foliolos, utilizando segmentación del índice espectral RGB y categorización del valor de píxeles, para mejorar la resolución y precisión en comparación con las evaluaciones tradicionales. Esto permite el análisis rápido de cientos de imágenes con una precisión comparable a la de los métodos visuales y superior a otros enfoques basados en imágenes. Este método evalúa la progresión de la roya en los guisantes, eliminando errores inducidos por el evaluador en los métodos tradicionales. La implementación de este nuevo enfoque para evaluar grandes colecciones de germoplasma mejorará nuestra comprensión de las interacciones entre plantas y patógenos y ayudará en el futuro mejoramiento de nuevos cultivares de guisantes con mayor resistencia a la roya.

En el cuarto capítulo se destaca que, a pesar de algunos esfuerzos para evaluar la variación natural en la resistencia de los guisantes, su explotación eficiente en el fitomejoramiento es limitada debido a la escasez de loci de resistencia identificados y la naturaleza desconocida de sus genes responsables. Para superar esta brecha de conocimiento, se llevó a cabo un estudio integral de asociación de todo el genoma (GWAS) sobre la roya del guisante, causada por *Uromyces pisi*, para descubrir loci genéticos asociados con la resistencia. Para ello se utilizaron los conjuntos de datos producidos en los dos capítulos anteriores. Así, utilizando una colección diversa de 320 accesiones de guisantes y las respuestas fenotípicas a dos aislados de roya utilizando métodos tradicionales y fenotipado avanzado basado en imágenes, se llevaron a cabo los estudios de asociación. Detectamos 95 asociaciones significativas de marcadores moleculares con los caracteres evaluados utilizando un conjunto de 26.045 marcadores polimórficos Silico-DArT. Nuestro análisis in-silico identificó 62 genes candidatos supuestamente involucrados en la resistencia a la roya, agrupados en diferentes categorías funcionales, como regulación de la expresión génica, tráfico de vesículas, biosíntesis de la pared celular y señalización hormonal. Esta investigación realizada en el quinto capítulo destaca el potencial de GWAS para

identificar fuentes de resistencia, marcadores moleculares asociados con la resistencia y genes candidatos contra la roya del guisante, ofreciendo nuevos objetivos para el mejoramiento genético de precisión. Al integrar nuestros hallazgos con los programas de mejoramiento actuales, podemos facilitar el desarrollo de variedades de guisantes con mayor resistencia a la roya, contribuyendo a prácticas agrícolas sostenibles y a la seguridad alimentaria. Por lo tanto, este estudio sienta las bases para futuros análisis genómicos funcionales y la aplicación de enfoques de selección genómica para mejorar la resistencia a enfermedades en los guisantes.

En el quinto y último capítulo, se utilizaron los mismos conjuntos de datos fenotípicos y genotípicos para un enfoque de selección asistida por marcadores (MAS) diferente de GWAS: selección genómica (GS). La predicción o selección genómica se ha convertido en una herramienta indispensable en el fitomejoramiento moderno, particularmente para rasgos complejos como la resistencia a la roya en los guisantes, que están fuertemente influenciados por factores ambientales. En este capítulo se evaluó la efectividad de GS para predecir la resistencia a la roya, utilizando el panel de 320 accesiones de guisantes y 26,045 marcadores Silico-DArT. Comparamos las capacidades predictivas de varios modelos GS, incluida la Mejor Predicción Genómica Lineal Imparcial (GBLUP), y exploramos el impacto de incorporar interacciones marcador × ambiente (MxE) como covariable en el modelo GBLUP. El análisis abarcó tanto los datos generados en campo como en condiciones controladas. Evaluamos la capacidad predictiva de diferentes estrategias de validación cruzada y comparamos la eficiencia del uso de rasgos únicos versus un enfoque de índice de multi-rasgo, específicamente FAI-BLUP, que combina rasgos evaluados en condiciones controladas. El modelo GBLUP, particularmente cuando se modificó para incluir interacciones MxE, superó consistentemente a otros modelos, lo que demuestra su idoneidad para rasgos afectados por interacciones complejas genotipo-ambiente. Específicamente, la mejor capacidad predictiva (0,635) se logró utilizando el enfoque FAI-BLUP dentro del modelo Bayesiano Lasso (BL). La inclusión de interacciones MxE mejoró significativamente la precisión de la predicción en diversos entornos en los modelos GBLUP, aunque no mejoró notablemente las predicciones para líneas no fenotipadas en ambientes conocidos. Estos hallazgos resaltan la variabilidad de las capacidades predictivas debido a las interacciones entre el genotipo y el entorno (GEI) y la eficacia de los enfoques de multi-rasgo para abordar tales complejidades. En general, en este capítulo se ilustra el potencial de GS, especialmente cuando se emplea un índice como FAI-BLUP y se consideran las interacciones MxE, en programas de mejoramiento de guisantes enfocados en la resistencia a la roya. Este enfoque proporciona un marco sólido para abordar los desafíos de GEI, lo que convierte a GS en una herramienta aplicable en la búsqueda de una mejor resistencia a la roya en los guisantes.

Chapter 1
General Introduction. Breeding for rust resistance in Legumes

1. Abstract

Rust diseases are a major concern in legume production worldwide causing heavy losses especially in developing countries that depend on grain legumes as staple food being a key protein source. Fungal species from *Uromyces*, *Phakopsora* and *Puccinia* genera are the main causal agents. They contribute to up to 100 % yield losses on susceptible cultivars and are emerging as a substantial threat to global food security. Developing durable resistance to rusts has thus become a critical plant breeding objective alongside efforts to improve cultural and disease management practices. This review specifically focuses on recent advances in understanding and enhancing genetic rust resistance across diverse legume crops. Key topics covered include: i) the diversity and host range of the rust species affecting legumes; ii) the disease management strategies from cultural practices to chemical control; iii) the available screening methods for identifying new sources of resistance; iv) the genetic basis of resistance, encompassing both major resistance genes and quantitative trait loci; v) insights into gene regulation and effector molecules leading legume-rust interactions; and vi) emerging genomic-assisted breeding techniques that can accelerate the development of durable rust resistance in legumes. Overall, this review highlights the progress made to date and the remaining challenges in sustainably managing rust diseases across diverse legume crops through integrated approaches spanning pathogen biology, advanced phenotyping, genetic resistance, and Mol Breed.

2. Introduction

Rusts are important plant diseases caused by pathogens belonging to the Pucciniales order, which is the most extensive taxonomic order of plant pathogenic fungi, encompassing over 8,000 species (Toome-Heller 2016). Widely distributed, rust-causing agents have specialized across various hosts and climates, being obligate basidiomycete pathogens of annual crops, shrubs, and even trees worldwide (Helfer 2014). Due to its negative impact on cropping systems, two species of rust have been included among the 10 plant pathogens with the greatest scientific and economic relevance. These are *Puccinia* spp., responsible for rust in cereals and, to a lesser extent, in some legumes, and *Melampsora lini*, which causes rust in flax (Dean et al. 2012). Although not included in this ranking, soybean rust caused by *Phakopsora pachyrhizi* warrants special attention due to its recent surge in incidence globally, particularly in regions where soybean is a main crop (Dean et al. 2012; Goellner et al. 2010).

Most rust species are macrocyclic heteroecious fungi, meaning they have complex cycles involving various spore types infecting different plant host species through their lifetime (Duplessis et al. 2021). Their combination of sexual and asexual life cycles renders them high-risk evolutionary pathogens, capable of overcoming

plant defences with relative ease (Mapuranga et al. 2022). The life cycle stages of rusts are traditionally referred to by Roman numerals:

• Pycniospores (Stage 0): Produced in pycnidia, these serve as haploid gametes in heterothallic rusts.

• Aeciospores (Stage I): Arising from aecia, these non-repeating, dikaryotic asexual spores infect the primary host.

• Urediniospores (Stage II): Formed in uredia, these repeating, dikaryotic vegetative spores can cause autoinfection on the primary host. They are often visible as rust-coloured pustules on the plant.

• Teliospores (Stage III): Produced in telia, these spores typically represent the overwintering stage and lead to the production of basidia and basidiospores.

• Basidiospores (Stage IV): Arising from teliospores, these wind-dispersed haploid spores typically infect an alternate host, playing a crucial role in the pathogen lifecycle.

Depending on the rust species, the epidemic cycle may involve stage I, caused by aeciospores, or stage II, caused by urediniospores (Singh et al. 2023; Beniwal et al. 2022). Symptoms are characterized by numerous small, rust-like, orange/yellow, or brown pustules forming on infected plant tissues (Figure 1). These pathogens extract nutrients from infected plant cells through specialized structures called haustoria (Voegele and Mendgen 2003). During sporulation, the fungus can form from light-yellow halo to dark necrotic area around diseased pustules. The disease severity leads to a loss of photosynthetic area in infected leaves (Figure 1a, b) or even in the stem and pods (Figure 1c), resulting in reduced overall plant yield depending on the crop and the favourable rust environment (Newcombe 2004; Gautam et al. 2022a).

The Fabaceae family, second in global agricultural importance after the Poaceae is fundamental in the context of food security and environmental sustainability (Graham and Vance 2003). Legume crops like beans, lentils, alfalfa, and peas constitute 27 % of the world primary crop production (Vance et al. 2000). These grain and forage legume crops, using 12 % to 15 % of arable land, are indispensable in various agronomic systems (Azooz and Ahmad 2015; FAOSTAT 2022). They are particularly crucial in low-income and developing countries, serving as the main source of grain and fodder for both human consumption and livestock feeding (Mitchell et al. 2022). Legumes are notable for their nutritional richness, providing essential plant-based proteins, vitamins, and minerals, critical for diets worldwide, especially for smallholders and subsistence farmers, as most legumes are recognized as low-input crops (Jha and Warkengin 2020; Venkidasamy et al. 2019; Didinger and Thompson 2021). Additionally, legumes offer environmental benefits, notably atmospheric nitrogen fixation, improving soil structure and benefiting rotations with

other annuals crop (Gungaabayar et al. 2023). Therefore, the production of grain and forage legumes continues to grow globally (FAOSTAT 2022), primarily to meet high demands in livestock feed for meat and dairy production and to a lesser extent for human consumption due to new plant-based dietary habits (Alexandratos 2012). However, global legume production faces challenges such as production limitations due to environmental adaptability issues and susceptibility to pest and diseases, with rust disease being a major agent of these problems (Rubiales et al. 2015). These factors hinder the capacity of legume production to meet the growing demands posed by demographic growth, emphasizing the need to improve agricultural practices and disease management, such as rust control, to boost legume cultivation.

Figure 1. Rust symptoms in two legume species. a) shows pustules of *Uromyces ciceris-arietini* on the adaxial surface of chickpea leaves inoculated under controlled conditions. b) represents the same disease under field conditions. c) the fungus *U. viciae-fabae* has sporulated on the leaves, stem, and pod of the faba bean plant

As an air-borne pathogen capable of surviving in the field for multiple seasons in alternative hosts, eradicating rust is challenging and can only be addressed by integrating various disease management methods. Among these, the use of rust resistant varieties is widely recognized as the most cost-effective, efficient, and environmentally friendly method to prevent the massive losses caused by this pathogen (Rubiales et al. 2015; Barilli et al. 2014).

This work reviews the efforts made in various aspects related to the management and breeding approaches of legume crops for resistance against rust. These efforts encompass a range of strategies, from cultural practices to conventional

and advanced breeding techniques, reflecting the importance and complexity of combating rust diseases in these crops.

3. Rust Diversity in Legumes

Understanding pathogen diversity is essential to design efficient disease management strategies, and to develop new rust resistant cultivars (Sillero et al. 2006). Legume rusts are mainly incited by fourteen fungal species (Table 1), most of them belong to the *Uromyces* genus, although some species from the *Phakopsora* and Puccinia genus can also be of importance for some legumes. Collectively, these rust species can exhibit a wide and overlapping host range with several *Uromyces* species able to infect the same host (Zhang et al. 2011). As for other pathosystems, numerous races and pathotypes have been described for several rust species according to their virulence pattern on different host genotypes.

Table 1. Causal agents of rust disease in legumes species.

Legume crop	Main specie/s	Main causal agent	References
Pigeon peas	*Cajanus cajan*	*Phakopsora pachyrhizi*	Nunkumar et al. 2008
Soybean	*Glicine max*	*P. pachyrhizi, P. meibomiae*	Bromfield 1984
Peanut	*Arachis hypogaea*	*Puccinia arachidis*	Mondal and Badigannavar 2015
Bambara groundnut	*Vigna subterranea*	*Puccinia spp.*	Hillocks et al. 2012
Common bean	*Phaseolus vulgaris*	*Uromyces appendiculatus*	de Jesús et al. 2001
Chickpeas	*Cicer arietinum*	*U. ciceris-arietini*	Sillero et al. 2012
Lupins	*Lupinus* spp.	*U. lupinicolus*	Huyghe 1997
Cowpea	*Vigna unguiculata*	*U. phaseoli* var. *vignae*	Edema and Adipala 1995
Grass pea	*Lathyrus sativus*	*U. pisi*	Vaz Patto and Rubiales 2013
Vetches	*Vicia sativa*	*U. pisi, U. viciae-fabae*	Rubiales et al. 2013a; Georgieva 2018; Rubio and Rubiales 2021
Peas	*Pisum sativum*	*U. pisi, U. viciae-fabae*	Barilli et al. 2009a, b
Faba bean	*Vicia faba*	*U. viciae-fabae*	Rashid and Bernier 1991
Lentils	*Lens culinaris*	*U. viciae-fabae*	Negussie and Pretorius 2012
Alfalfa	*Medicago sativa*	*U. striatus*	UK CAB et al. 1965
Clovers	*Trifolium* spp.	*U. striatus, U. trifolii*	Barbetti and Nichols 1991
Birdsfoot trefoil	*Lotus* spp.	*U. striatus* var. *loti, U. loti*	Zeiders 1985; Ciliuti et al. 2003

It is recognized that the resistance mechanisms of rust against *P. pachyrhizi* are race-specific, although these mechanisms are not well-defined and, comprehensive studies on the physiological races of the pathogen are still needed (Chanders et al. 2019). However, some studies identified 6 races of *P. pachyrhizi* on soybean and 4 on its wild alternative host plant kudzu (*Pueraria lobata*) in regions

of Japan (Yamaoka et al. 2002, 2014). In addition, preliminary studies have indicated the existence of at least two different races of the pathogen in South Africa and Brazil (Darben et al. 2020; Caldwell and McLaren 2004). These findings suggest a geographical and host-based pathogenic variation of *P. pachyrhizi*, highlighting the need for further research to understand the extent and implications of this diversity (Akamatsu et al. 2017).

In peanut crop, several studies have suggested the existence of races of *P. arachidis*, as susceptibility has been reported in plants presumed to be resistant under tropical climatic conditions (Kuo et al. 2021). However, physiological identification of these different races remains unclear so far (Subrahmanyam et al. 1993; Waliyar et al. 1993). These findings highlight the complexity of pathogen-plant interactions and the potential impact of environmental factors on disease dynamics. The inability to physiologically differentiate these pathogenic races underscores the challenges in managing peanut rust and suggests a need for ongoing research, particularly in understanding how climatic conditions influence pathogen virulence and host resistance (Kuo et al. 2021).

A wide global diversity has also been demonstrated for some *Uromyces* spp. populations, such as *U. appendiculatus* (syn. *U. phaseoli*), for which hundreds of races and pathotypes have been described in different regions of the world (Acevedo et al. 2013; Nyang et al. 2016; Liebenberg and Pretorius 2011). Research on the broad range of virulence on common bean genotypes has shown that *U. appendiculatus* races segregate into two distinct groups, Andean, and Mesoamerican (Pastor-Corrales and Aime 2004). Some of these pathotypes are limited to their geographic origin, as for the Andean races that usually infect common beans with the same Andean origin (Sandlin et al. 1999). By contrast, races belonging to the Mesoamerican gene pool present a broader range of virulence and are capable of infecting common beans of Andean, Middle American, and Mesoamerican origin (Pastor-Corrales 2004).

Two races have been described within *U. phaseoli* var. *vignae* affecting cowpea (Gay 1971). While most research have focused on race 1, whose resistance genes act independently of leaf age, the resistance genes of race 2 have been shown to act differentially depending on the leaf age, the site of infection, and the cultivar used (Heath 1994). Consequently, greater specificity has been suggested in race 2 than in race 1 of cowpea rust.

Although the existence of races has not been clarified within *U. pisi* population, it is recognized as the causal agent with the broadest host range among legumes. It significantly affects peas, grass pea and to a lesser extent lentils and vetches (Barilli et al. 2012). Although differences in the level of partial resistance expressed by specific host genotypes have been detected in response to different *U. pisi* isolates, differential patterns of the hypersensitive response (HR) were not detected impeding

the definition of differential races (Osuna-Caballero et al. *Under Review*). Interestingly, host range studies and phylogenetic analysis of *Uromyces* species suggests that the other legume infecting *Uromyces* species might have evolved from *U. pisi* (Emeran et al. 2008; Chung et al. 2004).

U. viciae-fabae can also affect a wide range of legumes, including faba bean, lentil, pea, and vetches (Conner 1982a; Gautam et al. 2022b). It is a complex species for which host specialization has been suggested (Emeran et al. 2005). Existence of races have been proposed within the faba bean infecting isolates, although not systematically monitored. Up to 9 races have been reported in Australia alone (Ijaz et al. 2020, 2021a), while and up to 16 races have been described from isolates of worldwide distribution (Emeran et al. 2001). This classification is based on the presence or absence of necrosis as a criterion for discrimination in broad bean cultivars. Some studies had also postulated existence of races based on pustule size (Conner 1982b; Rashid 1984). Recent studies have demonstrated differences in the pattern of HR expressed by *Lens* spp. genotypes in response to *U. viciae-fabae* isolates, suggesting the presence of four distinct races of this pathogen in lentils (Barilli and Rubiales 2023).

Although the available resources on *U. lupinicolus* are limited in terms of host diversity, one instance of inappropriate specificity between this pathogen and *M. truncatula* has been described (Vaz Patto and Rubiales 2014). Furthermore, available pathogenicity studies revealed a close relationship between *U. lupinicolus* and *U. ciceris-arietini* (Emeran et al. 2008). However, studies targeting the host range of *U. ciceris-arietini* showed successful infection and symptom manifestation on chickpeas and *Medicago* spp., including *M. truncatula*, but not on lupins (Stuteville et al. 2010). Therefore, given these contradictory results, further studies on host adaptation and virulence tests on both lupin and chickpea rusts species are needed.

Understanding the host range and diversity of rust isolates is crucial to design efficient management strategies, as it reveals how alternative hosts can serve as reservoirs for fungi, propagate the disease, and cause unexpected outbreaks. Moreover, if the same rust species or pathotype can infect two legume species, knowledge about the resistance developed for one of these species can also be useful for improving resistance in the other (Kawashima et al. 2016).

4. Disease Management

The very efficient spreading mechanism of rust that allow the transport of its urediniospores by winds or travellers over thousands of kilometres, coupled with its wide host range, make the eradication of the pathogen in the field a challenging task. Efficient control of rust requires the integration of different disease management approaches. The elimination or reduction of the pathogen propagules and of its aerial

dispersion are the primary objectives of these disease control measures (Chandrashekara et al. 2022).

4.1. Cultural Control

Agricultural practices can play a major role in reducing rust incidence in legumes. Accordingly, they are included in a sustainable integrated pest management approach in combination with other activities. Field assessment of previous crop, tillage, sowing date, cropping system, plant density and weed control are included as parameters that potentially decrease rust severity (Juroszek and von Tiedemann 2011).

Early sowing can facilitate the premature dispersal and germination of fungal spores, prompted by the advent of favourable temperatures and humidity levels. This phenomenon triggers an early emergence of the disease and increase the number of fungal cycles during the epidemic phase, thereby intensifying damage to the crop (Dawit and Andnew 2005; Das et al. 1999). Accordingly, numerous studies have corroborated that postponing planting diminishes the impact of rust in peanut (Das et al. 1999), faba bean or pea (Eshetu et al. 2018; Singh et al. 2014). This practice was also found efficient against some *Uromyces* species in cereals (Dawit and Andnew 2005), making it a suitable solution to prevent or reduce rust incidence in the field. The choice of the preceding crop in rotation also plays a pivotal role in the severity of rust infestation on the subsequent legume crop. If this crop is susceptible to rust, the remaining debris might serve as an inoculum reservoir, initiating plant infection under conducive environmental conditions.

The agricultural system, be it monoculture or mixed cropping, is another determinant of rust severity under field conditions. In intercropping systems, where legumes are mixed with other crops, these plants can form a physical barrier (Guo et al. 2021). This barrier impedes spore dispersion, thereby curtailing the number of fungal reproductive cycles in the epidemic stage and subsequently diminishing the disease impact on host plants. Recent studies underscore the superiority of intercropping over monoculture in managing diseases in legumes (Singh et al. 2014; Guo et al. 2021; Luo et al. 2022; Zhang et al. 2019). Moreover, the reduction of weeds which can serve as alternative hosts for rust, achieved with cropping mixtures, effectively lessens the disease severity in the field (Shtaya et al. 2021). Controlling the alternative host is also a key strategy in managing rust diseases in legumes, as evidenced by the historical success in controlling wheat stem rust by eradicating barberries (Zhao et al. 2016). This method reduces the likelihood of sexual recombination of the rust pathogen, which often occurs when infects on its alternate host. For instance, *U. pisi*, the pea rust pathogen, completes its life cycle on *Euphorbia cyparissias* and *E. esula*, which can grow in the vicinity of pea fields as spontaneous weeds and spread the fungal aeciospores over the crop (Pfunder and Roy 2000). By managing or eradicating such alternate hosts, the source of inoculum

is significantly reduced, thereby reducing the spread of the disease. This approach is crucial in integrated pest management programs.

Lastly, the density of plantations may influence the spread and severity of the fungus (Fernández-Aparicio et al. 2006). While certain studies observed a strong correlation between sowing density and rust severity (Eshetu et al. 2018; Fernández-Aparicio et al. 2006; McEwen and Yeoman 1989), others only detected a marginal effect if any with climatic conditions playing a more substantial role in the disease development (Olle and Sooväli 2020; More et al. 2020).

4.2. Biological Control

Biological control has primarily revolved around the use of living organisms such as predators, parasites, and pathogens to manage pest and disease populations in the field. However, the scope of biological control also encompasses the utilization of natural compounds derived from these organisms. This includes pheromones, hormones, and metabolism-derived products that may function as repellents, attractants, or growth inhibitors of pathogens. Both approaches have been documented in legume crops to manage rust disease.

Various microorganisms have been identified as biological control agents (BCAs) against rust disease. The study of host plant leaf microbiome allowed the discovery of antagonistic endophytic bacteria (Kiani et al. 2021). These beneficial bacteria limit fungal growth thereby reducing rust disease severity (Yuen et al. 2001). Several studies have demonstrated the effectiveness of bacteria from the *Bacillus* genera, against both cereal and legume rusts where they significantly mitigate disease severity in the field and under controlled conditions (Baker et al. 1983, 1985). In addition, bacteria from the *Pseudomonas* genera have also been described as potential BCAs against *U. appendiculatus* (Abo-Elyousr et al. 2021). Endophytic fungi able to induce resistance, antagonize rusts or even act as hyperparasites of the pathogen have also been described (Fontana et al. 2021). For instance, different strains of *Trichoderma* spp. have been reported to stimulate systemic resistance in common bean against *U. appendiculatus* (Burmeister and Hau 2009; Cruz-Triana et al. 2018). These strains can also antagonize the pathogen by inhibiting urediniospore germination and germ tube growth (Abeysinghe 2009). Further studies highlight the use of BCAs from *Simplicillium* and *Cladosporium* genera as hyperparasites of various rust species from the genera *Puccinia*, *Phakopsora*, and *Uromyces* genera (Si et al. 2022; Assante et al. 2004; Moricca et al. 2005; Barge et al. 2022).

A more accurate approach of biological control involves unveiling which specific products from these fungal and bacterial species can limit the growth and spread of rusts. This method would restrict the introduction of exogenous organisms into crop fields, potentially averting ecosystem destabilization if their growth becomes uncontrolled (Herskowitz et al. 2023). In this direction, the inhibitory effect

of several compounds isolated from plant essential oils or fungal secondary metabolism have been validated against different rust species. The antifungal effect of crude plant extracts has also been tested. For instance, crude extracts from *Ageratum conyzoides*, *Nigella sativa*, and *Pelargonium zonale* were found effective in reducing germination of *P. arachidis*, *U. appendiculatus*, and *U. viciae-fabae* urediniospores, respectively (Yusnawan and Inayati 2018; Arslan et al. 2009; El-Fawy et al. 2021). Notably, *Nigella sativa* extract reduced common bean rust severity by up to 96 % (Arslan et al. 2009). Evidence also suggests that plant derived essential oils can reduce the number of rust pustules in legumes. Application of lin seed oil, for example, was found to completely inhibit *U. appendiculatus* urediniospore germination in both in vivo and in planta experiments (Arslan 2014). Other trials on *U. viciae-fabae* demonstrated a reduction of rust severity of up to a 96 % after treating infected plants with basil oil three hours after inoculation (Oxenham et al. 2005) while hyssop and pumpkin seed oils were less efficient (Letessier et al. 2001; El-Fawy et al. 2022). While not achieving as high a reduction in rust severity on the complete plant, the application of these essential oils carries additional synergistic benefits for legumes, potentially enhancing plant height and yield, as demonstrated in greenhouse conditions (El-Fawy et al. 2022).

The isolation and analysis of secondary metabolites have also constituted an important area of research in combating rust. Effective substances produced by the secondary metabolism of both bacteria and fungi have been identified, with notable contributions from the *Bacillus* (Lim et al. 2017; Manjula et al. 2004), *Trichoderma* and *Cladosporium* genera (El-Hasan et al. 2022; Nasini et al. 2004). Similarly, several bio-compounds isolated from the secondary metabolism of phytopathogenic fungi such as *Seiridium cupressi*, *Diplodia quercivora*, and *Ascochyta lentil* can reduce the *U. pisi* severity on peas (Barilli et al. 2016, 2017, 2022). Additionally, evidence suggests that the accumulation of phytoalexins in non-host species inhibits the development of the pathogen within their plant tissue. For instance, phytoalexins such as medicarpin and scopoletin have been associated with resistance to *P. pachyrhizi* in the non-host species *M. truncatula* and *A. thaliana*, respectively, and their influence on soybean plants have been successfully tested against *P. pachyrhizi* (Beyer et al. 2019; Ishiga et al. 2015). Accumulation of these phytoalexins can also be induced by exogenous compounds that induce the systemic acquired response (SAR), such as BTH and BABA, as it has been demonstrated in pea against *U. pisi* (Barilli et al. 2010a, 2012, 2015). This line of research highlights a wide range of biological resources to enhance plant defence mechanisms against rust pathogens in an eco-friendlier way although their large-scale application in the field is so far not possible compromised by the low yield of the isolation methods that are in most cases not standardised and well-polished.

4.3. Chemical Control

The management of rusts in agricultural fields can be effectively achieved using chemical-synthesized fungicides. Among the primary phytochemicals employed for rust disease control, albeit with varying efficiencies, are triazoles, strobilurins, and carboxamides (Juliatti et al. 2017; Chen 2005; Alam et al. 2007). Triazoles function by inhibiting the enzyme 14α-sterol demethylase, thereby obstructing the binding of ergosterol, and subsequently disrupting the structural and functional integrity of the fungal cell wall. Additionally, triazoles exhibit systemic action, disseminating through both the leaves (translaminar movement) and the xylem (acropetal movement). Their effectiveness, whether applied solely or in combination with benzimidazoles, has been validated in several legume crops against rust species such as *U. viciae-fabae*, *U. appenditucalus*, and *U. lupinicolus* (Devi et al. 2020; Emeran et al. 2011; Etheridge and Bateman 1999; Modesto et al. 2005; Sugha et al. 2008). However, triazoles are categorized as posing an intermediate risk for fungicide resistance, with mutations in sterol demethylase identified in plant pathogens of cereals, leading to reduced triazole sensitivity (Cools et al. 2006).

Strobilurins impede mitochondrial respiration by targeting the electron transfer chain between cytochromes b and c1, which hampers ATP synthesis (Köle et al. 1997). Known as QoIs (quinoline outside inhibitors), these broad-spectrum fungicides have demonstrated efficacy against various rust species and, in some instances, have enhanced growth and yield (Rasha et al. 2021; Glaab and Kaiser 1999). Although the risk of rust species developing resistance to strobilurins is generally low, studies have indicated that a single point mutation in the mitochondrial cytochrome b (the target of strobilurins) can lead to QoIs fungicide resistance (Grasso et al. 2006a, b).

The action mechanism of carboxamides targets the enzyme succinate dehydrogenase (SDH), a crucial component of the tricarboxylic acid cycle (TCA) and the mitochondrial electron transport chain (Rheinheimer 2019). Carboxamides, thus, inhibit fungal cell respiration by blocking the TCA cycle at the oxidation stage from succinate to fumarate, culminating in the rapid cell death. These fungicides have also been tested against rust diseases in legumes; for instance, they limit rust damage in faba beans affected by *U. viciae-fabae* (Emeran et al. 2011). While carboxamides effectively mitigate rust disease across a spectrum of legumes and cereal rusts, the Fungicide Resistance Action Committee (FRAC) has developed resistance management recommendations for various crop pathogens to minimize the risk of resistance to this class of fungicides (Sierotzki and Scalliet 2013).

Despite their efficiency, the utilization of fungicides imposes a significant financial burden on legume production, especially in developing countries where legumes are the main protein source for human food (Emeran et al. 2011). The use of these chemicals can also pose health risks to users, adversely impact the

environment, and lead to the emergence of fungicide-resistant rust strains (Oliver 2014). Consequently, cultivating varieties with an adequate level of durable resistance represents the most effective strategy for rust disease control in legumes.

5. Basis of Resistance

The study of the resistance mechanisms that the host holds to respond the pathogen are intricately linked to the infection process of rust. This infection cycle, detailed in the Figure 2, begins when a spore lands on the tissue surface (Figure 2a). If the environmental conditions are favourable, the spore will form a germ tube. If this germ tube successfully locates a stoma, it can form an appressorium over it, serving to penetrate the host (Figure 2b). Successful penetration leads to the formation of a substomatal vesicle in the substomatal space (Figure 2c). From here, an initial infection hypha emerges and, upon contacting a mesophyll cell, can differentiate at its tip into a haustorial mother cell (HMC). Then the pathogen can enter the mesophyll cell via a neckband and forming a haustorium (Figure 2d). If this first haustorium is effective, the fungus will continue to develop secondary hyphae to infect more cells and continue extracting nutrients to expand the colony inside the host (Figure 2e). Once it has accumulated sufficient resources, sporogenic tissue begins to form, and spores emerge through an opening on the tissue surface created by pressure exerted from within (Figure 2f), leading to what we know as a pustule. This detailed understanding of the rust infection process is crucial for developing effective resistance strategies in the host plants, as it reveals the critical stages where intervention might be most effective.

5.1. Resistance Mechanisms against Rust

The detailed monitorisation of the infection process at microscopic level on a set of differential accessions allowed the detection of different resistance mechanism. The first resistance mechanism expressed by the plant is related with leaf morphology, reducing surface area and growth orientation, thus hindering spore deposition. It has been proposed that spore deposition (Figure 2a) would be lower in plants with vertical leaves compared to horizontal ones. However, the impact of leaf orientation on spore deposition is less significant than the effect of the foliar microclimate on germination. It has also been observed that bean rust germ tubes grow along trichomes on soybean plants, reducing the contact with the leaf surface (Wynn 1976). In this case, the trichome acted as a passive screen that can reduce disease severity although, this factor was not decisive in final plant severity under field conditions (Mmbaga et al. 1994). Some additional pre-infection mechanisms have been described including those preventing pathogen adhesion to the leaf surface (Mmbaga et al. 1994; Wynn and Staples 1981), diverting the thigmotropically sensitive germ tube away from stomata (Wynn and Staples 1981), impeding stomata recognition through atypical morphology of stomatal guard cells, and the secretion of

protective compounds on the leaf surface (Niks and Rubiales 2002; Prats et al. 2007). Genotypic differences that limit spore germination and directional growth of the germ tube have been detected against *U. pisi* and *U. viciae-fabae* (Vaz Patto et al. 2009). However, these mechanisms can, at best, reduce infection levels at the early epidemic cycles but are of marginal importance in natural conditions (Rubiales and Moral 2004; Vaz Patto et al. 2009).

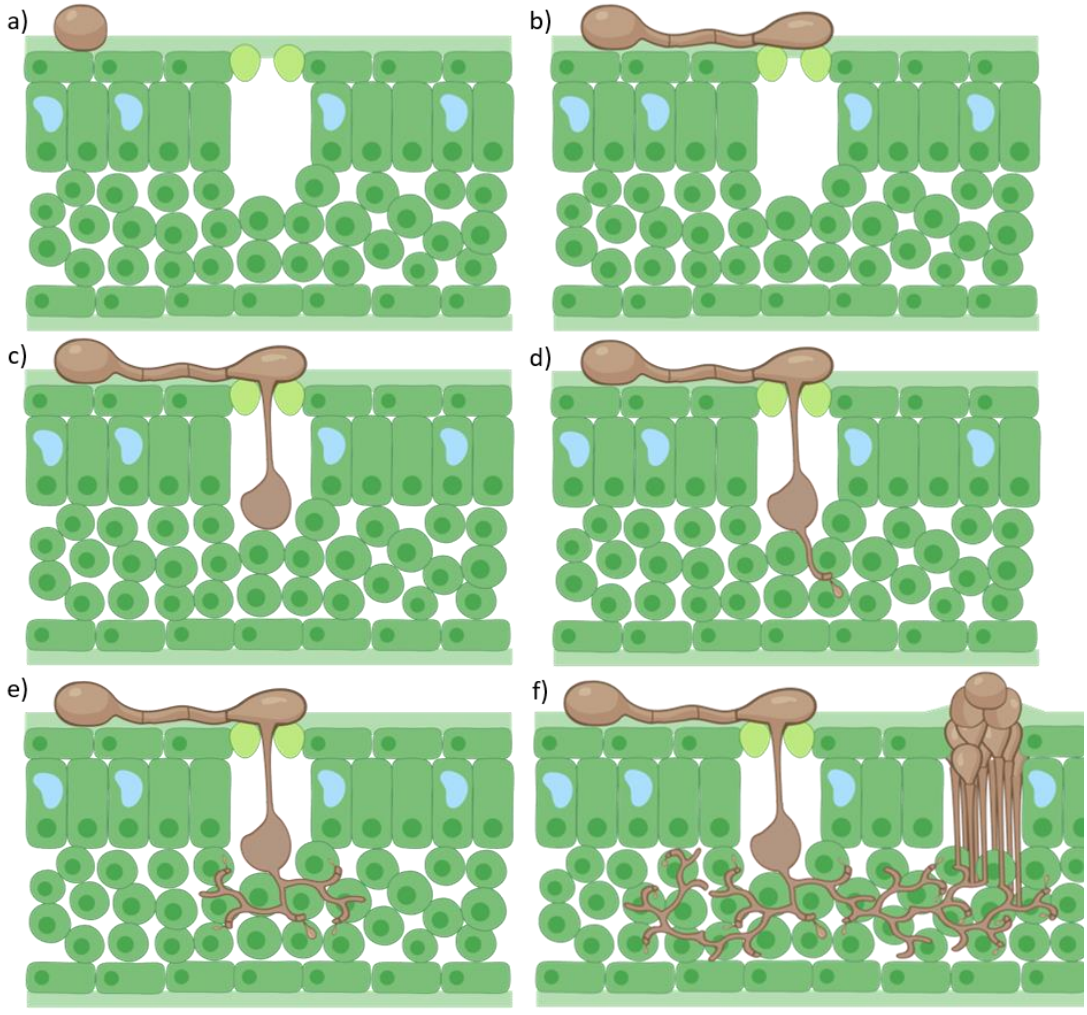

Figure 2. Rust infection process: a) spore deposition; b) spore germination and appressorium formation; c) stomatal penetration and substomatal formation; d) development of the first intracellular hyphae and haustorium formation: e) colonization; f) spore formation and release. Created with BioRender.com.

For pathogenic fungi that penetrate stomata, it is important that they locate them through an efficient chemical recognition (Cooper et al. 2007). The *U. viciae-fabae* fungus seems quite inefficient since typically only about 50 % of germ tubes find a stoma in faba beans, compared to figures ranging from 80 to 100 % for pea rusts caused by *U. pisi* (Sillero and Rubiales 2002; Barilli 2009c). Germ tubes of rust

that reach a stoma must stop growing and develop an appressorium to enter the leaf (Figure 2b). Reaching a stoma does not automatically result in stoma recognition and subsequent penetration (Chethana et al. 2021). There is evidence that urediniospore germs of *U. appendiculatus* detect morphological features of host stomata on which to develop appressoria in common bean (Wynn 1976; Hoch et al. 1987). Generally, stoma recognition is very efficient: typically, more than 90 % of germ tubes reaching a stoma form an appressorium. However, there are evidence of misplaced appressorium formation by the faba bean rust fungus, *U. viciae-fabae*. In this pathogen, the proportion of misplaced appressoria reach about 20 %, but it is rather uniformly distributed among faba bean accessions offering little opportunity for breeding (Sillero and Rubiales 2002).

The most efficient resistance mechanisms against rust occur after the formation of the substomatal vesicles, since changes before then, though significant, were too small to cause substantial epidemiological effects in the case of bean or pea rust (Barilli et al. 2009c). Non-host resistance, an inherent defence mechanism against non-adapted pathogens, is typically manifested before the formation of the first haustorium (Bettgenhaeuser et al. 2014). This type of resistance is also relevant to host-pathogen interactions, significantly contributing to partial resistance (PR), which is a quantitative mechanism characterized by a slower rate of disease development compared to susceptible plants (Parlevliet 1979). Being controlled by multiple genes, this mechanism showed an enhanced durability compared to monogenic R gene-mediated resistance (Niks and Rubiales 2002; Rubiales and Niks 1995). PR has been documented in a range of legumes including faba bean (Sillero and Rubiales 2002) and *M. truncatula* (Rubiales and Moral 2004), where a considerable proportion of infection units fail to establish haustoria. By contrast, host resistance mediated by R genes is characteristically induced after haustoria formation and is frequently correlated with the hypersensitive response, a localized cellular apoptosis designed to constrain pathogen propagation (Camagna and Takemoto 2018). Despite the efficacy of this response, the durability of R gene-mediated resistance is potentially compromised due to the pathogen evolutionary capacity to overcome specific resistance genes (Niks and Rubiales 2002).

The spectrum of rust resistance responses in legume crops are mostly categorized as incomplete. This classification encompasses instances where the host's affliction by the pathogen is mitigated relative to a susceptible control, albeit without the absolute inhibition of the pathogen life cycle. For instance, some faba bean and pea cultivars showed a partial hypersensitive resistance (HR) permitting some degree of sporulation in the presence of host cell necrosis around the infection site (Sillero et al. 2000; Osuna-Caballero et al. 2022).

Non-hypersensitive resistance constitutes an alternative form of incomplete resistance that impedes epidemic progression without eliciting programmed cell

death. Research indicates that this type of rate-reducing resistance is widespread within legumes species and frequently represents the sole form of defence (Sillero et al. 2012; Barilli et al. 2009a; Osuna-Caballero et al. 2022; Singh et al. 2015). This situation contrasts with other pathosystems dominated by HR and for which such PR is not common (Niks and Rubiales 2002).

5.2. Genetic Basis of Resistance against Rust

Precision genetic breeding for rust resistance requires an understanding of the genetic basis of resistance. For instance, through genome-wide association studies (GWAS) and linkage mapping, several types of resistance against different rust species have been localized among legumes. These qualitative and quantitative resistance mechanisms are dependent on one or multiple genes, respectively. This distinction between single gene and multiple resistance genes is crucial, as it influences the breeding methodology and the potential durability of the resistance. Linkage mapping and GWAS have enabled the identification of specific genetic loci and alleles responsible for resistance, thereby providing a foundation for targeted breeding strategies.

Monogenic resistance in rusts enable the cell programmed death when the haustorium forms inside the host. Although it is not the most common source of resistance in legumes, its use in breeding is available for some species. The known candidate resistance genes or QTLs and their location are displayed in Table 2 when the resistance sources contribute > 10 % to the phenotypic variance.

Table 2. Quantitative trait loci (QTLs) and candidate resistance genes and against rust infecting legumes, their genetic location (linkage group or chromosome) and linked markers

Legume crop	Rust specie	Linkage Group/ Chromosome	Resistance Genes/QTLs	Linked Markers	References
Grass pea	*U. pisi*	LG IV/Chr4	Psat4g145320	SNP_{1323}	Martins et al. 2022
		LG II/Chr6	Psat6g010840 and Psat6g006320	SNP_{2174}, SNP_{2175} and SNP_{2145}	Martins et al. 2022
Chickling pea	*U. pisi*	LG II	*UpDSIIa_field*, *UpDSIIb_field* and *UpDSIIc_field*	SSR_{LCI336}, $DArT_{39737826}$, $DArT_{100000564}$ and $DArT_{39732468a}$	Santos et al. 2022
		LG IV	*UpDSIV_chamber*, *UpDSIVa_field*, *GluvIVa* and *GlucIVb*	$SNP_{1000037810\_21}$, SSR_{LCI220} and $DArT_{100036350}$	Santos et al. 2022
Pea	*U. pisi*	LG VI/Chr1	127135829; 127115771; 127082329	$DArT_{3551012}$; $DArT_{5886489}$ and $DArT_{19788813}$; $DArT_{26138450}$	Osuna-Caballero et al. 2024
		LG I/Chr2	127117481; 127103325	$DArT_{3551269}$, $DArT_{3557565}$	Osuna-Caballero et al. 2024
		LG V/Chr3	127132076; 127125898; 127130208; 127127564; 127127894	$DArT_{3544108}$; $DArT_{5937399}$; $DArT_{5880972}$; $DArT_{3552072}$; $DArT_{3555519}$	Osuna-Caballero et al. 2024
		LG IV/Chr4	*UpDSIV*; *UpDSIV.2* 127138740	$DArT_{3563695}$, $DArT_{3569323}$, $DArT_{3560101\_51}$ and $DArT_{3536169}$; $DArT_{3536422}$ and $DArT_{3538789}$ $DArT_{4659565}$ and $DArT_{5947149}$	Barilli et al. 2018; Osuna-Caballero et al. 2024
		LG III/Chr5	*Up1* 127084018; 127084564; 127087291; 127087323; 127087508; 127105708	$RAPD_{OPY111316}$ and $RAPD_{OPV171078}$ $DArT_{3541671}$; $DArT_{3558891}$; $DArT_{3551119}$; $DArT_{8175311}$; $DArT_{4656208}$; $DArT_{5900633}$	Barilli et al. 2010b; Osuna-Caballero et al. 2024
		LG II/Chr6	*UpDSII* 127097832	SSR_{AD280}, $DArT_{3534625}$, $DArT_{3539148}$ and $DArT_{3567800}$ $DArT_{3557403}$	Barilli et al. 2018; Osuna-Caballero et al. 2024

Legume crop	Rust specie	Linkage Group/ Chromosome	Resistance Genes/QTLs	Linked Markers	References
Pea	*U. pisi*	LG VII/Chr7	127084730; 127108155	$DArT_{5897640}$; $DArT_{3549271}$, $DArT_{3541979}$ and $DArT_{4662232}$	Osuna-Caballero et al. 2024
	U. viciae-fabae		*Ruf*	$RAPD_{SC10\text{-}82360}$ and $RAPD_{SCRI\text{-}711000}$	Vijayalakshmi et al. 2005
		LG I/Chr2	*Qruf2*	SSR_{AA121} and SSR_{AD147}	Rai et al. 2016
		LG III/Chr5	*Qruf3*	SSR_{Ga20X} and SSR_{AD160}	Rai et al. 2016
		LG VII/Chr7	*Qruf*; *Qruf1*	SSR_{AA446} and SSR_{AA505}; SSR_{AD146} and SSR_{AA416}	Rai et al. 2011, 2016
Lentil	*U. viciae-fabae*			$RAPD_{OPX\text{-}15760}$ and $RAPD_{OPX\text{-}171075}$; $SSR_{Gllc527}$; $SSR_{GLLC106}$	Kant et al. 2004; Dikshit et al. 2016; Fikru et al. 2014
		LG III		$SRAP_{F7XEM4a}$	Saha et al. 2010
		LG I		$SSR_{LcSSR440}$ and $SSR_{LcSSR606}$	Singh et al. 2021
Faba bean	*U. viciae-fabae*		*Uvf-1*	$RAPD_{OPI20900}$	Avila et al. 2003
		Chr3	*Uvf-2*	$KASP_{Vf\_0703}$ and $KASP_{C250539}$	Ijaz et al. 2021b
		Chr5	*Uvf-3*	$KASP_{Ac\times F165}$ and $KASP_{vf\_1090}$	Ijaz et al. 2021b
Chickpea	*U. ciceris-arietini*	LG VII	*Uca1/uca1*	$STMS_{TA18}$ and $STMS_{TA180}$	Madrid et al. 2008
Common bean	*U. appendiculatus*	B1	*Ur9*	$RAPD_{OA4.1050}$	Park et al. 1999

Legume crop	Rust specie	Linkage Group/ Chromosome	Resistance Genes/QTLs	Linked Markers	References
Common bean	*U. appendiculatus*	B4/Pv04	*Ur5*; *Ur-Dorado*; *Ur-Ouro Negro*; *Ur14*; Phvul.004G012300; Phvul.004G012400; *Qur-1*	$RAPD_{OI19460}$; $SCAR_{BA08}$ and $SCAR_{F10}$; SSR_{R04596} and SSR_{04599}	Haley et al. 1993; Kelly et al. 2003; Corrêa et al. 2000;Valentini et al. 2017; Wu et al. 2022
		B11/Pv11	*Ur3*; *Ur6*; *Ur7*; *Ur11*	$RAPD_{OK14620}$; $KASP_{SS68}$; $SCAR_{SOBC06.308}$; $RAPD_{OAD12.550}$ and $RAPD_{OAF17.900}$; $RAPD_{OAC20490}$	Haley et al. 1994; Hurtado-Gonzales et al. 2017a; Park et al. 2003, 2004; Johnson et al. 1995
		B8/Pv08	*Ur13*; Phvul.008G061600; Phvul.008G065600; Phvul.008G065700; Phvul.008G253400; Phvul.008G270700	$SCAR_{KB126}$ and $CA_{KB4HhaI}$; SNP_{03379}; $DArT_{07386}$; SNP_{03385}; SNP_{03819}; SNP_{03850}	Mienie et al. 2005; Leitão et al. 2023
		B6/Pv06	*Ur4*; Phvul.006G152200; *Qur-3*	$RAPD_{OA141100}$; $DArT_{05945}$	Wu et al. 2022; Leitão et al. 2023; Miklas et al. 1993
		B7/Pv07	*Ur12*; Phvul.007G031000; Phvul.007G032266	$DArT_{06294}$; $DArT_{06303}$	Corrêa et al. 2000; Leitão et al. 2023
		Pv05	*Qur-2*		Wu et al. 2022
Cowpea	*U. vignae*	LG IX	*Rr1*; *Ruv1*	$SCAR_{ABRSAAG/CTG98}$; SNP_{2_01772}, SNP_{2_03292} and SNP_{2_04336}	Li et al. 2007; Wu et al. 2018a
		LG VII/Chr2	*Ruv2*	SNP_{2_00934}, SNP_{2_12503}, SNP_{2_09656} and SNP_{1_0906}; SNP_{2_00973}	Wu et al. 2018, b

Legume crop	Rust specie	Linkage Group/ Chromosome	Resistance Genes/QTLs	Linked Markers	References
Cowpea	*U. vignae*	LG VIII	*Ruv3*	SNP_{2_37041}, SNP_{2_07847} and SNP_{2_00497}	Wu et al. 2018a
Pigeon peas	*P. pachyrhizi*	LG V	*CcRpp1*	$CAPS_{52491}$ and SSR_{2152}	Kawashima et al. 2016
Soybean	*P. pachyrhizi*	LG G/Chr18	*Rpp1*; *Rpp4*; *Rpp6*	SSR_{Sct_187} and SSR_{Sat_064}; $SSR_{Satt288}$, $SSR_{Satt612}$ and $SSR_{AF162283}$; $SSR_{Satt324}$ and $SSR_{Satt394}$	McLean and Byth 1980; Hyten et al. 2007; Hartwig 1986; King et al. 2016; Bromfield et al. 1980, 1982; Garcia et al. 2008; Childs et al. 2018; Chanchu et al. 2022; Liu et al. 2016; Yu et al. 2015; Vuong et al. 2016; Lemons et al. 2011
		LG J/Chr16	*Rpp2*	$SSR_{Satt183}$, $SSR_{Sat-255}$, $SSR_{Satt620}$ and SSR_{Sct-01}	
		LG C2/Chr6	*Rpp3*	$SSR_{Satt658}$, $SSR_{Sat-263}$, $SSR_{Satt460}$ and $SSR_{Satt307}$	
		LG N/Chr3	*Rpp5*	$SSR_{Sat-166}$, $SSR_{Sat-275}$ and $SSR_{Sat-280}$	
		LG L/Chr19	*Rpp7*	$SNP_{GSM0547}$ and SNP_{0547}	
Peanut	*P. arachidis*	A03	Aradu.Z87JB, Aradu.RKA6 M, Aradu.T44NR, Aradu.IWV86 and Aradu.NG51Q	$RAPD_{J71300}$ and $RAPD_{J71350}$; $SSR_{pPGPseq4A05}$, and $SSR_{gi56931710}$; TE_{360} and TE_{498}; $SSR_{IPAHM103}$, SSR_{GM2009}, SSR_{GM1536}, SSR_{GM2301}, SSR_{GM1954}, SSR_{GM2079}; $SSR_{GO340445}$, SSR_{FRS72}	Mondal et al. 2008, 2012, 2014, 2018; Yol et al. 2016

In pea, only incomplete resistance has been identified against *U. viciae-fabae* and *U. pisi*. While some QTLs associated with resistance have been mapped, they are not yet suitable for marker-assisted selection (MAS) in breeding programs (Rubiales et al. 2011). There is evidence suggesting that partial resistance to *U. viciae-fabae* may be due to a single major gene (*Ruf*), with two RAPD markers identified nearby, but not close enough for effective MAS (Vijayalakshmi et al. 2005; Rai et al. 2011, 2016). For *U. pisi*, a QTL responsible for 63 % of resistance was located, with two associated RAPD markers, but further validation in different environments and genetic backgrounds is needed before these findings can be applied to MAS (Barilli et al. 2010b, 2018). In those cases, the development of standard markers and conversion of RAPDs to sequence-characterized amplified regions (SCARs) is necessary to improve their utility for MAS. On the other hand, new silico DArTseq makers have been associated to *U. pisi* partial resistance in pea where putative genes were proposed as resistance's causative agents for their use in breeding programs, but validation is still needed (Osuna-Caballero et al. 2024).

Likewise, researchers have found only incomplete resistance to rust caused by *U. ciceris-arietini* in chickpea (Sillero et al. 2012). A major QTL, accounting for 81 % of the resistance in adult plants, was mapped to linkage group 7 on the chickpea genetic map (Madrid et al. 2008). This resistance is thought to be controlled by a single gene (*Uca1*/*uca1*) closely flanked by two STMS markers suitable for reliable marker-assisted selection for rust resistance in chickpea breeding programs (Madrid et al. 2008).

In lentils, resistance to *U. viciae-fabae* is generally partial, but some sources show hypersensitive resistance (Rubiales et al. 2013b, Negussie et al. 2005, 2012; Barilli et al. 2023). There is known monogenic resistance, and research is advancing on identifying its chromosomal location and linked markers (Kant et al. 2004; Dikshit et al. 2016; Fikru et al. 2014; Saha et al. 2010; Singh et al. 2021). Significant association between the resistance and a specific SRAP and SSR markers has been found and could be used in MAS, though identification of markers closer to the gene would improve this approach (Kant et al. 2004; Dikshit et al. 2016; Fikru et al. 2014; Saha et al. 2010; Singh et al. 2021).

In common bean, researchers have identified various sources of resistance that are specific to individual races of *U. appendiculatus* (Hurtado-Gonzales et al. 2017b). However, some of these resistance sources have been overcome by the pathogen adaptation (Hurtado-Gonzales et al. 2017a). Recent studies have advanced our understanding of the genotypic basis of common bean resistance to diverse rust strains (Wu et al. 2022; Montejo-Domingez et al. 2022). These investigations encompass both partial and hypersensitive resistance mechanisms (Leitão et al. 2023). Therefore, several genes associated with these resistance forms have been

proposed, and several markers closely linked to these genes are now available for application in breeding programs (Table 2).

In faba bean, most resistance against *U. viciae-fabae* is of incomplete expression and non-hypersensitive (Sillero et al. 2010). The genetic basis of this resistance is not well understood, though race-specific genes reducing pustule size have been suggested (Conner 1982; Rashid and Bernier 1986). Recent mapping studies to identify genes associated with non-hypersensitive resistance have identified two genes, *Uvf-2* and *Uvf-3*, linked to RAPD markers (Ijaz et al. 2021b). Hypersensitive resistance in faba bean, controlled by major-effect genes, has also been identified (Avila et al. 2003). For instance, three RAPD markers linked to a resistance gene, *Uvf-1*, have been found, associated with two additional markers identified in repulsion phase (Mikas et al. 1993).

In cowpea, four QTLs have been proposed to induce resistance against rust with twelve linked markers available for MAS (Li et al. 2007; Wu et al. 2018a). Recently, the first QTL proposed, *Rr1* was coincident with the *Ruv1* in the Wu et al. (2018a) studies. Therefore, the SNPs markers are considered the most reliable in their use for breeding (Wu et al. 2018b).

In the case of pigeon pea, a single source of partial resistance against *P. pachyrhizi* known as the *CcRpp1* gene (*Cajanus cajan* Resistance *against Phakopsora pachyrhizi* 1) has been reported and successfully transferred to transgenic soybean plants (Kawashima et al. 2016).

5.3. Gene Regulation upon Rust Infection in Legumes

A transcriptional profiling during plant–pathogen interaction allows identifying both candidate resistance genes from the plant and genes involved in disease processes from the pathogen (Jha et al. 2021). Rust triggers important transcriptional changes in legume plants during infection, with several hundreds of genes being either up- or downregulated. RNA-seq and transcriptome analyses are powerful tools to identify key defence responsive genes and transcription factors in legume-rust interaction.

5.3.1. Defence/Resistance genes

In peas, an increase in glucanase activity has been observed during infection with *U. viciae-fabae* and *U. pisi* (Barilli et al. 2010a; Kushwaha et al. 2018). This enzyme activity is thought to contribute to the formation of phenolic compounds involved in lignin formation in cell walls, thereby strengthening the plant defence against the pathogen (Yadav et al. 2023). This aligns with transcriptomic analyses in grass pea, where resistance to *U. pisi* was correlated with the overexpression of an endo-beta-1,3-glucanase gene in resistant genotypes. Additionally, overexpressed genes in resistant genotypes of grass pea suggested a comprehensive molecular

response to rust infection which has also been indicated in pea partial resistant accessions (Almeida et al. 2014; Santos et al. 2018). These previous studies in grass pea indicated the overexpression of genes related to phytohormones and transcription factors in resistant genotypes, suggesting a shared genetic basis for resistance in these related legume species against the same rust pathogen and thereby enabling more breeding opportunities (Martins et al. 2022; Osuna-Caballero et al. 2024). In the case of *V. angularis*, a relative to *V. unguiculata*, a response to *U. vignae* infection was characterized by the activation of genes encoding glutamate receptor proteins (Yin et al. 2023).

Additionally, genetic expression studies in common bean inoculated with *U. appendiculatus* revealed significant changes in over five hundred genes when compared to control conditions at various time points post-inoculation (0, 12, and 84 hours) (Ayyappan et al. 2015). Among these, 90 genes were differentially expressed at all time points, including genes involved in stress responses such as calmodulin, cytochrome P450, chitinase, DNA polymerase II, and LRR, as well as transcription factors including WRKY, bZIP, MYB, HSFB3, GRAS, NAC, and NMRA (Ayyappan et al. 2015). These findings underscore the importance of these genes in the common bean-rust interaction which are also similar to those found in other rusts, such as peanut rust caused by *P. arachidis* (Ayyappan et al. 2015; Rathod et al. 2020). Similar differential expression patterns were observed in the "Sierra" cultivar of common bean harbouring the resistance gene *Ur3*, where genes containing NBS, LRR, and TIR signature motifs, along with WRKY-type transcription factors, were overexpressed at the onset of infection (Todd et al. 2017). Differential expression was also assessed in common bean to study the genetic architecture of *Ur4* resistance source. In that study, up to 90 genes were differentially expressed along *U. appendiculatus* infection and were mainly attributed to stress response, hormone regulation/signalling, transport, and cell wall formation (Thibivilliers et al. 2009). In faba bean, studies demonstrated a systemic plant response to localized leaf infection by *U. viciae-fabae*, involving changes in carbohydrate and amino acid metabolism as an adaptive strategy to the pathogen's entry into cells via the haustorium (Wirsel et al. 2001) which agrees with similar studies in *U. appendiculatus* (Puthoff et al. 2008).

Overall, several candidate resistance genes have been identified in plants by transcriptomic approaches which can complement the previously described genetic insights for the breeding of rust-resistant crops. However, functional studies are still missing to validate their role during plant–pathogen interaction.

Understanding both sides of the plant–pathogen interaction is important to completely unravel the molecular basis of resistance. However, most previous legume–rust interaction transcriptomic studies, only compared the plant transcripts induced in response to the pathogen due to low detection of fungal transcript. Identification of rust effector genes controlling pathogen host colonization must be

considered in transcriptomic studies focused on the identification of differentially expressed genes from the rust side and integrated with comparative rust genomics studies.

5.3.2. Candidate Effector Molecules

In the research of effector proteins, a significant focus has been placed on the legume rust pathogens of *U. appendiculatus*, *P. pachyrhizi*, and *U. viciae-fabae* which genomes are available (Link et al. 2014a). These candidate effectors are known to play a major role in activating response genes in the host plant and can suppress various resistance mechanisms. Specifically, in the pathosystems involving broad bean-*U. viciae-fabae* and common bean-*U. appendiculatus*, extensive studies have been conducted, proposing it as model systems for in-depth investigation of legume-rust interactions and for Asian soybean rust, respectively (Link et al. 2008; Thibivilliers et al. 2007). Preliminary studies on *U. appendiculatus* have utilized the haustoria transcriptome analysis to predict and identify effector molecules secreted by the pathogen (Link et al. 2014b). Among the discovered effectors of *U. appendiculatus*, some of them including Uaca_9, Uaca_12, Uaca_14, and Uaca_22, can suppress the hypersensitive response in the host plants (Qi et al. 2019). Additionally, effectors like Uaca_4, Uaca_5, Uaca_7, Uaca_9, Uaca_28, and Uaca_44 can suppress basal resistance in *Nicothiana benthamiana* against the bacterial pathogen *Pseudomonas syringae* (Qi et al. 2019). This indicates the broad impact these effectors might have across different species and pathogen types. It was also noted that some of the genes encoding these effector proteins contain highly conserved motifs within the *Pucciniales* family, suggesting a possible similarity in effector mechanisms across different rust species (Cooper et al. 2016).

A commonality in the action patterns between *U. appendiculatus* and *P. pachyrhizi* has been observed, where both pathogens initiate their infection by secreting families of hydrolase proteins to degrade the host plant's cell wall (245). They also produce structural proteins crucial for forming and stabilizing the haustorium within the host cells, which is a pivotal step in the infection cycle (Link et al. 2014b). The effector proteins from these pathogens are localized in the cytoplasm and nucleus of the host plant cells, where they exert their influence by activating or suppressing various plant responses (de Carvalho et al. 2017).

In the case of *U. viciae-fabae*, specific molecules responsible for the biotrophic interaction between the pathogen and its host have been identified (Voegele 2006). One such molecule, Uf-RTP1p (Rust Transferred Protein 1 from *Uromyces fabae*), secreted by the haustorium, is found within the infected cells, including their nucleus (Kemen et al. 2005). Similar molecules with homologous domains have been discovered whose analogous functions in other rust species have been proposed (Kemen et al. 2005; Vieira et al. 2012). The detection of these molecules facilitates accurate quantification of haustoria using RT-qPCR analysis (Voegele and Schmid

2011). Therefore, a deeper understanding of the substances secreted by the fungus and their functional roles enhances our knowledge of the effectors and the biotrophic interaction between rust-host (Link et al. 2005; Voegele et al. 2005). This knowledge is crucial for developing specific improvement strategies to breed plants that are fully resistant to rust since more effector genes are known, new resistance genes could be identified (Jakupović et al. 2006; Link 2020).

6. Breeding for Resistance

The main objective of breeding for rust resistance is to develop varieties that either show delayed disease onset, minimal symptom development, or slow disease progression, thereby minimizing crop damage. This process begins with the crucial step of identifying and characterizing potential resistance sources for integration into breeding programs.

6.1. Resistance Screening Methods

Efficient screening methods are essential for discovering new resistance sources against rust. In general, this process starts with mass screenings, where large germplasm collections, primarily from the same legume species or occasionally from its wild relatives are evaluated. These initial screenings aim to identify potential resistance sources. Following this, the resistance mechanisms of these promising candidates are further investigated through more in-depth screenings on a selected group of accessions. This two-tiered approach allows breeders not only to identify novel resistance sources but also to understand the underlying mechanisms, thereby aiding the development of rust-resistant varieties.

Mass screenings can be conducted either in natural field settings or under controlled conditions. It is a cornerstone in identifying aerial disease resistance in legumes (Sillero et al. 2006). These screenings employ a range of tools and techniques, to monitor symptom development on the whole plant or on the leaves, which are the most affected plant organs. Field screenings enable the simultaneous evaluation of extensive germplasm collections in conditions where natural inoculum is present allowing an understanding of the genetic and environmental factors that influence the phenotypic variances (Civantos-Gómez et al. 2022; Das et al. 2019). For more uniform and precise assessments, artificial inoculation with urediniospore is often employed and recommended when natural infestation is not high enough. This approach consists of spraying with aqueous suspension of rust spores or dusting mixture of spores in an inert carrier, ensuring consistency across the experimental trial (Sillero et al. 2000). However, natural conditions present challenges, such as the co-occurrence of other aerial diseases like ascochyta blight or powdery mildew, which can complicate rust assessments. The low initial inoculum densities of rust can also lead to the underestimation of its impact due to interference from these other diseases providing some risks of confusing escape with resistance (Porta-Puglia et al.

1993). To mitigate this, reinoculation with urediniospore may be necessary during field trials to ensure accurate evaluation of legume responses to rust (Barilli et al. 2009a). In addition, it is recommended to inoculate the plants after sunset to benefit from both the darkness and the high relative humidity of the night (Sillero et al. 2006).

In field conditions, the assessment of quantitative resistance to rust involves several methodologies. A common approach includes the visual estimation of foliar area affected by pustules, referred to as disease severity percentage (DS). When periodic evaluations of DS are performed, it provides insights into both the final severity of the disease (captured in the last DS data) and its progression overtime. Rust disease progression is estimate through the integration of the periodic DS evaluation into some parameters including the area under the disease progress curve (AUDPC) and the epidemic growth rate (r) (Arneson 2001; Jeger and Viljanen-Rollinson 2001), both critical in understanding the rust impact over time. Alongside DS, it is standard to record the infection type (IT) in the field. Various measurement scales have been developed for IT, which describe the plant reaction to rust disease. This reaction is characterized by the extent of necrosis or chlorosis at the infection sites, as well as the sporulation rate of the colonies that have formed on the tissue. One of the most widely used IT scales, developed for wheat rusts by Stakman et al. (1962), categorizes the reaction as follows: 0 = no symptoms, ; = necrotic flecks, 1 = tiny pustules without sporulation, 2 = necrotic halo surrounding small pustules, 3 = chlorotic halo surrounding pustules, and 4 = well-formed pustules without associated chlorosis or necrosis. On this scale, values between 0 - 2 indicate resistance, while 3 and 4 imply susceptibility. More comprehensive scales such as the scale developed by Bernier et al. (1984) for faba beans rust, combine IT with DS percentages for refined field assessments. This scale, for instance, ranges from 1 (highly resistant) to 9 (highly susceptible), considering both the leaf area and the whole plant affected. Similar scales exist for another legume rusts such peanut and pea (Sokhi et al. 1984; Subrahmanyam et al. 1995). Increasingly, traditional visual assessments are being supplemented, and in some cases replaced, by remote sensing technologies in many pathosystems. These methods, leveraging the contrast between damaged and healthy tissue, are developing new models for rust evaluation with comparable or higher accuracies than visual estimates (Simko et al. 2017). However, most current models are tailored to cereal rusts, where resources and research investment are more substantial (Rubiales et al. 2023). Therefore, adapting these remote sensing methodologies for rusts in legumes could enhance precision allowing timesaving in field evaluations under natural conditions.

A more detailed analysis of disease symptoms is feasible under controlled conditions using growth chambers or greenhouses. This setting enables evaluations at both seedling and adult plant stages. These systems are essential to test the efficacy and multiplication of rust isolates for subsequent evaluation. The most common

method for inoculation involves dusting plants with urediniospores diluted in an inert carrier such as talc powder (Chand et al. 2004). To achieve uniform spore deposition, the use of inoculation towers is recommended (Sillero et al. 2000). After inoculation, it is necessary to provide the environmental conditions required for urediniospore germination and successful plant infection. This typically involves incubation in darkness with 100 % relative humidity for 12 - 24 hours (More et al. 2018). Depending on the rust species, the first macroscopic symptoms are visible between 7 - 9 days post-inoculation (dpi), marking the start of evaluations symptoms. Unlike field evaluations, where DS is the most recorded parameter, controlled conditions allow for a more in-depth analysis of the disease. This includes counting pustules per unit area (infection frequency, IF), typically in a defined leaf area, and measuring pustule size in mm2 (Asare et al. 2019; Barilli and Rubiales 2023). IF facilitates the calculation of the latency period (LP), the time between inoculation and observation of 50 % of total pustules. Both DS percentage estimation and pustule counting is highly time consuming, especially when assessing large plant collections (Bock et al. 2020). Therefore, standard area diagrams (SADs) have been developed for some rust pathosystems to help reduce evaluator bias (Del Ponte et al. 2017). However, these SADs have not been adapted for most legume-infecting rust species, except for soybean rust (Franceschi et al. 2020). Efforts have also been made to automate the evaluation process under controlled conditions. For instance, through detached leaf assays, IF and DS can be calculated using easily acquired images such as RGB (red-green-blue) or thermal sensors, as done in pea and faba bean rust (Alves et al. 2020; Olivoto 2022; Osuna-Caballero et al. 2023). These developing techniques could be readily adapted to other pathosystems, as they share similar symptoms, improving evaluation precision and enabling the assessment of large germplasm collections. In addition, the common infection cycle shared by most rust species allow the evaluation of the different stages of the infection process by microscopic observation of infected leaves at an early stage of the interaction. For instance, in several rust-legume pathosystems, the formation of appressoria over the stomata has been assessed, allowing for the calculation of tissue penetration percentage (first 3-6 hours post-inoculation) (Figure 2b). Substomatal vesicle formation, hyphal development, and haustorium formation within cells (6-12 hours post-inoculation) are also evaluated in several cases (Figure 2c) (Dugyala et al. 2015; Sillero and Rubiales 2002). Colony size within plant tissue at 24- or 48-hours post-inoculation is another commonly assessed parameter (Figure 2d) (Barilli et al. 2009c; Kushwaha et al. 2016; Negussie et al. 2012; Sillero et al. 2012). These microscopic evaluations allow to characterise the resistance mechanisms expressed by the most resistant accessions and select cultivar with a specific resistance mechanism for breeding.

6.2. Conventional Breeding

Classical breeding techniques such as backcrossing, pedigree selection, and recurrent selection can be used to develop rust-resistant cultivars. These techniques

involve crossing elite cultivars with sources of rust resistance. The development of legume resistant cultivars against rust infection with an interesting agronomic potential is the main goal of any breeding program for disease resistance (Renzi et al. 2022). The search and identification of resistant sources is the first step in any classical breeding program for rust resistance and has also been the case for several legume breeding programs.

Once the source of resistance is identified, the introgression of the genomic regions conferring resistance to rust into non-resistant elite genotypes can be obtained by a complex crossing selection scheme. For instance, Conventional breeding for rust resistance in peanuts involves introgression of resistance genes from wild species into cultivated varieties (Stalker 2017). This is achieved through wide hybridization, where genes from cross-compatible wild species are transferred into the cultivated peanut. Efforts in India led to the development of rust-resistant peanut breeding lines such as VG 9514, derived from *A. cardenasii* which were subsequently used as parental lines to develop mapping populations for genetic and QTL mapping, enabling the development of molecular markers for rust resistance (Varman 1999).

In soybean breeding for rust resistance, conventional strategies like gene pyramiding have been applied (Chander et al. 2019). This involves combining multiple *Rpp* genes within a single genotype for broader and more durable resistance (Yamanaka et al. 2015). Molecular markers assist in identifying and selecting these genes, facilitating efficient breeding. Studies have shown that combinations of *Rpp* genes, like *Rpp2*, *Rpp3*, *Rpp4*, and *Rpp5*, provide enhanced resistance to *P. pachyrhizi* (Meira et al. 2022; Yamanaka et al. 2019). The effectiveness of these gene combinations varies with the genetic background of the soybean variety, indicating the importance of considering both specific genes and the overall genetic context in breeding programs.

In common bean cultivation, the optimal approach for traditional breeding also involves accumulating and pyramiding various race-specific resistance sources (Beaver et al. 2003), considering the isolate's specific climatic zones. Common bean varieties with rust resistance are typically developed through crossbreeding, backcrossing, and continuous disease pressure over successive generations, ensuring the acquisition of homozygous resistance genes. Unfortunately, not all registered plant varieties with rust resistance levels have validated reports of their development and resistance levels. Nonetheless, the extensive collaborations between the University of Puerto Rico and The USDA allow to develop various common bean ecotypes resistant to different races of *U. appendiculatus* (genes *Ur-3*, *Ur-5*, *Ur-4*, *Ur-6*, and *Ur-11*) (Beaver et al. 1999, 2015, 2020; Osorno et al. 2021; Pastor-Corrales et al. 2007).

In the case of chickpea, a single interspecific cross between *C. arietinum* and *C. reticulatum* enabled the wild parent to contribute the *Uca1*/*uca1* gene, resulting in segregating resistance lines within the offspring (Madrid et al. 2008). This allowed for the selection and registration of some rust-resistant material (Rubio et al. 2006).

For lentil and faba bean, simple crossings and single seed descendant selection have also made possible the registration of improved lines with significant levels of resistance to rust caused by *U. viciae-fabae* that are available to farmers (Idrissi et al. 2012; Rubiales and Khazaei 2022; Sakr et al. 2004). These breeding strategies demonstrate the integration of genetic resistance into cultivars, providing a sustainable approach to manage rust diseases in these legume crops, which have been developed to combat other legumes rusts (Deshmukh et al. 2020; Paul et al. 2010). However, the described conventional breeding approaches to obtain legume resistant varieties against rust are time-consuming and not very efficient for complex resistance traits. To increase the efficiency and speed of breeding programs, precision breeding approaches, based on molecular innovations, have been developed and applied for rust-resistant legume cultivars development.

6.3. Precision Breeding Strategies

Genomic technologies, including genome sequencing, resequencing, genetic mapping, and diverse omics strategies, are crucial in legume precision breeding. Advances such as next-generation sequencing (NGS) have led to techniques like genotyping by sequencing (GBS), diversity array technology sequencing (DArTseq), RNA-sequencing, and whole-genome sequencing (WGS), significantly improving marker technologies. These have enabled the discovery of numerous single nucleotide polymorphisms (SNPs) closely linked to genes or QTLs controlling rust resistance, enabling faster and more accurate breeding. A compilation of different types of molecular markers closely associated with legume rust resistance genes (previously described in Section 5.2) is presented, which could be beneficial for marker-assisted selection (MAS). These advancements in genomic tools and techniques signify a substantial leap in the ability to understand and manipulate genetic factors underlying rust resistance in legumes, potentially transforming breeding programs and enhancing crop resilience.

Precision breeding in peanuts for rust resistance involves the introgression resistance genes from wild species into cultivated varieties, utilizing MAS for efficient selection (Bertioli et al. 2016). For instance, markers like SSRGO340445 and SSRIPAHM103 have been identified near *P. arachidis* resistance loci (Varshney et al. 2014). These markers are then used in marker-assisted backcrossing to introgressive hybridization resistance into elite peanut genotypes, enhancing rust resistance in cultivated peanut varieties (Ramakrishnan et al. 2020).

Common bean serves as a prime example of a legume crop where, to date, the highest number of molecular markers have been identified in associated with *U. appendiculatus* resistance. Decades of dedicated efforts have led to a thorough understanding of different race-specific resistance genes, facilitating the development of various marker-assisted selection (MAS) strategies. The resistance gene *Ur-14*, present in the Ouro Negro cultivar, has been transferred to offspring using flanking markers RAPDOXY11 and SCARF10 (Ragagnin et al. 2009). Selecting within segregating populations using these polymorphic molecular markers in parental lines, along with others conferring resistance to different diseases, has enabled the development of elite varieties resistant to *U. appendiculatus* and other pathogens through a detailed MAS scheme (Ragagnin et al. 2009). Furthermore, the cultivar obtained in that study has also served as a parental donor of *Ur-14* in crosses and backcrosses with parental donors of resistance genes *Ur-5* (markers RAPDOPF10 and SCARSI19) and *Ur-11* (markers RAPDOPAC20 and SCARFSAE19) (Souza et al. 2014). This approach has allowed pyramiding diverse resistance sources against rust into elite varieties using MAS (Pilet-Nayer et al. 2017; Souza et al. 2014). In this context, the identification of high-quality SNP markers and specific genes will continue to expand knowledge and tools for MAS in common beans, as evidenced by recent GWAS studies (Leitão et al. 2023). Similarly, in other airborne diseases affecting common beans, SNPs linked to resistance genes have been identified, and through introgressions, they have been transferred to elite varieties exhibiting the same resistance level as the donor parent (Keller et al. 2015). These advancements demonstrate the significant progress in the application of genomic tools in breeding for rust resistance in legumes, particularly in enhancing the effectiveness of MAS.

However, the utilization of molecular markers to aid legume breeding for rust resistance has not been widely adopted in breeding programs so far. Various factors contribute to this limitation, but a significant one may be the substantial genetic distance between markers and resistance genes/QTLs. Most legume markers listed in Table 2 are not closely linked to rust resistance genes/QTLs. Large cM distances often identified in linkage maps make their application in precision breeding challenging. For instance, in lentils, some markers linked to rust resistance exceed distances of 5 cM, and others even surpass 10 cM, signifying a considerable gap between the marker and the resistance gene (Kant et al. 2004). Furthermore, not all markers are ideal for MAS. Specifically, OPX-15760 and OPX-171075, implicated in resistance to *U. viciae-fabae* in lentils, are RAPD markers with limitations in reproducibility and detecting allelic variants among heterozygotes (Jiang et al. 2013). Finally, while some polymorphic SSR markers associated with resistance traits have been described, the exact distance between the marker and the gene/QTL, or their location in linkage groups/chromosomes, is not always known (Dikshit et al. 2016; Fikru et al. 2014). These challenges highlight the complexity of integrating molecular

markers into legume breeding programs for rust resistance and underscore the need for continued research to refine these tools for more effective application.

The identification of SNP markers saturating the plant genome is gaining widespread acceptance due to their diverse applications in plant breeding and genetics (Hickey et al. 2019). These markers, numbering in the thousands, allow to study the genetic diversity within core collections of plants. The high-resolution data provided by SNPs allows for an in-depth examination of the genetic makeup, including analysis of linkage disequilibrium and population structure, which are essential components in whole-genome studies (Rispail et al. 2023). In the context of GWAS, these SNP markers are crucial for identifying allelic polymorphisms within genes that are involved in resistance mechanisms. This is particularly significant for enhancing marker-assisted breeding, as it allows for greater precision and efficiency in selecting for traits such as rust resistance in legumes (Susmitha et al. 2023). Moreover, genotyped collections derived from SNP markers are helpful for fitting genomic selection (GS) models. This GS strategy enables the prediction of phenotypes in various unknown plant varieties, considering different agroclimatic environments (Annichiarico et al. 2019). In legumes, both GWAS and GS studies have played a pivotal role in uncovering new genes linked to disease resistance and their utilization in breeding (Zargar et al. 2015). The markers identified through these studies facilitate the breeding of new varieties with enhanced resistance to diseases like rust.

The effectiveness of these precision breeding methodologies is not limited to legumes. Therefore, the advancements in genomic tools and procedures show a substantial improvement in breeders' ability to incorporate biotechnological methods into conventional breeding strategies. Post-genomic reverse genetics techniques, such as RNA interference (RNAi) and Targeting Induced Local Lesions IN Genomes (TILLING), are being used to confirm genetic functions and expedite the selection process for desirable traits (Padilla-Roji et al. 2023). Although initially more common in cereals for combating diseases like rust, the application of these techniques in legumes, such as peas, has shown promising results, for instance, allowing the characterization of nodulation trait mutants in peas (Tayeh et al. 2015). In *M. truncatula*, suppressing pathogenesis-related gene expression through gene silencing of a yeast protein MtSTP13 increased susceptibility to powdery mildew, while its transient overexpression enhances resistance against the disease in peas (Gupta et al. 2021). This expansion of genomic and molecular techniques in plant breeding, particularly in disease resistant, marks significant progress adaptable to other legumes. The ability to accurately quantify genetic diversity, identify disease-resistant genes, and predict phenotypic outcomes across different environments accelerates the development of improved crop varieties, ultimately enhancing crop resilience and productivity.

Similarly, the latest advancements in genetic transformation including CRISPR/Cas9 and single-guided RNA sequence (sgRNA) have achieved ambitious goals in rust resistance, though currently limited to cereals (Hickey et al. 2019). Using the CRISPR/Cas9 technique, it has been possible to silence Ca+ transporter genes involved in disease resistance, leading to the development of wheat varieties resistant to *Puccinia striiformis* f. sp. *tritici* (He et al. 2023). This breakthrough demonstrates the potential of advanced gene-editing techniques in enhancing rust resistance in crops. While this approach has primarily been applied to cereals, its successful application in wheat suggests promising prospects for its use in legumes, where some advances have been made in pea, cowpea, and common bean (de Koning et al. 2023; Ji et al. 2019; Li et al. 2023). The ability to precisely edit genes linked to rust resistance can significantly accelerate the breeding of resistant varieties, potentially revolutionizing the management of rust diseases in legume crops.

7. Conclusions and Future Prospects

Rust diseases present substantial challenges in legume breeding caused by a wide range of causal agents not limited to *Uromyces* genus. The management of these diseases demands integrated approaches that are both environmentally sustainable and cost-effective. Efforts to enhance rust resistance in legumes have led to the development of cultivars with varying levels of incomplete resistance. Despite these advancements, the resistance sources against rust are still limited, and current screening methods are laborious and time-consuming. This highlights the necessity for more accurate phenotyping, achievable through the integration of novel, high-throughput phenotyping platforms.

Significant strides in genomic technologies, including genome sequencing and the discovery of marker-trait associations, are essential in enhancing legume breeding strategies. The availability of optimized reference genomes in several legumes such as pea (Kreplak et al. 2019; Yang et al. 2022), common bean (Shmutz et al. 2014) or faba bean (Jayakodi et al. 2023) are proving invaluable at the molecular level. These resources aid in precise breeding and in unravelling complex trait genetics for better genetic gains. Collaboration among breeding programs is also crucial to share diverse genetic materials, facilitating the gene pyramiding of useful traits and implementing various hybridization regimes to stabilize resistance genes.

The complex nature of rust diseases in legumes requires multidisciplinary approaches that employ both biological knowledge and policy directives to enhance environmental sustainability and food security. Exploring resistance in lesser known but resilient legume species could provide valuable insights for breeding major legume crops. The resistant rust gene transferred from pigeon pea to soybean serve as a successful example (Kawashima et al. 2016). Therefore, investigating wild relative species for rust resistance has also the potential to significantly contribute to the improvement of other major legume crops.

Objectives

Considering rust one of the main diseases worldwide, this doctoral thesis focuses on the pathogen *U. pisi* for the study and identification of new sources/mechanisms of resistance in pea and its use in marker assisted selection in plant breeding. Taking this general objective into account, the specific objectives of this thesis are:

i. Identification of novel sources of resistance to *U. pisi* in a collection of *Pisum* spp. under field conditions and controlled conditions (Chapter 2 and 3).

ii. Identification of resistant accessions based on stability indices on field conditions, allowing the selection of potential resistance donors (Chapter 5).

iii. Characterization of the resistance mechanisms occurring in different pea accessions resistant to *U. pisi* at histologically level (Chapter 2).

iv. Develop an image processing workflow using R software to produce reliable and repeatable measurements of rust-infected pea leaf area, counting the number of pustules, and track disease progression parameters automatically (Chapter 3).

v. Identification of novel molecular markers associated with rust resistance enabling its use in marker assisted selection breeding (Chapter 4).

vi. To propose candidate genes responsible of rust susceptibility/resistance caused by *U. pisi* trough a genomic association approach (Chapter 4).

vii. To evaluate different genomic prediction models to select the more appropriate in future breeding scenarios for rust resistance (Chapter 5).

viii. To evaluate the genotype by effect interaction in different cross-validation strategies to enhance predictive abilities and accuracies in the best genomic selection models proposed (Chapter 5).

Chapter 2
Identification and Characterization of Novel Sources of Resistance to Rust Caused by *Uromyces pisi* in *Pisum* spp.

This Chapter has been published as:

Osuna-Caballero S, Rispail N, Barilli E, Rubiales D (2022) Identification and Characterization of Novel Sources of Resistance to Rust Caused by *Uromyces pisi* in *Pisum* spp. Plants 11(17):2268. https://doi.org/10.3390/plants11172268

1. Abstract

Pea rust is a major disease worldwide caused by *Uromyces pisi* in temperate climates. Only moderate levels of partial resistance against *U. pisi* have been identified so far in pea, urging for enlarging the levels of resistance available for breeding. Herein, we describe the responses to *U. pisi* of 320 *Pisum* spp. accessions, including cultivated pea and wild relatives, both under field and controlled conditions. Large variations for *U. pisi* infection response for most traits were observed between pea accessions under both field and controlled conditions, allowing the detection of genotypes with partial resistance. Simultaneous multi-trait indexes were applied to the datasets allowing the identification of partial resistance, particularly in accessions JI224, BGE004710, JI198, JI199, CGN10205, and CGN10206. Macroscopic observations were complemented with histological observations on the nine most resistant accessions and compared with three intermediates and three susceptible ones. This study confirmed that the reduced infection of resistant accessions was associated with smaller rust colonies due to a reduction in the number of haustoria and hyphal tips per colony. Additionally, a late acting hypersensitive response was identified for the first time in a pea accession (PI273209). These findings demonstrate that screening pea collections continues to be a necessary method in the search for complete resistance against *U. pisi*. In addition, the large phenotypic diversity contained in the studied collection will be useful for further association analysis and breeding perspectives.

2. Introduction

Pea (*Pisum sativum* L.) is a widely grown temperate grain legume. It is the second most cultivated legume in the world and the first in Europe, including both dry and green peas (FAOSTAT 2022). Its use extends to food and feed and represents a versatile and inexpensive protein source, bringing benefits to human health (Borges-Martínez et al. 2021; Clemente and Olias 2017; Tulbek et al. 2016). As for any other crop, pea production can be affected by a range of pests and diseases, among which pea rust has become a major concern worldwide (Rubiales et al. 2015).

Pea rust has been described to be incited by *Uromyces viciae-fabae* (Pers. de Bary) in tropical and subtropical regions (Singh et al. 2015) or by *U. pisi* (Pers.) (Wint.) in temperate areas (Barilli et al. 2009a; Emeran et al. 2005). *U. pisi* is a heteroecious macrocyclic fungus that completes its life cycle on *Euphorbia cyparissias* L. and *E. esula* L., which can grow in the vicinity of pea fields as spontaneous weeds and spread the fungal aeciospores over the crop (Pfunder and Roy 2000). When aeciospores infect pea, the uredial stage initiates a polycyclic infection, which results in the reduction in a photosynthetic area of an underdeveloped pod with yield losses up to 30 % (EPPO Standards Pea 2021).

Chemical control with fungicides is effective to control rust, but it is expensive and has environmental side effects (Emeran et al. 2011). Alternative control methods, such as application of natural substances with fungistatic effects (Barilli et al. 2017), the induction of systemic acquired resistance (Barilli et al. 2010, 2012), or agronomic practices, such as intercropping (Shtaya et al. 2021; Singh et al. 2014), are being explored but are not yet available at a commercial level. Therefore, it is important to pay attention to the inherent resistance within *Pisum* spp. diversity because the development of resistant varieties through plant breeding remains the most economical and eco-friendly approach to control foliar diseases, such rust in pea (Barilli et al. 2014). Some efforts have been achieved in that direction to identify sources of resistance to *U. pisi* and to understand the genetic basis of resistance. Large pea collections have been screened under field and controlled conditions, but complete resistance has not been found so far (Barilli et al. 2009a, 2009b). The development of a RIL population with the partially resistant *P. fulvum* accession IFPI3260 as donor allowed the detection of four QTLs related to phenotypic disease variation (Barilli et al. 2010, 2018).

The aim of this work was to expand the genetic background of *U. pisi* resistance in pea, evaluating new germplasm, including wild relatives, landraces, cultivars, and breeding lines from all over the world. The new resistant sources selected using a multi-trait index approach were characterized histologically to identify early resistance mechanisms. The components of resistance operating in each selected genotype are discussed according to their appropriate use in pea breeding programs for efficient and durable resistance to *U. pisi*.

3. Materials and Methods

3.1. *Pisum* spp. Germplasm Origin

This study used a worldwide germplasm collection containing 320 pea accessions kindly provided by USDA (Department of Agriculture, Quezon City, Philippines), JIC (John Innes Centre, Norwich, UK), CRF-INIA (Centro Nacional de Recursos Fitogenéticos, Madrid, Spain), CGN (CPRO-DLO, Wageningen, The Netherland), IPK (Gatersleben, Germany), and ICARDA (International Centre for Agricultural Research in the Dry Areas, Beirut, Lebanon). The core collection represents the *Pisum* genera in taxonomy, geographic distribution, and phenotypic variation (Additional file 1). All accessions were multiplied at the Institute for Sustainable Agriculture—CSIC at Cordoba, Spain, under field conditions before the experiments.

3.2. Pathogen Isolate and Multiplication

All experiments were performed with the *U. pisi* isolate Up-Co01 previously collected from naturally infested pea fields in Cordoba, Spain, and conserved at – 80 °C. Before use, rust spores were multiplied on susceptible pea cv. Messire under

controlled conditions (CC) to ensure availability of freshly collected spores at optimum conditions for inoculations, following the Sillero et al. 2000 procedure with modifications. For this, two-week-old Messire plants were inoculated by dusting the plants with 1 mg urediospores per pot, mixed in pure talc (1:10, v: v), and incubated for 24 h at 20 °C in complete darkness and 100 % relative humidity. Plants were then transferred to a growth chamber at 20 °C with a photoperiod of 14 h of light and 10 h of darkness and a light intensity of 148 µmol m^{-2} s^{-1}. After 2 weeks, the fresh urediospores were collected using a vacuum spore collection device, dried, and stored until inoculation assays.

3.3. Field Experiments and Data Assessments

The pea collection was phenotyped over three crop seasons (2017/2018, 2018/2019, and 2019/2020) at Cordoba, Spain (Table 3), using the rust susceptible pea cv. Messire as control check, following an alpha lattice design with three replicates. To ensure optimal germination, pea seeds were first scarified and then sown in the field by early December each year, according to local practice. The experimental unit consisted of a single 1-m long row per accession with 10 seeds per row, separated from the adjacent row by 0.7 m.

Table 3. Description of the environments of the trials for the multi-environment study during the crop cycle from December to May.

ENV	Season	Site	Soil Type	Soil pH	Organic Matter (g/110 g)	Available Phosphorus (mg/kg)	C:N Ratio	Avg T_{max} (°C)	Avg T_{min} (°C)	Avg RH (%) *	Rain (mm)
Co-18	2017–2018	37.862875, −4.791796	Vertisol	-	-	-	-	18.37	6.17	75.2	472
Co-19	2018–2019	37.864470, −4.789733	Vertisol	7.8	0.7	9.9	7.25	21.04	5.78	63.4	127
Co-20	2019–2020	37.866372, −4.787661	Vertisol	-	-	-	-	21.00	8.45	73.9	382

* Relative humidity data taken from *U. pisi* inoculation to disease severity assessment.

Plants were inoculated at mid-March to ensure high and uniform levels of rust infection. The inoculation consisted of spraying plants with an aqueous urediospores suspension (± 1.0 × 105 urediospores mL^{-1}) with Tween-20 (0.03 %, v:v) as surface-active agent after sunset to benefit from the darkness and high relative humidity of the night. Disease severity (DS) was visually estimated as the percentage of canopy covered by rust pustules 30 days after inoculation (dai) (Barilli et al. 2009b).

3.4. Controlled Condition Experiment and Assessments

Seeds of each accession were scarified and surface-sterilized for 20 min in a 20% solution of sodium hypochlorite and rinsed twice with sterile water for 20 min. Seed vernalization was induced for 3 days on wet tissue in a Petri dish at 4 °C in darkness and then shifted to 20 °C for 4 days for complete germination. Two germinated seeds per accession were sown in a 1:1 mixture of sand and peat per pot

(35 × 35 cm) to finally leave one grown plant per pot for the evaluation. Each accession was replicated once. Pots were placed in a randomized complete block design and seedlings were inoculated when the third leaf was completely expanded (±12 days after sowing). Inoculation was carried out as described above for the CC multiplication of pea rust spores on cv. Messire. Then, plants were transferred to a growth chamber at 20 °C with a photoperiod of 14 h of light and 10 h of darkness and 148 μmol m^{-2} s^{-1} of irradiance at plant canopy level. The whole experiment was repeated three times leading to the evaluation of a total of six plants per accession.

Two days after inoculation, one leaflet of the third leaf was cut from each seedling and processed for histological assessments. The rest of the plants were maintained in-tact for macroscopical observations of rust development from 7 to 14 dai by daily counting of the number of emerged pustules on a 1 cm^2 marked area of the third leaf. These daily scorings of the first rust cycle were used to calculate the time when 50% of pustules were formed (latency period, LP_{50}) and the monocyclic disease progress rate (MDPr) given by the slope of the regression line. To calculate MDPr, daily emerged pustules numbers were converted into relative pustule values expressed as the per-centage of the most susceptible cultivar in the collection (cv. Erygel-JI1210). The last count was used to determine the final number of pustules cm^{-2} (infection frequency, IF). By 14 dai, disease severity was also visually estimated as the percentage of canopy covered by rust, and infection type (IT) was assessed using the scale of Stakman et al. 1962.

3.5. Histological Assessments

The leaflet samples collected at 2 dpi were bleached on filter paper dipped in fixative solution (absolute ethanol/glacial acetic acid, 1:1, v:v) ,and then they were boiled in 0.05 % trypan blue in lactophenol/ethanol (1:2, v:v) for 10 min. Finally, they were cleared in a nearly saturated aqueous solution of chloral hydrate (5:2, w:v) to remove trypan blue from chloroplast membranes as described in Sillero and Rubiales 2002. Histological observations were made using a phase contrast Leica DM LS microscope at × 400 magnification. Assessments were based on the observation of 25 random infection units per leaflet with three independent replicated leaflets per accession. For each infection unit, the number of hyphal tips and haustoria were counted allowing estimation of the early abortion rate (colonies without haustoria). Presence or absence of host cell necrosis associated to the infection units was also noted through the detection of autofluorescence upon cell excitation by UV light. The colony size, including perimeter and area, was also determined using a Levenhuk M1400 PLUS camera and LevenhukLite software.

3.6. Data Manipulation and Statistical Analysis

The control condition (CC) and field experiment datasets were analysed separately. Control of data quality was performed individually for each trait through

graphical inspection of residuals to assess normality, homogeneity of variance, and outliers' detection. To ensure residuals normalization and variance stabilization, arcsine transformation was applied on the parameters expressed as percentages while square root transformation was performed for MDPr and IF and logarithmic trans-formation for LP_{50}. A two-way ANOVA and post-hoc Tukey test were performed for post-haustorium histological studies.

For CC traits (MDPr, IF, DSCC, IT, and LP_{50}), the experiment was analysed using a linear mixed-effect model (LMM) according to the following equation:

$$y_{ij} = \mu + \alpha_i + \tau_j + \varepsilon_{ij}$$

where yij is the trait observed value for the ith genotype in the jth replicate (i = 1, 2, … 320; j = 1, 2, … 6); αi is the random effect of the ith genotype; τj is the fixed effect of the jth replicate; and εij is the random error associated to yij.

For field data where multi-environment trials were conducted, the linear model with interaction effect was used to analyse data:

$$y_{ijk} = \mu + \alpha_i + \tau_j + (\alpha\tau)_{ij} + \gamma_{jk} + \varepsilon_{ijk}$$

where yijk is the trait observed value in the kth block of the ith genotype in the jth environment (i = 1, 2, … 320; j = 1, 2, 3; k = 1, 2, 3); μ is the grand mean; αi is the effect of the ith genotype; τj is the effect of the jth environment; (ατ)ij is the interaction effect of the ith genotype with the jth environment; γjk is the effect of the kth block within the jth environment; and εijk is the random error. In this case, the genotype effect, and the interaction genotype × environment (G × E) effect was selected as random effects and environment and replicates in environments were selected as fixed effects in the model.

In both models, the restricted maximum likelihood (REML) procedure was con-ducted to estimate the variance components of the linear mixed model to compute the predicted means (best linear unbiased prediction—BLUP) genotype values according to DeLacy et al. 1996. BLUPs were used as phenotypic data for subsequent correlations and genotype selection assessments. Variance components were also estimated in terms of coefficient of variation, following the formula:

$$CV = \left(\sqrt{\hat{\sigma}^2}/\mu\right) \times 100$$

where σ2 is the variance and μ is the grand mean. The broad-sense heritability (H2) on an entry mean basis in all growing conditions was estimated following the Toker (2004) study and calculated as:

$$H^2 = \frac{\hat{\sigma}_g^2}{\hat{\sigma}_g^2 + \hat{\sigma}_i^2 + \hat{\sigma}_e^2}$$

where σg2 is the genotypic variance, σi2 is the genotype-by-environment interaction variance, and σe2 is the residual variance.

To select rust resistant accessions through traits evaluated under controlled conditions, multi-trait genotype-ideotype distance (MGIDI) (Olivoto and Nardino 2021), Smith-Hazel (Smith 1936), and FAI-BLUP (Rocha et al. 2018) indexes were performed. For field data, the Linn and Binns superiority measures were assessed using a non-parametric method for genotype selection (Lin and Binns 1988). Every index ranks the accession based on their rust resistance level, and the selected resistant genotypes were those accessions that appeared in the best positions over all four indices.

All data analyses were performed in R Core Team (2021) with the "metan" (Olivoto and Lúcio 2020) package for fit-ting LM/LMM interpretation and "ggplot2" (Wickham 2016) package for visualization.

4. Results

4.1. Phenotypic Response, Variance Components and Broad-Sense Heritability

All accessions showed rust symptoms under both controlled and field conditions albeit with variable intensities. A large phenotypic variation was observed in all trials for all traits, although accessions with moderate levels of disease symptoms were the most frequent in revealing a positive skewness, except for IT, as most accessions showed well-formed pustules (IT = 4; Figure 3g). The susceptible check cv. Messire showed a DS under field conditions of 28, 35, and 50 in 2018, 2019, and 2020, respectively, which was in all cases higher than the total mean of these environments (Figure 3).

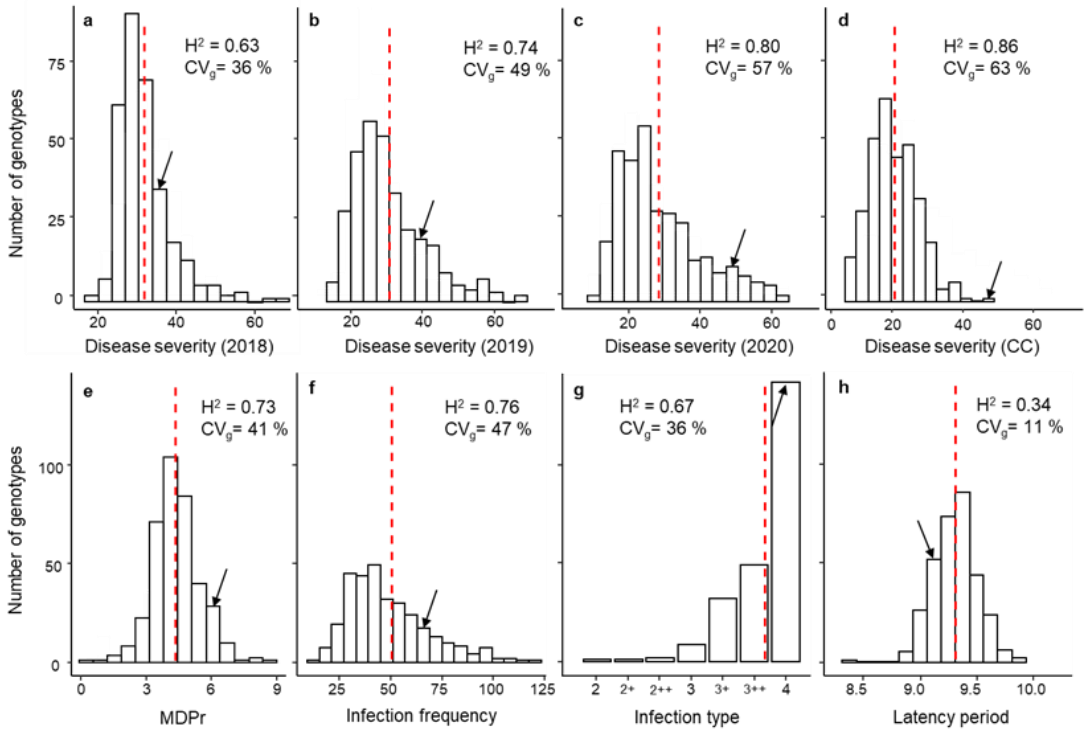

Figure 3. Phenotypic variation in rust response adjusted means (BLUPs) among 320 pea accessions after infection with *U. pisi*. (a–d) show the DS plants under field conditions during 2018, 2019, and 2020 seasons and DS seedlings under controlled conditions (CC), respectively. (e–h) show seedlings under CC, the monocyclic disease progress rate (MDPr), infection frequency (IF), infection type (IT), and latency period (LP50), respectively. Genotypic coefficient of variation (CVg) and heritability (H2) are also shown. Dashed red lines and black arrows indicate the overall mean and where the susceptible control Messire is located, respectively.

Under CC, cv. Messire showed higher values than the total mean for MDPr, IF, IT, and DS CC and lower values for LP50. These values were far from the min and max value, showing a range from incomplete resistant to highly susceptible accessions. The lowest IT value was observed in accession PI273209, with moderate levels of macroscopically visible necrosis associated with rust pustules (IT = 2), whereas all other accessions displayed a fully compatible interaction (IT > 3, with IT = 4 being the most frequent).

The likelihood ratio test revealed significant difference between genotypes for all traits ($p < 0.05$). In CC, 63 % of the phenotypic variance of DS was due to genetic differences between accessions. This trait also showed the highest broad-sense heritability ($H^2 = 0.86$). By contrast, genotypic effect explained only 11.2 % of the LP_{50} variance suggesting the low suitability of this parameter to predict the rust susceptibility/resistance response of a genotype. Under field conditions, the maximum genotypic effect was explained in 2020 with a 57 % of the phenotypic

variance and a broad-sense heritability of 0.80 (Figure 3). By contrast, the lowest genotypic effect was detected in 2018 explaining only 36 % of the phenotypic variance and a broad-sense heritability of 0.63 (Figure 3).

These variations between environments are also affected by genotype x environment interactions. The minimum interaction coefficient was detected for 2019 with 11 % and peaks in 2020 with 27 % (Table 4). In most cases, the accuracy of the LMM applied in CC and field conditions is >75 %, except for LP_{50}.

Table 4. Statistics performed for disease components studied in CC and under field conditions. Arithmetic mean ± standard error (SE), minimum and maximum values, skewness, accuracy of the selection in LMM applied, and their likelihood ratio test for genotype effect (LRT). The percentage of genotype-by-environment interaction coefficient of variation (CV_i) is also shown with a significance $p < 0.01$.

	Trait	Mean ± SE	Skewness	Min	Max	Accuracy	LRT	CV_i
Controlled Conditions	**MDPr**	5.7 ± 0.01	0.28	2.66	8.8	0.87	280	-
	IF	50.3 ± 1.19	2.33	1.00	387.0	0.87	264	-
	IT	3.8 ± 0.01	−2.05	2.00	4.0	0.82	180	-
	LP_{50}	9.3 ± 0.02	−0.02	6.71	12.6	0.58	11	-
	DS_{CC}	20.1 ± 0.29	0.53	2.00	60.0	0.93	549	-
Field Season	**DS_{2018}**	27.5 ± 0.49	1.73	2.00	60.0	0.79	111	27
	DS_{2019}	26.2 ± 0.56	1.06	1.00	65.0	0.86	205	11
	DS_{2020}	28.8 ± 0.59	0.95	1.50	65.0	0.89	299	17

4.2. Trait Correlations

Phenotypic correlations were calculated for each trait in each experimental condition. DS in the various field seasons were significantly correlated ($p \approx 0.5$, $p < 0.001$) (Table 5). Adult plant responses in the field (DS in the various season) were significantly correlated with seedling responses under controlled conditions, with IF showing higher correlations, followed by MDPr, DS, and IT. On the contrary, LP_{50} in seedlings was poorly correlated with DS in the field, although it was correlated with DS in seedlings ($p = -0.20$, $p < 0.01$).

The strongest positive correlation was detected between MDPr and IF under CC ($p = 0.96$, $p < 0.001$) while the strongest negative correlation was detected between MDPr and LP_{50} ($p = -0.21$, $p < 0.01$) under controlled conditions.

4.3. Selected Rust Resistant Accessions

Grouping accession according to the species and subspecies they belong to did not reveal a group of accessions with higher level of resistance, due to the large variance within groups (data not shown). In addition, the interaction between these factors and the environment hampers direct selection of most resistant accessions (Additional file 2).

Table 5. Pearson (*p*) correlation coefficient between traits evaluated under field and controlled conditions and calculated from adjusted mean (BLUPs) values from the 320 pea accessions.

	Field Conditions			**Controlled Conditions**			
	DS_{2018}	DS_{2019}	DS_{2020}	MDPr	IF	LP_{50}	DS_{CC}
Field conditions							
DS_{2019}	0.46***						
DS_{2020}	0.46***	0.55***					
Controlled conditions							
MDPr	0.21***	0.44***	0.39***				
IF	0.21***	0.46***	0.40***	0.96***			
LP_{50}	−0.04	0.01	−0.04	−0.21**	−0.05		
DS	0.14*	0.28***	0.30***	0.58***	0.57***	-0.20**	
IT	0.18*	0.29***	0.25***	0.45***	0.42***	-0.20**	0.33***

* $p < 0.05$, ** $p < 0.01$, *** $p < 0.001$.

Therefore, multi-trait indexes were applied to the dataset to drive selection of resistant accessions. This approximation points to several pea accessions that belong to different *Pisum* taxa and origin. Based on this multi-trait index selection of the nine most resistant accessions, the three most susceptible ones and three with intermediate levels were selected (Table 6).

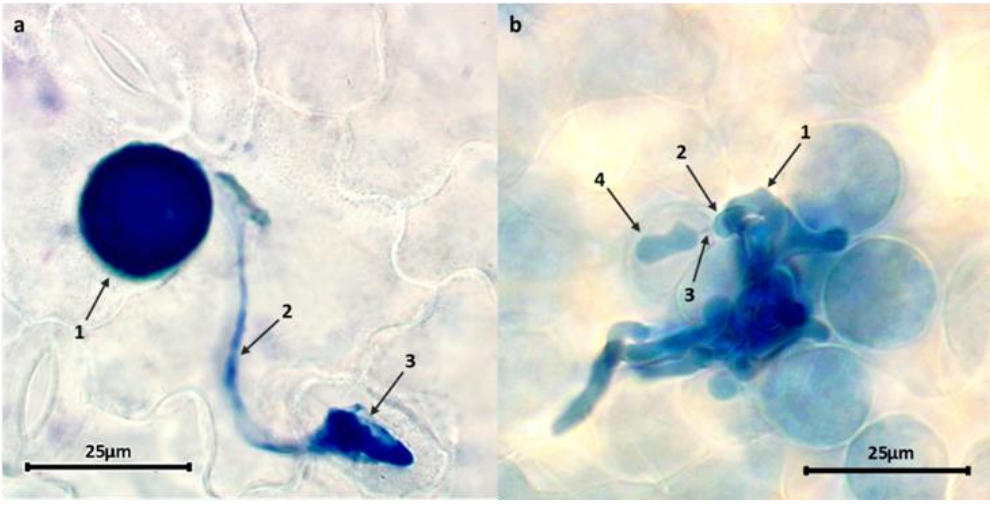

Figure 4. *U. pisi* structures infecting pea cells at 48 hpi. (a) Early rust infection event: a germinated urediospore (1) develops a germ tube (2) that differentiates an appressorium over a stoma (3). (b) A colony with hyphae growing between mesophyll cells (1) differentiates an haustoria mother cell (HMC) (2) which invaginates into the mesophyll cell via a neckband (3) forming an haustorium (4).

Table 6. Selected accessions representing three rust response levels (partial resistant, intermediate, and highly susceptible) through multi-trait index approach (FAI-BLUP, MGIDI, Smith-Hazel (SH), and Lin-Bin (LN), respectively).

Rust Level	Bank Code	Species	Origin	DS_{field} (%)	DS_{CC} (%)	Ranking Indices (1-320)			
						FAI-BLUP	MGIDI	SH	LIN
Resistant	CGN10206	*P. sativum* subsp. *elatius*	Unknown	3.0	5.2	1	1	1	4
	CGN10205	*P. sativum* subsp. *elatius*	Turkey	6.0	5.5	2	2	2	1
	PI273209	*P. sativum* subsp. *elatius*	Russia	3.3	3.0	3	3	3	2
	IFPI3260	*P. fulvum*	Syria	4.3	6.7	4	4	6	3
	BGE004710	*P. sativum* subsp. *sativum*	Portugal	7.7	6.5	7	8	7	10
	JI199	*P. sativum* subsp. *elatius*	Israel	5.0	6.5	5	5	4	5
	JI198	*P. sativum* subsp. *elatius*	Israel	5.8	11.6	6	6	8	6
	PI347321	*P. sativum*	India	11.0	4.5	9	9	10	11
	JI224	*P. fulvum*	Israel	4.3	10.0	10	10	12	9
Intermediate	PI347372	*P. sativum*	India	16.3	16.1	155	155	162	150
	PI143483	*P. sativum*	Azerbaijan	17.0	22.1	160	160	167	156
	PI324705	*P. sativum*	France	15.7	21.0	175	175	184	169
Susceptible	PI162910	*P. sativum*	Paraguay	34.5	27.6	318	318	318	320
	PI204667	*P. sativum* subsp. *sativum*	Netherland	30.0	45.8	319	319	319	318
	JI1210	*P. sativum* subsp. *sativum*	France	40.7	28.6	320	320	320	315

4.4. Pea Resistance Mechanisms against *U. pisi*

To complement the macroscopic characterization of the pea panel in response to *U. pisi* inoculation, the selected accessions were further analysed at histological level. The components of resistance of these selected accessions are presented in Table 7.

As expected, the most resistant accessions showed lower levels of infection with significantly lower values for all macro- and microscopical traits. No differences among accessions were observed at early stages of the infection (Figure 4a), with no significant differences for spore germination or appressoria formation. Post-

appressoria infection events (Figure 4b), including infection unit area, infection unit perimeter, number of hyphal tips, and haustoria, are lower in resistant accessions than in susceptible ones ($p < 0.05$). By contrast, infection unit area, infection unit perimeter, and hyphal tips were not significantly different between moderately and highly susceptible accessions. However, there is a significant difference between moderately and highly susceptible accessions in terms of haustoria number/infection unit.

Significant variation was also observed between partially resistant and susceptible accessions in terms of early abortion (infection units forming at least in HMC in contact with a mesophyll cell but failing to form any haustoria) not associated with host cell necrosis. Such early abortion was particularly high (over 23%) in JI198, JI199, and IFPI3260, followed by JI224, CGN10205, CGN10206, and PI347372 (over 12%) (Table 7). No or negligible levels of host cell necrosis were observed by 48 hpi on any of these early aborted colonies. Host cell necrosis was also absent or low (< 7 %) in established colonies of all studied accessions, except PI273209, where it reached 20 %, (Figure 5, Table 7); what was macroscopically visible as small pustules surrounded by necrotic halo (IT = 2) did not prevent sporulation but hampered it, resulting in incomplete resistance based on late acting hypersensitivity (Figure 6).

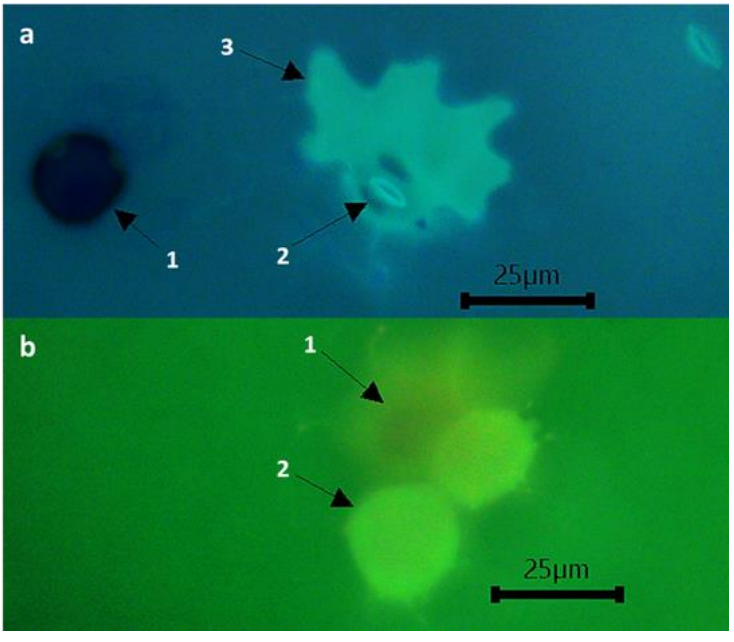

Figure 5. Different cells attacked by *U. pisi* colonies in PI273209 accession: (a) Epidermic tissue visualized with fluorescent blue filter at 48 h post inoculation showing a germinated urediospore (1), the stoma (2), and a dying epidermal cell (3); (b) Mesophyll tissue visualized with fluorescent green filter showing the substomatal space (1) and two dying mesophyll cells (2).

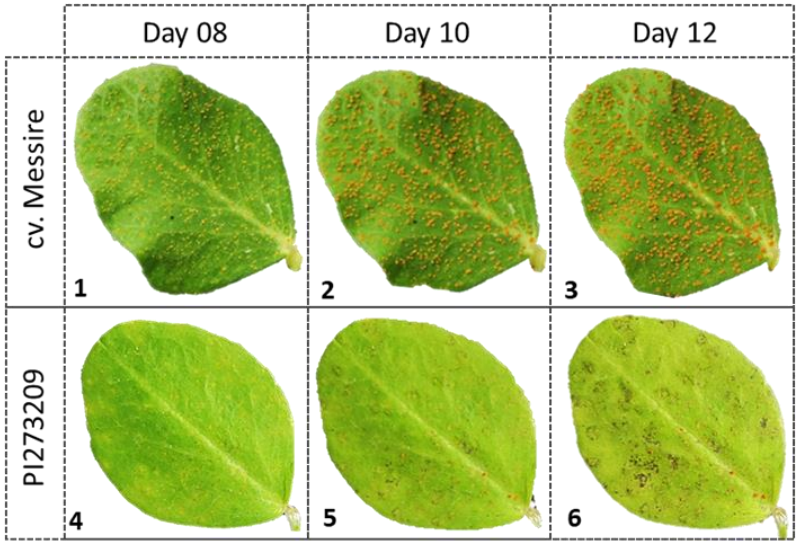

Figure 6. Rust symptoms progression in cv. Messire and PI273209 accession leaves. (1–3) show the macroscopic rust progression in cv. Messire at 8, 10, and 12 dpi, respectively. (4–6) show the macroscopic rust progression in PI273209 accession at 8, 10, and 12 dpi, respectively.

Table 7. Microscopic evaluation of *U. pisi* colonies 48 h post-inoculation in the selected genotypes. Values, per column, followed by different letters differ significantly at $p < 0.05$.

Bank Code	DS_{CC} (%)	IT	Infection Unit Area (µm²)	Infection Unit Perimeter (µm)	No. Hyphal Tips/ infection Unit	Early Abortion (%)	No. Haustoria/ Established Colony	Established Colonies Associated with Host Cell Necrosis (%)
PI347321	4.5 ^{d}	3++	490.8 ^{c}	184.0 ^{d}	3.3 ^{c}	8.3 ^{c}	1.9 ^{ab}	0 ^{d}
JI224	10.0^{bc}	3++	792.5 ^{b}	302.3 ^{b}	5.8 ^{ab}	12.5 ^{b}	1.7 ^{a}	2.5 ^{c}
BGE004710	6.5 ^{c}	3	592.6 ^{bc}	211.6 ^{cd}	3.6 ^{c}	10.6 ^{c}	1.6 ^{a}	4.3 ^{bc}
PI273209	3.0 ^{d}	2	784.3 ^{b}	277.5 ^{b}	5.4 ^{b}	10.0 ^{c}	1.9 ^{ab}	20.0 ^{a}
JI198	11.6 ^{bc}	3	941.2 ^{ab}	374.3 ^{a}	6.8 ^{a}	23.7 ^{a}	1.8 ^{ab}	0 ^{d}
JI199	6.5 ^{c}	3	765.0 ^{b}	270.3 ^{bc}	5.0 ^{b}	23.3 ^{a}	1.6 ^{a}	6.7 ^{b}
CGN10205	5.5 ^{cd}	3	545.4 ^{c}	195.7 ^{d}	3.8 ^{c}	13.3 ^{b}	1.6 ^{a}	0 ^{d}
CGN10206	5.2 ^{cd}	3	606.4 ^{bc}	240.2 ^{c}	4.8 ^{bc}	13.3 ^{b}	1.5 ^{a}	0 ^{d}
IFPI 3260	6.7 ^{c}	4	497.5 ^{c}	190.8 ^{d}	3.7 ^{c}	23.3 ^{a}	1.7 ^{a}	0 ^{d}
PI143483	22.1 ^{ab}	4	1170.7 ^{a}	360.5 ^{ab}	6.1 ^{ab}	0 ^{d}	2.3 ^{b}	0 ^{d}
PI347372	16.1 ^{b}	4	1074.9 ^{a}	356.5 ^{ab}	7.7 ^{a}	12.9 ^{b}	2.3 ^{b}	0 ^{d}
PI324705	21.0 ^{ab}	4	662.6 ^{b}	222.6 ^{c}	3.8 ^{c}	0 ^{d}	2.3 ^{b}	0 ^{d}
PI162910	27.6 ^{ab}	4	1202.0 ^{a}	395.7 ^{a}	7.9 ^{a}	0 ^{d}	3.4 ^{c}	0 ^{d}
PI204667	45.8 ^{a}	4	1024.8 ^{a}	334.0 ^{b}	6.2 ^{ab}	0 ^{d}	3.5 ^{c}	0 ^{d}
JI1210	28.6 ^{ab}	4	1006.1 ^{a}	292.0 ^{b}	5.9 ^{ab}	0 ^{d}	3.2 ^{c}	0 ^{d}

5. Discussion

Pea rust, caused by *U. pisi* and *U. viciae-fabae*, is a major disease responsible for serious yield losses worldwide (Rubiales et al. 2015). *U. pisi* is the principal agent causing pea rust in temperate regions (Emeran et al. 2008), while *U. viciae-fabae* is more widely distributed in tropical and sub-tropical areas (Anil-Kumar et al. 1994). Only moderate levels of resistance against *U. pisi* have been identified so far (Barilli et al. 2009a).

In this study, we macroscopically analysed the response to rust caused by *U. pisi* in a worldwide *Pisum* spp. collection of 320 accessions, meticulously selected to ensure a wide range of phenotypic and genetic variation ranges. The variability found within the collection under field conditions was moderately correlated between seasons supporting the strong influence of the weather conditions and the genotype x environment interactions as suggested previously for pea rust (Das et al. 2019; Singh et al. 2012). Rust DS was higher in 2020, which was characterized by a climate more favourable to *U. pisi* development due to a higher mid temperature and higher relative humidity (More et al. 2019) favouring disease infection, in agreement with previous studies on *U. viciae-fabae* (More et al. 2020; Negussie et al. 2005). Infection in 2018 were weakly correlated with traits measured under controlled conditions (CC) while field data recorded in 2019 and 2020 seasons were characterized by more favourable climates, which were better correlated with these traits. Correlation in adult plants and seedlings in response to rust disease can be affected not only by temperature and relative humidity but also by the polycyclic effect over the host and leaf age, which can express or not express the genes behind the resistance mechanism. Effect of temperature and leaf age has been well studied (Fondevilla et al. 2013) in other pea foliar disease, such as powdery mildew, but it is still unknown for rust.

Variability found in this collection according to disease severity of seedlings in CC to rust was higher than other studies performed in lathyrus (Vaz Patto and Rubiales 2009) and vetch (Rubio and Rubiales 2021) against *U. pisi* and comparable to pea studies in the same pathosystem where check cultivar Messire showed similar DS (~50%) (Barilli et al. 2009a). The screening techniques are well established and the *U. pisi*–legume pathosystem response confirmed the reproducibility of the method described by Sillero et al. 2006. All traits assessed under controlled conditions showed moderate to high positive correlation between them, except LP_{50}, which showed a negative one, in agreement with previous studies (Barilli et al. 2009a). Latency period of *U. pisi* development increases with the quantitative resistance level of pea genotypes similarly to other biotrophic pathogens (Précigout et al. 2020). Accordingly, it was negatively correlated with MDPr, IT, and DS. However, final IF was not correlated with the latency period in our collection, suggesting that the final number of pustules emerging on a leaf is an independent

event controlled by mechanisms distinct from those controlling the incubation period and the pre-sporulation symptoms involved in the latency period (Dehghani and Moghaddam 2004). In addition, latency period in plant diseases is very sensitive to variations in disease ex-pressions, including those due to phenotypic plasticity (Suffert and Thompson 2018), defined as the ability of in-dividual genotypes to produce different phenotypes when exposed to different environmental conditions (Pigliucci et al. 2006). A study carried out in wheat rust caused by *Puccinia triticina* revealed that, even in a clonal lineage population, significant differences were present in the latency period within identical pathotypes (Pariaud et al. 2012).

In this study, resistance based on DS reduction without host cell necrosis was the most common response of the collection under field and controlled conditions for adult plants and seedlings, respectively. This incomplete resistance not associated with hypersensitive response is known as partial resistance. It is characterized by a decrease in IF and DS while IT is high (Sillero et al. 2012), which means that plants harbour a lower number of pustules but those that do form develop normally. These components of quantitative resistance have demonstrated they are more durable than major gene resistance on average (Mundt 2014), so they are considered desirable traits for an effective field rust resistance, also in other crops, such as cereals (Rosewarne et al. 2013; Singh et al. 2008, 2011). The partial resistance reported here has been observed previously in pea against both *U. viciae-fabae* and *U. pisi* (Barilli et al. 2009a, 2009c). We support other studies in the identification of PI347321 and IFPI3260 accessions as partially resistant (Barilli et al. 2009a). In addition, we have identified novel sources of partial resistance in the accessions JI224, BGE004710, JI198, JI199, CGN10205, and CGN10206. The level of partial resistance of two of these accessions, JI224 and JI198, was similar to the highest level of resistance previously detected (DS ~ 10 %) (Barilli et al. 2009a). The additional resistant accessions, BGE004710, JI 199, CGN10205, and CGN10206, had a slightly higher level of partial resistant with DS < 7 %. Those results expand the genetic source of resistance by providing new accessions with levels of partial resistance similar to the previously described IFPI3260, which was to date the most resistant accession available against *U. pisi*.

On the one hand, there is only one *P. sativum* subsp. *sativum* accession described with high partial resistance levels, BGE004710. Its origin is assigned to Mogadouro in Portugal, according to its passport, where the incidence of rust caused by *U. pisi* and *U. viciae-fabae* is elevated (Talhinhas et al. 2019). Due to this taxonomy, its potential use to transfer the mi-nor genes conferring the partial resistance to pea cultivars in temperate climates is high. On the other hand, it is also possible to use other wild relatives and landraces described here as donor of partial resistance, since crosses between wild pea species and subsp. *sativum* cultivars have been already explored (Kosterin et al. 2019). In fact, it is known that wild pea relatives from *P. fulvum* work as a donor of resistance to biotic stresses, such as insect,

diseases, or weeds (Coyne et al. 2020). *P. sativum* subsp. *elatius* var. *elatius* has been used for breeding purposes increasing the nutritional value of peas, without being exploited as a source of resistance to biotic stresses so far (Clemente et al. 2015). In this context, the additional partial resistance sources detected here belonging to *P. sativum* subsp. *sativum* and *P. sativum* subsp. *elatius* var. *elatius* could allow the localization of new genome regions associated with rust resistance in pea, in addition to those currently described in the *P. fulvum* (Barilli et al. 2018). Recently, a panel of *Lathyrus sativus* inoculated with *U. pisi* revealed novel loci behind partial resistance mechanisms using an association mapping approach (Martins et al. 2022). Similarly, the present pea panel would be valuable to expand the genetic bases of resistance for future breeding of rust resistant pea.

To integrate all traits scored in controlled and field conditions a multi-trait index approach was applied to differentiate accessions. Since the first index was proposed by Smith 1936, multi-trait selection indices are established strategies to select superior genotypes in plant breeding and provide the breeder with an objective rule for evaluating and selecting several traits simultaneously (Cerón-Rojas and Crossa 2022). However, the Smith-Hazel index can be affected by multicollinearity problems, providing erroneous conclusions and inefficient conservation measures (Prunier et al. 2015). To offset this possibility, we applied in parallel two additional multi-trait indices, MGIDI and FAI-BLUP, that have been established for plant breeding selection and are free from weighting coefficients and multicollinearity issues (DeLacy et al. 1996; Olivoto and Nardino 2021). In addition, a non-parametric index that includes the genotype x environment interaction was used to select the most resistant pea genotypes to *U. pisi* in the field (Lin and Binns 1988). The results obtained from these indexes are quite similar in the cases of FAI-BLUP and MGDI, while SH and LIN provide different rankings of the superior genotypes. Even if one of the index criteria performed an erroneous selection, this was compensated by the other three indices supporting the usefulness of applying simultaneous indices. Based on this methodology the nine best-performing pea accessions in the four indices were selected and used to assay the underlying resistance mechanisms to *U. pisi* infection histologically.

In the microscopical study, the variation in urediospores germination and appressoria formation over stoma did not affect rust severity, suggesting that the resistance mechanisms took place after formation of substomatal vesicles (Niks and Rubiales 2002; Singh et al. 2014). One of the most efficient post-appressoria resistance mechanisms is the early abortion of colonies that failed to form any haustoria in mesophyll cells. Here, we detected a high proportion of early colony abortion in the resistant accessions JI198, JI199, and IFPI3260. Histological and biochemical studies in pea rust suggested early abortive colonies are explained by a physical barrier to successful infection due to a lignification process in the mesophyll cells around the infection unit (Barilli et al. 2012; Kushwaha et al. 2016). Additional

assessments are currently underway to confirm the involvement of host cell wall strengthening in these accessions. When this first mechanism failed and the first haustoria mother cells develop a haustorium into mesophyll cell, a second resistance mechanism may impede penetration of secondary hyphae, reducing the number of haustoria per infection unit and, therefore, decreasing the colony size and the number of hyphal tips. All selected accessions show some degree of this penetration resistance, which was particularly visible for IFPI3260, BGE004710, and PI347321, showing the smallest infection unit size and hyphae number. A similar resistance mechanism had been found in pea–rust studies against *U. viciae-fabae* (Barilli et al. 2009c) and *U. pisi* (Barilli et al. 2009a) and in another legume–rust pathosystems (Mundt 2014; Rubiales et al. 2011; Rubiales and Moral 2004).

Hypersensitive response (HR) is another post-appressorium formation mechanism associated with disease resistance. HR has been described previously against *U. viciae-fabae* in some legume crops, such lentil (Negussie et al. 2012; Rubiales et al. 2013) and faba bean (Adhikari et al. 2021; Sillero and Rubiales 2002), although it is not the most common resistance mechanism against rust (Sillero and Rubiales 2002; Stavely 1989). Here, low levels of hypersensitive reaction to U. pisi infection were observed in accessions JI224, BGE004710, and JI199 showing less than 7 % of infection units associated with cell death but revealing a compatible reaction with high infection type (IT = 3++, 3 and 3, respectively). On the contrary, PI273209 that displayed a considerable percentage of necrotic mesophyll cells (20 %) showed an incomplete reaction associated with macroscopically visible necrosis (IT = 2). In addition, this accession also showed non-hypersensitive resistance supported by histological results, reducing hyphal growth, and hampering haustorium formation resulting in reduced disease severity despite some well-formed pustules. These observations indicate that a combination of both hypersensitive and non-hypersensitive resistance operates in PI273209 against U. pisi, but that the early abortion of colonies is not associated with cell death. This mechanism reveals that non-hypersensitive reaction can occur before and after haustoria formation, but HR only takes place after haustoria formation. This type of incomplete resistance has been described as “late acting” hypersensitive rust resistance, and it allows some haustoria failing to form due to hypersensitive cell death but others forming successfully (Rubiales and Khazaei 2022). Incomplete resistance associated with HR has been reported before in pea against *U. pis*i or *U. viciae-fabae*. The use of fluorescence microscopy and digital image technology was particularly useful to study these resistance components, allowing the detection of necrotic host cells and precisely measuring the colony area and perimeter similar to Sillero and Rubiales 2002. In other legume–rust pathosystems, this HR type has been described as monogenic, allowing the identification of genes Uvf-1, Uvf-2, and Uvf-3 conferring hypersensitive resistance against *U. viciae-fabae* in faba bean (Avila et al. 2003; Ijaz et al. 2021) and gene Rpp2 conferring hypersensitive resistance against *Phakopsora*

pachyrihizi in soybean (Yu et al. 2015). Consequently, future studies are needed to determine the genetic inheritance behind this resistance mechanism that will complement the actual genetic basis conferred by QTL's *UpDSII*, *UpDSIV*, and *UpDSIV.2*, responsible for the genetic variance in partial resistance caused by *U. pisi* in pea wild relatives (Barilli et al. 2018).

In conclusion, this study allowed the identification of new resistance sources from a wide collection of pea accessions and confirmed the importance of crop core collection to identify traits of interest. In addition to identifying additional sources of partial resistance with a similar level to the highest previously described resistant accessions, we identified a moderate level of late-acting HR in one of our accessions, which had never been described before in the pea—*U. pisi* pathosystem. Including this accession, together with the additional sources of partial resistant in our breeding programs, should broaden the genetic bases of resistance, which is key for a more durable resistance. In addition, these novel resistance sources can be the base for further studies to establish the genetic, biochemical, and molecular nature of rust resistance in pea.

6. Additional files

Additional file 1. Accession list including bank code, bank origin, taxonomy, common name, germplasm origin and material type.

Bank code	Bank origin	Taxonomy	Common Name	Germplasm origin	Material type
PI 109865	USDA	*P. sativum* L.	Arvejas Amarillas	Venezuela	Landraces
PI 117910	USDA	*P. sativum* L.	Ervilha Ana	Brazil	Cultivar
PI 140297	USDA	*P. sativum* subsp. *sativum*	No. 6192	Iran	Landraces
PI 142442	USDA	*P. sativum* L.	Alberjon	Peru	Cultivar
PI 142774	USDA	*P. sativum* L.	G 1704	Mexico	Landraces
PI 142776	USDA	*P. sativum* L.	G 1705	Mexico	Landraces
PI 142776	USDA	*P. sativum* L.	G 1705	Mexico	Landraces
PI 143483	USDA	*P. sativum* L.	No. 7351	Azerbaijan	Landraces
PI 143484	USDA	*P. sativum* L.	Cpi 135298	Azerbaijan	Landraces
PI 143486	USDA	*P. sativum* L.	No. 7790	Iran	Landraces
PI 153351	USDA	*P. sativum* L.	Arvejas Verdes	Ecuador	Landraces
PI 162568	USDA	*P. sativum* L.	Orgullo Del Mercada	Argentina	Cultivar
PI 162692	USDA	*P. sativum* L.	Cuarentona	Argentina	Cultivar
PI 162693	USDA	*P. sativum* L.	Ojo Negro	Argentina	Cultivar
PI 162693	USDA	*P. sativum* L.	Ojo Negro	Argentina	Cultivar
PI 162910	USDA	*P. sativum* L.	L.P. No. 7	Paraguay	Landraces
PI 164568	USDA	*P. sativum* L.	Patani	India	Landraces
PI 166082	USDA	*P. sativum* subsp. *sativum*	Matar	India	Landraces
PI 195405	USDA	*P. sativum* L.	Quezaltenango	Guatemala	Landraces
PI 203065	USDA	*P. sativum* L.	G 6821	Finland	Landraces
PI 204305	USDA	*P. sativum* L.	Collegian	Australia	Cultivar
PI 204667	USDA	*P. sativum* subsp. *sativum* var. *sativum*	Stijfstro	Netherland	Cultivar
PI 220175	USDA	*P. sativum* L.	No. 150	Afganistan	Landraces
PI 220673	USDA	*P. sativum* L.	Moshong	Afganistan	Landraces
PI 222069	USDA	*P. sativum* L.	Moshong	Afganistan	wild
PI 234262	USDA	*P. sativum* L.	Carlon	USA	Cultivar
PI 254625	USDA	*P. sativum* L.	Kellerva	Finland	Landraces
PI 254626	USDA	*P. sativum* L.	Lima	Australia	Cultivar
PI 261678	USDA	*P. sativum* L.	Col. No. D-237	Netherland	Landraces
PI 262189	USDA	*P. sativum* L.	Big Pea	Costa Rica	Landraces
PI 266069	USDA	*P. sativum* L.	Line No. 110	Sweden	breeding lines
PI 269760	USDA	*P. sativum* subsp. *sativum* var. *arvense* (L.) Poir.	G 16701	UK	breeding lines

Bank code	Bank origin	Taxonomy	Common Name	Germplasm origin	Material type
PI 269763	USDA	*P. sativum* subsp. *jomardii* (Schrank) Kosterin	Aa86	UK	Landraces
PI 269786	USDA	*P. sativum* L.	Aa96	UK	Landraces
PI 272143	USDA	*P. sativum* subsp. *thebaicum*	Thebaicum Ruby	Germany	Landraces
PI 272151	USDA	*P. sativum* L.	Uniflorum	Germany	Landraces
PI 272153	USDA	*P. sativum* L.	Hiemale	Greece	Landraces
PI 272156	USDA	*P. sativum* L.	Hiemale	Greece	Landraces
PI 280621	USDA	*P. sativum* L.	Amplissimo Spartanec	Rusia	Landraces
PI 280623	USDA	*P. sativum* L.	Amplissimo Pulavskij	Poland	Landraces
PI 306592	USDA	*P. sativum* L.	G 19029	Hungary	Landraces
PI 312136	USDA	*P. sativum* L.	Alberga	Guatemala	Landraces
PI 319373	USDA	*P. sativum* L.	Chicharo Serrano	Mexico	Landraces
PI 326194	USDA	*P. sativum* L.	Col. No. 22340	Mexico	Landraces
PI 343326	USDA	*P. sativum* L.	G 18456	USA	Landraces
PI 343329	USDA	*P. sativum* L.	G 18459	USA	Landraces
PI 343935	USDA	*P. sativum* L.	6922	Ethiopia	Landraces
PI 343962	USDA	*P. sativum* L.	22662	Turkey	wild
PI 343965	USDA	*P. sativum* L.	22706	Turkey	Landraces
PI 343965	USDA	*P. sativum* L.	22706	Turkey	Landraces
PI 343969	USDA	*P. sativum* subsp. *sativum* var. *sativum*	Araka	Turkey	Landraces
PI 343981	USDA	*P. sativum* subsp. *sativum* var. *sativum*	22654	Turkey	Landraces
PI 343984	USDA	*P. sativum* subsp. *sativum*	22712	Turkey	Landraces
PI 343993	USDA	*P. sativum* subsp. *sativum* var. *arvense* (L.) Poir.	22652	Turkey	Landraces
PI 347282	USDA	*P. sativum* L.	Plp 11	India	Landraces
PI 347316	USDA	*P. sativum* L.	Plp 68	India	Landraces
PI 347317	USDA	*P. sativum* L.	Plp 71	India	Landraces
PI 347319	USDA	*P. sativum* L.	Plp 73	India	Landraces
PI 347321	USDA	*P. sativum* L.	Plp 88	India	Landraces
PI 347323	USDA	*P. sativum* L.	Plp 89	India	Landraces
PI 347326	USDA	*P. sativum* L.	Plp 93	India	Landraces
PI 347328	USDA	*P. sativum* L.	Plp 99	India	Landraces
PI 347330	USDA	*P. sativum* L.	Plp 102	India	Landraces
PI 347332	USDA	*P. sativum* L.	Plp 104	India	Landraces
PI 347333	USDA	*P. sativum* L.	Plp 105	India	Landraces
PI 347334	USDA	*P. sativum* L.	Plp 109	India	Landraces
PI 347335	USDA	*P. sativum* L.	Plp 113	India	Landraces
PI 347336	USDA	*P. sativum* L.	Plp 118	India	Landraces
PI 347338	USDA	*P. sativum* L.	Plp 126	India	Landraces
PI 347342	USDA	*P. sativum* L.	Plp 154	India	Landraces
PI 347343	USDA	*P. sativum* L.	Plp 156	India	Landraces
PI 347347	USDA	*P. sativum* L.	Plp 173	India	Landraces
PI 347348	USDA	*P. sativum* L.	Plp 182	India	Landraces
PI 347356	USDA	*P. sativum* L.	Plp 218	India	Landraces
PI 347357	USDA	*P. sativum* L.	Plp 219	India	Landraces
PI 347359	USDA	*P. sativum* L.	Plp 222	India	Landraces
PI 347366	USDA	*P. sativum* L.	Plp 266	India	Landraces
PI 347367	USDA	*P. sativum* L.	Plp 268	India	Landraces
PI 347370	USDA	*P. sativum* L.	Plp 278	India	Landraces
PI 347372	USDA	*P. sativum* L.	Plp 297	India	Landraces
PI 347373	USDA	*P. sativum* L.	Plp 301	India	Landraces
PI 347374	USDA	*P. sativum* L.	Plp 303	India	Landraces
PI 347375	USDA	*P. sativum* L.	Plp 304	India	Landraces
PI 347383	USDA	*P. sativum* L.	Plp 316	India	Landraces
PI 347385	USDA	*P. sativum* L.	Plp 320	India	Landraces
PI 347388	USDA	*P. sativum* L.	Plp 330	India	Landraces
PI 347389	USDA	*P. sativum* L.	Plp 332	India	Landraces
PI 347401	USDA	*P. sativum* L.	Plp 363	India	Landraces
PI 347471	USDA	*P. sativum* L.	Plp 450	India	Landraces
PI 358642	USDA	*P. sativum* subsp. *sativum* var. *arvense* (L.) Poir.	22793	Ethiopia	Landraces
PI 379612	USDA	*P. sativum* L.	Weibull 700	Sweden	Cultivar
PI 385981	USDA	*P. sativum* L.	Onward	UK	Cultivar
PI 399129	USDA	*P. sativum* L.	Florida	Germany	Cultivar
PI 494079	USDA	*P. sativum* L.	G 27917	Chile	Landraces
PI 560065	USDA	*P. fulvum* Sm.	Cpi 134669	Israel	wild
PI 560067	USDA	*P. fulvum* Sm.	Cpi 134471	Israel	wild
PI 595933	USDA	*P. fulvum* Sm.	Atc 113	Australia	wild
PI 595945	USDA	*P. fulvum* Sm.	Cpi 53306	Jordan	wild
PI 595947	USDA	*P. fulvum* Sm.	Vir 2523	Israel	wild
JI 85	JIC UK	*P. sativum* L.	P.Sativum-Afghanistan	Afganistan	Landraces
JI 156	JIC UK	*P. sativum* L.	P.Sativum-Ussr	Sudan	Landraces

Bank code	Bank origin	Taxonomy	Common Name	Germplasm origin	Material type
JI 156	JIC UK	*P. sativum* L.	P.Sativum-Ussr	Sudan	Landraces
JI 262	JIC UK	*P. sativum* subsp. *elatius* var. *elatius* (M. Bieb.) Alef.	P. Elatius	Turkey	wild
JI 263	JIC UK	*P. sativum* subsp. *sativum* var. *arvense* (L.) Poir.	P.Sativum-Balkans	Greece	wild
JI 228	JIC UK	*P. sativum* L.	P.Sativum-Bolivia	Bolivia	Landraces
JI 209	JIC UK	*P. sativum* subsp. *sativum* var. *arvense* (L.) Poir.	P.Sativum Arvense	India	Landraces
JI 209	JIC UK	*P. sativum* subsp. *sativum* var. *arvense* (L.) Poir.	P.Sativum Arvense	India	Landraces
JI 207	JIC UK	*P. sativum* subsp. *sativum* var. *sativum*	P.Sativum Choresmicum	UZBEKISTAN	Landraces
JI 224	JIC UK	*P. fulvum* Sm.	P. Fulvum	Israel	wild
JI 196	JIC UK	*P. sativum* subsp. *transcaucasicum* Govorov	P.Sativum-Georgia	Georgia	Landraces
JI 190	JIC UK	*P. sativum* L.	Wiraig	Sudan	Landraces
JI 189	JIC UK	*P. sativum* L.	Wiraig	Sudan	Landraces
JI 185	JIC UK	*P. sativum* L.	Wiraig	Sudan	Landraces
JI 267	JIC UK	*P. sativum* L.	P.Sativum-Greece	Greece	wild
JI 268	JIC UK	*P. sativum* L.	P.Sativum-Crete	Crete	wild
JI 275	JIC UK	*P. sativum* L.	P.Sativum-Crete	Crete	wild
JI 280	JIC UK	*P. sativum* L.	P.Sativum-Albania	Albania	wild
JI 288	JIC UK	*P. sativum* L.	P.Sativum-Greece	Greece	wild
JI 502	JIC UK	*P. sativum* L.	Rondo	Netherland	Cultivar
JI 701	JIC UK	*P. sativum* L.	P.Sativum-Italy	Italy	Landraces
JI 1030	JIC UK	*P. sativum* L.	P.Sativum-Iran	Iran	Landraces
JI 1057	JIC UK	*P. sativum* L.	Antioquia I Chilena	Colombia	Landraces
JI 1089	JIC UK	*P. sativum* subsp. *sativum* var. *arvense* (L.) Poir.	P.Elatius	Turkey	Landraces
JI 1107	JIC UK	*P. sativum* L.	Keerau Pea	Nepal	Landraces
JI 1213	JIC UK	*P. sativum* L.	Erylis	France	Cultivar
JI 1345	JIC UK	*P. sativum* L.	P.Sativum-Mongolia	Mongolia	Landraces
JI 1346	JIC UK	*P. sativum* L.	P.Sativum-Mongolia	Mongolia	Landraces
JI 2263	JIC UK	*P. sativum* L.	Wild Tunesian	Germany	Landraces
JI 2265	JIC UK	*P. sativum* L.	P.Sativum Var. Hiemale	Albania	Landraces
JI 2356	JIC UK	*P. sativum* L.	P.Sativum-Nepal	Nepal	Landraces
JI 2385	JIC UK	*P. abyssinicum* A. Braun	Pisum Sp.-Yemen	Yemen	Landraces
JI 2387	JIC UK	*P. sativum* L.	P.Sativum-Ethiopia	Ethiopia	Landraces
JI 2545	JIC UK	*P. sativum* L.	P. Sativum-Pakistan	Pakistan	Landraces
BGE001004	CRF INIA	*P. sativum* subsp. *sativum*	Garvanzo Enano	Spain	Landraces
BGE001034	CRF INIA	*P. sativum* subsp. *sativum* var. *sativum*	Pesol	Spain	Landraces
BGE001121	CRF INIA	*P. sativum* subsp. *sativum* var. *sativum*	Negrer	Spain	Landraces
BGE001121	CRF INIA	*P. sativum* subsp. *sativum* var. *sativum*	Negrer	Spain	Landraces
BGE001662	CRF INIA	*P. sativum* subsp. *sativum*	Chicharo	Spain	Landraces
BGE002168	CRF INIA	*P. sativum* subsp. *sativum*	Tito	Spain	Landraces
BGE002168	CRF INIA	*P. sativum* subsp. *sativum*	Tito	Spain	Landraces
BGE003315	CRF INIA	*P. sativum* subsp. *sativum*	Tirabeque	Spain	Landraces
BGE004710	CRF INIA	*P. sativum* subsp. *sativum*	Ervilha	Portugal	Landraces
BGE004713	CRF INIA	*P. sativum* subsp. *sativum*	Ervilha	Portugal	Landraces
BGE004958	CRF INIA	*P. sativum* subsp. *sativum*	Ervilhoto	Portugal	Landraces
BGE006125	CRF INIA	*P. sativum* subsp. *sativum*	Grizeu Farroba	Portugal	Landraces
BGE006126	CRF INIA	*P. sativum* subsp. *sativum* var. *sativum*	Ervilha	Portugal	Landraces
BGE019594	CRF INIA	*P. sativum* subsp. *sativum*	Arveja	Spain	Landraces
BGE022159	CRF INIA	*P. sativum* subsp. *sativum* var. *arvense* (L.) Poir.	Bisalto	Spain	Landraces
BGE020326	CRF INIA	*P. sativum* subsp. *sativum* var. *arvense* (L.) Poir.	Bisalto Del Terreno	Spain	Landraces
BGE023256	CRF INIA	*P. sativum* subsp. *sativum*	Guisante	Spain	Landraces
BGE025263	CRF INIA	*P. sativum* subsp. *sativum* var. *sativum*	Guisante Verde	Spain	Landraces
BGE025267	CRF INIA	*P. sativum* subsp. *sativum*	Mangano;Presol;Guisante Claro	Spain	Landraces
BGE025270	CRF INIA	*P. sativum* subsp. *sativum*	Guisante Negro	Spain	Landraces
BGE026428	CRF INIA	*P. sativum* subsp. *sativum* var. *sativum*	Guisante Rastrero	Spain	Landraces
BGE026429	CRF INIA	*P. sativum* subsp. *sativum*	Arvilla	Spain	Landraces
CGN16690	CGN	*P. sativum* L.		Italy	Landraces
CGN03277	CGN	*P. sativum* L.	Npe 378	Pakistan	Landraces
CGN13253	CGN	*P. sativum* L.	P.Sativum-Ethiopia	Ethiopia	Landraces
CGN16640	CGN	*P. sativum* L.	Khadraa	Sudan	Landraces
CGN16562	CGN	*P. sativum* L.	Ji 1543	Mongolia	wild
CGN16571	CGN	*P. sativum* subsp. *jomardii* (Schrank) Kosterin	P. Jomardii	Egypt	wild
CGN16581	CGN	*P. sativum* L.	Ji 93	Afganistan	Landraces
CGN16639	CGN	*P. sativum* L.	Ji 171	Ethiopia	Landraces

Bank code	Bank origin	Taxonomy	Common Name	Germplasm origin	Material type
CGN16679	CGN	*P. sativum* subsp. *cinereum* Govorov	Ji 204	Russia	wild
CGN16582	CGN	*P. sativum* L.	Keerau Pea	Nepal	Landraces
CGN16684	CGN	*P. sativum* L.		Greece	Landraces
CGN16646	CGN	*P. sativum* L.		Mongolia	Landraces
CGN16636	CGN	*P. abyssinicum* A. Braun	P. Abyssinicum	Ethiopia	Landraces
CGN03328	CGN	*P. sativum* L.	Npe 1210.362a	Pakistan	Landraces
CGN03170	CGN	*P. sativum* L.	Turkey-19	Irak	Landraces
CGN03190	CGN	*P. sativum* L.	Kulur	Turkey	Landraces
CGN03245	CGN	*P. sativum* L.	Ethiopia-32	Ethiopia	Landraces
CGN03165	CGN	*P. sativum* L.	Turkey-16	Turkey	Landraces
CGN03289	CGN	*P. sativum* L.	Npe 1175.346	Pakistan	Landraces
CGN03171	CGN	*P. sativum* L.	Selection 266/1	Turkey	breeding lines
CGN03290	CGN	*P. sativum* L.	Npe 1180.392	Pakistan	Landraces
CGN03305	CGN	*P. sativum* L.	Npe 1169.248	Pakistan	Landraces
CGN02921	CGN	*P. sativum* subsp. *sativum* var. *sativum*	Semi Nano Ideal	Italy	Cultivar
CGN03003	CGN	*P. sativum* subsp. *sativum* var. *sativum*	Petit Provencal	France	Cultivar
CGN03273	CGN	*P. sativum* L.	950 3e	Peru	breeding lines
CGN03229	CGN	*P. sativum* L.	Ethiopia-31	Ethiopia	Landraces
PI 413686	USDA	*P. sativum* L.	Felicitas	Hungary	Cultivar
PI 477371	USDA	*P. sativum* L.	Rosakrone	Denmark	Cultivar
PI 307666	USDA	*P. sativum* L.	Verja	Costa Rica	Landraces
PI 307666	USDA	*P. sativum* L.	Verja	Costa Rica	Landraces
PI 324693	USDA	*P. sativum* L.	Abesinijas	Hungary	Cultivar
PI 324705	USDA	*P. sativum* L.	No. 830	France	Unknown
PI 355905	USDA	*P. sativum* subsp. *sativum* var. *sativum*	Kairyo Aotenashi	Japan	Cultivar
PI 241593	USDA	*P. sativum* L.	G 6571	Taiwan	Unknown
PI 273207	USDA	*P. sativum* subsp. *elatius* (M. Bieb.) Asch. & Graebn.	9006/60	Bulgaria	Landraces
PI 266070	USDA	*P. sativum* subsp. *sativum* var. *sativum*	Line No. 930	Sweden	breeding lines
PI 198074	USDA	*P. sativum* L.	Gorsdagsart Iii	Sweden	Landraces
PI 357292	USDA	*P. sativum* subsp. *sativum* var. *sativum*	Kiflica	North Macedonia	Cultivar
PI 357293	USDA	*P. sativum* subsp. *sativum* var. *sativum*	Debarski	North Macedonia	Cultivar
PI 249645	USDA	*P. sativum* L.	B.R. 178	India	Landraces
PI 357048	USDA	*P. sativum* subsp. *elatius* (M. Bieb.) Asch. & Graebn.	Plp 514	India	wild
PI 357289	USDA	*P. sativum* subsp. *sativum* var. *sativum*	Ran	North Macedonia	Cultivar
PI 253968	USDA	*P. sativum* subsp. *elatius* (M. Bieb.) Asch. & Graebn.	Col. No. K1722	Afganistan	Landraces
PI 103058	USDA	*P. sativum* L.	No. 10	China	Cultivar
PI 180329	USDA	*P. sativum* L.	Watana	India	Landraces
PI 184131	USDA	*P. sativum* subsp. *sativum* var. *sativum*	No. 310	Serbia	Landraces
PI 124478	USDA	*P. sativum* L.	Matar	Pakistan	Landraces
PI 124479	USDA	*P. sativum* L.	Matar	Pakistan	Landraces
PI 124479	USDA	*P. sativum* L.	Matar	Pakistan	Landraces
JI 2480	JIC	*P. sativum* L.	Cgn 3352	Peru	breeding lines
JI 1951	JIC	*P. sativum* L.	P.Sativum-China	China	Cultivar
JI 2302	JIC	*P. sativum* subsp. *sativum* var. *sativum*	B76-197 (Stratagem)	Sweden	breeding lines
JI 1566	JIC	*P. sativum* L.	Almota	USA	Cultivar
PI 608038	USDA	*P. sativum* L.	74sn5	USA	Cultivar
PI 613100	USDA	*P. sativum* L.	Mini	USA	Cultivar
Atc-4235-53	Commercial	*P. sativum* L.	Atc-4235-53	Australia	breeding lines
Boreen	Commercial	*P. sativum* L.	Boreen	Australia	Cultivar
Danclale	Commercial	*P. sativum* L.	Danclale	Australia	Cultivar
Kagpa	Commercial	*P. sativum* L.	Kagpa	Australia	Cultivar
M5	Commercial	*P. sativum* L.	M5	Australia	Cultivar
Pinochio	Commercial	*P. sativum* L.	Pinochio	Denmark	Cultivar
B 99-114	Commercial	*P. sativum* L.	B 99-114	Czech Republic	breeding lines
AGT 205,21	Commercial	*P. sativum* L.	Agt 205,21	Czech Republic	breeding lines
Morris	Commercial	*P. sativum* L.	Morris	Czech Republic	Cultivar
JI 1210	JIC	*P. sativum* L.	Erygel	France	Cultivar
JI 1412	JIC	*P. sativum* L.	Marlin	USA	Cultivar

Bank code	Bank origin	Taxonomy	Common Name	Germplasm origin	Material type
JI 1559	JIC	*P. sativum* L.	Mexique 4	Mexico	Cultivar
JI 1747	JIC	*P. sativum* L.	Almires	Germany	Cultivar
JI 1760	JIC	*P. sativum* subsp. *sativum* var. *sativum*	Consort-Af	UK	Cultivar
JI 210	JIC	*P. sativum* L.	Lucknow Boniya	India	Cultivar
JI 252	JIC	*P. sativum* L.	P.Sativum-Ethiopia	Ethiopia	Landraces
JI 82	JIC	*P. sativum* L.	P.Sativum-Afghanistan	Afganistan	Landraces
Messire	IAS	*P. sativum* subsp. *sativum* var. *sativum*	Messire	France	Cultivar
Radley	IAS	*P. sativum* subsp. *sativum* var. *sativum*	Radley	UK	Cultivar
Ballet	IAS	*P. sativum* subsp. *sativum* var. *sativum*	Ballet	UK	Cultivar
W6 17515	USDA	*P. sativum* subsp. *sativum* var. *sativum*	Little Marvel	USA	Cultivar
W6 17516	USDA	*P. sativum* subsp. *sativum* var. *sativum*	Dark Skin Perfection	USA	Cultivar
W6 17517	USDA	*P. sativum* subsp. *sativum* var. *sativum*	New Era	USA	Cultivar
W6 17518	USDA	*P. sativum* subsp. *sativum* var. *sativum*	New Season	USA	Cultivar
W6 17520	USDA	*P. sativum* subsp. *sativum* var. *sativum*	Wsu 28	USA	Cultivar
KEBBY	Commercial	*P. sativum* subsp. *sativum* var. *sativum*	Kebby	UK	Cultivar
POLAR	Commercial	*P. sativum* subsp. *sativum* var. *sativum*	Polar	Spain	Cultivar
W6 17519	USDA	*P. sativum* subsp. *sativum* var. *sativum*	Wsu 23	Unknow	Cultivar
W6 17521	USDA	*P. sativum* subsp. *sativum* var. *sativum*	Wsu 31	Unknow	Cultivar
BGE023667	INIA	*P. sativum* subsp. *sativum*	Guisante	Spain	Landraces
BGE025727	INIA	*P. sativum* subsp. *sativum*	Guisante	Spain	Landraces
PI 358608	USDA-EEUU	*P. sativum* subsp. *sativum* var. *arvense* (L.) Poir.	22770b	Ethiopia	Landraces
PI 358609	USDA-EEUU	*P. abyssinicum* A. Braun	Wat	Ethiopia	wild
PI 173055	USDA-EEUU	*P. sativum* subsp. *elatius* var. *elatius* (M. Bieb.) Alef.	Hatun Bakleri	Turkey	Landraces
PI 120617	USDA-EEUU	*P. sativum* subsp. *elatius* var. *elatius* (M. Bieb.) Alef.	No. 738	Turkey	Landraces
PI 273209	USDA-EEUU	*P. sativum* subsp. *elatius* var. *elatius* (M. Bieb.) Alef.	9009/60	Russia	Landraces
PI 344003	USDA-EEUU	*P. sativum* subsp. *elatius* var. *elatius* (M. Bieb.) Alef.	22703	Turkey	wild
PI 344005	USDA-EEUU	*P. sativum* subsp. *elatius* var. *elatius* (M. Bieb.) Alef.	22611	Greece	wild
PI 344006	USDA-EEUU	*P. sativum* subsp. *elatius* var. *elatius* (M. Bieb.) Alef.	22618	Greece	wild
PI 343976	USDA-EEUU	*P. sativum* subsp. *elatius* var. *elatius* (M. Bieb.) Alef.	22716	Turkey	wild
PI 505059	USDA-EEUU	*P. sativum* subsp. *elatius* var. *elatius* (M. Bieb.) Alef.	Ilca 5076	Sudan	Landraces
PI 344010	USDA-EEUU	*P. sativum* subsp. *elatius* var. *elatius* (M. Bieb.) Alef.	22732	Greece	wild
PI 344011	USDA-EEUU	*P. sativum* subsp. *elatius* var. *elatius* (M. Bieb.) Alef.	22733	Greece	wild
PI 344013	USDA-EEUU	*P. sativum* subsp. *elatius* var. *elatius* (M. Bieb.) Alef.	22735	Greece	wild
PI 116056	USDA-EEUU	*P. sativum* subsp. *sativum*	Matar	India	Landraces
PI 505127	USDA-EEUU	*P. sativum* subsp. *sativum*	Ilca 5094	Albania	Landraces
PI 242027	USDA-EEUU	*P. sativum* subsp. *jomardii* (Schrank) Kosterin	G 11764	Denmark	Unknown
PI 269762	USDA-EEUU	*P. sativum* subsp. *jomardii* (Schrank) Kosterin	Aa38	UK	Landraces
PI 343987	USDA-EEUU	*P. sativum* subsp. *sativum* var. *sativum*	22718	Turkey	Landraces
PI 505080	USDA-EEUU	*P. sativum* subsp. *sativum*	Ilca 5039	Cyprus	Unknown
PI 505111	USDA-EEUU	*P. sativum* subsp. *sativum*	Ilca 5075	Syria	Landraces
PI 268480	USDA-EEUU	*P. sativum* subsp. *elatius* var. *pumilio* Meikle	Col. No. 317	Afganistan	Landraces
JI 45	JIC	*P. sativum* subsp. *transcaucasicum* Govorov	P.Transcaucasicum	Georgia	wild
JI 198	JIC	*P. sativum* subsp. *elatius* var. *elatius* (M. Bieb.) Alef.	P. Elatius	Israel	wild
JI 199	JIC	*P. sativum* subsp. *elatius* var. *elatius* (M. Bieb.) Alef.	P. Elatius	Israel	wild
JI 225	JIC	*P. abyssinicum* A. Braun	P. Abyssinicum	Ethiopia	Landraces
JI 227	JIC	*P. abyssinicum* A. Braun	P. Abyssinicum	Ethiopia	Landraces
JI 241	JIC	*P. sativum* subsp. *elatius* var. *pumilio* Meikle	P. Humile	Israel	wild

Bank code	Bank origin	Taxonomy	Common Name	Germplasm origin	Material type
JI 254	JIC	*P. sativum* subsp. *elatius* var. *elatius* (M. Bieb.) Alef.	P. Elatius	Ethiopia	wild
JI 804	JIC	*P. sativum* subsp. *sativum* var. *sativum*	P.Tibetanicum	Unknow	Landraces
JI 1398	JIC	*P. sativum* L.	P.Sativum	China	Landraces
JI 1428	JIC	*P. sativum* subsp. *sativum* var. *sativum*	P.Tibetanicum	Tibet	wild
JI 1854	JIC	*P. sativum* subsp. *elatius* var. *pumilio* Meikle	P. Humile	Israel	Landraces
JI 2116	JIC	*P. sativum* subsp. *sativum* var. *sativum*	P.Speciosum	Spain	Landraces
JI 2202	JIC	*P. abyssinicum* A. Braun	P. Abyssinicum	Yemen	Landraces
PIS 1318/91	IPK	*P. sativum* subsp. *elatius* (M. Bieb.) Asch. & Graebn.		Unknow	Unknown
CGN10205	CGN	*P. sativum* subsp. *elatius* var. *elatius* (M. Bieb.) Alef.	1140175	Turkey	Landraces
CGN10206	CGN	*P. sativum* subsp. *elatius* var. *elatius* (M. Bieb.) Alef.	1145176	Unknow	breeding lines
CGN10193	CNG	*P. sativum* subsp. *sativum* var. *arvense* (L.) Poir.		Unknow	Unknown
IFPI 3365	ICARDA-Siria	*P. sativum* subsp. *elatius* var. *elatius* (M. Bieb.) Alef.	Ig 52524	Turkey	wild
IFPI 3370	ICARDA-Siria	*P. sativum* subsp. *elatius* var. *elatius* (M. Bieb.) Alef.	Ig 52529	Turkey	wild
IFPI 387	ICARDA-Siria	*P. sativum* subsp. *thebaicum*	Ig 49546	USSR	wild
IFPI 436	ICARDA-Siria	*P. sativum* subsp. *jomardii* (Schrank) Kosterin	Ig 49595	Egypt	Landraces
IFPI 2348	ICARDA-Siria	*P. sativum* subsp. *sativum* var. *arvense* (L.) Poir.	Ig 51507	Ethiopia	Landraces
IFPI 2350	ICARDA-Siria	*P. sativum* subsp. *sativum* var. *arvense* (L.) Poir.	Ig 51509	Ethiopia	Landraces
IFPI 2351	ICARDA-Siria	*P. sativum* subsp. *sativum* var. *arvense* (L.) Poir.	Ig 51510	Ethiopia	Landraces
IFPI 2352	ICARDA-Siria	*P. sativum* subsp. *sativum* var. *arvense* (L.) Poir.	Ig 51511	Ethiopia	Landraces
IFPI 2353	ICARDA-Siria	*P. sativum* subsp. *sativum* var. *arvense* (L.) Poir.	Ig 51512	Ethiopia	Landraces
IFPI 2354	ICARDA-Siria	*P. sativum* subsp. *sativum* var. *arvense* (L.) Poir.	Ig 51513	Ethiopia	Landraces
IFPI 2356	ICARDA-Siria	*P. sativum* subsp. *sativum* var. *arvense* (L.) Poir.	Ig 51515	Ethiopia	Landraces
IFPI 2357	ICARDA-Siria	*P. sativum* subsp. *sativum* var. *arvense* (L.) Poir.	Ig 51516	Ethiopia	Landraces
IFPI 2358	ICARDA-Siria	*P. sativum* subsp. *sativum* var. *arvense* (L.) Poir.	Ig 51517	Ethiopia	Landraces
IFPI 2360	ICARDA-Siria	*P. sativum* subsp. *sativum* var. *arvense* (L.) Poir.	Ig 51519	Ethiopia	Landraces
IFPI 2362	ICARDA-Siria	*P. sativum* subsp. *sativum* var. *arvense* (L.) Poir.	Ig 51521	Ethiopia	Landraces
IFPI 2363	ICARDA-Siria	*P. sativum* subsp. *sativum* var. *arvense* (L.) Poir.	Ig 51522	Ethiopia	Landraces
IFPI 2364	ICARDA-Siria	*P. sativum* subsp. *sativum* var. *arvense* (L.) Poir.	Ig 51523	Ethiopia	Landraces
IFPI 2365	ICARDA-Siria	*P. sativum* subsp. *sativum* var. *arvense* (L.) Poir.	Ig 51524	Ethiopia	Landraces
IFPI 2367	ICARDA-Siria	*P. sativum* subsp. *sativum* var. *arvense* (L.) Poir.	Ig 51526	Ethiopia	Landraces
IFPI 2369	ICARDA-Siria	*P. sativum* subsp. *sativum* var. *arvense* (L.) Poir.	Ig 51528	Ethiopia	Landraces
IFPI 2370	ICARDA-Siria	*P. sativum* subsp. *sativum* var. *arvense* (L.) Poir.	Ig 51529	Ethiopia	Landraces
IFPI 2371	ICARDA-Siria	*P. sativum* subsp. *sativum* var. *arvense* (L.) Poir.	Ig 51530	Ethiopia	Landraces
IFPI 2372	ICARDA-Siria	*P. sativum* subsp. *sativum* var. *arvense* (L.) Poir.	Ig 51531	Ethiopia	Landraces
IFPI 2441	ICARDA-Siria	*P. sativum* subsp. *jomardii* (Schrank) Kosterin	Ig 51600	Denmark	Unknown
IFPI 2495	ICARDA-Siria	*P. sativum* subsp. *jomardii* (Schrank) Kosterin	Ig 51654	UK	Landraces
IFPI 3232	ICARDA-Siria	*P. fulvum* Sm.	Ig 52391	Syria	Wild
IFPI 3250	ICARDA-Siria	*P. sativum* L.	Ig 52409	Syria	wild
IFPI 3252	ICARDA-Siria	*P. sativum* subsp. *elatius* (M. Bieb.) Asch. & Graebn.	Ig 52411	Syria	wild

Bank code	Bank origin	Taxonomy	Common Name	Germplasm origin	Material type
IFPI 3253	ICARDA-Siria	*P. fulvum* Sm.	Ig 52412	Syria	wild
IFPI 3257	ICARDA-Siria	*P. fulvum* Sm.	Ig 52416	Syria	wild
IFPI 3260	ICARDA-Siria	*P. fulvum* Sm.	Ig 52419	Syria	wild
IFPI 3261	ICARDA-Siria	*P. fulvum* Sm.	Ig 52420	Syria	wild
IFPI 3262	ICARDA-Siria	*P. fulvum* Sm.	Ig 52421	Syria	wild
IFPI 3280	ICARDA-Siria	*P. sativum* subsp. *elatius* (M. Bieb.) Asch. & Graebn.	Ig 52439	Syria	wild
IFPI 3282	ICARDA-Siria	*P. sativum* subsp. *elatius* (M. Bieb.) Asch. & Graebn.	Ig 52441	Syria	wild
IFPI 3330	ICARDA-Siria	*P. sativum* subsp. *elatius* var. *elatius* (M. Bieb.) Alef.	Ig 52489	Turkey	wild
IFPI 3334	ICARDA-Siria	*P. sativum* subsp. *elatius* var. *elatius* (M. Bieb.) Alef.	Ig 52493	Turkey	wild
IFPI 3338	ICARDA-Siria	*P. sativum* subsp. *elatius* var. *elatius* (M. Bieb.) Alef.	Ig 52497	Turkey	wild
IFPI 3358	ICARDA-Siria	*P. sativum* subsp. *elatius* var. *elatius* (M. Bieb.) Alef.	Ig 52517	Turkey	wild
	IAS - CSIC	*P. sativum* subsp. *elatius* var. *elatius* (M. Bieb.) Alef.		Unknow	wild
JI 1006	JIC	*P. fulvum* Sm.	Wbh 2142	Israel	wild

Additional file 2. Differences between groups in pea panel grouped by material type, growth condition and taxonomy.

Grouped by[a]	Group 1	Group 2	Signif.[b]
Material type	Breeding Line	Cultivar	*
	Cultivar	Landraces	****
	Cultivar	Wild	****
Growing Condition	DS_{2018}	DS_{2019}	***
	DS_{2018}	DS_{2020}	****
	DS_{2019}	DS_{2020}	****
	DS_{2018}	DS_{CC}	****
	DS_{2019}	DS_{CC}	****
	DS_{2020}	DS_{CC}	****
Taxonomy	*P. fulvum* Sm.	*P. sativum* subsp. *sativum* var. sativum	**
	P. sativum L.	*P. sativum* subsp. *sativum* var. sativum	****
	P. sativum subsp. *sativum* var. arvense	*P. sativum* subsp. *sativum* var. sativum	**
	P. sativum subsp. *sativum* var. sativum	*P. sativum* subsp. *elatius* var. elatius	****

[a] Grouped by column attend to Material type (Breeding Line, Cultivar, Landrace, Wild or Unknown), Growth Condition (Disease severity in Controlled Conditions (DSCC) or Disease Severity in environments Co-2018, Co-2019 or Co-202 (DS2018, DS2019 and DS2020, respectively)) and *Pisum* taxonomy.

[b] Signif. column reveals the statistical significance in the Wilcoxon test: * = $p < 0.05$, ** = $p < 0.01$, *** = $p < 0.001$, **** = $p < 0.0001$.

Chapter 3
RGB image-based method for phenotyping rust disease progress in pea leaves using R

This Chapter has been published as:

Osuna-Caballero S, Olivoto T, Jiménez-Vaquero MA, Rubiales D, Rispail N (2023) RGB image-based method for phenotyping rust disease progress in pea leaves using R. Plant Methods 19:86. https://doi.org/10.1186/s13007-023-01069-z

1. Abstract

Rust is a disease that damages important crops like pea, and researchers are still struggling to identify genotypes with high levels of resistance. To find new sources of resistance, it is crucial to accurately measure the level of infection on large number of accessions. This is where an image analysis system proves useful. By applying an easy-to-use and affordable system, researchers can quickly count and measure the pustules caused by rust on pea samples. The goal of this study was to develop an automated image analysis pipeline that can accurately calculate disease progression parameters of rust, while also ensuring that the data collected are reliable. To validate the method and determine the best approach, a set of 600 pea leaflets affected by rust symptoms were analysed at different resolutions using distinct segmentation indices. The processing time varied depending on the compression level, with lower resolution resulting in faster processing and reduced storage space. Among the segmentation indices tested, the Normalized Green Red Difference Index (NRGDI) was the fastest at 60 % resolution, taking a total of 62 seconds to analyse the 600 leaflets using parallel processing. Lin's concordance correlation coefficient was the metric used to evaluate the accuracy of image-based analyses compared to visual pustule counting. The highest accuracies (> 0.98) were obtained at full resolution, but a compression level of 60 % was not statistically different for most disease progression parameters. Overall, NRGDI was the optimal segmentation, providing high accuracy and less accumulated error over time for pustule counting. A new image-based method for pea rust disease phenotyping has been proposed, using RGB spectral indices segmentation and pixel value thresholding to improve resolution and precision. It can analyse hundreds of images in seconds and has accuracy comparable to visual methods and better than other image-based methods. It captures the full complexity of rust disease in pea and eliminates errors introduced by raters in traditional approaches. This method can help identify QTLs for pea genetic resistance and improve breeding efforts.

2. Introduction

Rusts are a group of plant diseases caused by species of the Pucciniales order which is one of the largest orders of plant fungal pathogens comprising more than 8,000 species (Toome-Heller 2016). They are obligate biotrophs that compromise yields of important crops worldwide and exhibit complex lifecycles with up to five different stages (i.e., pycnidial, aecial, uredial, telial, and basidial stages) (Helfer 2014). Rust lifecycle begins when the spores, carried by wind or water, germinate, and infect the aerial tissue of the host. Once inside the plant, it produces specialized structures called haustoria mother cells, which penetrate the plant cells via a neckband, and form haustoria to extract nutrients. Then, the fungus produces secondary spores, which can spread to other parts of the same plant or to new host plants. This infection cycle and spore production can be repeated several times along

the cropping season, leading to the development of visible symptoms such as yellowing, spotting or rust-coloured pustules on the leaves, stems, or fruit of the host, depending on the rust species or host reaction (Helfer 2014; Newcombe 2004). In many cases two taxonomically unrelated hosts are required to complete the life cycle. Different species of rust fungi have different host ranges, but many can infect a wide variety of plant species within a particular plant family or group, hindering their management in the field (Duplessis et al. 2021). In pea (*Pisum sativum* L.), a valuable, versatile, and inexpensive protein source for human food and animal feed (Tulbek et al. 2016), rust is a major disease spread worldwide (Rubiales et al. 2015). Two rust species, *Uromyces pisi* (Pers.) (Wint.) and *U. viciae-fabae* (Pers. de Bary) (Barilli et al. 2009b), have been described as causal agent of pea rust. The uredial stage of *U. pisi* produces the infective structures that affects pea crops in temperate regions while in warmest countries the aecial stage of *U. viciae-fabae* is the epidemic one (Beniwal et al. 2022). Although agronomical practices and chemical control of pea rusts have been explored to reduce their incidence (Shtaya et al. 2021; Luo et al. 2022; Barilli et al. 2017; Barilli et al. 2022; Khalil et al. 2023; Villegas-Fernández et al. 2023), the use of resistant cultivars is considered as the most effective, economic, and eco-friendly strategy for rust control (Li et al. 2021). To face the challenge of developing new rust resistant varieties, the reference genomes recently available provide important resources for pea breeding (Yang et al. 2022; Kreplak et al. 2019; Martins et al. 2022; Bari et al. 2023). The constant reduction in sequencing cost coupled with the technological advances that refine marker-trait association and genome editing approaches are expected to boost future development of pea resistance breeding. However, these methods need to be fed with detailed and accurate phenotypic data to guide breeding and deepen our understanding of the genetic variations controlling complex traits, such as rust disease resistance. Phenotyping is therefore becoming the main bottleneck for breeding. It is particularly challenging when assessment of very large collection of several thousand lines which is the typical size of nested association mapping (NAM) populations (Gireesh et al. 2021; Diers et al. 2018; Li et al. 2016).

It is therefore urgent to improve and optimize the available methods of phenotyping. The phenotypic characterization of pea response to rust has relied on disease assays conducted under controlled or field condition, in seedlings or adult plants, and with natural or artificial infestation. In these assays, disease was evaluated by measuring qualitative and/or quantitative measurements. Qualitative assessment of rust disease, known as infection type (IT) usually use a scale ranging from 0 to 4, as described by Stakman et al. 1963 in wheat. The IT depends on the host reaction to the pathogen. This reaction could be incompatible, when the host shows no symptoms or develops a hypersensitive response, or compatible when typical rust pustule develops on the susceptible host (Duplessis et al. 2021). Quantitative assessment of rust symptoms is conventionally assessed as a visual estimation of the

percentage of leaf area covered by rust pustules (disease severity, DS). This can be decomposed in more detailed components such as the infection frequency (IF) and colony size (CS). IF is the number of lesions (herein, pustules) within a limited area, usually 1 cm^2. These parameters defined as objective are weakly affected by user bias but highly time consuming when screening large germplasm collections. Contrary to IF or CS, DS is a subjective parameter highly dependent on the user interpretation that requires specialized training (Del Ponte et al. 2022). DS is also affected by IT, so the user can confound the area surrounding pustules that sometimes develop chlorotic/ necrotic regions. In several foliar diseases, standard area diagrams (SAD) can offer increased precision over DS calculations (Modesto et al. 2022; Castellar et al. 2021; Lopes et al. 2022). However, SADs are not readily available for pea rust. Traditionally, qualitative, and quantitative measurements have been performed to better understand the resistance mechanisms that operate in pea-rust pathosystem, together with other ones considering the pustule size (Barilli et al. 2009a, 2009b, 2009c). Periodical evaluation of these quantitative parameters allows to estimate disease progression factors such as the Area Under Disease Progress Curve (AUDPC), the Latency Period (LP50) and the Monocyclic Disease Progress rate (MDPr) (Smiko et al. 2012; Arneson et al. 2001). Through these factors, it is possible to capture most of the complexity of rust disease evolution. Little advances have been achieved toward automatization of pea rust phenotyping in comparison with other aerial fungal pathosystems, for which many platforms and methodologies have been developed to increase accuracy and precision of disease estimation including from other fungal pathogens in legumes (McDonald et al. 2022) to bacterial pathogens in citrus plants (Bock et al. 2009; Bock et al. 2008). Among these so-called high-throughput methods, development of image-based phenotyping techniques has largely increased in the last decade partly thanks to the decrease in imaging technologies cost and the increase in computing power that contributed to make them more affordable and accurate (Bock et al. 2010). These approaches take advantage of the clear contrast between the lesion emerging on the leaf surface and the healthy leaf background. These methods, through the application of appropriate threshold, isolate lesions from coloured images (in CMYK, RGB, CIELAB, or HSV format) of the infected leaf to count their number and size in pixel. Some systems using RGB images are already available to evaluate leaf rust disease in other rust pathosystems, such oat leaf rust (*Puccinia coronate* f. sp. *avenae* Fraser & Led.) in oat (*Avena sativa* L.) (Gallego-Sánchez et al. 2020). More complex methods using multi- and hyperspectral sensors that collect information outside the visible light spectrum have also been developed to quantify disease severity in various pathosystem including soybean rust, wheat leaf rust, and wheat steam rust (Cui et al. 2010; Ashourloo et al. 2014; Abdulridha et al. 2023). In particular, it has been applied to quantify leaf rust (*Puccinia triticina* Eriks.) diseases under controlled conditions in wheat (*Triticum aestivum* L.) through vegetation indices (Ashourloo et al. 2014) and their application in the field have

already been explored using unmanned aerial vehicles (UAV) (Guo et al. 2021). However, there are currently no high-throughput image-based method that can be used to estimate rust disease evolution during the complete cycle and to estimate disease progression parameters, particularly in pea. The growing interest in image-based disease phenotyping has driven the development of various image analysis platforms. Particularly promising are the platforms based on free and open-source environments that align with the principles of open science, with Python language being a notable example. Python's versatility and ease of use have made it a popular choice for various scientific disciplines, including plant disease phenotyping trough packages such as PlantCV (Gehan et al. 2017; Fahlgren et al. 2015). In parallel, the R language, known for its extensive use in statistical computing and graphics, is also gaining traction in the field of plant phenotyping. Researchers are increasingly recognizing the capabilities of R for handling and analysing complex datasets, making it a valuable tool for studying plant diseases (Beare et al. 2018; Miller et al. 2023; Olivoto et al. 2022). This study aimed to develop an image processing workflow using R software that achieves several goals, including producing reliable and repeatable measurements of rust-infected pea leaf area, counting the number of pustules, and measuring them on the leaf surface, combining leaf information over time to track disease progression, automating the process to analyse thousands of images, and allowing for data tracking from image acquisition to output.

3. Materials and Methods

3.1. Plant materials, Pathogen isolate and Inoculation

The plant material used in the image analysis to set up and validate our method was a randomly selected subset of 33 accessions from a pea core collection of 320 genotypes which previously reported to show a wide variability of responses to rust caused by *Uromyces pisi* (Osuna-Caballero et al. 2022). Disease assays were performed at seedling stage under controlled conditions. The experiment followed a randomized complete block design with three biological replicates being planted at a time, using pea cv. Messire as a high-susceptible rust control, meaning a total of 100 experimental units. Seeds of each accession were surface-sterilized, scarified and vernalized to ensure optimal germination. Three germinated seeds per accession were sown in a sand:peat mixture (1:1, w/w) in a 15 cm^2 plastic pot. At 7 days post germination, plants were thinned to one plant per pot to maximize light distribution. The growth chamber was maintained at 20 ºC with a photoperiod of 14 h of light and 10 h of darkness and 148 µmol m^{-2} s^{-1} of irradiance at plant canopy level. Once the third leaf of each plant was fully expanded, plants were inoculated with freshly collected urediospores of the highly virulent isolate UpKeS-05 of *U. pisi* (Barilli et al. 2012) previously multiplied on cv. Messire seedlings. Inoculation was performed by dusting the plants with 1 mg urediospores per pot, mixed in pure talc (1:10, v:v) and the infected plants were incubated for 24 h at 20 ºC in complete darkness and 100%

relative humidity as previously described [75]. Then, plants were transferred back to the growth chamber. Pustules associated with rust symptoms started to emerge on pea plants eight days after inoculation (dai).

3.2. Image Acquisition

In order to cover the first rust disease cycle that goes from 8 to 13 dai, a leaflet from the third leaf of each plant (n = 100) was cut at 7 dai and transferred to square Petri dishes filled with water:agar (0.5%) media and 0.005% Benzimidazole as fungicide with nine leaflets per Petri dish (Figure 7). Petri dishes were maintained in the growth chamber until the end of the experiment. RGB images of the whole Petri dishes were then acquired daily from 8 to 13 dai, with a smartphone brand Xiaomi, carrying a Sony IMX363 Exmor RS Sensor with a focal ratio $f/$ 1.9 with a 12-megapixel resolution. To ensure homogeneity of the RBG images, the smartphone was set on a tripod 0.35 m above the Petri dish and images were acquired on a plain black background under fluorescent light tubes set at 35° angles on both side of the plate. White balance, shutter speed, aperture and ISO speed of the camera was adjusted according to default parameters without flash. Each Petri dish was opened before image acquisition to avoid light reflection and closed thereafter to prevent contaminations (Figure 7). Daily RGB images were saved in .jpg format with an original resolution of 3024 × 3024 pixels.

Figure 7. Example of a stored RGB image. The image represents a typical Petri dish containing nine inoculated pea leaflets and their labels. Each row contains the same genotype, and the columns are their biological replicates. The example shows the genotypes 302, 301, and 280 at 8 dai.

3.3. Disease assessments

Infection frequency (IF) was estimated by counting the number of rust pustules emerging daily on each leaflet from 8 to 13 dai, visually or through the image analysis procedure. The resulting daily counting were then integrated in three parameters representing disease progression:

- AUDPC. The Area Under Disease Progress Curve (Jeger et al. 2001) following the formula:

$$AUDPC = \sum_{i=1}^{n-1} \frac{y_i + y_{i+1}}{2} \times (t_{i+1} - t_i)$$

  where y_i is the IF at the ith observation, t_i is days at the ith observation, and n is the total number of observations.
- MDPr. The Monocyclic Disease Progress rate, as described by Arneson (2001), is a proportionality constant that represents the rate of disease progress per unit of inoculum.
- LP_{50}. The Latency Period is the elapsed time between inoculation day and the day when 50 % of pustules are formed.

3.4. Image Segmentation

Image-based quantification of rust damage requires a two-stage segmentation of the original images to separate leaves from the background and to distinguish rust damage from healthy tissue. This segmentation was performed for each image subset allowing the estimation of DS, IF and PS.

The colour differences between foreground and background in our images are represented by different values from the red (R), green (G), and blue (B) channels in the RGB colour space, allowing the object segmentation in the images. Accordingly, the first segmentation was performed by applying a HUE index prevailing the green region to isolate the leaflets from the background with the formula:

$$HUE = \frac{\text{atan}\big(2(R - G - R)\big)}{30.5(G - B)}$$

The threshold used to separate the background from the leaflets were based on the Otsu method (Otsu 1979).

To isolate rust pustules from the healthy tissue, a second segmentation step was performed. Four indices commonly used in remote sensing and phytopathometry were tested for their capacity to detect rust pustules (Best and Harlan 1985; Blancon et al. 2019; Gitelson et al. 2002; Motohka et al. 2010), three operating in the RGB channels and one in the CIELAB colour space stack. The selected indices were the Normalized Green Red Difference Index $\left(NGRDI = \frac{G-R}{G+R}\right)$ (Chapu et al. 2022),

Primary Colours Hue Index $\left(HI = \frac{2(R-G-B)}{G-B}\right)$, Green Leaf Area Index $\left(GLAI = \frac{25(G-R)}{(G+R-B)+1.25}\right)$, and the a*- chrominance channel from CIELAB band $\left(a^* = 0.55\frac{(R-(0.2126\,R+0.7152\,G+0.0722\,B))}{1-0.2126}\right)$. Each index applies a different transformation of RGB values, therefore, each one requires a different threshold. The thresholds used were set as 0, 1, 1, and 0.50 for NGRDI, HI, GLAI, and a*- respectively. To maximize the accuracy of image-based pustules counting, the Watershed algorithm was also implemented, permitting to segment pustules connected by a few pixels that could be considered as two distinct lesions (Beucher et al. 1979).

3.5. Image Compression and Processing Time

Image compression can improve the processing time while saving store capacity in RAM and ROM memories. To get the optimum processing time without compromising precision and accuracy, four different compression levels ranged from full resolution (3024 × 3024 pixels) to 40% of the full resolution (1210 × 1210 pixels) were tested. Images compression were performed by applying the image_resize() function from "pliman" R package (Olivoto et al. 2022). The processing time required to analyse all images at each compression level was calculated using mark() function from "bench" R package (Hester and Vaughan 2023).

3.6. Method Validation

To validate and select the best segmentation index and optimum image compression, the Lin's concordance correlation coefficient (ccc, ρ_c) (Lin 1989) was computed between visual counting and software-estimation for each dai (from 8 to 13) and disease progression parameter (AUDPC, MDPr and LP50). The Lin's ccc not only evaluates how well the software-predicted values align with the visual counting values but also considers their systematic differences and scale variations. It provides a comprehensive assessment of the agreement by measuring both the correlation and the bias between the predicted and real values. Therefore, the ccc has been widely recommended and utilized in studies that involve comparing estimated severity values with actual severity values in phytopathometry (Del Ponte et al. 2017, 2022; Pereira et al. 2020). This parameter was calculated using a resampling approach between predicted and visual values for each parameter using the R package "yardstick" (Kuhn et al. 2023). In addition, the root-mean-square error (RMSE) were also calculated for an additional accuracy estimation between visual and software-based calculations. ρ_c values range from 0 to 1 while RMSE values are in the same units as the original data.

3.7. Description of Rust evaluation Method

The script controlling the image analysis method was developed in R software version 4.2.2 (R Core Team 2021) under RStudio version 2022.07.2.576, using the R

packages “pliman” (Olivoto et al. 2022), “EBImage” (Pau et al. 2010), and “Tidyverse” (Wickham et al. 2019). The approach to analyse the images using batch processing were also implemented with the R package “foreach”, which facilitates to compute the analyses in a parallel process. This parallel strategy allows to split the jobs across multiple cores in the CPU, regarding an extra processing time saving. All the analyses were performed on a PC equipped with an AMD Ryzen 9 CPU (16 cores) with 3.4 GHz frequency, a NVIDIA GTX 1660 Ti GPU, and 32 GB of RAM memory.

The method was developed using the set of 600 individual leaflets with different levels of rust disease symptoms. The symptoms ranged from no disease to leaflets heavily covered with pustules. The image processing pipeline (Additional file 4), developed as a R script (Osuna-Caballero et al. 2023), consists of a function which imports and analyses the images following a batch processing strategy. First, the input plate image is loaded following a name pattern inside the file path, then it is resized, before the nine leaflets within plate image are split according to the first index segmentation (HUE index). Then the split samples are analysed individually through a for loop using the measure_disease() function that estimates the total leaflet area, the number of pustules, the leaflet area covered by pustules and the mean pustule size, and saves these values for each sample in the output data frame. Furthermore, the developed function integrates an additional argument to analyse the input images in parallel (“parallel” argument set to “TRUE”) or sequentially (if parallel argument set to “FALSE”).

Therefore, the method can rapidly and accurately count the number of pustules (IF), report the percentage of leaf area covered by pustules (DS) and the average pustules size (PS) for each genotype daily from 8 to 13 dai. The daily values obtained for the same leaflet/genotype are then stored and combined into the AUDPC, MDPr and LP_{50} parameters, also stored in the output data frame.

4. Results

4.1. Pea Rust Monitoring

The developed R script enables the tracking of rust progression through image analysis, as shown in Figure 8A. The method allows the accurate detection of the pustules and the storage of the results in a readily usable data frame for further calculation. The evaluation of 33 diverse pea genotypes randomly selected revealed their variability in response to rust infection caused by *U. pisi*. A moderate variation was detected in disease severity (DS) which ranged from 1 to 14%. The average pustule size (PS) also exhibited variability between 0.3 and 1.0 mm^2, reflecting the presence of some resistance mechanism reducing the rust pustules size in some genotypes. As expected, a more pronounced variability was detected for the infection frequency (IF) that ranged from 10 to 82 pustules per cm^2 at 13 days after inoculation (dai) (Figure 8B). Monitoring the evolution of these disease parameters over time showed a steady

increase of DS and PS throughout the experiment (Figure 8B), although the increment rate varies according to the genotype. IF also increment over time although in this case the increment follows an exponential evolution with a slow increase from 8 to 9 dai followed by a rapid increase from 9 to 11 dai and thereafter a saturation plateau (Figure 8B). As for DS and PS, the increment rate of the different IF phase varied according to the genotypes. Integration of these daily disease estimates from 8 to 13 dai allowed the calculation of AUDPC, LP50, and MDPr progression parameters which capture most of the complexity of rust resistance and facilitate the selection and discrimination of genotypes (Additional file 3). As expected, the susceptible genotypes GEN261 exhibited the highest AUDPC and MDPr values and one of the shortest latency periods (LP_{50}), while the susceptible GEN62 displayed the lowest AUDPC and MDPr values and the longest LP_{50}, as expected (Additional file 3). These progression parameters, combined with daily point resistance mechanisms (IF, DS, and PS), enable a more precise estimation of the resistance or susceptibility levels of the pea genotypes to the pathogen. Similar results were obtained with the visual counting. Accordingly, these results showcase the potential of the image-based method to accurately assess rust disease progression in pea leaves and its capability to discriminate between genotypes based on their disease severity and pustule size variations.

4.2. Processing Time optimization and RGB Segmentation Selection

To validate the method and select the optimal criterion, a set of 100 leaflets x 6 time-points images were randomly selected. The 600 pea samples affected by rust symptoms were analysed following a parallel or sequential batch processing approach to detect the fastest one. In all cases, parallel strategy was five time faster than sequential strategy on average (Additional file 5). Only small processing time differences was detected with the parallel strategy between segmentation index independently of the image resolution (Figure 9). In most cases NGRDI (Normalized Green Red Difference Index) tend to be faster than the other segmentation index although the difference was only statistically significant with images at 60% resolution. At this resolution the analysis of the 600 leaflets with the NGRDI index took 62 s.

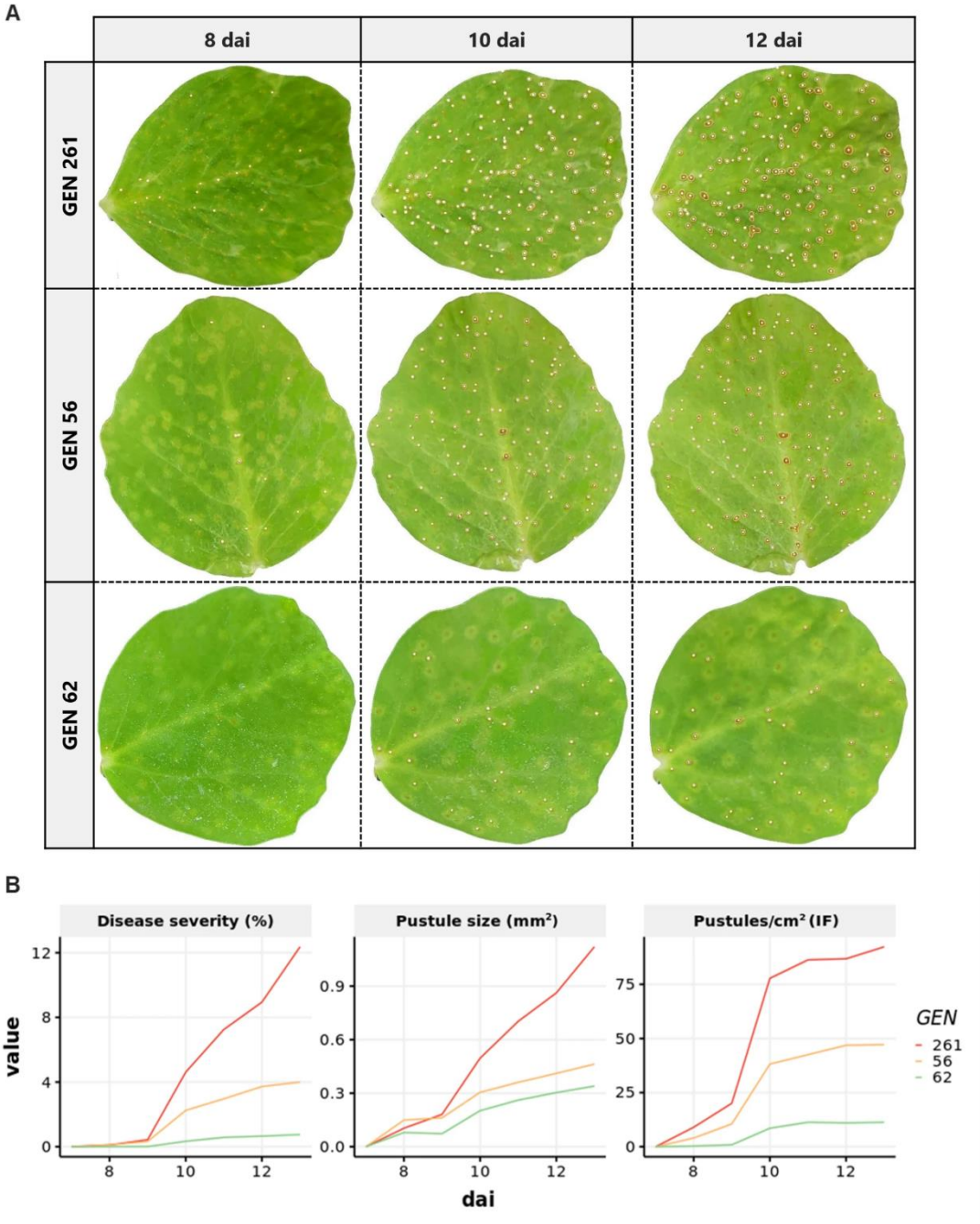

Figure 8. Pea rust evolution assessed with the RGB-based method. (A) The images show the evolution of rust pustule development at three different days after inoculation (8 dai, 10 dai, and 12 dai) on a representative leaflet of three differential genotypes (GEN62, GEN56, and GEN261) covering the wide range of susceptibility detected in the collection. White spots on the images indicate rust pustules detected by the image-based analysis methods. (B) Line plots showing the progression of disease severity (DS), pustule size (PS) and infection frequency (IF) over time estimated from these genotypes with the RGB-based method.

Clear differences in processing time were observed between compression levels. The processing time required to analyse a single leaflet image varied from an average of 65.7 ms at 40% resolution to 274 ms at full resolution (Table 8). Therefore, reducing the image resolution allowed decreasing processing time from up to 76% at 40% resolution (Table 8). The image compression also allowed reducing storage space required in the ROM memory. The average input image size in megabytes (Mb) varied from 3.5 to 1.0 between full resolution to 40% resolution, respectively, resulting in a store saving of up to 71% at maximum compression in comparison to full resolution (Table 8).

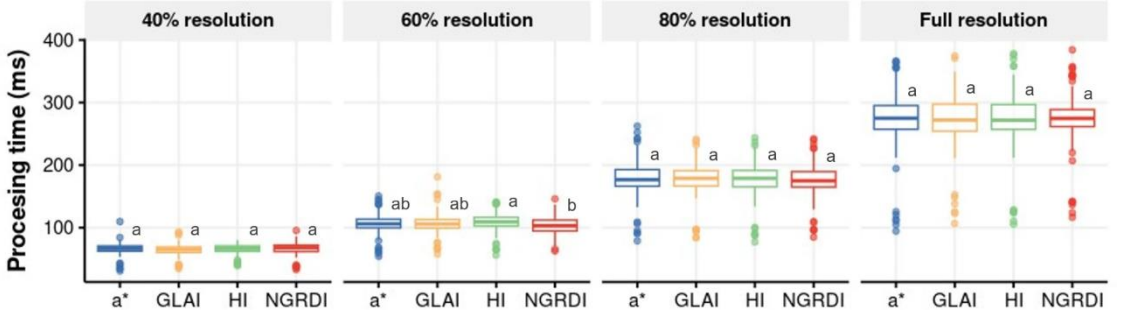

Figure 9. Boxplots showing the effect of image compression on processing time per leaflet by index applied to segment the pustules from healthy tissue. Different letters above the box indicate the statistical differences between indices for each image resolution estimated by Tukey HSD test at p = 0.05 for n = 600.

Table 8. Effect of image compression over processing time and image size.

Resolution	*Time by leaflet (ms)*	*Input Image size (Mb)*	*Speed increase vs full resolution (%)*	*ROM saving vs full resolution (%)*
full (3024 px)	274	3.5	-	-
80 % (2419 px)	178	3.1	35	11
60 % (1814 px)	106	2.0	61	43
40 % (1210 px)	65.7	1.0	76	71

To select the most appropriate compression level without compromising accuracy of rust pustule estimation, concordance correlation coefficient (ccc) using a resampling approach were evaluated between visual pustule counting and image-based analysis. As expected, the averaged indices ccc and RMSE varied largely depending on the compression level. As expected, accuracy for all traits was proportional to the image compression level (Figure 10A) while RMSE was inversely proportional to image compression level (Figure 10B). The highest accuracies and lowest RMSE were always obtained at full resolution. However, the accuracies and RMSE obtained for all traits at 80% resolution were not statistically different to the full resolution (Figure 10). At these resolutions, the accuracy of AUDPC and MDPr estimates ranged from 0.952 to 0.962 for AUDPC and from 0.918 to 0.922 for MDPr.

LP_{50} was more difficult to estimates with accuracies varying from 0.811 to 0.852. Increasing the compression level reduced accuracy and increased RMSE although accuracies of AUDPC and MDPr estimations at 60% resolution was still higher than 0.9 (ρc = 0.918 and ρc = 0.901 for AUDPC and MDPr, respectively) (Figure 10).

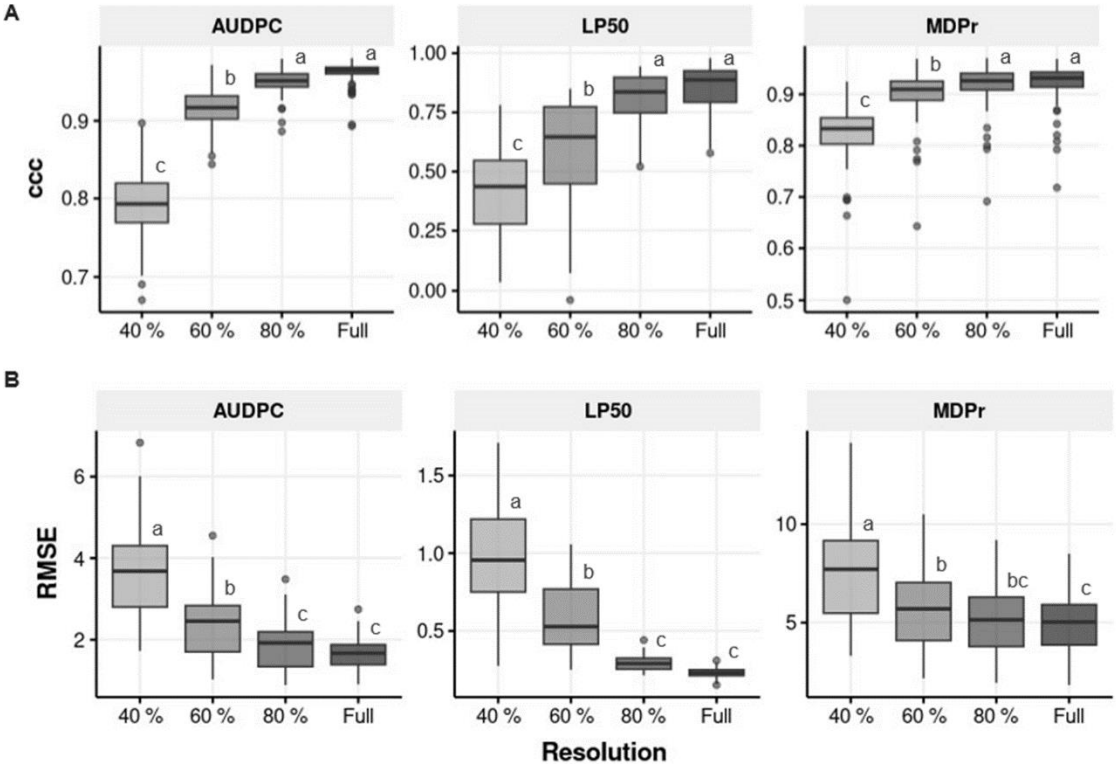

Figure 10. Boxplots showing the effect of image compression in the precision of comparison, by accuracy (A) and RMSE (B), between visual calculation and image-based calculation on LP50, MDPr and AUDPC. Different letters above the boxes indicate statistically significant differences at p = 0.05 according to the Tukey HSD test for n = 600.

Significant differences in accuracy and RMSE were also detected between segmentation index for all estimated disease parameters (Figure 11 and Figure **12**). In all cases, the NGRDI index was the best index accumulating significantly less error and providing a significantly higher accuracy while a* chrominance from LAB colour space and GLAI (Green Leaf Area Index) were the worst. The average accuracies of NGRDI were 0.975, 0.945, and 0.957 for AUDPC, LP50, and MDPr, respectively. The average accuracy of HI (Primary Colours Hue Index) was also higher than 0.9 in all cases, suggesting that this index also provided suitable rust estimation, may be useful to analyse leaves from other species.

Variations were also detected in the estimation capacity of each model over time. Indeed, accuracy and RMSE obtained from the estimations obtained from the different indices were more variable at 8 and 9 dai then at later stages (Figure 12). In general, accuracy increase while time advances and RMSE decrease. NGRDI was the

only index which gave accuracies higher than 0.9 for all time points, reaching an accuracy of 0.98 at 11 dai. Although accuracy of HI was slightly lower, the estimation capacity of HI was still acceptable (Figure 12).

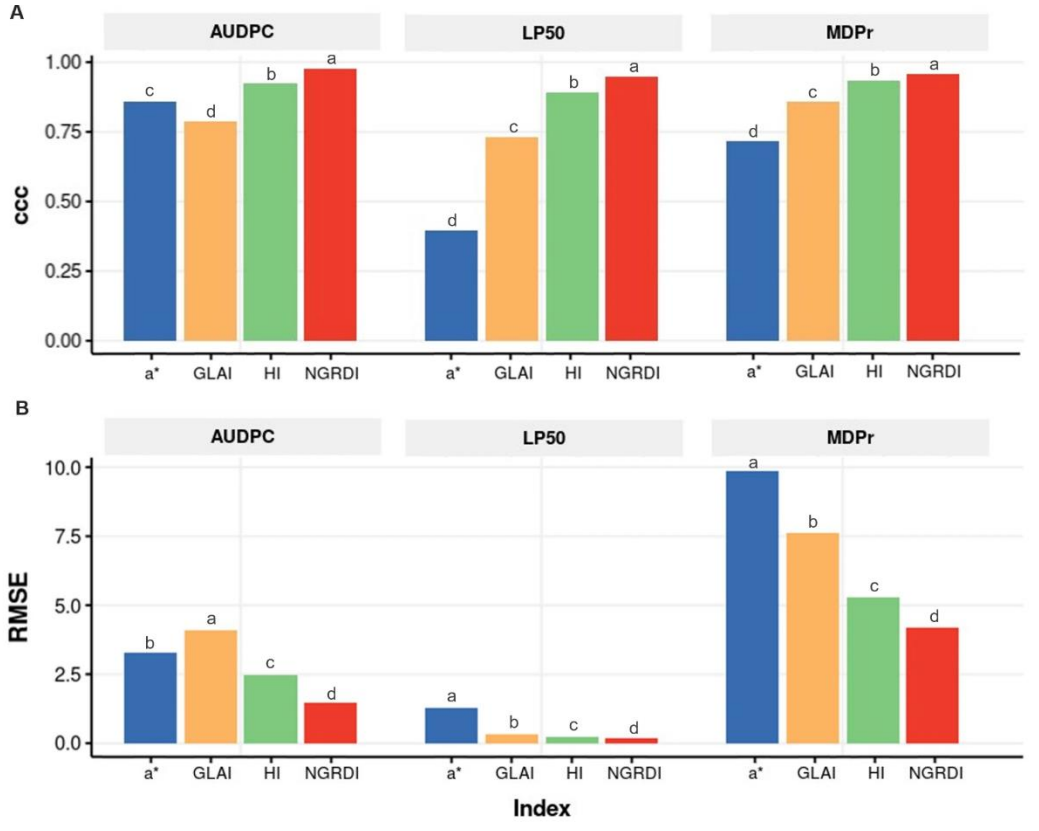

Figure 11. Bar plots showing the effect of the different indices on accuracy (A) and RMSE (B) when visual method and image-based method are compared by each parameter studied from images at 60% of the full resolution. Different letters above the boxes indicate statistically significant differences at p = 0.05 according to the Tukey HSD test for n = 600.

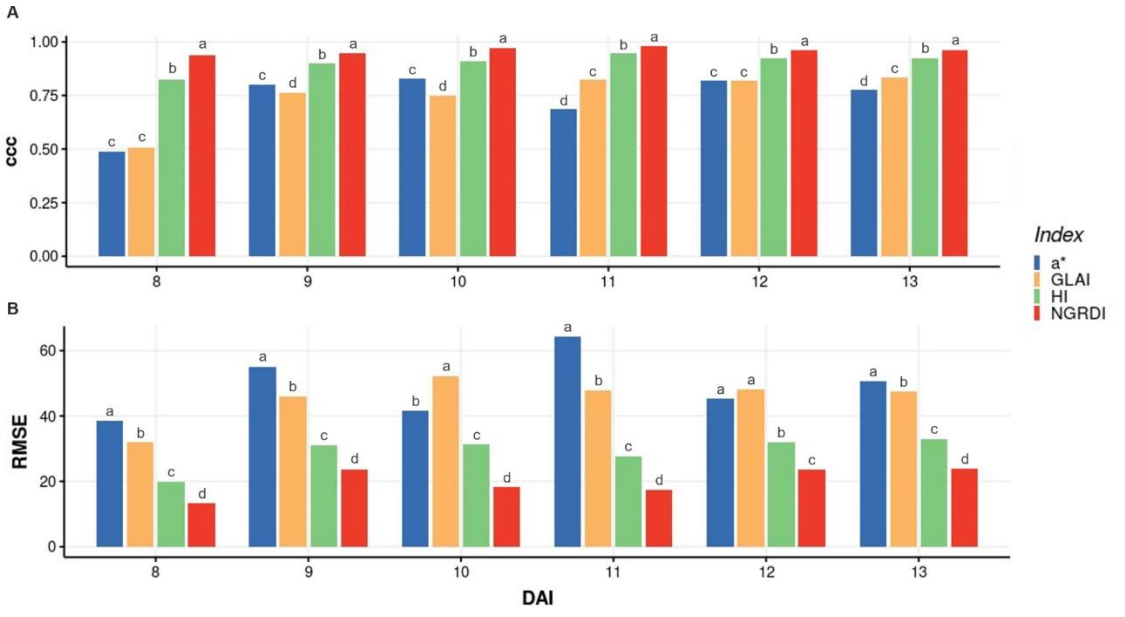

Figure 12. Bar plots showing the effect of the different indices on accuracy (A) and RMSE (B) when visual method and image-based method are compared for each parameter studied at 60% resolution. Different letters above the boxes indicate statistically significant differences at p = 0.05 according to the Tukey HSD test for n = 600.

5. Discussion

In recent years, advancements in image analysis software and computing power have enabled the use of high-throughput methods for plant disease phenotyping. These methods are nowadays used to analyse plant diseases at different architecture levels, including stems, leaves, and roots (Bock et al. 2010). Remote sensing techniques are playing a major role in modern breeding programs, providing accurate and high-resolution methods for identifying and quantifying novel natural variations within crops (Dissanayake et al. 2020; Watanabe et al. 2017; Yang et al. 2021). This present study describes a new method for the automatic assessment of daily rust disease parameters from RGB images and their integration into rust disease progression parameters fastening both disease ratings and phenotype data analysis. The method, developed on the R programming environment, counts, measures, and reports the damage caused by rust on pea leaflets. Moreover, when images are provided in a temporal sequence, the method can accurately integrate the damage into the most common disease progression parameters and report them by genotype in a ready-to-use data frame. Overall, the image-based method proposed here to analyse rust disease progression in pea provides breeders with a powerful tool to improve the efficiency and effectiveness of their breeding programs. It enables the rapid and accurate screening of large germplasm collections against rust, which will facilitate the future development of pea cultivars with high level of rust resistance.

Although not tested, the method proposed should be easily applied to evaluate rust in other plant species.

5.1. Automatization of Pea Rust Progress Monitoring

Traditional image-based methods for evaluating plant aerial diseases have been destructive and do not allow comprehensive disease tracking. The proposed method enables the periodic evaluation of several disease parameters throughout the first cycle of rust disease on the same sample and to integrated them into disease progression parameters (AUPDC, MDPr and LP_{50}) providing a comprehensive analysis of the pea genotype response to rust. This approach is an adaptation of previously designed detached leaf assay used to assess other foliar diseases such as powdery mildew in legumes (Barilli et al. 2019) and cereals (Rubiales and Carver 2000) which enable the preservation of viable leaflet simples throughout the first cycle of rust disease and ensure standardize condition for image acquisition. One of the key advantages of the proposed method is the improved efficiency in data collection. The image analysis workflow (Additional file 4) allows for disease monitoring and captures maximum information regarding disease progression in an automatic process, which, as far as we know, could not be achieved by the previously developed methods (Alves et al. 2022; Dissanayake et al. 2020; Gallego-Sánchez et al. 2020; Pierz et al. 2023). Here, estimation of the daily resistance components (IF, DS, and PS) for each leaflet allows the calculation of disease progression parameters such as AUDPC, LP50, and MDPr for each genotype. Application of this method was suitable to discriminate between genotypes and identify pea genotypes with high partial resistance such as GEN62 (Figure 8) providing seminal works for the implementation of this method to evaluate large pea collection. The fast, accurate and comprehensive information gathered by this method is crucial for future breeding efforts of pea with higher resistance to rust (Rubiales et al. 2015).

Very few image-based analysis methods tackle temporal analysis of fungal infection in plants (Heineck et al. 2019; Pavicic et al. 2021). Beside some studies in different *Arabidopsis thaliana* (L.) pathosystems (Pavicic et al. 2021), Only one study targeted rust and compared rust disease progression parameters estimated by image analysis in R or visual rating (Mattos et al. 2020). This study that counted rust pustules on ryegrass leaves with the "EBImage" R package allowed to estimate AUDPC with an accuracy of 0.77 which is lower than the accuracy we obtain in pea with the present method ($\rho_c = 0.975$). In addition, by contrast with all previous method, calculation of disease progression parameters is integrated in the R script, resulting in an automated process that incorporates all quantitative assessments obtained through RGB image analysis that will help researchers to better understand disease progression and resistance mechanisms in aerial diseases.

5.2. Processing Time Optimization

Image-based disease assessments face the challenge of balancing storage capacity, processing time, and accuracy. The present R-based approach is based on the "pliman" package functions. This package, recently launched by Olivoto et al. (2022a), is specifically designed for plant disease image phenotyping. It is a promising tool faster than other software such as the widely used license-based APS Assess 2.0 software or the LeafDoctor free-app, while still maintaining high levels of accuracy (Olivoto et al. 2022b). The processing speed of the R package "pliman" has been considerably increased compared to the first stable version available on CRAN (v 1.0.0). For example, the processing time required to analyse one image of ~ 3 mega-pixels (1367 × 2160) with only one leaflet was previously reported as ~ 1 and 3 s, for a parallel and sequential strategy, respectively (Olivoto et al. 2022b). Considering the average time to process one Petri dish (~ 900 ms) with 9 leaves using an image of ~ 3.3 mega-pixels (1814 × 1814), we have shown that the processing time per leaflet is almost nine time faster. The greater speed observed here is attributed to recent improvements of the packages that now use C + + language for the most critical functions (Eddelbuettel and Francois 2011) which offers faster computation speeds compared to other languages such as JavaScript or Python (https://github.com/niklas-heer/speed-comparison). The potential of "pliman" to quantify disease severities was initially explored on infected *Populus* spp. leaves, and it was found to be faster and more efficient than manual analyses with ImageJ software to estimate necrotic area percentages (Dreischhoff et al. 2023). However no previous studies used "pliman" to assess rust disease.

The present method can analyse 100 pea samples in 27.4 segs at full resolution, or in 10.6 segs at 60% resolution, provide estimates with accuracies higher than 0.91 at all time-points. This is a significant improvement compared to the previously developed RUST software developed on Image-J that took 20 to 80 min to estimate IF on 100 oat samples in automatic and semi-automatic mode, respectively (Gallego-Sánchez et al. 2020; Milus et al. 2009). Additional methods using free or licensed image-based analysis software are able to predict rust IF with good accuracy. Although not all studies reported processing time. The present method appears, as far as we know, 100 to 200 times faster than previously existing method to quantifying rust IF. In addition, these previous methods did not allow estimation of disease progression parameters such as AUDPC while they are automatically estimated by the present method within the processing time. In others pathosystems, incorporation of additional colour space transformations or implementation of machine learning tool was shown to improve lesion segmentation and accuracy however each additional step increased processing time. For example, McDonald et al. proposed an automated method for measuring soybean [*Glycine max* (L.) Merr] frogeye leaf spot that involves converting RGB images to HSB (hue, saturation,

brightness) and then to LAB (lightness, a* chrominance, b* chrominance) to remove the background and isolate the lesion (McDonald et al. 2022). While the method was highly accurate, reaching accuracy of 0.99 it took 16.7 min to analyse 100 leaf samples. Although, this method was slightly more accurate, it was around 100 times slower than the method proposed here. Implementation of machine learning to segment and quantify cassava (Manihot esculenta Crantz) bacterial blight disease severity also improved accuracy but takes 250 min to analyse 100 cassava leaves due to higher computer requirements (Elliott et al. 2022). The method proposed here is simpler and more cost-effective allowing the comprehensive fast analysis of pea rust disease without compromising accuracy. It is based on RGB spectral indices segmentations discussed by Alves et al. (2022). These authors also coincide in the use of NGRDI and HI as the optimal one for foliar diseases segmentations when compared to others (Alves et al. 2022).

The high accuracy provided for all disease parameters compared with the present method coupled with it unprecedent speed which should be even more reduced by reducing image resolution to 60% if needed allow it is implementation to evaluate large collections. It could be the method of choice for the evaluation of NAM population, typically comprising several thousand genotypes (Diers et al. 2018; Gireesh et al. 2021) that cannot be evaluated by current rust evaluation methods.

5.3. Rust Resistance Mechanisms Estimations through RGB Images

The proposed RGB image-based method in controlled conditions showed high accuracies (ρc) exceeding 0.9, and in most stages of the disease cycle. This method requires neither a large budget nor specific training, making it a cost-effective and feasible option for phenotyping rust in pea and other crops. In contrast to other complex techniques like multi- or hyperspectral imaging, which have also proven useful in rust phenotyping in different rust pathosystems (Zhang et al. 2012, 2014), our approach stands out as a more accessible and user-friendly alternative. The acquisition of these sophisticated phenotyping platforms can be prohibitively expensive and demands specialized training, limiting their widespread application (Simko et al. 2017).

Traditionally, DS is the measure used to assess the extent of damage caused by plant diseases, especially those affecting the aerial parts (Alves et al. 2022). The colour thresholding method used in this study is considered the most reliable method to accurately determine DS in phytopathometry (Bock et al. 2020). To automate DS assessment, the capacity to accurately predict DS of several free open-source or licensed software have been explored (Barbedo 2016; Bock et al. 2008; Schneider et al. 2012; Vale et al. 2003). In the context of the R environment, Mattos et al. (2020) developed models that indirectly determined the percentage of injured area from images of Septoria leaf spot in tomatoes (*Solanum lycopersicum* L.), achieving accuracies of 0.925 and 0.98 for the percentage of necrotic area and the necrotic plus

chlorotic area, respectively. These accuracies are similar to the accuracies obtained with the present method, but the method proposed by Mattos et al. required to manually delimit the injured area using an image software (GIMP) which is not require for our method. Previous study on crown and stem rust in perennial ryegrass (*Lolium perenne* L.), using the "EBImage" R package predicted crown rust with similar accuracy (0.93) but only allow evaluation of from single-leaf samples at a single time point and it was around 10 time slower (Heineck et al. 2019).

Despite being widely used, visual DS estimations can be imprecise and biased for diseases with small and numerous lesions like rust (Del Ponte et al. 2022). Therefore, researchers usually also analyse IF and/or PS that are less prone to user bias to quantify more precisely partial resistance in pea (Barilli et al. 2014). Some previous studies reported the estimation of some of these disease components through RGB image analysis with variable efficiency (Bade and Carmona 2011; Díaz-Lago et al. 2003; Gallego-Sánchez et al. 2020; Milus et al. 2009).

For instance, the widely used license based Assess 2.0 software seems efficient to estimate rust PS in wheat (Bade and Carmona 2011) although its accuracy to estimate IF was more limited as shown by a study on maize (*Zea mays* L.) leaves ($R2 = 0.49$) (Díaz-Lago et al. 2003). By contrast, highly accurate estimation of rust IF in oat was obtained with the license-based Image Pro or the free ImageJ software that reported accuracies of 0.97 in pustules counting but with image resolution doubling the image resolution required by the present method (Gallego-Sánchez et al. 2020; Milus et al. 2009). Heineck et al. also estimate IF in their methodology of crown and stem rust in perennial ryegrass images, although the reported accuracies were lower reaching 0.77 and 0.84 respectively (Henieck et al. 2019).

Moreover, our image-based approach provides a more detailed and precise characterization of rust disease resistance mechanisms and its progression. Traditional methods may suffer from subjectivity and limitations in capturing subtle variations in rust disease development. In contrast, our method captures the high complexity of rust disease by analysing daily symptoms and integrating them into disease progression parameters, allowing for a more comprehensive understanding of the plant-pathogen interaction.

6. Conclusion

Accurate and detailed information on the phenotype of rust disease in pea crop is crucial to develop new cultivars with improved genetic resistance. The proposed method for image-based rust phenotyping uses RGB spectral indices segmentation and pixel value thresholding to separate important features from the image, such as the leaf and pustule lesions if present. This enables the measurement of disease severity by calculating the percentage of the leaflet area affected and counting the number of pustules on a leaflet. With minimal computational requirements, the

program can analyse hundreds of images in seconds and has accuracy comparable to visual methods. The proposed method is significantly faster than previously developed image-based workflows for plant disease phenotyping without compromising accuracy. In addition, this is the first methods that allow to capture most of the complexity of rust disease in pea by assessing daily DS, IF and PS and integrating them into three disease progression parameters through an automated process. Being developed as an R script, the proposed method can also easily adjust to evaluate rust in other pathosystems where these detailed measurements are necessary to comprehend partial disease resistance. In addition, the application of image processing alleviates the raters bias that can be introduce in traditional methods, making it a convenient and precise approach to gather data on rust disease symptoms. As a results, application of the proposed method can have implications for both basic research and plant breeding, paving the way for more effective disease management strategies and the development of pea varieties with higher resistance in the future.

7. Additional files

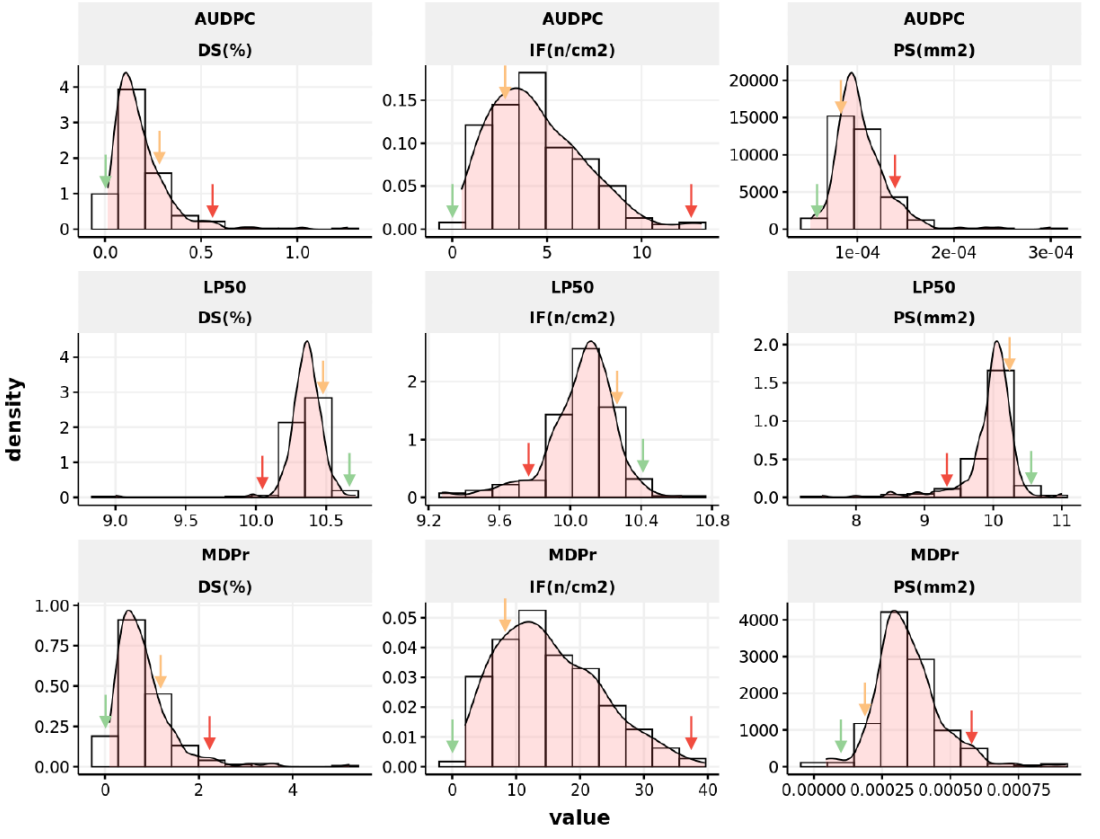

Additional file 3. Histograms showing disease parameters distributions. Red, yellow, and green arrows indicate the values for GEN261, GEN56 and GEN62, respectively.

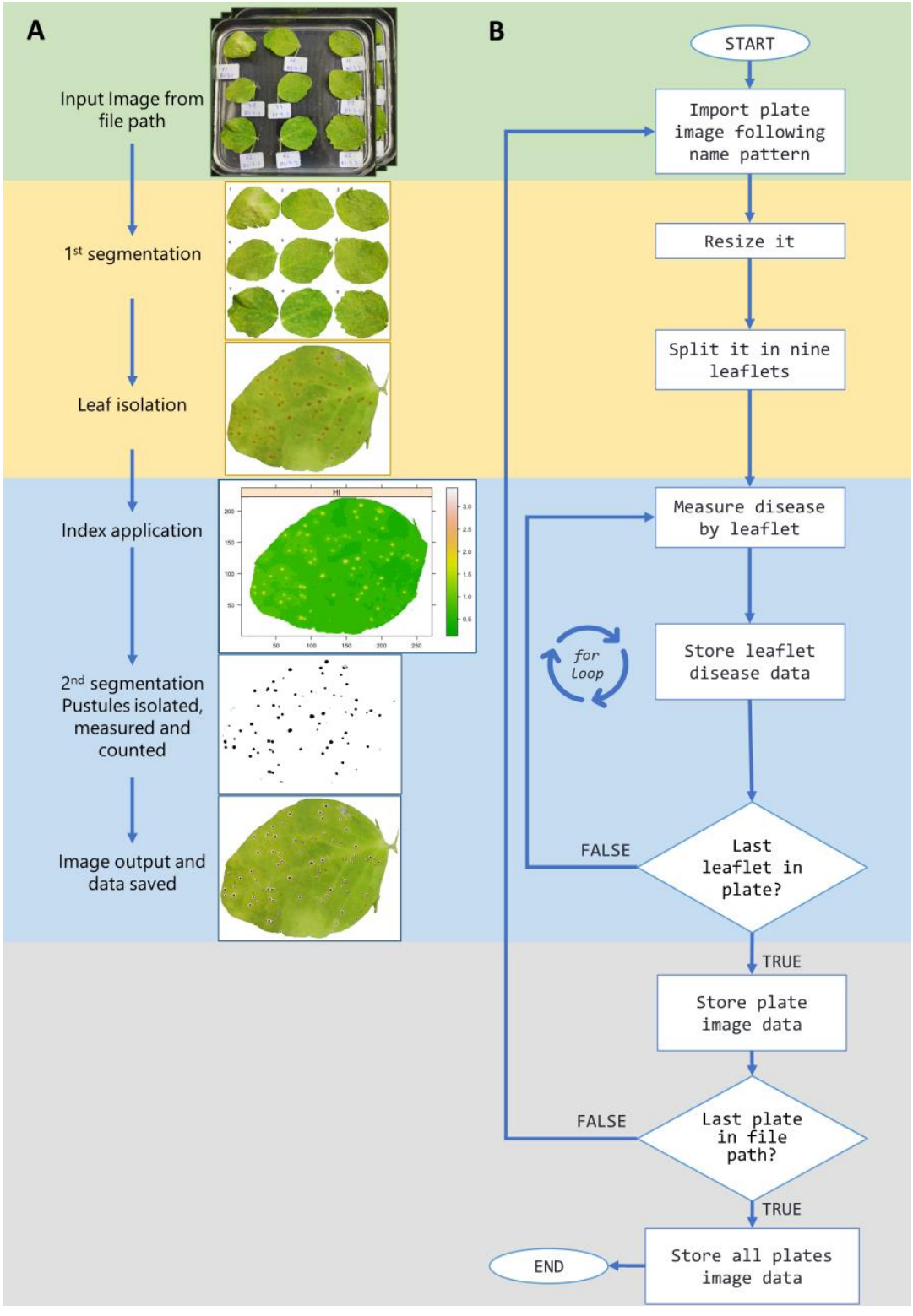

Additional file 4. Image processing pipeline. (A) shows the image modifications from the original image to the individual leaflet output and (B) represents the function flowchart summarized in the script. Every coloured region represents the four main steps. In green, the

image loading; in yellow, the leaflet segmentation; in blue, the lesion segmentation and, in grey, the storing of the collected data and reporting.

Additional file 5. This table shows the processing time for 600 leaflets of the CPU in hh:mm:ss format by index, processing strategy and resolution applied.

			Pustules index segmentation			
			NGRDI	**HI**	**GLAI**	**a***
Processing strategy	Sequential	Full resolution	00:12:40	00:12:55	00:12:27	00:12:10
		80 % resolution	00:08:23	00:08:53	00:08:21	00:08:13
		60 % resolution	00:05:18	00:05:44	00:05:10	00:05:06
		40 % resolution	00:03:06	00:03:19	00:03:19	00:02:58
	Parallel	Full resolution	00:02:22	00:02:27	00:02:26	00:02:25
		80 % resolution	00:01:39	00:01:40	00:01:40	00:01:39
		60 % resolution	00:01:02	00:01:09	00:01:05	00:01:05
		40 % resolution	00:00:42	00:00:42	00:00:42	00:00:42

Chapter 4
Genome-Wide association study uncovers pea candidate genes and pathways involved in rust resistance

1. Abstract

Pea is an important temperate legume crop providing plant-based proteins for food and feed worldwide. Pea yield can be limited by a number of biotic stresses, among which, rust represents a major limiting factor. Some efforts have been made to assess the natural variation in pea resistance, but its efficient exploitation in breeding is limited since the resistance loci identified so far are scarce and their responsible gene(s) unknown. To overcome this knowledge gap, a comprehensive Genome-Wide Association Study (GWAS) on pea rust, caused by *Uromyces pisi*, has been performed to uncover genetic loci associated with resistance. Utilizing a diverse collection of 320 pea accessions, we evaluated phenotypic responses to two rust isolates using both traditional methods and advanced image-based phenotyping. We detected 95 significant trait-marker associations using a set of 26,045 DArT-seq polymorphic markers. Our in-silico analysis identified 62 candidate genes putatively involved in rust resistance, grouped into different functional categories such as gene expression regulation, vesicle trafficking, cell wall biosynthesis, and hormonal signalling. This research highlights the potential of GWAS to identify resistance sources, molecular markers associated with resistance and candidate genes against pea rust, offering new targets for precision breeding. By integrating our findings with current breeding programs, we can facilitate the development of pea varieties with improved resistance to rust, contributing to sustainable agricultural practices and food security. This study sets the stage for future functional genomic analyses and the application of genomic selection approaches to enhance disease resistance in peas.

2. Introduction

Pea (*Pisum sativum* L. 2n = 14) is one of the principal legume crops grown globally, ranking as the third most produced pulse in the world after dry beans and chickpeas (FAOSTAT 2021). This crop is a vital source of plant-based protein for both animal feed and human food, offering significant health benefits (Tulbek et al. 2016; Clemente and Olias 2017). Additionally, pea plays a crucial role in agricultural sustainability through nitrogen fixation enhancing soil fertility and structure, making it a valuable component of crop rotation or intercropping systems, particularly in conjunction with cereals (Skoufogianni et al. 2019; Gungaabayar et al. 2023).

Despite its global significance, peas have received less attention compared to other crops such as soybeans or wheat, where yields have significantly increased over the years due to the development of new varieties and improved farming practices (Rubiales et al. 2019). One of the main reasons for the lower yield of peas is their high susceptibility a wide range of diseases and pests (Rubiales et al. 2015, 2023). A major disease affecting peas is rust, which can be caused by two different biotrophic fungus: *Uromyces viciae-fabae* (Pers. de Bary) or *U. pisi* (Pers.) (Wint.). In warm and humid climates, the disease is attributed to *U. viciae-fabae*, whereas in more temperate

climates, *U. pisi* is the causal agent (Barilli et al. 2012a). Both fungi can cause yield losses of up to 50% and 30%, respectively (Singh et al. 2023). The impact of pea rust on both yield and seed quality highlights the pressing need for targeted breeding and management strategies to mitigate this disease.

Rust control with fungicides is effective (Emeran et al. 2011) but requires repeated treatments which is hardly economical for low input field crops like pea. Also, concerns are raised on environmental issues of pesticide control. To address this, efforts have been made to control pea rust inducing systemic acquired resistance (Barilli et al. 2009b) or using natural compounds, that were shown promising although the available formulations are only partly effective, and their long-term environmental impacts remain unverified (Barilli et al. 2012b, 2017, 2022). Therefore, further emphasis is needed to develop cultivars resistant to rust. In this line, large pea germplasm collections have been evaluated for resistance to *U. pisi*, disclosing and characterizing variable levels of incomplete resistance, with no complete resistance available so far (Barilli et al. 2009a; Osuna-Caballero et al. 2022). Partial resistance (PR) is characterized by a non-hypersensitive response and reduced disease severity (DS). It is very frequent in other legumes against various rusts, and it is the common source of resistance found in peas against rust (Rubiales et al. 2011). Conversely, hypersensitive resistance (HR), often monogenic in origin, has also been observed in other rust pathosystems caused by *U. viciae-fabae* in lentils and faba beans (Avila et al. 2003; Negussie et al. 2012; Rubiales et al. 2013; Adhikari et al. 2021). Recent screenings of a pea core collection have uncovered new sources of PR and identified for the first time a pea accession combining HR and PR against *U. pisi* (Osuna-Caballero et al. 2022). Furthermore, new, and more efficient image-based phenotyping methods are improving the limitations of traditional breeding in this pathosystem (Olivoto et al. 2022; Osuna-Caballero et al. 2023). Nevertheless, despite previous efforts to unravel the genetic control underlying resistance to this fungal disease—where QTL responsible for resistance in *P. fulvum* were identified—clarifying the genetic architecture of HR and PR to rust caused by *U. pisi* remains necessary (Barilli et al. 2018). Furthermore, identification of candidate genes could be instrumental in foreground selection of favourable alleles.

The phenotypic information available in pea germplasm, combined with new high-throughput phenotyping systems focused on rust, and the availability of high-quality reference pea genomes (Kreplak et al. 2019; Yang et al. 2022), enables more in-depth genomic studies (Pandey et al. 2021). Genome-wide association studies (GWAS) have emerged as a powerful approach to dissect the complex genetic underpinnings of quantitative traits within diverse plant populations. By scanning the genome for polymorphisms correlated with phenotypic variance, GWAS has facilitated the identification of both single nucleotide polymorphisms (SNPs) and DArT-seq derived markers that are intricately linked with key traits, providing candidate genes associated with traits of interest across numerous legume species

(Susmitha et al. 2023). Specifically, recent GWAS in peas have been useful to identify favourable alleles for agronomic traits or disease resistance (Alemu et al. 2022; Leprévost et al. 2023), but there is still a lack of such studies for rust disease.

In the present study, we bring new sources of resistance against two *U. pisi* isolates by employing both traditional screening methods and innovative image-based methodologies across an extensive germplasm collection of 320 pea accessions, representative of global diversity. Moreover, we explored the genetic architecture of partial resistance to rust infection through GWAS, as a preliminary step towards more efficient precision breeding. To achieve this, the phenotypic response of the world collection of pea accessions inoculated with *U. pisi* was integrated with previously generated DArT-seq polymorphic markers, revealing significant associations between them. Our in-silico analysis of the genes containing or in the vicinity of the associated markers led to the discovery of previously uncharted metabolic pathways potentially implicated in rust response. These findings open new avenues for precision breeding, offering novel targets for rust resistance improvement and enhancement of crop resilience and productivity through the development of new pea rust-resistant varieties.

3. Material and Methods

3.1. Plant and Fungal Material

Plant material consisted in a diverse core collection of 320 *Pisum* accessions of worldwide origin gathered previously at Institute for Sustainable Agriculture – CSIC to ensure an extensive range of characteristics in terms of phenotype and their genetic makeup (Rispail et al. 2023). The collection includes accessions that have already demonstrated their potential for resistance to several pea diseases including rust (accessions IFPI3260, PI347352, PI347343, PI347353 and PI347389) (Barilli et al. 2009a).

To assess the resistance levels within the collection to rust disease, we used in this study two highly virulent isolates of *Uromyces pisi* that specifically affect pea crop, UpCo-01 and UpKeS-05, preserved at IAS – CSIC (Barilli et al. 2012a).

3.2. Phenotyping

Three series of experiments were conducted to assess the rust resistance components of the pea collection. One series of experiments took place under field conditions over three cropping seasons, involving adult plants, while the other two experiments were conducted in controlled conditions (CC) using seedlings infected with the *U. pisi* isolate UpCo-01 or UpKeS-05.

For the field experiment, the pea collection was evaluated over three consecutive crop seasons from 2018 to 2020 in Cordoba, Spain, as described in Osuna-Caballero et al. (2022). Briefly, ten seeds per accession were sown in 1-meter

rows, spaced 0.7 meters apart, in an alpha lattice design with three replicates. Mature plants were artificially inoculated with the *U. pisi* isolate UpCo-01, and Disease Severity (DS) was assessed as the percentage of rust coverage 30 days after inoculation (dai).

The first CC experiment, involved evaluating the pea collection against the UpCo-01 isolate, followed a randomized complete block design (RCBD), and the inoculations were performed as described in Osuna-Caballero et al. (2022). Screening was done with six replicates per genotype, visually counting pustules (Infection Frequency, IF) from 7 to 13 dai to estimate Area Under Disease Progress Curve (AUDPC), Latency Period (LP50) and Monocyclic Disease Progress rate (MDPr). Additionally, at 13 dai, DS and infection type (IT) was visually evaluated.

The second CC experiment, using UpKeS-05 isolate, replicated this design but with a different approach. In this case, we applied a detached leaflets procedure, as described in Barilli et al. (2022), to maintain the viability of the pea leaves and capture the rust evolution through imaging. Daily photographs of Petri dishes containing pea leaflets, from 7 to 13 dai, were analysed to determine IF, DS, and PS (pustule size, mm2), along with the corresponding disease progression parameters (AUDPC, LP50 and MDPr), using the RGB-method as described in Osuna-Caballero et al. (2023).

3.3. Phenotypic data analysis

The statistical analysis of the three phenotypic data sets (field, CCUpCo-01, and CCUpKeS-05) was conducted using R 4.2.2 (R Core Team, 2021) and the lme4 package (Bates et al. 2015) for mixed models. The linear model with interaction effect used to analyse the field data from multi-environment trials was applied using the genotype effect as fixed factor, while the remaining sources of variance, such as environment, environment x genotype interaction, and replicated block nested in environments, were included as random effects variables. Prior to analysis, field data set underwent an arcsine transformation to achieve normal distribution of disease severity percentages (DS), which was confirmed by checking the assumptions of residual normality and variance homogeneity. Heritability on the mean basis (H2) was calculated following the formula:

$$H^2 = \frac{\hat{\sigma}_g^2}{\hat{\sigma}_g^2 + \hat{\sigma}_i^2/e + \hat{\sigma}_e^2/(eb)}$$

Where $\hat{\sigma}_g^2$, $\hat{\sigma}_i^2$, and $\hat{\sigma}_e^2$ are the genotypic, the genotype-by-environment interaction, and the residual variance, respectively; and e and b are the number of environments and blocks, respectively.

For both controlled conditions (CC) phenotypic data sets, DS was transformed with an arcsine transformation, and other parameters related to disease progression

and daily resistant components (IF and PS) were transformed with a square root transformation to achieve normal distribution. The genotype effect was included as a fixed factor, and the replicate, block, and combination of genotype and replicate were treated as random effects variables in the mixed model analysis. In case of CC, the H2 was calculated as follows:

$$H^2 = \frac{\hat{\sigma}_g^2}{\hat{\sigma}_g^2 + \hat{\sigma}_e^2/rep}$$

Where *rep* means the number of replicates within the experiment.

For the three data sets, mean separation between accessions and the overall mean was determined using Dunnett's test ($p \leq 0.05$). The distributions are presented as best linear unbiased estimations (BLUEs) obtained from the mixed model. Correlation between estimated means under controlled or field conditions was assessed using the Pearson correlation coefficient. To simplify the complexity of the 21 traits evaluated, a Principal Component Analysis (PCA) was performed using factoextra R package (Kassambara and Mundt 2020).

3.4. Genotyping

The process of DNA extraction, DArTseq protocol, and data analysis were previously detailed in Rispail et al. (2023). In summary, the genotyping of the pea core collection was carried out using the DArTSeq approach, as described by Barilli et al. (2018). DNA was extracted from pooled leaves of 20 seedlings per accession and subjected to high-density Pea DArTSeq 1.0 array analysis. Data cleaning was performed to remove markers with low quality or lacking polymorphism, following the recommendations of Pavan et al. (2020). As a result, 26,045 polymorphic Silico-DArT markers were retrieved. The filtered markers were then mapped onto the improved *Pisum* reference genome sequences (Kreplak et al. 2019; Yang et al. 2022).

3.5. Genome-wide association mapping

The GWAS analysis between 26,045 DArTseq markers spread across the pea genome were tested for their association with rust disease variation on 320 pea phenotypes. In this study, a single-trait GWAS was conducted using two different models: the single locus mixed linear model (MLM) and the multi-locus Bayesian information and linkage disequilibrium iteratively nested keyway (BLINK) model (Huang et al. 2019). Both models were performed within GAPIT 3.0 (Wang and Zhang 2021) and have different assumptions: the MLM model allows for the identification of individual markers associated with the trait, while the BLINK model considers multiple markers simultaneously, considering the joint effects of nearby markers. Therefore, the analysis can capture both major and minor genetic effects contributing to the rust response variation.

The Bayesian information criterion (BIC)-based model selection procedure was used to determine the optimum number of principal components (PCs) required to efficiently control for population structure of the collection Additionally, the Astle kinship matrix was used to estimate relatedness among individuals, further accounting for potential genetic correlations (Astle and Balding 2009).

To determine significant DArTseq markers, two different threshold levels were applied. The Bonferroni corrected LOD threshold, calculated based on the number of markers (26,045), offers a more stringent criterion to minimize false positives. On the other hand, the false discovery rate (FDR) method, proposed by Storey and Tibshirani (2003), provides a less restrictive threshold, allowing for the identification of potentially interesting markers that might be missed by the Bonferroni correction. FDR limit was set for each model and trait combination to ensure less than one false positive association with the R package qvalue (Storey and Bass 2022).

To visualize the results, Manhattan plots were generated, displaying the -log10(p-value) for each marker along the seven chromosomes, highlighting regions where significant associations occur. Quantile-quantile (Q-Q) plots were also performed to assess the overall distribution of p-values and evaluate whether any genomic inflation or deflation occurred though the calculation of lambda (λ) using QQperm R package (Petrovski and Wang 2016). All models with genomic inflation (λ) below 0.8 or higher than 1.2 were not considered. Manhattan and Q-Q plots were generated using CMplot R package (Lilin-Yin 2023).

3.6. Candidate Genes and Pathways selection

To identify potential candidate genes, we scrutinized the genomic regions surrounding the significant DArTseq markers using the Cameor and ZW6 pea reference genome browsers (https://urgi.versailles.inra.fr/jbrowse/gmod_jbrowse/?data=myData/Pea/Psatv1a/data; https://www.peagdb.com/index/). We considered genes either containing a DArTseq marker or residing within a 30 kb window from the marker as putative candidate genes.

The process of gene annotation involved associating these candidate genes with enzyme codes to investigate their metabolic pathways using the Kyoto Encyclopaedia of Genes and Genomes (KEGG). In cases where the proteins encoded by these genes were not characterized in the KEGG database, we extended our search to include orthologous sequences. For this purpose, the TAIR database was mined to identify corresponding orthologous proteins in Arabidopsis thaliana. This extensive annotation approach facilitated the elucidation of the potential function of each gene and the delineation of pathways relevant to resistance mechanisms against pea rust. To enrich our analysis, we integrated this genomic data with existing literature and

performed comprehensive in silico analyses, thereby enhancing our understanding of the genetic factors contributing to rust resistance in peas.

4. Results

4.1. Variance components, Heritability and Correlations between Traits

The pea collection demonstrated a wide diversity of response to rust underscoring the large genetic heterogeneity of the pea collection. Under controlled conditions (CC), the response of the pea collection to each ruts isolate was different (Table 9). The UpCo-01 isolate exhibited higher virulence, with more pronounced AUDPC and DS average values (36.1 and 20.2%, respectively) compared to the UpKeS-05 isolate, which recorded an AUDPC_IF of 29.9 and a DS of 10.9% in average. Notably, symptoms development initiated earlier with UpKeS-05 than with UpCo-01, as indicated by their LP50_IF, with values of 8.98 and 9.28 days, respectively. Moreover, the MDPr_IF — representing the rate of disease symptom per time unit — was also higher for UpKeS-05. For both isolates, the highest coefficient of variation (CV%) values were obtained for AUDPC, MDPr, DS and IF, while LP50 presented the lowest CV% values. In terms of heritability, UpCo-01 consistently outperformed UpKeS-05 across most comparable traits, implying that a high portion of variability stemmed from genetic differences. A notable exception was IT, which exhibited a moderate H^2 value of 0.67, and LP50, with a lower H^2 value of 0.21.

Table 9. Variance components, heritability and descriptive statistic by phenotypic data set and its trait.

Data set	Trait	Average	SE	Range	Skewness	CV (%)	H^2	Accuracy
$CC_{UpCo-01}$	AUDPC_IF	36.07	1.24	173.07	1.77	61.52	0.77	0.87
	DS	20.21	0.48	55.44	0.59	42.44	0.86	0.93
	IF	50.48	1.8	252.31	2.34	63.95	0.76	0.87
	IT	3.79	0.01	1.6	-1.94	6.88	0.67	0.82
	LP_{50}_IF	9.28	0.02	2.76	0.18	4.12	0.21	0.45
	MDPr_IF	11.41	0.13	16.13	0.27	20.8	0.73	0.86
$CC_{UpKeS-05}$	AUDPC_DS	21.99	1.04	148.67	2.56	85.11	0.51	0.71
	AUDPC_IF	29.95	1.23	117.4	1.83	73.89	0.5	0.7
	AUDPC_PS	0.1	0.01	0.23	0.34	29.62	0.44	0.66
	DS	10.86	0.2	23.62	0.96	33.27	0.51	0.72
	IF	51.28	1.81	156.09	0.94	63.17	0.49	0.7
	LP_{50}_DS	9.31	0.08	3.69	-0.95	15.07	0.24	0.49
	LP_{50}_IF	8.98	0.07	3.51	-0.79	13.65	0.11	0.33
	LP_{50}_PS	9	0.07	3.66	-0.8	13.91	0.28	0.53
	MDPr_DS	0.93	0.03	3.38	1.41	60.19	0.51	0.72
	MDPr_IF	13.62	0.43	44.03	0.96	56.97	0.36	0.6
	MDPr_PS	0.38	0.01	0.98	1	45.41	0.4	0.63
Field $_{UpCo-01}$	DS2018	31.02	0.40	53.98	1.72	23.05	0.62	0.79
	DS2019	29.73	0.52	51.58	0.85	31.07	0.74	0.86
	DS2020	31.62	0.53	47.41	0.80	29.76	0.81	0.90
	DS_field	30.79	0.39	42.56	0.94	22.91	0.75	0.87

Field conditions revealed a slightly different picture (Table 9). As a result of the polycyclic evolution of the disease in the field, DS in the three field seasons were higher than in controlled conditions. While the three campaigns and their estimated average (DS_field) had similar mean values and ranges, the 2018 campaign displayed a lower H^2, accompanied by a pronounced positive skewness of 1.72. This suggests that most pea accessions exhibited reduced DS in 2018 campaign which is further corroborated by its lower CV% relative to the subsequent two field campaigns.

In general, the accuracy values—interpreted as the square root of H^2—consistently exceeded 0.7 for most traits, confirming the reliability of the experimental measurements. On the other hand, strong positive (> 0.50) and strong negative (< -0.50) skewness was detected for most traits confirming the need to transform raw values to achieve a normal distribution before fitting the mixed models and predicting the estimated means (BLUEs) for each trait.

Phenotypic correlations of BLUEs for each trait across different experimental conditions are depicted in Figure 13 in terms of Pearson correlation (ρ). As expected, the most pronounced correlations were observed within individual datasets. For instance, traits from the CCUpCo-01 dataset, including AUDPC, MDPr, and IF, exhibited strong and significant interrelations ($\rho > 0.9$, $P < 0.001$). A similar trend was observed for traits of the CCUpKeS-05 dataset, such as AUDPC_DS, AUDPC_IF, MDPr_DS, and MDPr_IF, and the DS measurements across the three field seasons. Several significant correlations were also detected between traits from different datasets. DS and IF consistently displayed notable correlations regardless the rust isolate, evidenced by values of $\rho = 0.57$ and $\rho = 0.58$ for UpCo-01 and UpKeS-05 isolates, respectively. Similarly, IT maintained slight but consistent correlations with DS across isolates, with $\rho = 0.34$ for UpCo-01 and $\rho = 0.35$ for UpKeS-05. Intriguingly, IT correlation with IF varied depending on the rust isolate from a low correlation for UpKeS-05 ($\rho = 0.15$) to a moderate correlation for UpCo-01 ($\rho = 0.54$). When correlation with Latency period was significant, this trait was always inversely proportional to the other trait. Accordingly, a moderate correlation was detected between LP50_IF and DS and its associated AUDPC with the UpKeS-05 isolate ($\rho = -0.36$). Unexpectedly, the latency period for pustule size (LP50_PS) directly correlated with MDPr_PS ($\rho = 0.47$) and, to a lesser extent, with AUDPC_PS ($\rho = 0.19$). This suggests that a delayed pustule size growth accelerates the disease rate (MDPr) and affects positively the AUDPC in terms of pustule size.

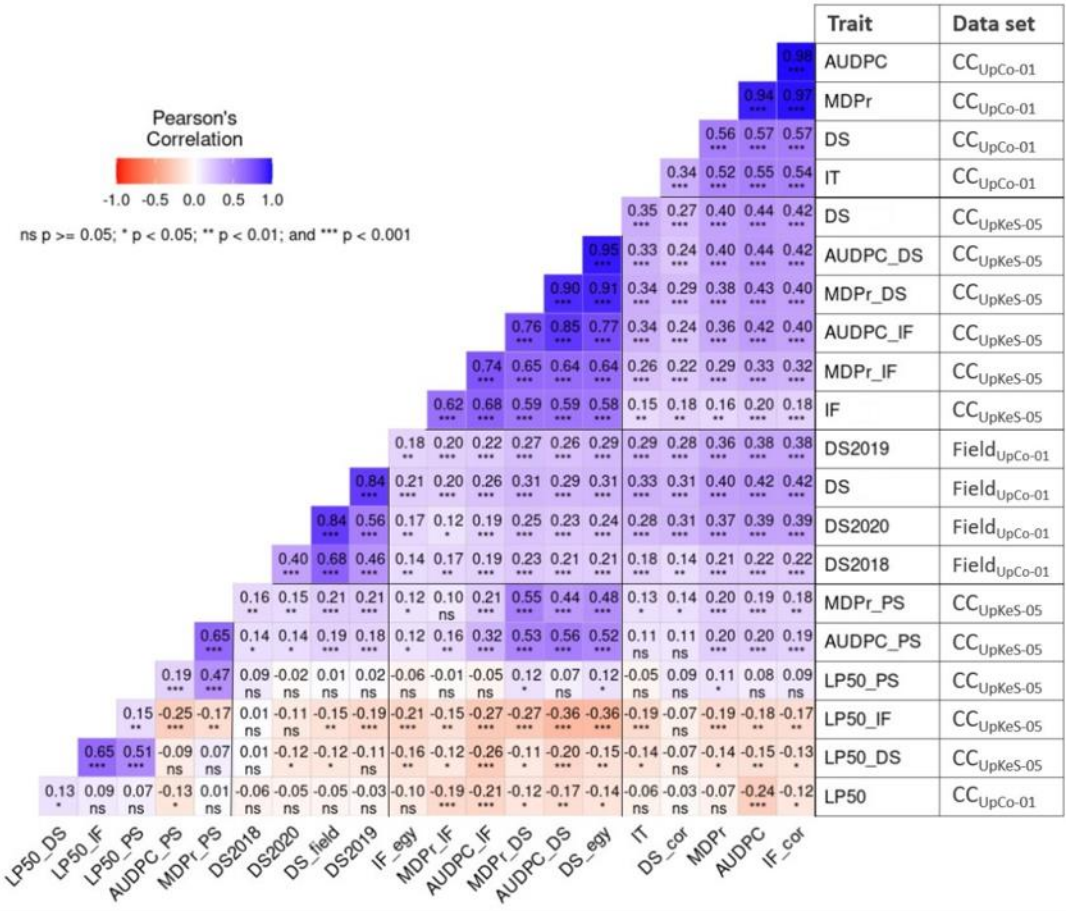

Figure 13. Cor plot based on Pearson's correlation values between phenotypic traits across the three-dataset evaluated with two different *U. pisi* isolates (UpCo-01 and UpKeS-05).

The PCA biplot provides a comprehensive visual representation of the primary patterns of variability among the twenty-one traits across the three datasets (Figure 14). The first two principal components (PCs), accounted for over 47% of the total trait variability. Dim1 differentiated traits based on their influence on rust symptoms. Traits positively contributing to rust symptoms clustered on the right, while those playing a protective role, such as latency periods, positioned on the left. By contrast, Dim2 effectively delineated traits based on the rust isolate. Specifically, traits assessed for UpCo-01 were situated at the top of the biplot, while those associated with UpKeS-05 are anchored at the bottom. Mirroring the patterns observed in the PCA biplot (Figure 14), the correlogram (Figure 13) also indicated that the DS values from the field campaigns exhibited stronger correlations with CC traits evaluated for UpCo-01.

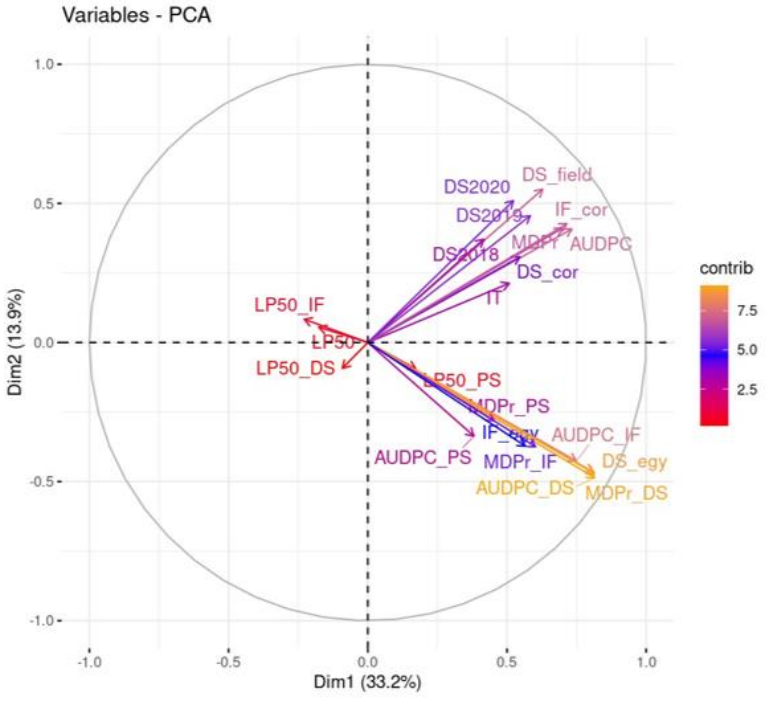

Figure 14. PCA biplot by trait contribution to phenotypic variance.

4.2. Detection of Associated Markers

To identify genetic variations associated with rust symptoms in pea, a GWAS was conducted using two different models, MLM and BLINK, for each of the 21 traits evaluated in three conditions across 320 pea accessions. A total of 95 DArTseq markers were found to be significantly associated with some of the evaluated traits in combination with the two models applied (Figure 15 and Additional file 6). Examining the BIC estimates, the genomic inflation factor (λ) and the QQ plot revealed that population structure was efficiently controlled by the Kinship matrix without the need to add other population structure covariates (PCs) (Figure 16, Table 10, and Additional file 7).

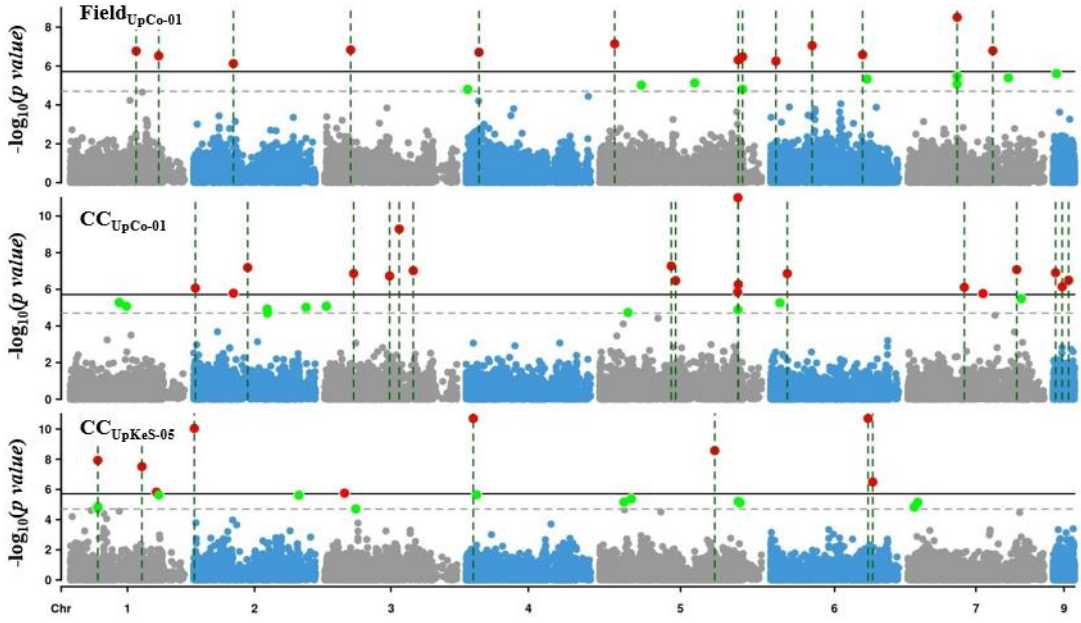

Figure 15. Manhattan plots showing marker significance in a combination of MLM and BLINK models by phenotypic data base across pea genome. Chromosome 9 shows unmapped markers onto reference genome. Associated markers through Bonferroni-based LOD are highlighted in red and the genomic region with dashed lines while in green are the associated markers retrieved based on FDR adjustment method.

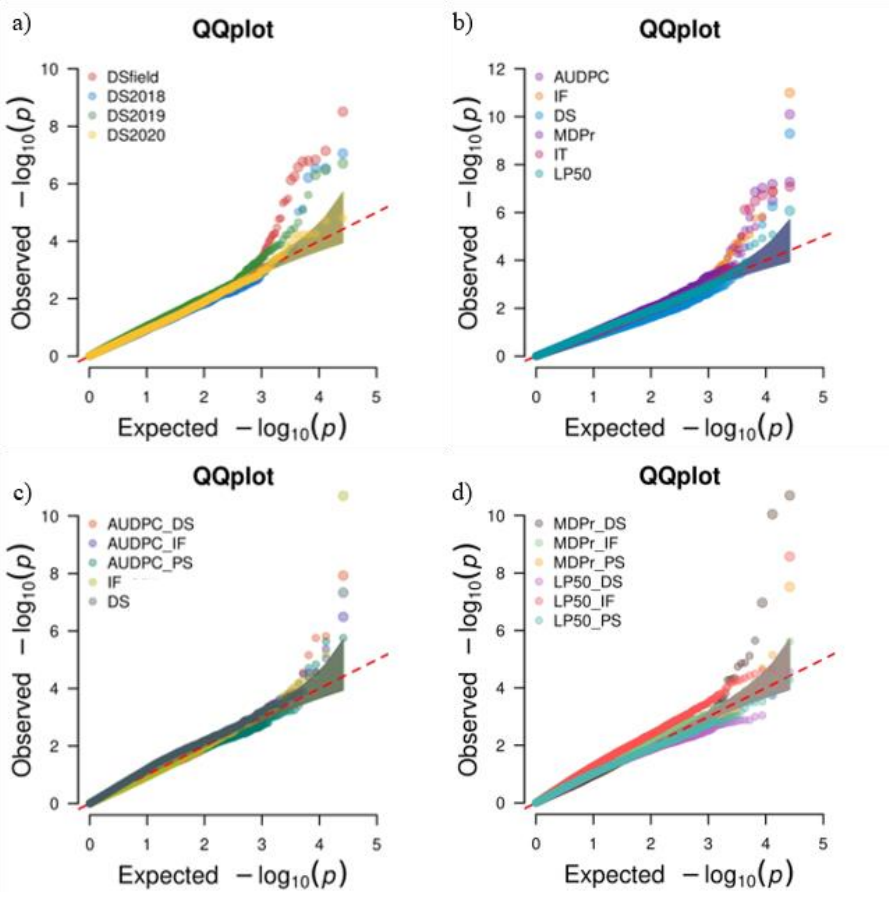

Figure 16. Q-Q plots between theoretic and observed p values using the BLINK model. a) and b) show p values from UpCo-01 isolate in field and controlled conditions, respectively. c) and d) show p values from UpKeS-05 results in controlled conditions.

The BLINK approach identified 70 markers linked to pea rust of which 49 were unique to this model while the MLM model detected 46 associated markers of which 25 were unique to this method. Notably, 21 associated markers were common to more than one trait or model (Figure 17a) while one marker was identified from all three data sets (Figure 17b).

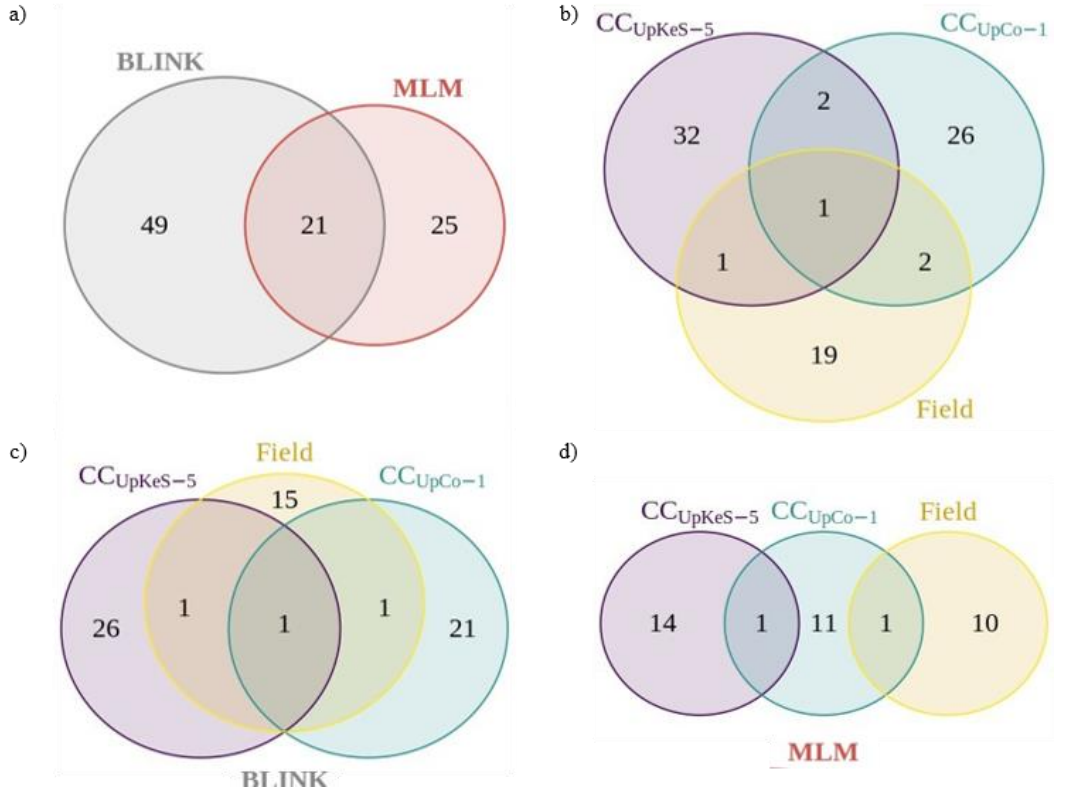

Figure 17. Venn diagram of common markers across data sets. a) and b) represent the common associated markers by applied model and the common associated markers by phenotypic dataset in combination of both models' outputs. c) and d) show the linked markers to pea rust from BLINK and from MLM results, respectively.

In general, the BLINK method yielded a higher number of significantly associated markers with lower p-value and higher LOD (Table 10). The total phenotypic variation explained by the associated marker for each trait (PVE) varied also greatly depending on the GWAS model. As the BLINK model identified more significant marker-trait associations for each trait, their corresponding PVE_{sum} was generally higher (Table 10). The highest number of associated markers for a single trait was identified with the BLINK method for DS_field, with a total of 13 markers explaining 86.2% of the total phenotypic variance while the MLM model only uncover 3 associated markers for this trait accounting for 10.2% of the phenotypic variance (Table 10). By contrast, the MLM method uncovered 7 markers associated with AUDPC for UpCo-01 under CC while BLINK only uncovered 5 significantly associated marker for this trait although associated markers identified by both methods explained around 70% of PVE_{sum}.

Table 10. BLINK and MLM model outputs obtained for each trait from the three phenotypic data sets. N indicates the number of significant marker-trait associations; λ is the genomic inflation factor; the LODrange is the range of the -log10(p-value); PVE_{range} is

the range of the phenotypic variance explained by each individual marker and PVE_{sum} is the total phenotypic variance explained by the associated markers.

		BLINK MODEL					MLM MODEL				
Data set	**Trait**	**N**	**λ**	**LOD_{range}**	**PVE_{range}**	**PVE_{sum}**	**N**	**λ**	**LOD_{range}**	**PVE_{range}**	**PVE_{sum}**
$CC_{UpCo-01}$	AUDPC	5	0.9	5.1-10.1	3.4-17.8	69.2	7	1.1	5.3-7.1	2.5-16.1	73.7
	DS	3	0.8	6.0-9.3	7.5-10.5	26.6	1	1.0	4.6	6.1	6.1
	IF	3	0.9	5.4-13.0	1.5-8.4	47.6	7	1.0	5.5-6.2	6.0-17.5	78.5
	IT	7	0.9	5.8-7.2	2.2-16.1	73.6	2	1.1	4.5-6.3	2.2-9.6	11.7
	LP_{50}	3	1.0	4.4-6.1	6.1-7.6	20.1	1	1.0	4.7	6.3	6.3
	MDPr	5	1.0	6.5-7.5	3.0-15.4	52.9	2	1.1	4.7-4.7	3.9-6.2	10.1
$CC_{UpKeS-05}$	AUDPC_DS	4	1.0	4.6-7.9	2.6-10.6	24.3	3	1.0	4.5-5.3	2.6-5.2	13.1
	AUDPC_IF	5	1.1	4.6-6.5	3.6-10.5	39.7	2	1.0	4.4-4.4	2.8-3.6	6.3
	AUDPC_PS	2	1.0	5.8-6.2	3.2-5.0	8.1	2	1.0	5.0-5.0	6.3-12.0	18.3
	DS	3	1.1	4.8-7.4	4.4-14.4	29.6	2	1.0	5.0-5.3	6.9-12.8	19.7
	IF	3	1.0	5.2-10.7	14.1-17.6	17.6	1	0.9	4.5	2.2	2.2
	LP_{50}_DS	1	1.0	4.4	5.3	5.3	1	1.0	4.5	5.3	5.3
	LP_{50}_IF	7	1.2	4.9-8.7	0.4-7.6	19.6	2	1.0	4.8-4.8	4.5-6.3	10.8
	LP_{50}_PS	1	1.0	4.5	6.6	6.1	1	0.9	4.4	4.4	4.4
	MDPr_DS	6	0.9	5.1-10.7	3.8-15.3	58.5	6	1.0	5.3-5.9	2.5-15.3	56.1
	MDPr_IF	3	1.1	4.5-5.7	1.1-7.5	13.8	2	1.0	4.4-4.4	5.2-7.5	12.7
	MDPr_PS	3	1.0	5.2-7.5	2.6-9.9	20.5	2	1.1	4.5-5.5	5.2-9.9	15.1
$Field_{UpCo-01}$	DS_field	13	1.0	5.5-8.5	0.3-14.5	86.2	3	1.0	5.1-5.4	0.5-6.8	10.2
	DS2018	5	0.9	6.3-7.0	4.6-10.2	36.5	4	1.0	5.6-6.5	4.9-10.2	29.7
	DS2019	6	1.0	5.2-7.6	1.1-22.8	77.4	6	1.0	4.7-5.5	3.5-19.5	67.7
	DS2020	2	1.0	4.6-5.0	2.9-3.1	5.9	1	0.9	4.4	1.4	1.4

It is worth noting that the sum of the phenotypic variation explained by the associated markers for each trait was closely related to heritability for the BLINK model (Additional file 8), except for DS2020.

4.3. In silico Identification of Candidate Genes

To identify putative candidate genes the genomic regions surrounding the significantly associated markers was examined. Out of the 95 associated markers detected (Additional file 6), 75 markers were located within or next to 62 genes from the Cameor and/or ZW6 reference genomes (Table 11). It is interesting to note several of these candidate genes contained more than one significant associated marker, underscoring their importance in contributing to the phenotypic variation of the trait. By chromosome, the gene annotation results were as follows:

A total of 10 candidate genes were detected on chromosome 1. Among them, two genes, 127087512 and 127115771, each marked by two associated markers were related to vesicle trafficking within cells. Two additional genes 127115471 and 127137201 were related with wax and cell wall biosynthesis. Interestingly, one

uncharacterized gene, marked by three associated markers, was related to BFA1 assembly which is required for ATP synthesis in A. thaliana.

On chromosome 2, 7 candidate genes were detected. Four of these genes (127120834, 127121528, 127118910 and 127117580) are related with carbohydrate and amino acid metabolism. Two genes, 127117481 encoding an F-box protein, and 127118667 encoding a MADS-box transcription factor were related to defence response to stresses in plants (Table 11) while the last identified candidate genes engaged in cell trafficking.

On chromosome 3, 9 candidate genes were detected. Among them, two genes, 127132076 and 127127305, encoded protein kinases related to plant development, stress responses and hormone signalling. Two genes, 127130208 and 127127894, were also associated with vesicle trafficking. Additionally, two genes were related with secondary metabolism while another one was related to auxin homeostasis as gene 127080599 from chromosome 1.

From the three genes detected on chromosome 4, two genes (127138368 and 127076644) encoded proteins related with the secondary metabolism and cell wall biosynthesis while the last one, gene 127138740 putatively encodes a haloacid dehalogenase-like hydrolase (HAD).

Chromosome 5 harboured the highest number of candidate gene with 18 genes identified from 23 associated markers. A notable hotspot in chromosome 5 consisted of three closely spaced markers within a 1.2 Mb window, located within genes 127082537, 127087291, and 127087323. Interestingly, two of these genes 127082537 and 127087323 were related with mobile elements in A. thaliana while the third one together with genes 127087766 and 127084564 were related with DNA transcription regulation. As in chromosomes 1 and 4, several genes related with cell wall biosynthesis and maintenance were detected on chromosome 5. Several genes related with transport and signalling, and with fatty acid or secondary metabolism were also detected on this chromosome.

From the five candidate genes identified on chromosome 6, three were related with DNA formation and transcription. The last two genes were related to inositol phosphate metabolism and abscisic acid (ABA) signalling, respectively.

Chromosome 7 harbour 11 genes in the vicinity of 13 associated markers. Among them, the function of three genes were not known in peas but the ortholog of two of them, 127105234 and 127105763, in A. thaliana have been related to tissue development. Similarly, to the other chromosomes, several candidate genes related with the regulation of DNA transcription regulation (127108155 and 127105708), the amino acid metabolism (127103253), the vesicle trafficking (127102730) and the response to stresses (127105022, 127104606 and 127104295) were identified in this chromosome.

Table 11. Potential candidate genes containing or in the vicinity of significant markers. * Function annotation deduced from the role of its closest orthologous protein in *A. thaliana*.

N	Gene ID_{NCBI}	Gene description	Pathway	DArT ID	Position ZW6	LD
1	127087512	Coatomer subunit beta'-2 in COPI	Vesicle trafficking: from Golgi to ER	3536217	Chr1_638769913	in
				5922176	Chr1_638767256	in
2	127115471	Cytochrome P450 86B1	Cutin, suberin and wax biosynthesis	3540396	Chr1_96490148	0.23 kb
3	127121867	Uncharacterized protein	Assembly of BFA1*	41128912	Chr1_128396385	in
				5916127	Chr1_128396397	in
				5933458	Chr1_128395696	in
4	127101876	Uncharacterized protein	Unknown function*	5944598	Chr1_249806845	11.83 kb
				3542029	Chr1_249828952	3.94 kb
5	127135829	Guanine nucleotide-binding protein	Signal transmission outside the cell	3551012	Chr1_346012159	6.01 kb
6	127137201	Glycosyltransferase BC10	Cell wall biosynthesis*	19178657	Chr1_368992937	in
7	127115771	Putative clathrin assembly protein	Vesicle trafficking: Clathrin-mediated endocytosis	5886489	Chr1_367783858	0.37
				19788813	Chr1_335454587	31.2 kb
8	127080599	WAT1-related protein	Auxin homoeostasis	3568148	Chr1_435743430	in
9	127082329	Splicing factor 3B subunit 2	Spliceosome	26138450	Chr1_446396667	in
10	127085672	Potassium channel AKT2/3	Regulation of membrane potential, Response to abscisic acid	5926320	Chr1_461368879	in
11	127117481	F-box/kelch-repeat protein	Negative regulation of defence response	3551269	Chr2_2285562	7.45 kb
12	127117580	Nicotinamide/nicotinic acid mononucleotide adenylyltransferase	Nicotinate and nicotinamide metabolism Metabolic pathways Biosynthesis of cofactors	5943946	Chr2_8124874	in

N	Gene ID$_{NCBI}$	Gene description	Pathway	DArT ID	Position ZW6	LD
13	127118910	Aminoacylase	Arginine biosynthesis Metabolic pathways Biosynthesis of secondary metabolites 2-Oxocarboxylic acid metabolism Biosynthesis of amino acids	3544074	Chr2_207090849	in
14	127118667	MADS-box protein AGL24-like	Transcription factor	3545236	Chr2_160200620	in
				8174445	Chr2_160210451	in
15	127103325	Uncharacterized GPI-anchored protein	Vesicle trafficking	3557565	Chr2_293250588	in
16	127120834	Hexokinase	Sugars metabolism Starch and sucrose metabolism Amino sugar and nucleotide sugar metabolism Metabolic pathways Biosynthesis of secondary metabolites Carbon metabolism Biosynthesis of nucleotide sugars	4660875	Chr2_488496120	18.91 kb
17	127121528	Pectate lyase	Pentose and glucuronate interconversions Metabolic pathways	3557551	Chr2_453678844	6.68 kb
18	127132076	CDPK-related kinase 3	Plant development, stress responses and hormone signalling	3544108	Chr3_7935806	in
19	127125898	WAT1-related protein	Auxin homoeostasis	5937399	Chr3_149104224	in
20	127130208	Plasmodesmata-located protein	Intercellular transport	5880972	Chr3_160776867	in
21	127126068	Transcription factor EMB1444-like	Regulation of DNA transcription	4660018	Chr3_172692251	in
22	127126145	ATP-dependent RNA helicase DHX8/PRP22	Spliceosome	4659692	Chr3_185293539	6.59 kb

N	Gene ID$_{NCBI}$	Gene description	Pathway	DArT ID	Position ZW6	LD
23	127127305	Serine/threonine-protein kinase PBL18	Plant development, stress responses and hormone signalling	3544804	Chr3_307444551	in
24	127127564	Fructose-1,6-bisphosphatase, chloroplastic	Glycolysis / Gluconeogenesis Pentose phosphate pathway Fructose and mannose metabolism Carbon fixation in photosynthetic organisms Metabolic pathways Biosynthesis of secondary metabolites Carbon metabolism	3552072	Chr3_344541908	in
25	127127894	Phragmoplastin DRP1E	Defence response to fungus and vesicle-mediated transport	3555519	Chr3_390153145	in
26	127133145	Small nucleolar RNA R71		5916636	Chr3_458654213	20.98 kb
27	127138368	Peroxidase 42	Phenylpropanoid biosynthesis Metabolic pathways Biosynthesis of secondary metabolites	3559464	Chr4_10427626	22.00 kb
28	127138740	Uncharacterized protein	Haloacid dehalogenase-like hydrolase	4659565	Chr4_41816686	in
29	127076644	Aldehyde decarbonylase	Cutin, suberine and wax biosynthesis Biosynthesis of secondary metabolites	3551373	Chr4_493077319	in
30	127087766	Chromodomain-helicase-DNA-binding protein	ATP-dependent chromatin remodeling	3538596	Chr5_90360668	in
31	127087924	ATP-dependent zinc metalloprotease FTSH 4	Proteolysis and meristem maintenance*	5934956	Chr5_99840368	in
32	127079825	Uncharacterized protein	Unknown function*	3569894	Chr5_156765071	in

N	Gene ID$_{NCBI}$	Gene description	Pathway	DArT ID	Position ZW6	LD
33	127080906	Uncharacterized protein	Unknown function*	3556574	Chr5_169393625	0.09 kb
34	127082843	Long-chain acyl-CoA synthetase	Metabolic pathways Fatty acid metabolism Peroxisome	5941026	Chr5_201861329	21.33 kb
				5958686	Chr5_201824241	9.87 kb
35	127082981	Pectic arabinogalactan synthesis-related protein	Cell wall pectin biosynthetic process*	3567360	Chr5_211456207	in
36	127084018	Trichome birefringence-like protein	Plant-type secondary cell wall biogenesis*	3541671	Chr5_293235930	0.10 kb
37	127084160	Uncharacterized protein	Intracellular signal transduction*	3566561	Chr5_305106410	in
38	127084564	Zinc finger CCCH domain-containing protein	Regulation of DNA transcription and translation*	3558891	Chr5_346387511	in
39	127084634	Alpha-glucan phosphorylase, H isozyme	Starch and sucrose metabolism Metabolic pathways Biosynthesis of secondary metabolites	19230512	Chr5_354090893	in
40	127084730	4-coumarate--CoA ligase	Ubiquinone and other terpenoid-quinone biosynthesis Phenylpropanoid biosynthesis Metabolic pathways Biosynthesis of secondary metabolites	5897640	Chr5_364545534	in
41	127086095	Actin-related protein 8	Actin filament-based process*	41124830	Chr5_528086379	in
42	127087180	Dolichol-phosphate mannosyltransferase	N-Glycan biosynthesis Metabolic pathways	5948001	Chr5_621702676	in
43	127082537	Uncharacterized protein	Plant mobile domain*	3552142	Chr5_627629549	in
44	127087291	NLP9-like protein	Regulation of DNA-templated transcription*	3551119	Chr5_627951949	in
45	127087323	Plant transposase	Plant mobile domain*	8175311	Chr5_628892227	in

N	Gene ID$_{NCBI}$	Gene description	Pathway	DArT ID	Position ZW6	LD
46	127087508	Sulfate transporter 3	Phosphate ion transport*	4656208	Chr5_638399837	in
47	127096746	Chromodomain-helicase-DNA-binding	ATP-dependent chromatin remodeling	3540395	Chr6_26605159	in
48	127097832	Rho-N domain-containing protein, chloroplastic	DNA-templated transcription termination*	3557403	Chr6_68402207	in
49	127096589	Inositol polyphosphate 5-phosphatase 4	Inositol phosphate metabolism	3540217	Chr6_82691906	in
50	127091595	Retarded root growth-like protein	Involved in ABI4-mediated mitochondrial retrograde signalling*	3543069	Chr6_167359798	in
51	127097692	Guanylate kinase 1-like	Nucleotide metabolism	3535374	Chr6_449699858	in
52	127105022	Phosphatase 1 regulatory subunit 7 protein	Abscisic acid-activated signaling pathway	3543068	Chr7_27387876	in
53	127101904	Uncharacterized protein		5941166	Chr7_39362330	27.69 kb
54	127103253	Amidase	Arginine and proline metabolism Phenylalanine metabolism Tryptophan metabolism Metabolic pathways	3556244	Chr7_131668232	in
55	127108155	Cell division cycle-associated protein 7	Regulation of DNA-templated transcription	3549271	Chr7_207690490	in
				3541979	Chr7_207717206	26.66 kb
				4662232	Chr7_207717206	26.66 kb
56	127105708	Cyclic dof factor 3-like isoform X1	Regulation of DNA-templated transcription*	5900633	Chr7_237959555	in
57	127102730	Transport protein SEC31 (COPII)	Protein processing in endoplasmic reticulum, cell wall formation	3553784	Chr7_403662597	0.386 kb
58	127105234	Uncharacterized protein	Root and shoot system development*	5963353	Chr7_286715392	in
59	127105763	Uncharacterized protein	Root and tissue development*	3569870	Chr7_302256784	in
60	127104295	Secreted RxLR effector protein 161-like	Defence response (CRK8) *	3641999	Chr7_448189894	8.27 kb

N	Gene ID$_{NCBI}$	Gene description	Pathway	DArT ID	Position ZW6	LD
61	127104606	Uncharacterized protein	Response to ABA and defence response*	3555097	Chr7_486340934	in
62	127105963	Queuine tRNA-ribosyltransferase subunit	tRNA modification factors	3562429	Chr7_506822033	in

5. Discussion

Rust is a world-wide distributed disease that severely affects pea crop yield (Rubiales et al. 2015). In warm and humid areas, the main causative pathogen is *Uromyces viciae-fabae*, while *U. pisi* is responsible for pea rust in more temperate regions (Singh et al. 2023). Complete resistance to rust in peas has not yet been identified, with partial resistance being the primary source of genetic resistance available so far to control this disease in pea (Barilli et al. 2014). In this study, we applied a GWAS approach to identify regions of the pea genome associated with traits linked to the partial resistance response. To achieve this, a collection of 320 pea accessions was evaluated under field and control conditions in response to two rust isolates (UpCo-01 and UpKeS-05).

5.1. Phenotypic Variance and GWAS Model Outputs

The phenotypic response of the collection against the rust isolate UpCo-01 was previously described in Osuna-Caballero et al. (2022). Comparing those results with the response of the pea collection to the UpKeS-05 isolate, revealed some commonalities and differences. Similarly, to the situation with UpCo-01, complete resistance to UpKeS-05 was not detected in the collection. In addition, the reduced number of well-developed pustules and low IT detected on the accession PI273209 in response to UpKeS-05 suggest that this accession also exhibits a late hypersensitive resistance response against this isolate (Additional file 9). Disease ratings were nonetheless lower in response to UpKeS-05 than to UpCo-01 and the response to each isolate were clearly differentiated on the PCA suggesting that the collection responded differentially to the isolates As mild to moderate relationship was also observed for most traits between isolates, these differences are more likely revealing differences in the overall virulence level of the isolates although the existence of *U. pisi* races in peas could not be ruled out.

Previous studies performed on the pea core collection demonstrated a rapid LD decay and a broad distribution of the polymorphic DArT markers throughout the pea genome (Rispail et al. 2023). Although a significant portion of the population resulted admixed in phylogenetic terms, the collection was found to be structured into six groups consistent with the taxonomy of the *Pisum* species and subspecies (Rispail et al. 2023). However, BIC selection models indicated that population structure was efficiently controlled in the GWAS models by the kinship matrix alone and did not require adding the initial PCs to the models as it was previously demonstrated on GWAS studies performed on plant populations with a high percentage of admixture (Kaur et al. 2023). The BLINK method improves the statistical power and enhances the robustness of association signals compared to MLM (Huang et al., 2019). Furthermore, the extensive coverage of the DArT markers across the pea genome is ideal for multi-locus methods like BLINK, making it a frequently used model in

GWAS studies to analyse complex traits in legumes (Tibbs Cortes et al. 2021; Susmitha et al. 2023). Accordingly, this method detected a high number of markers associated with rust disease development.

The two GWAS methods applied here detected a total of 95 markers significantly associated with one or more of the 21 rust disease traits, among which 21 markers were detected by both methods which will be instrumental for future breeding for rust resistance in pea. Previous studies based on linkage mapping identified three QTLs located in LGII and LGIV which correspond with chromosome 6 and 4, respectively (Barilli et al. 2018). Our findings support these results providing a total of 4 and 3 candidates genes surrounding QTL UpDSII in chromosome 6 and QTLs UpDSIV and UpDSIV.2 on chromosome 4. On the other hand, this is the first GWAS targeting rust resistance in pea while similar studies addressing rust disease in legumes remains scarce. Most previous studies were based on the MLM method while only one study on soybean (Glycine max) – rust (Phakopsora pachyrhizi) applied the BLINK method (Martins et al. 2022; Montejo Domínguez et al. 2022; Wu et al., 2022; Xiong et al. 2023). The number of significant marker-trait associated largely depended on the number and distribution of the available markers. Accordingly, 100 and 129 marker-trait associations were identified in response to rust in soybean and common bean in studies with more than 20,000 genome-wide markers (Wu et al. 2022; Xiong et al. 2023) while only 7 DS associated markers was identified in response to *U. pisi* in grass pea from a marker set of 5,651 SNPs (Martins et al. 2022). Interestingly, aligning these 7 grass pea markers onto pea reference genomes allowed the identification of 19 candidates genes among which 5 have similar function to those detected in the present study (Martins et al. 2022).

5.2. Candidate Genes Represent Diverse Functional Roles

Examining the surrounding regions of the 95 associated markers detected in the present study allowed the identification of 62 candidate genes with potential function in rust resistance. According to their annotation, these candidate genes participate in a variety of function, including primary and secondary metabolism, cell wall synthesis, cell trafficking, DNA transcription regulation and defence response.

5.2.1. Regulators of Gene Expression

Among the 62 candidate genes, 12 are related to the regulation of DNA transcription/translation, RNA modification, and transposable elements. Seven of them are transcription factors (TFs), including a Nodule inception-like 9 protein (NLP9, 127087291) a Cycling DOF factor 3 (CDF3, 127105708) and a Zinc finger transcription factor orthologous to Tandem Zinc Finger 9 (TZF9, 127084564). Previous studies on TZF9 identified it as an important regulator of plant immune defence in A. thaliana (Maldonado-Bonilla et al. 2014; Tabassum et al. 2020). While NLP9 and CDF3 have been mainly associated with nitrogen use efficiency in plants

some studies in tomato and soybean linked them to the response to biotic and abiotic stresses (Renau-Morata et al. 2017; Domínguez-Figueroa et al. 2020; Konishi et al. 2021; Amin et al. 2023). Interestingly, two candidate genes (127087323 and 127082537) encoding plant mobile domains are located within a 1.2Mb distance on both side of NPL9. While the role of these two genes in genomic regulation is under study, their involvement in plant defence has yet to be clarified (Fambrini et al. 2020). Apart from these TFs, two candidate genes (12782329 and 127126145), encoding a splicing factor (SF3b) of the U2 spliceosome complex and an RNA helicase (PRP22) respectively, are related to mRNA splicing via the spliceosome, which play an important role in the plant response to biotic stresses (Shang et al. 2017). Accordingly, knock-out mutation in SMD3, other subunits of the U2 complex, increase the susceptibility to *Pseudomonas syringae* in *A. thaliana* (Golisz et al. 2021). In addition, the orthologous gene of RNA helicase in *A. thaliana* (At1g32490) have been implicated in the negative regulation of numerous genes related to cell wall formation (Howles et al. 2016), which could improve the physical barrier against haustoria formation inside the plant cells.

5.2.2. Regulators of Vesicle Trafficking and Cell Wall Components

Several of the candidate genes containing or closely related to the associated markers are related to vesicle trafficking and cell wall biosynthesis suggesting the importance of the cell wall and cell trafficking in response to rust. Among them, three genes (127087512, 127102730, and 127115771) encode proteins of the coat protein complex I (COPI), coat protein complex II (COPII), and clathrin-mediated endocytosis vesicles that mediate basic functions of protein export/import to the ER in plant cells (Zeng et al. 2023). COPII has been directly involved in the process of autophagy, which enable the ABA-mediated cell nutrient recycling in response to stress (Li et al. 2022). In addition, the gene 127086095 encodes an actin-related protein (ARP8) that participates in cytoskeleton-related functions (Kandasamy et al. 2008). Recent studies in A. thaliana have shown that related ARPs, such as ARP4 and ARP6, are involved in both biotic and abiotic environmental changes (Nie and Wang 2021; Jakada et al. 2023). This suggest that vesicle trafficking, and particularly the endomembrane cell system, could play an important function in response to rust in pea.

On the other hand, eight candidate genes (127086095, 127076644, 127115471, 127137201, 127084018, 127082981, 127076644 and 127115471) are related to cell wall formation or to the biosynthesis of cell-wall related secondary metabolites such as lignin. Among them, gene 127137201 encodes a glycosyltransferase BC10 that have been related to the cellulose and lignin biosynthesis at the cell wall (Zhou et al. 2009; Zhang et al. 2016) while two genes (127082981 and 127084018) are related to the synthesis of rhamnogalacturonan-I (RG-I), one of the pectic components of the cell wall (Stonebloom et al. 2016). This suggests that changes in the cell wall composition

may participate in the plant cell response to rust. Interestingly, two additional genes (127076644 and 127115471), encoded an Eceriferum (CER1) -like enzyme and a mid-chain alkane hydroxylase (MAH1), respectively, are important players of wax on the cell wall (Lewandowska et al. 2020; Wang et al. 2020) which play an important role in the host recognition by rust in several species (Niks and Rubiales 2002) and on the modulation of plant susceptibility to necrotrophic fungus such as Sclerotinia sclerotiorum (Bourdenx et al. 2011).

5.2.3. Regulators of Hormone Signalling and Defence Response

Eleven of the identified genes in the vicinity of the significantly associated markers were related to hormone signalling and defence. Among them, two genes (127080599 and 127125898) encoded two copies of a nodulin like proteins homologs to Medicago truncatula NODULIN 21 (MtN21) and A. thaliana WAT1 (walls are thin 1) genes that have been involved in auxin metabolism and play a significant role in secondary cell wall formation of (Ranocha et al. 2010). Recent studies showed that additional MtN21-related homologs in A. thaliana, such as RTP1 negatively regulates plant resistance to biotrophic pathogens through cell death and auxin-mediated production of reactive oxygen species (Pan et al. 2016; Gao et al. 2023) linking these genes to auxin signalling and defence. Apart for auxin, several genes pointed to the potential involvement of ABA in response to rust since four genes (127085672, 127091495, 127105022 and 127104606) encoded ABA-responsive genes including orthologs of the potassium channel AKT2/3, the regulatory subunit of protein phosphatase 1 (PP1R3), the Abscisic Acid Insensitive 4 (ABI4) and a SEC14-like protein (Chérel et al. 2002; Wang et al. 2016; Chandrasekaran et al. 2020; Zhang et al. 2020). Among their distinct functions, several studies in A. thaliana or Nicotiana benthamiana showed that AKT2/3, ABI4 and the SEC14 proteins contributed to plant defence being important actors of the plant resistance to different pathogens (Kiba et al. 2012; Zhou et al. 2014; Yop et al. 2023).

Several genes identified in this study are also directly involved in the plant defence mechanisms against pathogen attacks, involving some regulatory proteins and kinases. Accordingly, three of the identified genes encoded protein kinases including a PBS1-like protein kinase, a calcium-dependent protein kinase (CDPK3) and cysteine-rich receptor-like kinase (CRK8). Previous studies reported the crucial role of PBS1 in bacterial and viral resistance in A. thaliana and soybean (Pottinger et al. 2020). PBS1 was also shown to play a role in herbivore resistance in interaction with CDPK3 (Miyamoto et al. 2019; Desaki et al. 2023) hinting the involvement of both gene in a common defence pathway. Interestingly, one marker significantly associated with pea rust resistance was located at 8.27 kb of the receptor-like kinase CRK8 that have been shown previously to play a crucial role in rust resistance in wheat (Gu et al. 2020; Kamel et al. 2023). In addition to these kinases, this study identified an ortholog of a F-box protein CPR1/CPR30 (127117481), that acts,

between other function, as a negative regulator of salicylic acid-dependent resistance (R) proteins like SNC1 (Gou et al. 2012), and a dynamin-related protein 1E (DRP1E; 127127894) which knock-out mutation was found in A. thaliana to induce stronger hypersensitive response to powdery mildew (Tang et al. 2006; Leibman-Markus et al. 2022; Mc Gowan et al. 2022).

Altogether, this GWAS study shed light on the complex genetic architecture underpinning partial resistance to rust in pea. In addition to the detection of 95 new molecular markers associated with partial resistance, this study detected 62 candidate genes that contains or was intricately linked to these markers, which offer several promising targets to improve our understanding of rust resistance in pea and future plant breeding strategies. These genes span a diverse array of biological functions providing the basis for further gene functional mapping. The identification of several candidate genes known to participate in rust resistance in cereal (i.e., wax genes, CRK8) suggest that at least some of these candidate genes might be the responsible gene underlying the detected QTL confirming the usefulness of GWAS studies to uncover new resistance QTL and genes. Therefore, this study opens the possibility to characterize further, via gene expression studies or TILLING, the function of these candidate genes to explore their implication in rust disease in pea. The significantly associated DArT-seq markers also provides a basis for future marker-assisted selection and the development of more efficient genomic prediction models for rust resistance. Therefore, this study contributes to understanding the genetic make-up of rust resistance in pea and promotes future crop improvement. By focusing on the candidate genes uncovered, breeding programs can develop more targeted approaches, upon their validation, leveraging genetic variation to improve the resilience of pea crops against rust disease. This not only contributes to secure yield and quality in the face of biotic stress but also supports sustainable agricultural practices by reducing the reliance on chemical fungicides.

6. Additional files

Additional file 6. The 95 Silico-DArT markers associated with rust disease traits. N = Linked or same marker related to a genomic region. Marker_ID = DArTseq marker identificatory. Chr_ZW6 = chromosome location of DArT marker on ZW6 reference genome. Pos_ZW6 = DArT marker position (pb) on ZW6 reference genome. P.value = significance of association. MAF = minor allele frequency. H.B.P.Value = False Discovery Rate (FDR) control of p value developed by Benjamini and Hochberg. Effect = marker effect on phenotypic variance. Model = GWAS model applied. Trait = current trait. DataSet = current data set. Lambda = genomic inflation factor. LOD = $-\text{Log}_{10}$(p value). Criterion = marker retrieved by FDR or Bonferroni adjustment. PVE = phenotypic variance explained (%) by each marker.

N	Marker_ID	Chr_ZW6	Pos_ZW6	P.value	MAF	H.B.P.Value	Effect	Model	Trait	DataSet	Lambda	LOD	Criterion	PVE
1	3536217	chr5	638769913	1.29E-04	0.40	0.87	-0.04	MLM	AUDPC_DS	CC_egy	0.97	4.48	FDR adjusted	4.52
1	5922176	chr5	638767256	2.12E-04	0.42	0.97	-0.04	MLM	AUDPC_IF	CC_egy	0.98	4.45	FDR adjusted	2.79
2	3540396	chr1	96490148	2.48E-05	0.11	0.15	-0.17	BLINK	LP50_IF	CC_egy	1.16	5.25	FDR adjusted	3.05
3	41128912	chr1	128396385	4.20E-05	0.27	0.61	-0.02	BLINK	AUDPC_DS	CC_egy	0.99	4.65	FDR adjusted	2.25
3	41128912	chr1	128396385	2.84E-05	0.27	0.25	0.00	MLM	AUDPC_DS	CC_egy	0.99	5.02	FDR adjusted	2.65
3	41128912	chr1	128396385	1.40E-05	0.27	0.12	-0.01	MLM	MDPr_DS	CC_egy	1.00	5.34	FDR adjusted	2.46
3	5916127	chr1	128396397	1.18E-08	0.45	0.00	0.00	BLINK	AUDPC_DS	CC_egy	0.93	7.93	Gapit Default	5.92
3	5916127	chr1	128396397	2.81E-05	0.45	0.68	0.01	BLINK	AUDPC_IF	CC_egy	1.01	4.58	FDR adjusted	3.55
3	5916127	chr1	128396397	4.64E-08	0.45	0.00	0.00	BLINK	DS_egy	CC_egy	1.00	7.33	Gapit Default	6.92
3	5916127	chr1	128396397	1.08E-07	0.45	0.00	0.01	BLINK	MDPr_DS	CC_egy	0.94	6.96	Gapit Default	7.30
3	5916127	chr1	128396397	5.00E-06	0.45	0.13	0.00	MLM	AUDPC_DS	CC_egy	0.99	5.30	FDR adjusted	5.92
3	5916127	chr1	128396397	8.36E-05	0.45	1.00	0.01	MLM	AUDPC_IF	CC_egy	0.95	4.42	FDR adjusted	3.55
3	5916127	chr1	128396397	1.02E-05	0.45	0.13	0.00	MLM	DS_egy	CC_egy	1.03	5.30	FDR adjusted	6.92
3	5916127	chr1	128396397	1.08E-05	0.45	0.12	0.01	MLM	MDPr_DS	CC_egy	1.00	5.34	FDR adjusted	7.30
3	5933458	chr1	128395696	1.81E-05	0.39	0.12	-0.01	MLM	MDPr_DS	CC_egy	1.00	5.34	FDR adjusted	5.11
4	5944598	chr1	249806845	5.25E-06	0.09	0.00	2.28	MLM	AUDPC	CC_cor	1.72	7.08	Gapit Default	2.54
4	3542029	chr1	249828952	2.79E-05	0.13	0.08	0.00	MLM	MDPr_PS	CC_egy	1.15	5.52	FDR adjusted	5.17
5	3551012	chr1	346012159	1.70E-07	0.11	0.00	-1.73	BLINK	DS_field	Field	0.96	7.37	Gapit Default	14.44
6	19178657	chr1	368992937	3.03E-08	0.07	0.00	0.00	BLINK	MDPr_PS	CC_egy	0.99	7.54	Gapit Default	9.91
6	19178657	chr1	368992937	4.69E-05	0.07	0.88	0.00	MLM	MDPr_PS	CC_egy	1.00	4.48	FDR adjusted	9.91
7	5886489	chr1	367783858	2.22E-05	0.06	0.49	-3.76	MLM	DS2019	Field	0.97	4.73	FDR adjusted	16.03
7	19788813	chr2	335454587	3.53E-05	0.07	0.02	-0.10	MLM	IT	CC_cor	1.20	6.33	Gapit Default	2.17
8	3568148	chr1	435743430	1.51E-06	0.20	0.04	0.04	BLINK	AUDPC_DS	CC_egy	0.96	5.82	Gapit Default	5.52
9	26138450	chr1	446396667	2.99E-07	0.09	0.00	2.10	BLINK	DS2018	Field	0.89	7.00	Gapit Default	10.24
9	26138450	chr1	446396667	3.10E-07	0.09	0.01	2.83	MLM	DS2018	Field	1.02	6.51	Gapit Default	10.24

N	Marker_ID	Chr_ZW6	Pos_ZW6	P.value	MAF	H.B.P.Value	Effect	Model	Trait	DataSet	Lambda	LOD	Criterion	PVE
9	26138450	chr1	446396667	2.33E-06	0.09	0.02	0.00	BLINK	AUDPC_PS	CC_egy	0.90	6.23	Gapit Default	3.17
10	5926320	chr1	461368879	1.24E-04	0.17	0.99	-2.84	MLM	DS2020	Field	0.95	4.42	FDR adjusted	1.44
11	3551269	chr2	2285562	9.33E-11	0.23	0.00	-0.05	BLINK	MDPr_DS	CC_egy	0.95	10.33	Gapit Default	13.58
12	5943946	chr2	8124874	8.54E-07	0.07	0.02	0.04	BLINK	LP50	CC_cor	0.98	6.08	Gapit Default	6.11
13	3544074	chr2	207090849	5.12E-05	0.05	1.00	-0.06	MLM	LP50_PS	CC_egy	0.93	4.42	FDR adjusted	4.36
14	3545236	chr2	160200620	7.46E-07	0.24	0.00	-1.57	BLINK	DS_field	Field	0.96	6.97	Gapit Default	5.44
14	8174445	chr2	160210451	1.63E-06	0.06	0.01	0.05	BLINK	MDPr	CC_cor	1.04	6.49	Gapit Default	5.58
15	3557565	chr2	293250588	6.49E-08	0.23	0.00	0.02	BLINK	MDPr	CC_cor	1.04	7.50	Gapit Default	15.31
16	5918466	chr2	346062476	1.96E-05	0.07	0.51	0.04	MLM	LP50	CC_cor	1.02	4.71	FDR adjusted	6.32
16	5918466	chr2	346062476	9.12E-05	0.07	0.95	0.00	BLINK	LP50	CC_cor	0.98	4.44	FDR adjusted	6.40
17	4660875	chr2	488496120	1.32E-05	0.07	0.11	-0.04	BLINK	MDPr_DS	CC_egy	0.95	5.36	FDR adjusted	6.86
17	4660875	chr2	488496120	2.44E-06	0.07	0.06	-0.06	BLINK	MDPr_IF	CC_egy	1.23	5.73	FDR adjusted	7.52
17	4660875	chr2	488496120	8.79E-05	0.07	0.98	-0.08	MLM	MDPr_IF	CC_egy	0.97	4.42	FDR adjusted	7.52
18	3557551	chr2	453678844	9.58E-06	0.21	0.04	0.04	BLINK	IT	CC_cor	0.94	5.80	Gapit Default	16.13
19	3544108	chr3	7935806	2.84E-05	0.09	0.13	-39.84	MLM	AUDPC	CC_cor	1.03	5.30	FDR adjusted	9.67
19	3544108	chr3	7935806	5.82E-05	0.09	0.31	0.16	BLINK	LP50_IF	CC_egy	1.01	4.93	FDR adjusted	7.62
19	3544108	chr3	7935806	8.41E-06	0.09	0.05	-12.28	MLM	IF_cor	CC_cor	1.01	5.68	FDR adjusted	10.33
20	3553494	chr3	79799764	1.75E-06	0.09	0.05	0.00	BLINK	AUDPC_PS	CC_egy	1.01	5.76	Gapit Default	4.96
20	3553494	chr3	79799764	2.80E-05	0.09	0.36	-1.02	BLINK	AUDPC_IF	CC_egy	1.02	4.85	FDR adjusted	10.46
21	5937399	chr3	149104224	1.47E-07	0.19	0.00	-1.44	BLINK	DS_field	Field	0.96	7.37	Gapit Default	13.10
22	5880972	chr3	160776867	1.38E-07	0.10	0.00	0.06	BLINK	IT	CC_cor	0.94	7.20	Gapit Default	14.15
23	4660018	chr3	172692251	3.99E-05	0.06	0.52	0.89	BLINK	DS_egy	CC_egy	1.20	4.77	FDR adjusted	4.44
24	5940996	chr3	125011420	1.95E-05	0.08	0.25	0.00	MLM	AUDPC_PS	CC_egy	1.03	5.02	FDR adjusted	12.00
25	4659692	chr3	185293539	1.13E-04	0.24	0.58	0.04	BLINK	MDPr_IF	CC_egy	1.23	4.77	FDR adjusted	1.05
26	3544804	chr3	307444551	4.56E-05	0.49	0.20	-0.02	BLINK	MDPr_DS	CC_egy	0.95	5.12	FDR adjusted	3.84

N	Marker_ID	Chr_ZW6	Pos_ZW6	P.value	MAF	H.B.P.Value	Effect	Model	Trait	DataSet	Lambda	LOD	Criterion	PVE
27	3552072	chr3	344541908	1.87E-07	0.05	0.00	-0.10	BLINK	IT	CC_cor	0.94	7.20	Gapit Default	15.44
28	3555519	chr3	390153145	5.15E-10	0.13	0.00	-4.25	BLINK	DS_cor	CC_cor	0.77	9.29	Gapit Default	7.54
29	5916636	chr3	458654213	9.52E-08	0.35	0.00	-0.02	BLINK	MDPr	CC_cor	1.04	7.50	Gapit Default	13.71
30	3559464	chr4	10427626	1.59E-05	0.08	0.21	3.69	MLM	DS_field	Field	0.97	5.11	FDR adjusted	6.79
31	4659565	chr4	41816686	2.70E-05	0.36	0.52	0.35	BLINK	DS_egy	CC_egy	1.20	4.77	FDR adjusted	10.75
31	4659565	chr4	41816686	2.07E-11	0.36	0.00	0.04	BLINK	MDPr_DS	CC_egy	0.95	10.68	Gapit Default	15.34
31	4659565	chr4	41816686	2.06E-05	0.36	0.18	0.00	BLINK	MDPr_PS	CC_egy	0.99	5.19	FDR adjusted	7.90
31	4659565	chr4	41816686	2.14E-06	0.36	0.03	0.04	MLM	MDPr_DS	CC_egy	0.99	5.95	Gapit Default	15.34
31	5947149	chr4	41816686	2.25E-06	0.42	0.03	-0.04	MLM	MDPr_DS	CC_egy	0.99	5.95	Gapit Default	13.50
32	3551343	chr4	51609223	1.96E-07	0.19	0.00	-2.07	BLINK	DS2019	Field	1.06	6.82	Gapit Default	19.51
32	3551343	chr4	51609223	4.38E-05	0.19	0.49	-2.32	MLM	DS2019	Field	0.97	4.73	FDR adjusted	19.51
33	3565209	chr4	401865193	3.68E-05	0.21	0.22	-0.01	BLINK	LP50_IF	CC_egy	1.32	5.19	FDR adjusted	0.39
34	3550659	chr4	406124171	5.05E-05	0.28	0.22	-0.01	BLINK	LP50_IF	CC_egy	1.32	5.19	FDR adjusted	0.76
35	3551373	chr4	493077319	3.64E-05	0.06	0.19	-2.94	BLINK	DS2019	Field	1.06	5.17	FDR adjusted	5.17
36	3538596	chr5	90360668	7.17E-08	0.06	0.00	2.69	BLINK	DS_field	Field	0.96	7.37	Gapit Default	2.88
36	3538596	chr5	90360668	2.90E-07	0.06	0.00	2.68	BLINK	DS2018	Field	0.89	7.00	Gapit Default	7.72
36	3538596	chr5	90360668	8.41E-06	0.06	0.21	3.38	MLM	DS_field	Field	0.97	5.11	FDR adjusted	2.88
36	3538596	chr5	90360668	2.23E-06	0.06	0.03	3.29	MLM	DS2018	Field	1.02	5.95	Gapit Default	7.72
37	4660557	chr5	138612700	6.91E-06	0.18	0.09	0.04	BLINK	AUDPC_DS	CC_egy	0.96	5.46	FDR adjusted	10.60
38	5934956	chr5	99840368	2.24E-05	0.06	0.22	0.02	BLINK	LP50_IF	CC_egy	1.32	5.19	FDR adjusted	0.61
39	3569894	chr5	156765071	3.00E-05	0.12	0.13	38.95	MLM	AUDPC	CC_cor	1.03	5.30	FDR adjusted	8.84
40	3556574	chr5	169393625	4.26E-06	0.48	0.06	0.02	BLINK	AUDPC_IF	CC_egy	1.11	5.71	FDR adjusted	10.32
40	3556574	chr5	169393625	4.98E-05	0.48	0.19	0.03	BLINK	IF_egy	CC_egy	1.19	5.19	FDR adjusted	1.46
41	5941026	chr5	201861329	5.67E-05	0.31	0.69	1.81	BLINK	DS2020	Field	0.92	4.58	FDR adjusted	3.05
41	5958686	chr5	201824241	5.56E-05	0.23	0.14	2.39	MLM	DS_field	Field	1.20	5.36	FDR adjusted	0.52

N	Marker_ID	Chr_ZW6	Pos_ZW6	P.value	MAF	H.B.P.Value	Effect	Model	Trait	DataSet	Lambda	LOD	Criterion	PVE
42	3567360	chr5	211456207	9.54E-06	0.06	0.06	3.27	MLM	DS2018	Field	1.02	5.62	FDR adjusted	4.93
43	3541671	chr5	293235930	3.80E-05	0.48	0.20	14.65	BLINK	AUDPC	CC_cor	0.90	5.12	FDR adjusted	14.88
44	3566561	chr5	305106410	3.12E-05	0.34	0.27	0.02	BLINK	AUDPC_IF	CC_egy	1.11	5.02	FDR adjusted	9.59
45	3558891	chr5	346387511	5.35E-08	0.49	0.00	0.02	BLINK	MDPr	CC_cor	1.04	7.50	Gapit Default	15.38
46	19230512	chr5	354090893	3.20E-05	0.10	0.22	0.01	BLINK	LP50_IF	CC_egy	1.32	5.19	FDR adjusted	0.86
47	5897640	chr5	364545534	3.36E-07	0.43	0.00	-0.03	BLINK	IT	CC_cor	0.94	7.08	Gapit Default	12.96
48	3537837	chr5	441607030	7.40E-06	0.06	0.06	3.07	MLM	DS2018	Field	1.02	5.62	FDR adjusted	6.81
49	41124830	chr5	528086379	2.66E-09	0.06	0.00	-0.02	BLINK	LP50_IF	CC_egy	1.32	8.69	Gapit Default	6.32
49	41124830	chr5	528086379	4.07E-05	0.06	0.41	-0.02	MLM	LP50_IF	CC_egy	1.02	4.81	FDR adjusted	6.32
50	5948001	chr5	621702676	4.47E-05	0.08	0.41	-0.02	MLM	LP50_IF	CC_egy	1.02	4.81	FDR adjusted	4.51
51	3552142	chr5	627629549	1.03E-05	0.17	0.09	-37.06	MLM	AUDPC	CC_cor	1.03	5.46	FDR adjusted	14.26
51	3552142	chr5	627629549	1.44E-06	0.17	0.02	-11.71	MLM	IF_cor	CC_cor	1.01	6.23	Gapit Default	16.25
52	3551119	chr5	627951949	1.32E-05	0.22	0.07	-8.67	MLM	IF_cor	CC_cor	1.01	5.58	FDR adjusted	13.95
52	3544538	chr5	627951949	7.70E-11	0.16	0.00	-32.21	BLINK	AUDPC	CC_cor	0.90	10.11	Gapit Default	16.10
52	3544538	chr5	627951949	1.01E-13	0.16	0.00	-11.34	BLINK	IF_cor	CC_cor	0.90	13.00	Gapit Default	17.64
52	3544538	chr5	627951949	5.21E-06	0.16	0.07	-42.13	MLM	AUDPC	CC_cor	1.03	5.58	FDR adjusted	16.10
52	3544538	chr5	627951949	8.40E-07	0.16	0.02	-13.00	MLM	IF_cor	CC_cor	1.01	6.23	Gapit Default	17.64
53	8175311	chr5	628892227	5.42E-07	0.15	0.01	-2.23	BLINK	DS_cor	CC_cor	0.77	6.57	Gapit Default	10.49
53	8175311	chr5	628892227	3.37E-05	0.15	0.09	-1.12	BLINK	DS_field	Field	0.96	5.47	FDR adjusted	14.54
53	8175311	chr5	628892227	4.87E-07	0.15	0.00	-2.09	BLINK	DS2019	Field	1.06	6.82	Gapit Default	22.77
53	8175311	chr5	628892227	6.22E-06	0.15	0.08	-0.27	BLINK	IF_egy	CC_egy	0.95	5.51	FDR adjusted	7.71
53	8175311	chr5	628892227	2.11E-05	0.15	0.13	-40.04	MLM	AUDPC	CC_cor	1.03	5.30	FDR adjusted	15.36
53	8175311	chr5	628892227	1.77E-06	0.15	0.02	-12.87	MLM	IF_cor	CC_cor	1.01	6.23	Gapit Default	17.54
54	4656208	chr5	638399837	9.03E-06	0.34	0.24	-0.56	MLM	DS_egy	CC_egy	0.98	5.04	FDR adjusted	12.83
54	4656208	chr5	638399837	7.63E-06	0.34	0.07	-0.04	MLM	MDPr_DS	CC_egy	0.99	5.60	FDR adjusted	12.39

N	Marker_ID	Chr_ZW6	Pos_ZW6	P.value	MAF	H.B.P.Value	Effect	Model	Trait	DataSet	Lambda	LOD	Criterion	PVE
55	3538568	chr5	647525119	3.35E-07	0.38	0.00	-1.51	BLINK	DS2019	Field	1.06	6.82	Gapit Default	13.83
55	3538568	chr5	647525119	1.40E-05	0.38	0.12	-2.52	MLM	DS2019	Field	1.14	5.38	FDR adjusted	13.57
55	26137611	chr5	647525119	1.56E-05	0.24	0.27	-1.51	BLINK	DS2020	Field	1.12	5.01	FDR adjusted	2.90
56	3540395	chr6	26605159	5.61E-07	0.10	0.00	-2.09	BLINK	DS_field	Field	0.96	7.03	Gapit Default	4.88
57	3557403	chr6	68402207	5.46E-06	0.42	0.04	16.38	BLINK	AUDPC	CC_cor	0.90	5.86	Gapit Default	16.98
57	3557403	chr6	68402207	1.14E-05	0.42	0.10	4.76	BLINK	IF_cor	CC_cor	0.90	5.42	FDR adjusted	14.13
58	3540217	chr6	82691906	1.38E-07	0.15	0.00	-0.04	BLINK	MDPr	CC_cor	1.04	7.46	Gapit Default	2.97
59	3543069	chr6	167359798	8.82E-08	0.13	0.00	-1.62	BLINK	DS2018	Field	0.89	7.05	Gapit Default	7.11
60	3565836	chr6	403894626	2.64E-07	0.18	0.00	-1.49	BLINK	DS_field	Field	0.96	7.28	Gapit Default	3.47
61	5921762	NA	NA	4.67E-06	0.35	0.01	0.87	BLINK	DS_field	Field	0.96	6.29	Gapit Default	0.29
62	5900228	chr6	429004258	1.94E-11	0.47	0.00	-0.28	BLINK	IF_egy	CC_egy	0.95	10.71	Gapit Default	8.44
62	5900228	chr6	429004258	3.63E-05	0.47	0.87	-0.02	BLINK	MDPr_IF	CC_egy	1.00	4.48	FDR adjusted	5.19
62	5900228	chr6	429004258	4.56E-05	0.47	0.97	-0.02	MLM	MDPr_IF	CC_egy	0.99	4.43	FDR adjusted	5.19
63	3535374	chr6	449699858	3.21E-07	0.10	0.01	-0.05	BLINK	AUDPC_IF	CC_egy	1.11	6.53	Gapit Default	5.76
64	3543068	chr7	27387876	1.47E-05	0.16	0.25	0.00	MLM	AUDPC_PS	CC_egy	1.03	5.02	FDR adjusted	6.29
65	5941166	chr7	39362330	7.17E-06	0.22	0.09	0.00	BLINK	MDPr_PS	CC_egy	0.99	5.47	FDR adjusted	2.65
66	5932021	chr7	51930899	6.15E-04	0.19	0.95	0.02	BLINK	LP50_DS	CC_egy	0.96	4.44	FDR adjusted	5.34
66	5932021	chr7	51930899	1.87E-04	0.19	0.93	0.01	MLM	LP50_DS	CC_egy	1.00	4.47	FDR adjusted	5.34
67	3556244	chr7	131668232	4.81E-05	0.49	0.20	-0.02	BLINK	MDPr_DS	CC_egy	0.95	5.12	FDR adjusted	11.59
68	3549271	chr7	207690490	6.15E-07	0.17	0.00	-1.34	BLINK	DS2018	Field	0.89	6.81	Gapit Default	6.81
68	3549271	chr7	207690490	2.27E-08	0.17	0.00	-3.73	BLINK	DS2019	Field	0.99	7.64	Gapit Default	15.03
68	3549271	chr7	207690490	3.11E-09	0.17	0.00	-3.13	BLINK	DS_field	Field	1.08	8.54	Gapit Default	11.77
68	3549271	chr7	207690490	3.70E-05	0.17	0.48	-3.33	MLM	DS2019	Field	0.96	4.73	FDR adjusted	15.03
68	3541979	chr7	207717206	3.98E-05	0.33	0.15	-2.36	MLM	DS2019	Field	1.14	5.27	FDR adjusted	4.04
68	3541979	chr7	207717206	3.32E-06	0.33	0.03	-2.36	BLINK	DS_field	Field	1.16	5.99	Gapit Default	3.61

N	Marker_ID	Chr_ZW6	Pos_ZW6	P.value	MAF	H.B.P.Value	Effect	Model	Trait	DataSet	Lambda	LOD	Criterion	PVE
68	4662232	chr7	207717206	8.44E-06	0.35	0.08	-1.72	MLM	DS2019	Field	1.15	5.55	FDR adjusted	3.54
68	4662232	chr7	207717206	1.72E-05	0.35	0.07	NA	BLINK	DS_field	Field	1.26	5.60	FDR adjusted	2.15
69	5900633	chr7	237959555	1.14E-04	0.17	0.91	0.06	MLM	IT	CC_cor	1.01	4.47	FDR adjusted	9.59
69	5900633	chr7	237959555	7.73E-07	0.17	0.02	0.04	BLINK	IT	CC_cor	1.06	6.12	Gapit Default	9.67
70	3553784	chr7	403662597	1.70E-06	0.09	0.04	68.32	MLM	AUDPC	CC_cor	1.03	5.77	Gapit Default	6.93
70	3553784	chr7	403662597	2.01E-05	0.09	0.07	17.41	MLM	IF_cor	CC_cor	1.01	5.54	FDR adjusted	5.98
70	3553784	chr7	403662597	2.80E-05	0.09	0.50	0.06	MLM	MDPr	CC_cor	1.07	4.72	FDR adjusted	3.86
71	5963353	chr7	286715392	1.63E-07	0.09	0.00	-2.21	BLINK	DS_field	Field	0.96	7.37	Gapit Default	8.19
71	5963353	chr7	286715392	1.06E-06	0.09	0.01	-2.06	BLINK	DS2018	Field	0.72	6.27	Gapit Default	4.63
72	3569870	chr7	302256784	2.61E-05	0.20	0.23	-0.02	BLINK	LP50	CC_cor	0.98	5.07	FDR adjusted	7.60
73	3641999	chr7	448189894	4.07E-06	0.46	0.01	0.95	BLINK	DS_field	Field	0.96	6.29	Gapit Default	1.44
74	3555097	chr7	486340934	8.42E-08	0.11	0.00	-0.06	BLINK	IT	CC_cor	0.94	7.20	Gapit Default	3.01
75	3558830	chr7	500294438	3.37E-05	0.45	0.77	-0.25	MLM	IF_egy	CC_egy	0.95	4.53	FDR adjusted	5.04
76	3562429	chr7	506822033	3.25E-06	0.48	0.03	1.48	BLINK	DS_cor	CC_cor	0.77	5.96	Gapit Default	8.61
77	3542176	NA	NA	1.96E-05	0.09	0.07	-11.34	MLM	IF_cor	CC_cor	1.01	5.54	FDR adjusted	12.64
78	3542944	NA	NA	4.02E-06	0.45	0.03	18.14	BLINK	AUDPC	CC_cor	0.90	5.87	Gapit Default	17.84
78	3542944	NA	NA	1.24E-07	0.45	0.00	5.70	BLINK	IF_cor	CC_cor	0.90	7.21	Gapit Default	15.88
79	3547116	NA	NA	2.47E-06	0.42	0.02	-1.23	BLINK	DS2019	Field	1.06	6.24	Gapit Default	1.13
80	4657913	NA	NA	7.20E-07	0.09	0.00	0.06	BLINK	IT	CC_cor	0.94	6.84	Gapit Default	2.21
81	5898238	NA	NA	1.75E-04	0.22	0.90	0.03	BLINK	LP50_PS	CC_egy	0.99	4.48	FDR adjusted	6.06
82	5933084	NA	NA	3.20E-07	0.08	0.00	26.70	BLINK	AUDPC	CC_cor	0.90	6.80	Gapit Default	3.37
82	5933084	NA	NA	3.81E-05	0.08	0.50	0.07	MLM	MDPr	CC_cor	1.07	4.72	FDR adjusted	6.24
83	5962639	NA	NA	4.52E-05	0.11	0.66	-3.62	MLM	DS_cor	CC_cor	1.06	4.61	FDR adjusted	6.06

Additional file 7. Bayesian Information Criteria (BIC) analysis for the number of Principal Components (PCs) by each trait and Data set.

DataBase	Trait	Number of PCs/Covariates	BIC (larger is better) - Schwarz 1978	log Likelihood Function Value
$CC_{UpCo-01}$	AUDPC	0	-1836.629324	-1827.976842
$CC_{UpCo-01}$	AUDPC	1	-1839.357944	-1827.821302
$CC_{UpCo-01}$	AUDPC	2	-1841.986658	-1827.565855
$CC_{UpCo-01}$	AUDPC	3	-1842.063123	-1824.75816
$CC_{UpCo-01}$	AUDPC	4	-1844.832186	-1824.643063
$CC_{UpCo-01}$	AUDPC	5	-1843.266178	-1820.192894
$CC_{UpCo-01}$	AUDPC	6	-1846.178743	-1820.221298
$CC_{UpCo-01}$	AUDPC	7	-1846.626064	-1817.784459
$CC_{UpCo-01}$	AUDPC	8	-1847.545339	-1815.819573
$CC_{UpCo-01}$	DS	0	-1084.431685	-1075.779204
$CC_{UpCo-01}$	DS	1	-1087.313626	-1075.776984
$CC_{UpCo-01}$	DS	2	-1089.616766	-1075.195964
$CC_{UpCo-01}$	DS	3	-1090.724519	-1073.419556
$CC_{UpCo-01}$	DS	4	-1093.65717	-1073.468046
$CC_{UpCo-01}$	DS	5	-1091.603944	-1068.53066
$CC_{UpCo-01}$	DS	6	-1094.656057	-1068.698613
$CC_{UpCo-01}$	DS	7	-1093.688932	-1064.847327
$CC_{UpCo-01}$	DS	8	-1094.164427	-1062.438661
$CC_{UpCo-01}$	IF	0	-1452.3178	-1443.665319
$CC_{UpCo-01}$	IF	1	-1455.09815	-1443.561508
$CC_{UpCo-01}$	IF	2	-1457.702211	-1443.281408
$CC_{UpCo-01}$	IF	3	-1457.422793	-1440.11783
$CC_{UpCo-01}$	IF	4	-1459.952167	-1439.763043
$CC_{UpCo-01}$	IF	5	-1456.602125	-1433.528841
$CC_{UpCo-01}$	IF	6	-1459.472561	-1433.515116
$CC_{UpCo-01}$	IF	7	-1459.017409	-1430.175804
$CC_{UpCo-01}$	IF	8	-1459.502987	-1427.777222
$CC_{UpCo-01}$	IT	0	151.0841163	159.7365978
$CC_{UpCo-01}$	IT	1	148.2602911	159.7969331
$CC_{UpCo-01}$	IT	2	145.4529507	159.8737532
$CC_{UpCo-01}$	IT	3	144.2539844	161.5589474
$CC_{UpCo-01}$	IT	4	141.4872734	161.6763969
$CC_{UpCo-01}$	IT	5	139.7072834	162.7805674
$CC_{UpCo-01}$	IT	6	138.5311374	164.4885819
$CC_{UpCo-01}$	IT	7	135.671465	164.51307
$CC_{UpCo-01}$	IT	8	138.3100282	170.0357937
$CC_{UpCo-01}$	LP50	0	362.5797033	371.2321848
$CC_{UpCo-01}$	LP50	1	359.8990089	371.4356509
$CC_{UpCo-01}$	LP50	2	357.7542508	372.1750533
$CC_{UpCo-01}$	LP50	3	355.0243478	372.3293108
$CC_{UpCo-01}$	LP50	4	354.0435762	374.2326996
$CC_{UpCo-01}$	LP50	5	351.0034247	374.0767086
$CC_{UpCo-01}$	LP50	6	348.0597713	374.0172158
$CC_{UpCo-01}$	LP50	7	344.885435	373.72704
$CC_{UpCo-01}$	LP50	8	343.6626757	375.3884411
$CC_{UpCo-01}$	MDPr	0	360.6956472	369.3481287
$CC_{UpCo-01}$	MDPr	1	357.9664604	369.5031024

$CC_{UpCo-01}$	MDPr	2	355.6475095	370.068312
$CC_{UpCo-01}$	MDPr	3	355.3337176	372.6386806
$CC_{UpCo-01}$	MDPr	4	352.4887957	372.6779192
$CC_{UpCo-01}$	MDPr	5	352.752123	375.8254069
$CC_{UpCo-01}$	MDPr	6	350.2535358	376.2109802
$CC_{UpCo-01}$	MDPr	7	349.1245157	377.9661207
$CC_{UpCo-01}$	MDPr	8	351.0736744	382.7994399
$CC_{UpKeS-05}$	AUDPC_DS	0	198.7668081	207.4192896
$CC_{UpKeS-05}$	AUDPC_DS	1	196.0140767	207.5507187
$CC_{UpKeS-05}$	AUDPC_DS	2	193.349389	207.7701915
$CC_{UpKeS-05}$	AUDPC_DS	3	191.5341026	208.8390656
$CC_{UpKeS-05}$	AUDPC_DS	4	188.8571973	209.0463208
$CC_{UpKeS-05}$	AUDPC_DS	5	192.3317425	215.4050265
$CC_{UpKeS-05}$	AUDPC_DS	6	189.1672834	215.1247278
$CC_{UpKeS-05}$	AUDPC_DS	7	186.1903702	215.0319752
$CC_{UpKeS-05}$	AUDPC_DS	8	184.4372792	216.1630447
$CC_{UpKeS-05}$	AUDPC_IF	0	241.3528511	250.0053326
$CC_{UpKeS-05}$	AUDPC_IF	1	238.6027033	250.1393453
$CC_{UpKeS-05}$	AUDPC_IF	2	235.8901153	250.3109178
$CC_{UpKeS-05}$	AUDPC_IF	3	233.8715846	251.1765476
$CC_{UpKeS-05}$	AUDPC_IF	4	231.543843	251.7329665
$CC_{UpKeS-05}$	AUDPC_IF	5	232.316143	255.3894269
$CC_{UpKeS-05}$	AUDPC_IF	6	230.0283542	255.9857987
$CC_{UpKeS-05}$	AUDPC_IF	7	227.5242585	256.3658635
$CC_{UpKeS-05}$	AUDPC_IF	8	227.1184141	258.8441796
$CC_{UpKeS-05}$	AUDPC_PS	0	3217.346974	3225.999455
$CC_{UpKeS-05}$	AUDPC_PS	1	3214.445472	3225.982114
$CC_{UpKeS-05}$	AUDPC_PS	2	3211.777535	3226.198337
$CC_{UpKeS-05}$	AUDPC_PS	3	3209.304442	3226.609405
$CC_{UpKeS-05}$	AUDPC_PS	4	3206.484016	3226.67314
$CC_{UpKeS-05}$	AUDPC_PS	5	3203.811321	3226.884605
$CC_{UpKeS-05}$	AUDPC_PS	6	3202.386999	3228.344444
$CC_{UpKeS-05}$	AUDPC_PS	7	3199.950601	3228.792206
$CC_{UpKeS-05}$	AUDPC_PS	8	3197.026778	3228.752544
$CC_{UpKeS-05}$	DS	0	-608.768544	-600.1160626
$CC_{UpKeS-05}$	DS	1	-611.6021578	-600.0655158
$CC_{UpKeS-05}$	DS	2	-614.3050938	-599.8842913
$CC_{UpKeS-05}$	DS	3	-615.8150839	-598.5101209
$CC_{UpKeS-05}$	DS	4	-618.7633	-598.5741765
$CC_{UpKeS-05}$	DS	5	-614.7145816	-591.6412976
$CC_{UpKeS-05}$	DS	6	-617.6961305	-591.738686
$CC_{UpKeS-05}$	DS	7	-620.0673767	-591.2257717
$CC_{UpKeS-05}$	DS	8	-621.9240275	-590.198262
$CC_{UpKeS-05}$	IF	0	-410.867552	-402.2150705
$CC_{UpKeS-05}$	IF	1	-413.5723697	-402.0357277
$CC_{UpKeS-05}$	IF	2	-416.5070376	-402.0862351
$CC_{UpKeS-05}$	IF	3	-418.7826601	-401.4776971
$CC_{UpKeS-05}$	IF	4	-421.6318321	-401.4427086
$CC_{UpKeS-05}$	IF	5	-422.9055249	-399.832241
$CC_{UpKeS-05}$	IF	6	-425.9432575	-399.985813
$CC_{UpKeS-05}$	IF	7	-428.4016068	-399.5600018
$CC_{UpKeS-05}$	IF	8	-431.0086043	-399.2828388

$CC_{UpKeS-05}$	LP50_DS	0	492.3210673	500.9735488
$CC_{UpKeS-05}$	LP50_DS	1	489.9531865	501.4898285
$CC_{UpKeS-05}$	LP50_DS	2	487.0584892	501.4792917
$CC_{UpKeS-05}$	LP50_DS	3	489.4036102	506.7085732
$CC_{UpKeS-05}$	LP50_DS	4	487.3603746	507.5494981
$CC_{UpKeS-05}$	LP50_DS	5	484.7451698	507.8184538
$CC_{UpKeS-05}$	LP50_DS	6	482.4362628	508.3937073
$CC_{UpKeS-05}$	LP50_DS	7	479.7161193	508.5577243
$CC_{UpKeS-05}$	LP50_DS	8	477.4677256	509.1934911
$CC_{UpKeS-05}$	LP50_IF	0	664.4158492	673.0683307
$CC_{UpKeS-05}$	LP50_IF	1	661.5765637	673.1132057
$CC_{UpKeS-05}$	LP50_IF	2	658.6611067	673.0819092
$CC_{UpKeS-05}$	LP50_IF	3	655.7499985	673.0549615
$CC_{UpKeS-05}$	LP50_IF	4	652.9067076	673.0958311
$CC_{UpKeS-05}$	LP50_IF	5	650.0254523	673.0987363
$CC_{UpKeS-05}$	LP50_IF	6	647.3820004	673.3394448
$CC_{UpKeS-05}$	LP50_IF	7	644.4443717	673.2859767
$CC_{UpKeS-05}$	LP50_IF	8	641.6487432	673.3745087
$CC_{UpKeS-05}$	LP50_PS	0	313.5855246	322.2380061
$CC_{UpKeS-05}$	LP50_PS	1	310.9583475	322.4949895
$CC_{UpKeS-05}$	LP50_PS	2	307.9213953	322.3421978
$CC_{UpKeS-05}$	LP50_PS	3	305.196908	322.501871
$CC_{UpKeS-05}$	LP50_PS	4	302.5965982	322.7857216
$CC_{UpKeS-05}$	LP50_PS	5	309.1446295	332.2179135
$CC_{UpKeS-05}$	LP50_PS	6	306.8233849	332.7808294
$CC_{UpKeS-05}$	LP50_PS	7	304.0504556	332.8920606
$CC_{UpKeS-05}$	LP50_PS	8	301.2081306	332.9338961
$CC_{UpKeS-05}$	MDPr_DS	0	210.4625909	219.1150724
$CC_{UpKeS-05}$	MDPr_DS	1	207.7157248	219.2523668
$CC_{UpKeS-05}$	MDPr_DS	2	205.2524441	219.6732466
$CC_{UpKeS-05}$	MDPr_DS	3	203.919043	221.224006
$CC_{UpKeS-05}$	MDPr_DS	4	201.0786518	221.2677753
$CC_{UpKeS-05}$	MDPr_DS	5	206.4461219	229.5194058
$CC_{UpKeS-05}$	MDPr_DS	6	203.2239402	229.1813847
$CC_{UpKeS-05}$	MDPr_DS	7	200.3843595	229.2259645
$CC_{UpKeS-05}$	MDPr_DS	8	197.8880741	229.6138396
$CC_{UpKeS-05}$	MDPr_IF	0	126.6897689	135.3422504
$CC_{UpKeS-05}$	MDPr_IF	1	123.8148325	135.3514745
$CC_{UpKeS-05}$	MDPr_IF	2	121.3865352	135.8073377
$CC_{UpKeS-05}$	MDPr_IF	3	119.412142	136.717105
$CC_{UpKeS-05}$	MDPr_IF	4	116.5488945	136.738018
$CC_{UpKeS-05}$	MDPr_IF	5	118.8402935	141.9135775
$CC_{UpKeS-05}$	MDPr_IF	6	116.7198564	142.6773009
$CC_{UpKeS-05}$	MDPr_IF	7	116.5958193	145.4374243
$CC_{UpKeS-05}$	MDPr_IF	8	118.1126726	149.8384381
$CC_{UpKeS-05}$	MDPr_PS	0	1653.943456	1662.595937
$CC_{UpKeS-05}$	MDPr_PS	1	1651.104104	1662.640746
$CC_{UpKeS-05}$	MDPr_PS	2	1648.164795	1662.585598
$CC_{UpKeS-05}$	MDPr_PS	3	1645.408209	1662.713172
$CC_{UpKeS-05}$	MDPr_PS	4	1642.434048	1662.623172
$CC_{UpKeS-05}$	MDPr_PS	5	1643.689891	1666.763175
$CC_{UpKeS-05}$	MDPr_PS	6	1641.283304	1667.240748

$CC_{UpKeS-05}$	MDPr_PS	7	1638.811825	1667.65343
$CC_{UpKeS-05}$	MDPr_PS	8	1635.668485	1667.39425
$Field_{UpCo-01}$	DS_field	0	-969.096726	-960.4442445
$Field_{UpCo-01}$	DS_field	1	-971.7952153	-960.2585733
$Field_{UpCo-01}$	DS_field	2	-974.7089842	-960.2881818
$Field_{UpCo-01}$	DS_field	3	-975.9296814	-958.6247184
$Field_{UpCo-01}$	DS_field	4	-977.7769702	-957.5878467
$Field_{UpCo-01}$	DS_field	5	-977.1602916	-954.0870077
$Field_{UpCo-01}$	DS_field	6	-979.4395547	-953.4821102
$Field_{UpCo-01}$	DS_field	7	-981.9978888	-953.1562839
$Field_{UpCo-01}$	DS_field	8	-984.9265113	-953.2007458
$Field_{UpCo-01}$	DS_2018	0	-936.1170249	-927.4645434
$Field_{UpCo-01}$	DS_2018	1	-939.0509782	-927.5143362
$Field_{UpCo-01}$	DS_2018	2	-941.771783	-927.3509805
$Field_{UpCo-01}$	DS_2018	3	-944.4845542	-927.1795912
$Field_{UpCo-01}$	DS_2018	4	-946.4971521	-926.3080286
$Field_{UpCo-01}$	DS_2018	5	-948.3202499	-925.2469659
$Field_{UpCo-01}$	DS_2018	6	-949.8942639	-923.9368194
$Field_{UpCo-01}$	DS_2018	7	-952.9389032	-924.0972983
$Field_{UpCo-01}$	DS_2018	8	-955.9977196	-924.2719541
$Field_{UpCo-01}$	DS_2019	0	-1034.601155	-1025.948674
$Field_{UpCo-01}$	DS_2019	1	-1037.010733	-1025.474091
$Field_{UpCo-01}$	DS_2019	2	-1039.911396	-1025.490594
$Field_{UpCo-01}$	DS_2019	3	-1040.76812	-1023.463157
$Field_{UpCo-01}$	DS_2019	4	-1041.764394	-1021.575271
$Field_{UpCo-01}$	DS_2019	5	-1038.665906	-1015.592622
$Field_{UpCo-01}$	DS_2019	6	-1040.926593	-1014.969148
$Field_{UpCo-01}$	DS_2019	7	-1041.154473	-1012.312868
$Field_{UpCo-01}$	DS_2019	8	-1043.825191	-1012.099425
$Field_{UpCo-01}$	DS_2020	0	-1100.28252	-1091.630038
$Field_{UpCo-01}$	DS_2020	1	-1103.044926	-1091.508285
$Field_{UpCo-01}$	DS_2020	2	-1105.868679	-1091.447877
$Field_{UpCo-01}$	DS_2020	3	-1106.913756	-1089.608793
$Field_{UpCo-01}$	DS_2020	4	-1109.74129	-1089.552167
$Field_{UpCo-01}$	DS_2020	5	-1110.871206	-1087.797922
$Field_{UpCo-01}$	DS_2020	6	-1113.855119	-1087.897675
$Field_{UpCo-01}$	DS_2020	7	-1116.944602	-1088.102997
$Field_{UpCo-01}$	DS_2020	8	-1119.975702	-1088.249937

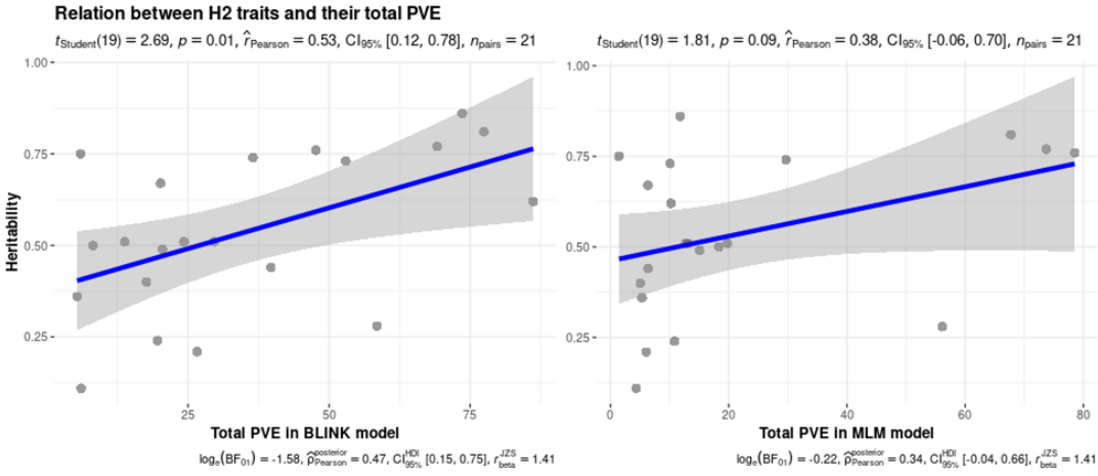

Additional file 8. Scatterplot between heritability of each trait by its cumulative phenotypic variance explained (PVE_{sum}) by the markers obtained through BLINK model (left) or MLM model (right). Inferential statistics with effect size plus CIs are at the top of the plot while Bayesian hypothesis-testing and estimation are at the bottom.

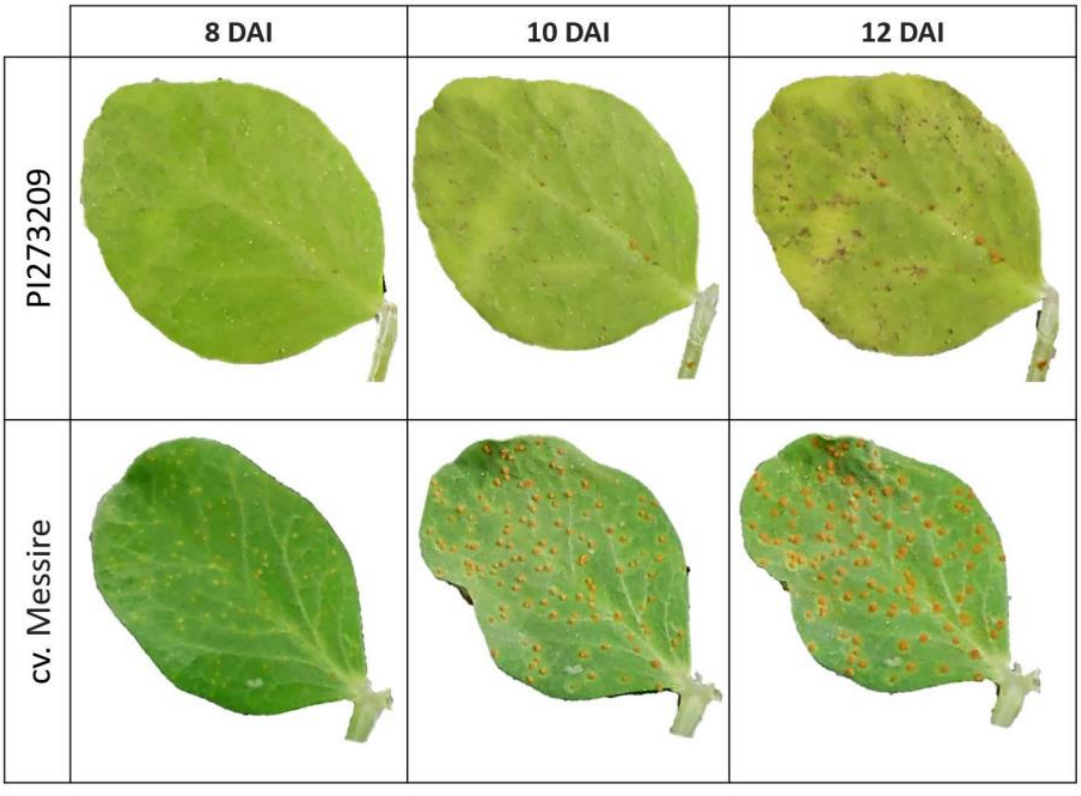

Additional file 9. Rust (UpKe-05 isolate) symptoms progression by 8, 10 and 12 days after inoculation (dai) in cv. Messire and PI273209 accession leaflets.

Chapter 5
Genomic Prediction for Rust Resistance in Pea

1. Abstract

Genomic selection (GS) has become an indispensable tool in modern plant breeding, particularly for complex traits like rust resistance in peas (*Pisum sativum* L.) that are heavily influenced by environmental factors. This study evaluates the efficacy of GS in predicting rust resistance, using a panel of 320 pea accessions and 26,045 DArT-Seq markers. We compared the prediction abilities of several GS models, including genomic best linear unbiased prediction (GBLUP), and explored the impact of incorporating marker × environment (MxE) interactions as a covariate in the GBLUP model. The analysis encompassed data from both field and controlled conditions. We assessed the predictive accuracies of different cross-validation strategies and compared the efficiency of using single traits versus a multi-trait index approach, specifically the FAI-BLUP, which combines traits from controlled conditions. The GBLUP model, particularly when modified to include MxE interactions, consistently outperformed other models, demonstrating its suitability for traits affected by complex genotype-environment interactions. Notably, the best predictive ability (0.635) was achieved using the FAI-BLUP approach within the Bayesian Lasso (BL) model. The inclusion of MxE interactions significantly enhanced prediction accuracy across diverse environments in GBLUP models, although it did not markedly improve predictions for not-phenotyped lines. These findings underscore the variability of predictive abilities due to genotype by environment (GEI) interactions and the effectiveness of multi-trait approaches in addressing such complexities. Overall, our study illustrates the potential of GS, especially when employing a multi-trait index like FAI-BLUP and accounting for MxE interactions, in pea breeding programs focused on rust resistance. This approach provides a robust framework for handling GEI challenges, making GS a valuable asset in the quest for improved rust resistance.

2. Introduction

Pea, *Pisum sativum* L. (7n = 14), is a significant cool-season legume crop cultivated predominantly in temperate climates. With an annual global production exceeding 14 million tons of dry and 21 million tons of green peas (FAOSTAT, 2022), it holds substantial nutritional value, being a rich source of proteins, starch, fibers, vitamins, and minerals. Its symbiotic relationship with nitrogen-fixing bacteria underscores its role in enhancing soil fertility, making it a vital component in sustainable cropping systems (Guo et al., 2021). Cultivars of pea are primarily inbred lines, largely homozygous, developed through several generations of self-fertilization following initial hybridization (van de Wouw et al., 2010). This breeding process is time-intensive, requiring years to yield genetically and phenotypically stable lines suitable for field trials and eventual commercialization. Hence, there is a pronounced need for more efficient breeding strategies, such as high-throughput genotyping or

phenotyping, to expedite the identification and development of elite lines (Annicchiarico et al., 2023).

One of the main objectives in the development of elite pea lines is the introduction of new resistance sources to pests and diseases, which are major constraints to global pea production (Rubiales et al., 2023). Therefore, disease resistance is a key focus in pea breeding programs, and significant advances have been made using marker-assisted selection (MAS) for diseases controlled by single gene traits. For instance, polymerase chain reaction (PCR) markers facilitate the identification of breeding lines carrying DNA polymorphisms linked to resistance against viruses such as Pea seedborne mosaic virus (Grimm & Porter, 2021) and Pea enation mosaic virus (Jain et al., 2013), as well as fungal diseases like powdery mildew which resistance are controlled by *er1*, *er2* and *Er3* genes (Fondevilla & Rubiales, 2012). However, challenges persist in managing diseases with polygenic resistance nature, including root rot caused by *Aphanomyces eusteiches* (Leprévost et al., 2023) or fusarium wilt (Sampaio et al., 2020) and aerial diseases such as ascochyta blight (Barilli et al., 2016) or rust (Osuna-Caballero et al., 2022). Rust disease, caused by *Uromyces* spp., can reduce pea yields by up to 50%, varying with environmental conditions and the specific pathogen involved. *U. viciae-fabae* predominantly affects peas in tropical and subtropical climates, while *U. pisi* is more prevalent in temperate regions, both causing significant epidemics cycles during the crop season (Singh et al., 2023). Complete resistance to rust has yet to be identified in peas, and measuring partial resistance is challenging due to the influence of environmental factors like rainfall, temperature, and inoculum levels on disease prevalence in field (Das et al., 2019). Partial resistance to *U. pisi*-induced rust is multigenic, with some QTLs identified in biparental populations using wild relatives as resistance donors (Barilli et al., 2010; 2018). In addition, GWAS analysis has identified 95 DArT-seq polymorphic markers linked to rust resistance, pointing to 62 candidate genes putatively involved in resistance to *U. pisi* (Osuna-Caballero et al., 2024a). Genomic selection (GS), utilizing a wide array of genetic markers across the genome, offers a promising approach to select elite breeding lines for complex, multigenic traits such as rust resistance, where complete resistance is not available.

Genomic prediction, originally pioneered in the livestock industry, has expanded its utility across a diverse range of plant species, encompassing fruit and timber trees (Resende et al., 2012; Wang et al., 2023), as well as major crops such maize and wheat (Crossa et al., 2017). GS accelerates the breeding cycle in annual inbred crops, enabling earlier selection of breeding parents based on Genomic Estimated Breeding Values (GEBV) in successive filial generations (Lin et al., 2017). The focus of GS studies has often been on genotype-environment interactions (GEI) to improve prediction accuracy highlighting those effects as a crucial factor and allowing the development of novel complex models which integrate those effects as covariates (Tolhurst et al., 2022). This includes predicting GEBVs for lines lacking

phenotypic data and extending predictions across various environments for partially phenotyped lines. The application of GS in plant breeding varies significantly among crops and traits, influenced by each genetic architecture and specific breeding and cultivation systems (Akdemir & Isidro-Sánchez, 2019). In pea breeding, GS has been employed to assess important agronomic traits such as thousand-seed weight, seed number per plant, and flowering date (Tayeh et al., 2015). Remarkably, prediction accuracies for traits like thousand-seed weight reached as high as 0.83, underscoring the potential of GS in pea breeding, particularly when traits are relatively easy to measure and highly heritable. In addition, the size and composition of the training population, carefully selected, significantly affect prediction accuracy (Akdemir & Isidro-Sánchez, 2019). In recent research, GS has also been applied to predict pea grain yield, protein content, and morphological traits using Genotyping-by-Sequencing (GBS) data (Annicchiarico et al., 2019, 2020; Crosta et al., 2022, 2023). For instance, those approaches yielded accurate intrapopulation (0.84) and interpopulation (0.71) prediction accuracies for grain yield, proving to be cost-effective as phenotyping costs were notably higher than genotyping costs (Annicchiarico et al., 2019). These findings suggest that GS could be a valuable tool in pea breeding programs. However, its efficacy for disease traits in peas remains an area for further exploration where some advances have only performed in ascochyta blight resistance (Carpenter et al., 2018).

GS requires comprehensive genotypic data, typically acquired through methods like high-density arrays or GBS. Among GBS approaches, DArTSeq genotyping has emerged as a suitable genomic method for GS, genetic mapping and population genetics approaches in many plant species (Alam et al., 2018; Alemu et al., 2022). This method, which enables the generation both SNP and SilicoDArT markers, is particularly effective for crops with large genomes abundant in repetitive sequences, such as peas (Barilli et al., 2018). It sequences regions adjacent to restriction enzyme sites, and by employing methylation-sensitive enzymes, preferentially targets coding regions over repetitive DNA (Akbari et al., 2006). In GS analyses, prediction accuracy is often gauged by the correlation between predicted and observed trait values. However, beyond estimating the breeding value (BV) for entire populations, plant breeders are particularly interested in accurately predicting top-performing individuals for selection as elite cultivars or parental lines for subsequent breeding cycles (Bassi et al., 2016). GS presents a dual advantage in pea genetic improvement: it facilitates the prediction of GEBV for individuals lacking phenotypic data and enhances the precision of BV estimates for phenotyped individuals, especially for traits that are challenging to measure (Rubiales et al., 2021). This is achieved by integrating trait data from multiple environments and/or years with genotypic information. Moreover, leveraging molecular data for BV estimation offers inherent advantages over traditional pedigree-based approaches (Hayes et al., 2009). Molecular data provide a 'realized relationship matrix,' reflecting the actual genetic

relationships among individuals, as opposed to the 'expected values' used in pedigree-based matrices, where relative individuals are assumed to have average and equal genetic contributions (Crossa et al., 2010). This nuanced understanding of genetic relationships afforded by molecular data underpins the enhanced accuracy of GS, making it a transformative tool in modern plant breeding.

Assessments of the different models used for genomic selection have not revealed a single model that always surpass the others, since model performance depends on the number of genomic regions influencing a trait and the magnitude of its effects (Habier et al., 2011; Heffner et al., 2011). Furthermore, different models make assumptions that may or may not match the genetic architecture of the traits of interest. Therefore, in this study we present a comprehensive evaluation of GS models for rust resistance in peas, tailoring our approach to align with the practical demands of current pea breeding programs (Annicchiarico et al., 2023). Utilizing genotypic data from Rispail et al. (2023) and phenotypic data against *U. pisi* from Osuna-Caballero et al. (2022), we trained and validated several GS models. Our objectives included comparing the predictive abilities of these models for phenotype prediction, examining the influence of multi-trait indices on their predictive accuracy, and investigating the role of genotype by environment interactions in the context of field condition predictions. The study encompassed an in-depth analysis using the three most prevalent cross-validation schemes, recognized for their relevance and applicability in validating genomic selection equations in plant breeding. This methodical approach allowed us not only to assess the efficacy of different GS models in a breeding context but also to explore how the integration of complex data, such as multi-trait indices and environmental interactions, can optimize predictive accuracies. Our findings aim to contribute valuable insights into the deployment of GS strategies for enhancing rust resistance in pea crops, thereby aiding breeders in their selection and genetic improvement endeavours.

3. Material and Methods

3.1. Plant Material

The pea panel utilized in this study comprise an extensive collection of 320 accessions of *Pisum* spp., encompassing a diverse range of genetic material, including wild relatives, landraces, cultivars, breeding lines, and unidentified genotypes sourced from various continents. The selection of these genotypes was carried out meticulously, with an aim to cover a broad spectrum of genotypic and phenotypic variance, as highlighted by Rispail et al. (2023). This approach ensures a comprehensive representation of the *Pisum* genera, capturing the genetic diversity across the three main species – *P. sativum*, *P. fulvum*, and *P. abyssinicum* – as well as the *P. sativum* subspecies, namely *sativum*, *arvense*, *jomardi*, *elatius*, and *humile*. The selection was also based on specific criteria including historical resistance

performance, genetic diversity, and unique phenotypic profile that are potentially linked to disease resistance and favorable agronomic traits (Rispail et al., 2023). The inclusion of genotypes collected worldwide not only adds to the genetic mixture but also allows for the examination of genotype-environment interactions.

3.2. Phenotyping and Statistical Analysis

The pea panel was evaluated under rain-fed conditions in three autumn-sown environments in Cordoba, southern Spain. These environments are referred to as Cordoba 2018 (DS-2018), Cordoba 2019 (DS-2019), and Cordoba 2020 (DS-2020). According to the Köppen–Geiger classification system, this location represents the hot dry-summer Mediterranean climate, a common form of the Mediterranean climate characterized by hot, dry summers and mild, wet winters (Kottek et al., 2006).

Each growing season, the experiment was conducted in an alpha lattice design with three replications, using cv. Cartouche as check control. The experimental procedures and evaluations are detailed in Osuna-Caballero et al. (2022). The primary recorded trait was disease severity, expressed as the proportion of pustules covering the experimental unit. Additionally, four traits related to rust disease in pea were assessed in a growth chamber for the entire panel: (i) infection frequency (IF), measured as the number of pustules per cm^2 of leaf, counted daily from day 7 to day 14 post-inoculation; (ii) the area under the disease progress curve (AUDPC) based on the daily IF scores; (iii) infection type (IT), classified according to Stackman et al. (1962) and (iv) disease severity (DS), quantified as the percentage of tissue damaged by pustules.

Each accession underwent four evaluation rounds through inoculation, with three inoculations performed as described in Osuna-Caballero et al. (2022). An analysis of variance (ANOVA) was conducted to assess variation among accessions, genotype material, and between environments (controlled conditions or field), wherein the genotype × environment interaction (GEI) variation was dissected using an additive main effects and multiplicative interaction (AMMI) analysis. This approach is particularly valuable for unravelling patterns of GEI, and it was employed to determine the range of genotype stability and adaptability among the nine most resistant and the three most susceptible lines identified in the study by Osuna-Caballero et al. (2022). Additionally, the AMMI analysis provided further insights into the environmental consistency regarding GEI effects. In this approach, the Yij response—denoting the reaction of genotype i in environment j—follows the model proposed by Olivoto et al. (2019). The analysis was performed using the 'metan' package in R (Olivoto et al., 2020).

The genetic correlation (r_g) for genotype rust responses across traits and environments was estimated according to Howe et al. (2000). For each environment,

components of variance relative to genotype variation (CV_g) and experimental error (CV_e) were estimated using the restricted maximum likelihood (REML) in the linear mixed model, where the factor of interest (accession) was included as fixed effect, and the remaining sources of variance were fitted as random variables. The fitted model, using the R package lme4 (Bates et al., 2015), allowed the calculation of the best linear unbiased prediction (BLUP) by genotype for every single trait following the methodology of DeLacy et al. (1996). In addition, multi- environment trial (MET) allowed the calculation of the BLUPs of the merged data from the three field seasons (megaENV). The BLUPs estimated for each trait collected under controlled conditions served as phenotypic data for computing a multi-trait index (FAI-BLUP) based on factor analysis and ideotype-design proposed by Rocha et al. (2018), and for subsequent genomic prediction assessments. Broad-sense heritability on an accession mean basis was estimated for each trait and environment as per Nizam et al. (1994).

3.3. Genotyping and Data Filtering

The pea core collection was genotyped using the DArTSeq approach by DiversityArray Ltd, Australia. For this process, the third compound leaves from twenty-two-week-old seedlings of each accession, grown under controlled conditions, were harvested. These samples were pooled, flash-frozen in liquid nitrogen, and subsequently lyophilized. DNA extraction was then carried out following the method prescribed by Diversity Arrays P/L, Canberra, Australia. The extracted DNA was adjusted to a concentration of 20 ng/µl prior to DArT marker analysis. This analysis was conducted using the high-density Pea DArTseq 1.0 array, which consists of 50,000 markers and is specially adapted for wild *Pisum* spp. accessions. The genotyping process involved complexity reduction using PstI-MseI restriction enzymes, followed by library construction, amplification, and Illumina sequencing. These steps were performed by Diversity Arrays Technology Pty Ltd, Canberra, Australia, as detailed in Barilli et al. (2018). The DArTSeq sequence analysis yielded two sets of markers: Single Nucleotide Polymorphisms (SNPs) and presence-absence sequence variants (Silico-DArT), where Silico-DArT was the genetic information used in the GS analysis.

Data cleaning was then meticulously performed for DArT markers. This process was undertaken to eliminate low-quality and non-polymorphic markers, as described by Rispail et al. (2023). Markers exhibiting more than 20% missing data, a minor allele frequency (MAF) below 5%, and heterozygosity exceeding 0.1% were excluded from the analysis. Missing data were imputed using the Singular Value Decomposition (SVD) method, adhering to the recommendations of Nazzicari et al., (2016).

3.4. Genomic Regression Models and Data Configurations

Genome-enabled predictions in this study were primarily based on Silico-DArT markers. We focused on three genomic prediction models known for their predictive ability in legume species, particularly in relation to pea traits: Ridge regression BLUP (rrBLUP), Bayesian Lasso (BL), and Genomic BLUP (GBLUP), as identified in previous comparisons (Annicchiarico et al., 2017; Carpenter et al., 2018).

The rrBLUP model, proposed by Meuwissen et al. (2001), assumes a common variance across all loci, making it suitable for traits influenced by many minor genes. Its linear mixed additive model equation is:

$$y = \mu + Gu + \varepsilon$$

where y is the vector of observed phenotypes, μ is the mean of y, G is the genotype matrix (i.e., {0, 1} for absence/presence sequence variants Silico-DArT markers), $u \sim N(0, I\sigma^2 u)$ is the vector of marker effects, and $\varepsilon \sim N(0, I\sigma^2 \varepsilon)$ is the vector of residuals. The solution, utilizing standard ridge-regression methods, is:

$$u = G'(G' + \lambda\, I)^{-1}(y - \mu)$$

where $\lambda = \frac{\sigma_e^2}{\sigma_u^2}$ is the ridge parameter, representing the ratio between residual and markers variance (Searle et al. 2006) estimated by a REML method implemented by a spectral decomposition algorithm (Hyun et al. 2008). Given the vector of markers effects, it is then possible to predict phenotypes and GEBV.

The GBLUP model follows a similar equation to rrBLUP but uses a marker-based genomic relationship matrix (GRM) instead of the marker matrix (Hayes et al., 2009). Allele frequencies in this GRM were estimated from the observed genotype data. This model was also trained after incorporating the marker x environmental (MxE) effect matrix as covariate to evaluate its influence over the predictions.

Bayesian models, such as Bayesian Lasso (BL), permit different effects and variances for markers, typically few with large effects (Wang et al., 2018). These models assign prior densities to marker effects and induce various types of shrinkage. Solutions are obtained by sampling from the posterior density via a Gibbs sampling approach (Casella & George, 1992), with BL implementation as per Park and Casella, (2008).

Predictive ability (r_ab) of these genome-enabled models for rust traits in the pea panel was assessed using the R package GROAN (Nazzicari & Biscarini, 2022). r_ab was estimated as Pearson's correlation between observed and predicted phenotypes, following three cross-validation (CV) strategies: (i) single trait and intra-environment cross-validation, training and testing each trait per environment [CV0]; (ii) single trait and cross-environment validation, predicting known lines over an environment used in the training model [CV1]; (iii) single trait and inter-environment cross-validation, predicting new lines in an untrained environment [CV2].

Overall, we assessed 11-model configurations represented by combinations of three genomic prediction models (rrBLUP, GBLUP or BL) in which MxE interaction is evaluated in GBLUP model and three CV procedures with one marker data set (DArT-seq).

Finally, the accuracy (r_ac) of these models was estimated from r_ab and the square root of broad-sense heritability on an entry mean basis in the validation environment (H), following Lorenz et al. (2011): $r_{ac} = \frac{r_{ab}}{H}$

4. Results

4.1. Phenotypic data

The phenotypic data revealed consistent patterns across different years under field condition and between traits measured under controlled conditions as shown in Osuna-Caballero et al. (2022). Here, we further explored the phenotypic correlation (rp) between the FAI-BLUP index, and the single traits measured under controlled and field conditions, as well as their genetic correlations (Figure 18). Notably, the integration of traits measured under controlled conditions into the FAI-BLUP index improved Pearson correlations between traits. Consequently, the rp values between FAI-BLUP and DS in 2018 (DS-2018), 2019 (DS-2019), 2020 (DS-2020), and in the MegaENV were 0.24, 0.47, 0.41, and 0.46, respectively. Higher than those between DS in controlled conditions and DS-2018 (rp = 0.14), DS-2019 (rp = 0.32), DS-2020 (rp = 0.39), and MegaENV (rp = 0.44). In addition, correlations between FAI-BLUP and field data were also higher than those estimated between any other single trait measured under controlled conditions (AUDPC, IT and IF) and the corresponding field data (Figure 18).

Under controlled conditions, we also observed that the FAI-BLUP index correlated more strongly with individual traits. The correlation between the AUDPC and FAI-BLUP was the highest (rp = 0.90), while the correlation between IT and FAI-BLUP was comparatively lower but still robust (rp = 0.70).

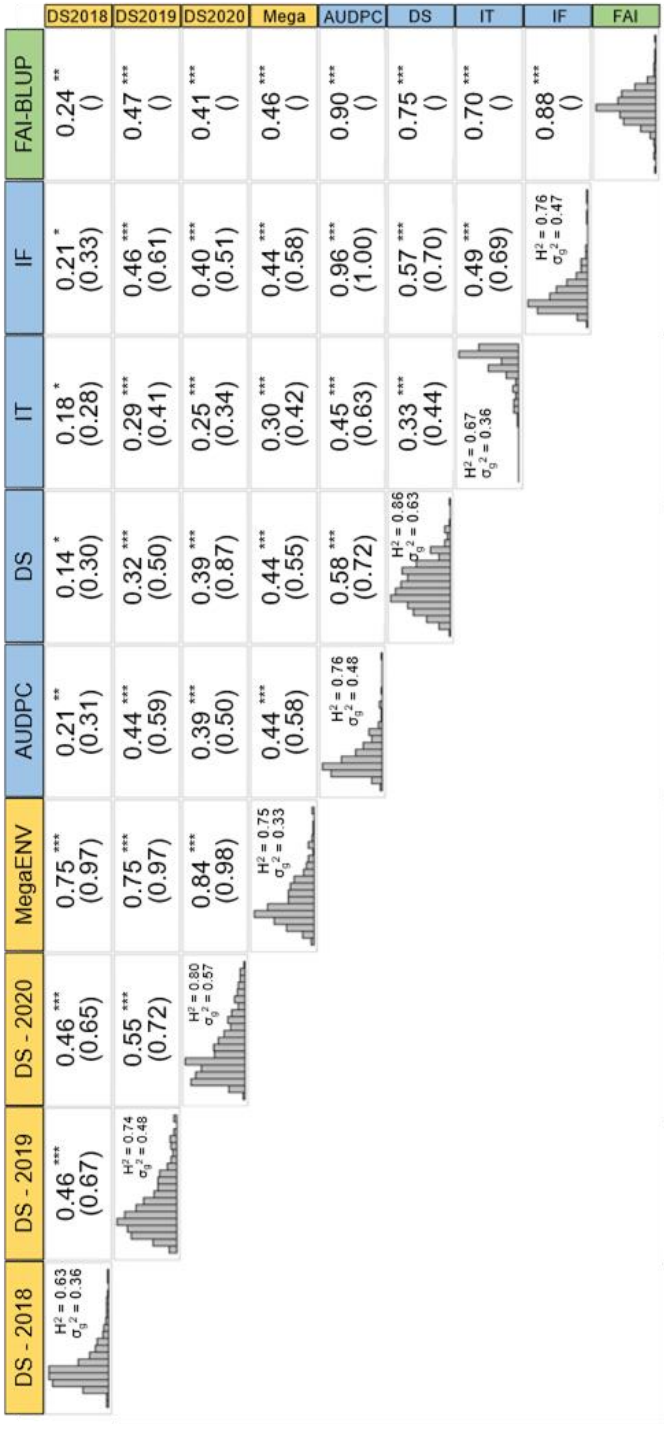

Figure 18. Trait correlation between field (yellow), controlled conditions (blue) and FAI-BLUP index (green). Phenotypic correlation (rp) and genotypic correlation (rg) under brackets are depicted in each trait's intersection. Each trait shows its distribution, heritability, and genetic variance. *, ** and *** represent the significance of the rp at 0.05, 0.01 and 0.001, respectively.

The genetic correlation, rg, which assesses the extent to which the same genes influence a trait across different environments (such as different field seasons or traits under controlled conditions), also revealed differences between traits/environments. The highest genetic correlation was observed between DS-2020 and DS-2019 (rg = 0.72), suggesting that rust severity in those years was influenced by similar genetic factors. In contrast, genetic correlations were generally lower between traits measured under controlled conditions and in the field, with the notable exception of DS, which exhibited a high genetic correlation (rg = 0.80) with DS-2020 (Figure 18).

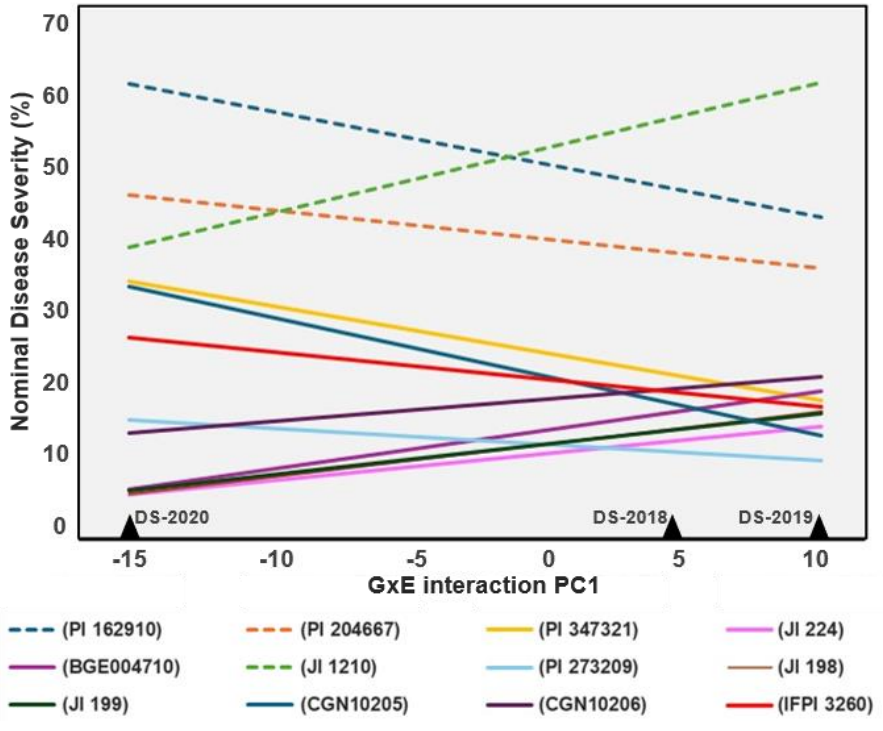

Figure 19. Estimated nominal disease severity (DS%) of nine most resistance (straight lines) and three susceptible (dashed lines) accessions based on FAI-BLUP index along the GEI PC1 axis.

AMMI analysis of DS percentages revealed that the first GEI principal component axis (PC1) was highly significant ($P < 0.001$), explaining 80% of the GEI variance (Additional file 10). This axis notably distinguished the 2020 field season from the two preceding years in terms of genotype responses, as depicted in Figure 19. The AMMI model illustrated pronounced cross-type GEI interactions, characterized by a range shift between the resistant and susceptible lines across the different environments. Particularly in the 2020 field environment, there was an observable increase in line variation (Figure 19). Notably, resistant and susceptible accessions form two cluster that did not intersect across environments, indicating consistency in their response patterns, as visualized in Figure 19. Specifically, lines JI

224, PI 273209, JI 199, and CGN 10206 demonstrated a distinct advantage in terms of both resistance and stability, even within these significant contrasting environments (Figure 19).

4.2. Genome-enabled modelling

4.2.1. Predictive abilities of rrBLUP, BL and GBLUP under CV0 scenario

This study assessed the intra-environment ability of three genomic prediction models (rrBLUP, BL and GBLUP) trained with a Silico-DArT marker data set to predict pea rust across controlled and field conditions. The average predictive abilities (rab) obtained for each trait under the intra-environment scenario of cross-validation (CV) are depicted in Table 12.

rrBLUP and BL models showed similar predictive abilities for all traits. Under controlled conditions, predictive abilities (rab) of BL varied from 0.569 for IF predicted by BL to 0.635 for FAI-BLUP. In this scenario, rab of the G-BLUP model were slightly lower ranging from 0.510 for IF to 0.633 for FAI-BLUP (Table 12). For all three models, the highest predictive ability was reached for FAI-BLUP trait (rab = 0.635).

Table 12. Intra-environment predictive ability of Ridge regression BLUP (rrBLUP), Bayesian Lasso (BL) or Kernel Genomic BLUP model trained with a Silico-Dart data set to predict pea rust disease parameter in four environments [a].

	Controlled Conditions					Field Conditions			
Model	**AUDPC**	**IF**	**IT**	**DS**	**FAI-BLUP**	**DS-2018**	**DS-2019**	**DS-2020**	**Mega-ENV**
rrBLUP	0.602	0.572	0.579	0.601	0.633	0.258	0.544	0.308	0.460
BL	0.602	0.569	0.571	0.604	0.635	0.261	0.541	0.302	0.459
GBLUP	0.576	0.510	0.544	0.590	0.633	0.270	0.558	0.310	0.446

[a] Predictions were based on 50 repetitions of 10-fold stratified cross validations per individual analysis.

For the field data, the predictive abilities of the three models were notably lower. In this case, the G-BLUP model achieved the highest predictive abilities for all single environment ranging from 0.27 for DS-2018 to 0.558 for DS-2019 while its ability to predict MegaENV (rab = 0.446), which encapsulates the overall environmental variance, was slightly lower than rrBLUP and BL that reached 0.460 and 0.459, respectively under this CV scenario.

4.2.2. Predictive abilities of rrBLUP, BL and GBLUP under CV1 scenario

The genomic selection models were also trained and tested across different environments to evaluate their ability and accuracy in predicting rust disease in peas. Under the CV1 scenario, moderate predictive abilities were obtained for all three

models when they were trained with DS values obtained under controlled conditions and tested on the MegaENV data. In this case, the highest predictive ability value was reached by GBLUP (rab = 0.382) followed by rrBLUP (rab = 0.378) and BL (rab = 0.369. GBLUP also outperformed the other models in terms of predictive accuracy (rac), with a score of 0.441, while rrBLUP and BL exhibited rac values of 0.436 and 0.426 respectively. Training models with the FAI-BLUP index dataset and testing them on MegaENV data improved the model predictive abilities with GBLUP exhibiting the highest predictive ability (rab = 0.500) and accuracy (rac =0.577).

Table 13. Cross-environment [CV1] predictive ability (rab) and predictive accuracy (rac) of pea rust across different traits and two environments estimated with Ridge regression BLUP (rrBLUP), Bayesian Lasso (BL) or Kernel Genomic BLUP model trained on a Silico-DArT marker data set [a].

Training set	Test set	r_{ab}			r_{ac}		
		rrBLUP	**BL**	**GBLUP**	**rrBLUP**	**BL**	**GBLUP**
DS	MegaENV	0.378	0.369	0.382	0.436	0.426	0.441
FAI-BLUP	MegaENV	0.419	0.402	0.500	0.484	0.464	0.577
DS-2018	DS-2019	0.498	0.491	0.605	0.579	0.571	0.703
DS-2018	DS-2020	0.384	0.411	0.465	0.430	0.460	0.520
DS-2019	DS-2018	0.357	0.358	0.369	0.450	0.451	0.465
DS-2019	DS-2020	0.463	0.465	0.503	0.518	0.520	0.562
DS-2020	DS-2018	0.357	0.386	0.388	0.450	0.486	0.489
DS-2020	DS-2019	0.605	0.596	0.627	0.703	0.693	0.730

[a] Prediction were based on 50 repetitions of 10-fold stratified cross validations per individual analysis.

For the field data with this CV1scenario, the models trained on DS-2018 and tested with DS-2019 exhibited high predictive abilities and accuracies, especially for GBLUP (rab = 0.605, rac = 0.703). Conversely, models trained on DS-2019 and tested on DS-2018, led to lower predictive abilities and accuracies. The highest predictive abilities and accuracies were observed after training the models on DS-2020 and testing them on DS-2019 (Table 13). Once again, GBLUP outperformed rrBLUP and BL, exhibiting predictive ability and accuracy of 0.627 and 0.730 respectively.

4.2.3. Predictive abilities of rrBLUP, BL and GBLUP under CV2 scenario

In the last cross-validation scheme (CV2), the genomic selection models were trained on one set of data and validated on a different, untrained environment, simulating the prediction of new pea lines performance (Table 14). When the models were trained on controlled condition DS and validated on MegaENV, predictive abilities were moderate, with GBLUP exhibiting a slightly higher ability (rab = 0.332) compared to rrBLUP (rab = 0.329) and BL (rab = 0.319). The predictive accuracies

for these models were closely matched, with GBLUP leading at 0.383. Training on FAI-BLUP and validating on MegaENV data improved the model predictive abilities, with GBLUP displaying again the highest ability (rab = 0.427) and accuracy (rac = 0.493).

Table 14. Cross-environment [CV2] predictive ability (rab) and predictive accuracy (rac) of pea rust traits estimated with Ridge regression BLUP (rrBLUP), Bayesian Lasso (BL) or Kernel Genomic BLUP model trained on a Silico-DArT marker data set [a].

Training set	Validation set	r_{ab}			r_{ac}		
		rrBLUP	BL	GBLUP	rrBLUP	BL	GBLUP
DS	MegaENV	0.329	0.319	0.332	0.380	0.368	0.383
FAI-BLUP	MegaENV	0.331	0.400	0.427	0.382	0.462	0.493
DS-2018	DS -2019	0.377	0.330	0.519	0.438	0.384	0.603
DS -2018	DS -2020	0.223	0.217	0.295	0.249	0.243	0.330
DS -2019	DS -2018	0.198	0.197	0.177	0.250	0.220	0.223
DS -2019	DS -2020	0.326	0.307	0.352	0.365	0.384	0.394
DS -2020	DS -2018	0.198	0.204	0.201	0.250	0.236	0.253
DS -2020	DS -2019	0.479	0.435	0.510	0.557	0.502	0.593

[a] Prediction were based on 50 repetitions of 10-fold stratified cross validations per individual analysis.

For the field datasets, models trained on DS-2018 and validated on DS-2019 showed notable predictive abilities and accuracies, particularly GBLUP (rab = 0.519, rac = 0.603) while validating these models with DS-2020 decrease predictive abilities and accuracies. Training models with DS-2019 led to low predictive abilities and accuracies. Conversely, training models on DS-2020 and validating them with DS-2019 exhibited again the highest predictive ability (rab = 0.479 for GBLUP) and accuracy (rac = 0.593 for GBLUP) within this CV2 scenario (Table 14).

4.2.4. Influence of the MxE Interaction in the GBLUP Prediction

In an effort to improve the predictive abilities and accuracies of the GBLUP model, we incorporated the marker × environment interaction (MxE) matrix as covariate within two cross-validation strategies: CV1 and CV2 (Table 4). When models were trained on controlled condition DS and tested on MegaENV dataset, the inclusion of the MxE interaction as covariate improved predictive abilities and accuracies under both CV1 and CV2 scenarios reaching rab values of 0.457 and 0.443 and rac values of 0.528 and 0.511respectively. Addition of the MxE covariate also improves predictive abilities and accuracies of GBLUP models trained on FAI-BLUP index data and validated on MegaENV data reaching rab value of 0.500 and 0.465 and rac values of 0.578 and 0.537 for CV1 and CV2 scenarios respectively (Table 15).

Again, FAI-BLUP data was found as the best training-controlled condition trait to predict accession response to rust in the field.

Table 15. Predictive ability (rab) and predictive accuracy (rac) fitting the GBLUP model with the effect of the marker x environment interaction (MxE) as covariate in two Cross-Validation strategies.

Training set	Validation set	r_{ab}		r_{ac}	
		CV1	CV2	CV1	CV2
DS	MegaENV	0.457	0.443	0.528	0.511
FAI-BLUP	MegaENV	0.500	0.465	0.578	0.537
DS-2018	DS -2019	0.592	0.536	0.688	0.623
DS -2018	DS -2020	0.343	0.297	0.383	0.332
DS -2019	DS -2018	0.400	0.261	0.504	0.329
DS -2019	DS -2020	0.455	0.300	0.509	0.335
DS -2020	DS -2018	0.371	0.264	0.467	0.333
DS -2020	DS -2019	0.670	0.541	0.779	0.623

Using single field DS to predict another accession response to rust in another field season revealed varying results. Training in 2018 and validating in 2019 data showed high predictive abilities (rab = 0.592 in CV1 and rab = 0.536 in CV2) and accuracies (rac = 0.688 in CV1 and rac = 0.623 in CV2), indicating that the model could accurately capture the year-to-year environmental variance. The models trained in 2020 and validated in 2019 exhibited the highest predictive ability (rab = 0.670 and 0.541 under CV1 and CV2 respectively) and accuracy (rac = 0.779 and 0.623 under CV1 and CV2 respectively). However, training models on DS-2019 and validating on DS-2018 decreased predictive ability and accuracy. In summary, while the incorporation of the MxE matrix into the GBLUP model does not significantly influence the average predictive abilities and accuracies under CV1 scenario, it improves by 11% on average the predictive abilities under CV2 scenario (Additional file 11). This underscores the potential for the GBLUP model, with the Marker × Environment interaction, to predict disease resistance with considerable accuracy, especially when data can be validated with DS collected in field seasons with high and homogeneous rust infestation levels.

5. Discussion

The integration of quantitative genomic methodologies into plant breeding has opened a new era for variety development, characterized by reduced cycle times and cost savings through diminished reliance on extensive phenotyping (Crossa et al., 2017). Among these techniques used in marker-assisted selection (MAS) are Genome-Wide Association Studies (GWAS) and Genomic Selection (GS). GS has gained attraction in legume breeding for the selection of lines with key agronomic

traits. However, the accurate prediction of complex traits, especially those like disease resistance with quantitative inheritance and strong environmental interactions, remains a significant barrier in the effective integration of GS into routine plant breeding workflows (Rubiales et al., 2021). In our study, we have assessed the ability and accuracy of three GS models to predict disease severity of rust in peas, an important trait controlled by such complex quantitative responses. We investigated various disease-related parameters as predictors of rust severity under controlled and field conditions. Our approach included the consolidation of controlled condition traits into a multi-trait index, enhancing our understanding of the trait's performance in field scenarios. Through this, we were able to assess the stability of certain accessions deemed resistant or highly susceptible, spanning three distinct environments. This enabled a thorough evaluation of the GEI and of the consistency of environmental response on the accessions' response to rust. Upon identifying the most promising model, we incorporated additional covariates, namely Marker × Environment interactions, to refine predictive performance. This strategic adjustment aimed to identify an optimal configuration for practical application in ongoing breeding programs.

The population size and the quantity and quality of molecular markers employed are crucial to the efficacy of GS models (Zhang et al., 2017). Our pea collection, comprising 320 individuals, is consistent with the scope of analogous studies that utilize structured populations of comparable size to train GS models in pea (Annicchiarico et al., 2019; 2017; Tayeh et al., 2015). Our population size is also similar to those of other studies aiming the prediction of agronomically significant traits in other legume species (Biazzi et al., 2017; Pecetti et al., 2023). In line with previous findings, the Silico-DArT type marker dataset used here allow similar GS model fitting than SNPs datasets (Tayeh et al., 2015). It has been observed that the precision of GS models can be moderately enhanced by increasing the marker numbers (Heffner et al., 2011). Genotyping of our broadly diverse pea collection generated 26,046 high-quality polymorphic Silico-DArT markers covering all pea chromosomes after thorough data filtering. This robust marker framework lays the groundwork for evaluating genomic prediction models tailored to complex quantitative traits. Comparable GS studies that have calibrated models with a few thousand SNPs typically report lower predictive abilities ranging from 0.29 to 0.46 than those reached here for intra-environment predictions (0.63) (Bonnett et al., 2013; Oakey et al., 2016). Hence, the extensive marker coverage of our Silico-DArT marker largely improves the model's predictive accuracy compared to studies including fewer markers. The comprehensive genetic diversity analysis by Rispail et al. (2023) demonstrated that the pea collection is structured and divided into either three or six clusters, encompassing the various species and subspecies of the *Pisum* genera. Nevertheless, this study also uncovered the presence of significant genetic admixture within the collection, indicating prevalent gene flow between sub-

populations and attenuating the impact of population structure of the collection. Given that pronounced population structure can potentially reduce accuracy in cross-validation schemes of GS, the weak/moderate structure observed in the pea collection is considered beneficial for the validation and application of our models.

It is well-known that GEI is a significant factor influencing DS of rust, as shown for several pea studies in the field (Das et al. 2019; Osuna-Caballero et al., 2022). This influence is confirmed by by the present AMMI analysis (Additional file 11). Despite the complexity introduced by GEI, the phenotypic and genotypic correlations of DS under field conditions and the stability of selected accessions across environments allowed to consolidate three individual field evaluations into a Mega-Environment (MegaENV). The MegaENV reduce the effect of GEI and allow researchers to extract valuable information about accessions more effectively, making it a suitable solution for trait highly affected by GEI such as rust DS (González-Barrios et al., 2019). The BLUP values derived from the MegaENV successfully integrate the variance of the three environments while retaining high correlation with each environment, as illustrated in Figure 18. Consequently, this MegaENV dataset, which reflects analogous climatic and edaphic conditions, acts as a robust validation set for models trained on controlled conditions data as confirmed by other authors (Lado et al., 2016).

Field phenotyping of extensive collections is critical for elucidating GEI, a cornerstone for the successful deployment of GS schemes (Budhlakoti et al., 2022). Nonetheless, this necessity stands in contrast to the associated high costs and intensive labour. In this study, we have explored the potential of using controlled condition data to predict rust severity observed under field conditions, where disease-related parameters can be measured with greater accuracy. While some multi-trait GS models that incorporate various parameters for model training and validation have reported promising results (Gill et al., 2021), others have found that the improvements are not consistently marked across different traits (Jarquín et al., 2014). Our study introduces an alternative approach that consolidates traits measured under controlled conditions into a single index: FAI-BLUP (Rocha et al. 2018). This index, similar to MGDI, accounts for the multicollinearity among parameters, yielding more favourable outcomes than traditional indices founded on linear models (Rocha et al. 2018; Olivoto et al. 2020). Accordingly, the FAI-BLUP index showed the best predictive abilities of the controlled condition traits in the intra-environment GS scheme regardless of the model, highlighting its efficacy, and validating its application for other GS scenarios. Other authors who evaluated the consistency of multi-trait GS models obtained lower predictive abilities compared to the application of the FAI-BLUP index proposed here in intra-environment and across-environment configurations (Gill et al., 2021; Ward et al., 2019).

In the initial GS scheme, the predictive abilities of three models were evaluated for each trait within controlled and field conditions. While rrBLUP and BL models showed comparable predictive abilities under controlled conditions, GBLUP excelled under field conditions, boasting superior predictive abilities as previously shown in other related studies (Nazzicari & Biscarini, 2022; Wang et al., 2018). Notably, this enhancement in predictive performance was not mirrored for the FAI-BLUP index, which exhibited uniform prediction abilities across all three models. Additionally, the predictive ability of GBLUP was diminished for the MegaENV assessment. These discrepancies may be attributed to the distinct methodologies and assumptions inherent to each model. GBLUP, like rrBLUP, assumes that traits are influenced by many genes with small effects. However, GBLUP advantage emerges when considering the population structure and genetic relationships, which are critical factors under field conditions (Habier et al., 2007). We propose that field conditions reflect more accurately DS across the complete lifecycle of rust on pea plants, unlike controlled conditions that evaluate only the initial rust disease cycle on seedlings. Such controlled settings may not fully capture the phenotypic expressions that characterize each sub-population—such as leaf size and overall plant size—that could impact disease variation. Conversely, in the field, these sub-population traits are considered by the GBLUP model leading to more accurate predictions. This observation aligns with other studies where GBLUP has been preferred over rrBLUP and BL, particularly when modelling traits under field conditions that are influenced by population structure (Guo et al., 2014; Roorkiwal et al., 2016).

In the following GS framework, which is more relevant for plant breeding, models were cross trained using data from two distinct conditions, and predictions were made for the validation set, which was also part of the training set (CV1). This strategy is particularly informative when the environments are homogeneous and exhibit strong interrelatedness. Indeed, our results confirm that environments with greater genetic or phenotypic similarity yielded higher predictive abilities as previously shown (Carpenter et al., 2018; Crosta et al., 2023). Consistently, the GBLUP model provided the most robust predictions, achieving a predictive accuracy of 0.730 when trained on DS-2020 and validated on DS-2019, and 0.577 when employing the FAI-BLUP index for training and validation on MegaENV. This highlighted the enhanced predictive potential of multi-trait index over single traits measured under controlled conditions (Table 13). Comparatively, these predictive accuracies signify an advancement over other GS research focused on pea diseases employing a similar cross-validation scheme (CV1) (Carpenter et al., 2018), and they even surpass those documented for rust resistance in wheat, ranging from 0.33 to 0.44, using the same validation strategy and the GBLUP model (Daetwyler et al., 2014). In the context of plant breeding, the most valuable scheme is the one that allows the prediction of phenotypic values in novel lines and untrained environments, a configuration referred to as CV2. In this study, CV2 assessment for rust resistance

in peas mirrored the pattern seen in CV1, albeit with lower rab and rac values. This outcome aligns with previous studies that documented a decline in predictive performance from CV1 to CV2 across legumes (Carpenter et al., 2018; Gill et al., 2021). Despite this drop, the GBLUP model continued to exhibit moderate and still useful predictive abilities and accuracies, outperforming other models. The most effective approach to predict rust response in the field with controlled conditions data was to train models with the FAI-BLUP index and validating them on MegaENV. By contrast, to predict rust responses under field conditions with DS collected under field condition, the most accurate predictions were obtained when DS-2019 was used as validation dataset. This strategy achieved higher predictive values for plant disease resistance compared to other GS approaches using similar strategies (Juliana et al., 2017; Rutkoski et al., 2011), confirming the utility of our models in practical breeding applications for rust resistance.

In the final GS arrangement, we revisited the CV1 and CV2 cross-validation scenario of GBLUP model, which consistently provided superior predictive abilities and accuracies for the evaluated traits. In this iteration, we introduced the DArT-seq marker matrix's interaction with the environments (MxE) as covariate model (Lopez-Cruz et al., 2015). This addition confirms the critical role of GEI interaction, enabling refined adjustments to enhance the model predictive abilities, as demonstrated in other studies targeting disease resistance in pea (Carpenter et al. 2018). This modification is especially beneficial for traits with complex genetic architectures such as rust resistance in pea, which are shaped by the interplay of genetic and environmental factors. By incorporating the MxE interaction, the model gains the capacity to account for the unique expression of genetic markers across different environments, a factor essential for the accurate prediction of phenotypes in variable conditions (Cuevas et al., 2016). As other researchers have shown for rust disease in other species, modifying the GBLUP model to include the MxE matrix empowers it to discern marker effects that may be prominent in one environment but not others, an aspect that is critically important in the CV2 scheme, where validation occurs in an environment not represented in the training dataset (Fois et al., 2021; Lopez-Cruz et al., 2015). Accounting for these interactions has yielded more precise predictions in new environments, improving accuracy by up to 11% in this study. We suggest that integrating the MxE effect might reduce model bias. Without this interaction, the model might be overfitting the conditions of the training set, particularly in the CV1 scheme. Thus, the inclusion of the MxE covariate is instrumental to generalize the model, ensuring stability, and enhancing the accuracy of predictions across a spectrum of environmental scenarios.

This study embarked on a comprehensive exploration of GS models to enhance the prediction of rust resistance in pea, a trait of paramount importance in legume breeding (Osuna-Caballero et al., 2024b). Our investigation, spanning various genomic selection schemes, provides critical insights into the applicability and

optimization of GS models for complex traits influenced by both genetic and environmental factors. Among the GS models evaluated, GBLUP model consistently emerged as the most effective, exhibiting superior predictive abilities and accuracies across different environments and traits. This model's strength lies in its ability to account for the intricate genetic architecture of rust resistance, a trait governed by numerous genes with minor effects and substantially influenced by environmental interactions. The success of GBLUP underscores its potential as a powerful tool in plant breeding programs, particularly for traits that are challenging to phenotype and influenced by environmental conditions. Our study also highlighted the importance of accounting for GEI in GS models. By integrating Marker x Environment (MxE) interactions as a covariate, we achieved a notable enhancement in the model's predictive accuracy, especially under the CV2 cross-validation scenario where predictions were made for untested environments. This adjustment demonstrates the critical role of environmental factors in shaping phenotypic expression and the necessity of modelling these interactions for precise genomic predictions. The practical implications of our findings are significant in plant breeding, where efficiency and accuracy are paramount, the ability to predict rust resistance in peas using GS models, particularly GBLUP with MxE interactions, represents a substantial advancement. This approach not only contribute to the breeding process but also reduces reliance on extensive phenotyping, which is often resource-intensive and environmentally constrained. Our results are especially encouraging for breeding programs aimed at developing rust-resistant pea varieties, as they offer a method to identify promising lines rapidly and accurately. Moreover, the use of a multi-trait index, particularly the FAI-BLUP index, further refined our predictions. This index, by integrating multiple traits associated with disease resistance under controlled conditions, provided a more holistic view of the genetic potential of each accession, outperforming the predictions based on single traits measured under controlled conditions. This suggests that incorporating multi-dimensional trait data into GS models can yield more robust predictions, a strategy that could be extended to other complex traits in plant breeding. In conclusion, our study not only reaffirms the efficacy of genomic selection in plant breeding but also advances our understanding of how to effectively model complex traits like rust resistance in pea. The insights gained here have broader applications in the field of agricultural genetics, providing a roadmap for harnessing genomic tools to accelerate the development of crop varieties that are resilient to diseases and adaptable to varying environmental conditions. As we look to the future, the integration of advanced genomic tools, such as those explored in this study, will be instrumental in meeting the growing challenges of global food security and sustainable agriculture.

6. Additional files

Additional file 10. AMMI analysis table. Two interactions principal component axis (IPCA) were fitted and significant at 5% probability error.

Source	Df	Sum Sq	Mean Sq	F value	Pr(>F)	Proportion	Accumulated
ENV	2	68194	34097	147.43	6.19E-60	NA	NA
REP(ENV)	6	139557	23260	100.57	5.08E-109	NA	NA
BLOCK (REP*ENV)	162	81240	501	2.17	4.49E-14	NA	NA
GEN	323	277957	861	3.72	1.39E-69	NA	NA
GEN:ENV	646	485286	751	3.25	5.04E-84	NA	NA
PC1	324	385781	1191	5.15	0.00E+00	79.3	79.3
PC2	322	100731	313	1.35	1.00E-04	20.7	100
Residuals	1764	407964	231	NA	NA	NA	NA
Total	3549	1946710	549	NA	NA	NA	NA

Additional file 11. Prediction accuracy of GBLUP model in two cross-validation schemes (CV1 at the top and CV2 at the bottom) based in the training/validation test described at the bottom of each boxplot.

General Conclusions

i. This thesis has successfully identified novel sources of rust resistance within a diverse collection of pea accessions, underlining the value of extensive crop core collections in pinpointing key traits. Beyond revealing additional sources of partial resistance comparable to the most resistant accessions known previously, we have also discovered a unique case of moderate, late-acting hypersensitive response (HR) in one accession. This particular response to *U. pisi* in peas has not been documented before. Integrating this accession, along with the newly identified partial resistance sources, into our breeding programs is expected to expand the genetic base of resistance (Chapter 2).

ii. This thesis introduces a novel, image-based phenotyping method for rust disease in peas, utilizing RGB spectral indices segmentation and pixel thresholding for accurate disease assessment. This efficient technique, which rapidly processes images with minimal computational demands, accurately measures disease severity and pustule count on leaflets. Its speed and precision, comparable to traditional visual methods, mark a significant advancement over existing workflows. Uniquely capable of daily tracking complex disease progression parameters, this R script-based approach also offers adaptability for studying rust in other pathosystems. By reducing subjective bias inherent in manual assessments, this method enhances both fundamental research and plant breeding, paving the way for more effective disease management and the development of genetically resistant pea varieties (Chapter 3).

iii. The GWAS study proposed here significantly advances our understanding of rust resistance in peas, revealing 95 molecular markers and 62 candidate genes linked to partial resistance. These findings not only validate the power of GWAS in identifying new resistance-associated QTL but also provide a diverse set of potential gene targets for future research and breeding strategies. The identification of genes analogous to those in cereal rust resistance suggests a shared resistance mechanism. These insights are instrumental for developing targeted breeding programs and genomic prediction models, enhancing pea crop resilience against rust disease, and supporting sustainable agricultural practices by reducing fungicide reliance (Chapter 4).

iv. The GBLUP model's superiority was highlighted in accommodating the complex genetic and environmental factors influencing rust resistance in pea. Notably, incorporating Marker x Environment interactions into GBLUP significantly enhanced predictive accuracy, especially in scenarios involving untested environments and lines. This advancement underscores the potential of GS in efficiently identifying rust-resistant pea varieties, thereby reducing reliance on labour-intensive phenotyping. The use of the FAI-BLUP index,

integrating multiple disease resistance traits, further improved the robustness of our predictions. Our findings offer valuable insights for plant breeding, suggesting a promising approach to developing disease-resilient crops and contributing to global food security and sustainable agriculture (Chapter 5).

Bibliography

Abdulridha J, Min A, Rouse MN, Kianian S, Isler V, Yang C. Evaluation of Stem Rust Disease in Wheat Fields by Drone Hyperspectral Imaging. Sensors. 2023;21(8):23.

Abeysinghe S (2009) Systemic resistance induced by Trichoderma harzianum RU01 against *Uromyces appendiculatus* on *Phaseolus vulgaris*. J Natl Sci Found Sri Lanka 37(3):203. https://doi.org/10.4038/jnsfsr.v37i3.1214

Abo-Elyousr KAM, Abdel-Rahim IR, Almasoudi NM, Alghamdi SA (2021) Native Endophytic *Pseudomonas putida* as a Biocontrol Agent against Common Bean Rust Caused by *Uromyces appendiculatus*. J Fungi 7(9):745. https://doi.org/10.3390/jof7090745

Acevedo M, Steadman JR, Rosas JC (2013) *Uromyces appendiculatus* in Honduras: Pathogen Diversity and Host Resistance Screening. Plant Dis 97(5):652–61. https://doi.org/10.1094/PDIS-02-12-0169-RE

Adhikari KN, Khazaei H, Ghaouti L, Maalouf F, Vandenberg A, Link W et al (2021) Conventional and Mol Breed Tools for Accelerating Genetic Gain in Faba Bean (*Vicia faba* L.). Front Plant Sci 12:1–17. https://doi.org/10.3389/fpls.2021.744259

Akamatsu H, Yamanaka N, Soares RM, Ivancovich AJG, Lavilla MA, Bogado AN et al (2017) Pathogenic Variation of South American *Phakopsora pachyrhizi* Populations Isolated from Soybeans from 2010 to 2015. Japan Agric Res Q JARQ 51(3):221–32. https://doi.org/10.6090/jarq.51.221

Akbari M, Wenzl P, Caig V, Carling J, Xia L, Yang S, et al (2006). Diversity arrays technology (DArT) for high-throughput profiling of the hexaploid wheat genome. Theor and Appl Gen, 113(8), 1409–1420. https://doi.org/10.1007/s00122-006-0365-4

Akdemir D & Isidro-Sánchez J (2019). Design of training populations for selective phenotyping in genomic prediction. Sci Rep, 9(1), 1–15. https://doi.org/10.1038/s41598-018-38081-6

Alam MM, Sadat MA, Hoque MZ, Rashid MH, Officer S, Division PP (2007) Management of Powdery Mildew and Rust Diseases of Garden Pea Using Fungicides. Int J Sustain Crop Prod 2(3):56–60.

Alam M, Neal J, O'Connor K, Kilian A, Topp B (2018). Ultra-high-throughput DArTseq-based silicoDArT and SNP markers for genomic studies in macadamia. PLOS ONE, 13(8), e0203465. https://doi.org/10.1371/journal.pone.0203465

Alemu A, Brantestam AK, Chawade A (2022) Unraveling the Genetic Basis of Key Agronomic Traits of Wrinkled Vining Pea (*Pisum sativum* L.) for Sustainable Production. Front Plant Sci 13. https://doi.org/10.3389/fpls.2022.844450

Alexandratos JNB (2012) World agriculture towards 2030 / 2050: the 2012 Revision. https://www.fao.org/agrifood-economics/publications/detail/en/c/147899. Accessed 4 December 2023.

Almeida NF, Leitão ST, Krezdorn N, Rotter B, Winter P, Rubiales D et al (2014) Allelic diversity in the transcriptomes of contrasting rust-infected genotypes of *Lathyrus sativus*, a lasting resource for smart breeding. BMC Plant Biol 14(1):376. http://doi.org/10.1186/s12870-014-0376-2

Alves KS, Guimarães M, Ascari JP, Queiroz MF, Alfenas RF, Mizubuti ESG et al (2022) RGB-based phenotyping of foliar disease severity under controlled conditions. Trop Plant Pathol 47(1):105–17. https://doi.org/10.1007/s40858-021-00448-y

Amin N, Ahmad N, Khalifa MAS, Du Y, Mandozai A, Khattak AN et al (2023) Identification and Molecular Characterization of RWP-RK Transcription Factors in Soybean. Genes 14:369. https://doi.org/10.3390/genes14020369

Anil-Kumar TB, Rangaswamy KT, Ravi K (1994) Assessment of Tall Field Pea Genotypes for Slow Rusting Resistance. Legum Sci 17, 79–82

Annicchiarico P, Nazzicari N, Pecetti L, Romani M, Russi L (2019) Pea genomic selection for Italian environments. BMC Genomics 20(1):1–18. https://doi.org/10.1186/s12864-019-5920-x

Annicchiarico P, Russi L, Romani M, Notario T, Pecetti L (2023) Value of heterogeneous material and bulk breeding for inbred crops: A pea case study. Field Crops Res 293,108831. https://doi.org/10.1016/j.fcr.2023.108831

Annicchiarico P, Nazzicari, N, Laouar M, Thami-Alami I, Romani M, Pecetti L (2020) Development and proof-of-concept application of genome-enabled selection for pea grain yield under severe terminal drought. Int J Mol Sci 21(7) 1–20. https://doi.org/10.3390/ijms21072414

Annicchiarico P, Nazzicari N, Pecetti L, Romani M, Ferrari B, Wei Y, Brummer EC (2017) GBS-Based Genomic Selection for Pea Grain Yield under Severe Terminal Drought. The Plant Genome 10(2). https://doi.org/10.3835/plantgenome2016.07.0072

Annicchiarico P, Nazzicari, N, Wei Y, Pecetti L, Brummer EC (2017) Genotyping-by-sequencing and its exploitation for forage and cool-season grain legume breeding. Front Plant Sci 8 1–13. https://doi.org/10.3389/fpls.2017.00679

Arneson PA (2001) Plant Disease Epidemiology: Temporal Aspects. The Plant Health Instructor. https://doi.org/10.1094/PHI-A-2001-0524-01

Arslan U, Ilhan K, Karabulut OA (2009) Antifungal activity of aqueous extracts of spices against bean rust (*Uromyces appendiculatus*). Allelopath J 24(1):207–13

Arslan U. (2014) Efficacy of plant oils on the control of bean rust and wheat leaf rust. Fresenius Environ Bull. 23:2259–65.

Asare AT, Mensah TA, Tagoe SMA, Asante DKA (2019) Identification of New Sources of Rust Resistance in Cowpea (*Vigna Unguiculata* L. Walp) Germplasm Using Simple Sequence Repeat Markers. Legum Res 43(2):185-9. https://doi.org/10.18805/LR-488.

Ashourloo D, Mobasheri M, Huete A. Developing two spectral disease indices for detection of Wheat Leaf Rust (*Puccinia triticina*). Remote Sens. 2014;6(6):4723–40.

Assante G, Maffi D, Saracchi M, Farina G, Moricca S, Ragazzi A (2004) Histological studies on the mycoparasitism of *Cladosporium tenuissimum* on urediniospores of *Uromyces appendiculatus*. Mycol Res 108(2):170–82. https://doi.org/10.1017/S0953756203008852

Astle W, Balding DJ (2009) Population Structure and Cryptic Relatedness in Genetic Association Studies. Stat Sci 24. https://doi.org/10.1214/09-STS307

Avila CM, Sillero JC, Rubiales D, Moreno MT, Torres AM (2003) Identification of RAPD markers linked to the Uvf-1 gene conferring hypersensitive resistance against rust (*Uromyces viciae-fabae*) in *Vicia faba* L. Theor Appl Genet 107(2):353–8. https://doi.org/10.1007/s00122-003-1254-8

Ayyappan V, Kalavacharla V, Thimmapuram J, Bhide KP, Sripathi VR, Smolinski TG et al (2015) Genome-Wide Profiling of Histone Modifications (H3K9me2 and H4K12ac) and Gene Expression in Rust (*Uromyces appendiculatus*) Inoculated Common Bean (*Phaseolus vulgaris* L.). PLoS One 10(7):0132176. https://doi.org/10.1371/journal.pone.0132176

Azooz MM, Ahmad P (2015) Legumes under environmental stress: yield, improvement and adaptations. Oxford UK. https://doi.org/10.1002/9781118917091

Bade CIA, Carmona MA. Comparison of methods to assess severity of common rust caused by *Puccinia sorghi* in maize. Trop Plant Pathol. 2011;36(4):264–6.

Baker CJ (1983) Inhibitory Effect of Bacillus subtilis on *Uromyces phaseoli* and on Development of Rust Pustules on Bean Leaves. Phytopathology 73(8):1148. http://doi.org/10.1094/Phyto-73-1148

Baker CJ, Stavely JR, Mock N (1985) Biocontrol of bean rust by *Bacillus subtilis* under field conditions. Plant Dis. 1985;69(9):770–2. https://doi.org/10.1094/PD-69-770

Barbedo JGA. A review on the main challenges in automatic plant disease identification based on visible range images. Biosyst Eng. 2016;144:52–60.

Barbetti M, Nichols P (1991) Herbage and seed yield losses in six varieties of subterranean clover from rust (*Uromyces trifolii-repentis*). Aust J Exp Agric 31(2):225. https://doi.org/10.1071/EA9910225

Barge EG, Leopold DR, Rojas A, Vilgalys R, Busby PE (2022) Phylogenetic conservatism of mycoparasitism and its contribution to pathogen antagonism. Mol Ecol 31(10):3018–30. https://doi.org/10.1111/mec.16436

Bari MA, Al Fonseka D, Stenger J, Zitnick-Anderson K, Atanda SA, Morales M et al (2023) A greenhouse-based high-throughput phenotyping platform for identification and genetic dissection of resistance to Aphanomyces root rot in field pea. Plant Phenome J. 2023;7(1):6.

Barilli E, Agudo FJ, Masi M, Nocera P, Evidente A, Rubiales D (2022) Anthraquinones and their analogues as potential biocontrol agents of rust and powdery mildew diseases of field crops. Pest Manag Sci 78(8):3489–97. https://doi.org/10.1002/ps.6989

Barilli E, Cimmino A, Masi M, Evidente M, Rubiales D, Evidente A (2016a) Inhibition of Spore Germination and Appressorium Formation of Rust Species by Plant and Fungal Metabolites. Nat Prod Commun 11(9). http://doi.org/10.1177/1934578X1601100940

Barilli E, Cimmino A, Masi M, Evidente M, Rubiales D, Evidente A (2017) Inhibition of early development stages of rust fungi by the two fungal metabolites cyclopaldic acid and epi-epoformin. Pest Manag Sci 73(6):1161–8. https://doi.org/10.1002/ps.4438

Barilli E, Cobos MJ, Carrillo E, Kilian A, Carling J, Rubiales D (2018) A high-density integrated DArTseq SNP-based genetic map of *Pisum fulvum* and identification of QTLs controlling rust resistance. Front Plant Sci 9:1–13. https://doi.org/10.3389/fpls.2018.00167

Barilli E, González-Bernal MJ, Cimmino A, Agudo-Jurado FJ, Masi M, Rubiales D et al (2019) Impact of fungal and plant metabolites application on early development stages of pea powdery mildew. Pest Manag Sci. 2019;18:ps5351.

Barilli E, Moral A, Sillero JC, Rubiales D (2012a) Clarification on rust species potentially infecting pea (*Pisum sativum* L.) crop and host range of *Uromyces pisi* (Pers.) Wint. Crop Prot 37:65–70. https://doi.org/10.1016/j.cropro.2012.01.019

Barilli E, Prats E, Rubiales D (2010a) Benzothiadiazole and BABA improve resistance to *Uromyces pisi* (Pers.) Wint. in *Pisum sativum* L. with an enhancement of enzymatic activities and total phenolic content. Eur J Plant Pathol 128(4):483–93. http://doi.org/10.1007/s10658-010-9678-x

Barilli E, Rubiales D (2023) Identification and Characterization of Resistance to Rust in Lentil and Its Wild Relatives. Plants 31;12(3):626. https://doi.org/10.3390/plants12030626

Barilli E, Rubiales D, Amalfitano C, Evidente A, Prats E (2015) BTH and BABA induce resistance in pea against rust (*Uromyces pisi*) involving differential phytoalexin accumulation. Planta 242(5):1095–106. http://doi.org/10.1007/s00425-015-2339-8

Barilli E, Rubiales D, Castillejo MA (2012b) Comparative proteomic analysis of BTH and BABA-induced resistance in pea (*Pisum sativum*) toward infection with pea rust (*Uromyces pisi*). J Proteomics 75:5189–5205. https://doi.org/10.1016/j.jprot.2012.06.033

Barilli E, Satovic Z, Rubiales D, Torres AM (2010b) Mapping of quantitative trait loci controlling partial resistance against rust incited by *Uromyces pisi* (Pers.) Wint. in a *Pisum fulvum* L. intraspecific cross. Euphytica 175(2):151–9. https://doi.org/10.1007/s10681-010-0141-z

Barilli E, Sillero JC, Fernández-Aparicio M, Rubiales D (2009a) Identification of resistance to *Uromyces pisi* (Pers.) Wint. in *Pisum* spp. germplasm. Field Crop Res 114(2):198–203. https://doi.org/10.1016/j.fcr.2009.07.017

Barilli E, Sillero JC, Moral A, Rubiales D (2009c) Characterization of resistance response of pea (*Pisum* spp.) against rust (*Uromyces pisi*). Plant Breed 128(6):665–70. https://doi.org/10.1111/j.1439-0523.2008.01622.x

Barilli E, Sillero JC, Prats E, Rubiales D (2014) Resistance to rusts (*Uromyces pisi* and *U. viciae-fabae*) in pea. Czech J Genet Plant Breed. 50(2):135–43. https://doi.org/10.17221/125/2013-CJGPB

Barilli E, Sillero JC, Rubiales D (2009b). Induction of Systemic Acquired Resistance in Pea against Rust (*Uromyces pisi*) by Exogenous Application of Biotic and Abiotic Inducers. J Phytopathol 158:30-34. https://doi.org/10.1111/j.1439-0434.2009.01571.x

Barilli E, Sillero JC, Serrano A, Rubiales D (2009d) Differential response of pea (*Pisum sativum*) to rusts incited by *Uromyces viciae-fabae* and *U. pisi*. Crop Prot 28(11):980–6. http://doi.org/10.1016/j.cropro.2009.06.010

Barilli, Eleonora, Cobos, M. J., & Rubiales, D. (2016b). Clarification on host range of didymella pinodes the causal agent of pea ascochyta blight. Front Plant Sci 7. https://doi.org/10.3389/fpls.2016.00592

Bassi FM, Bentley AR, Charmet G, Ortiz R, Crossa J (2016). Breeding schemes for the implementation of genomic selection in wheat (*Triticum* spp.). Plant Science 242, 23–36. https://doi.org/10.1016/j.plantsci.2015.08.021

Bates D, Mächler M, Bolker BM, Walker SC (2015) Fitting linear mixed-effects models using lme4. J Stat Softw 67. https://doi.org/10.18637/jss.v067.i01

Beare R, Lowekamp B, Yaniv Z (2018) Image Segmentation, Registration and characterization in R with SimpleITK. J Stat Softw. 2018;86(8):1–35.

Beaver JS, González A, Godoy-Lutz G, Rosas JC, Hurtado-Gonzales OP, Pastor-Corrales MA et al (2020) Registration of PR1572-19 and PR1572-26 pinto bean germplasm lines with broad resistance to rust, BGYMV, BCMV, and BCMNV. J Plant Regist 14(3):424–30. https://doi.org/10.1002/plr2.20027

Beaver JS, Rosas JC, Myers J, Acosta J, Kelly JD, Nchimbi-Msolla S et al (2003) Contributions of the Bean/Cowpea CRSP to cultivar and germplasm development in common bean. Field Crop Res 82(2–3):87–102. https://doi.org/10.1016/S0378-4290(03)00032-7

Beaver JS, Rosas JC, Porch TG, Pastor-Corrales MA, Godoy-Lutz G, Prophete EH (2015) Registration of PR0806-80 and PR0806-81 White Bean Germplasm Lines with Resistance to BGYMV, BCMV, BCMNV, and Rust. J Plant Regist 9(2):208–11. http://doi.org/10.3198/jpr2014.09.0061crg

Beaver JS, Zapata M, Miklas PN (1999) Registration of the PR9443-4 Dry Bean Germplasm Resistant to Bean Golden Mosaic, Common Bacterial Blight, and Rust. Crop Sci 39(4):1262–1262. https://doi.org/10.2135/cropsci1999.0011183X003900040066x

Beniwal D, Dhall RK, Yadav S, Sharma P (2022) An overview of rust (*Uromyces viciae-fabae*) and powdery mildew (*Erysiphe polygoni* DC) of pea (*Pisum sativum* L.). Genetika 54(1):499–512. https://doi.org/10.2298/GENSR2201499B

Bernier CC, Hanounik SB, Hussen MM, Mohamed HA (1984) Field manual of common bean diseases in the Nile Valley. ICARDA Inf Bull 3:40

Bertioli DJ, Cannon SB, Froenicke L, Huang G, Farmer AD, Cannon EKS et al (2016) The genome sequences of *Arachis duranensis* and *Arachis ipaensis*, the diploid ancestors of cultivated peanut. Nat Genet 48(4):438–46. https://doi.org/10.1038/ng.3517

Best RG, Harlan JC (1985) Spectral estimation of Green leaf area index of oats. Remote Sens Environ 17(1):27–36.

Bettgenhaeuser J, Gilbert B, Ayliffe M, Moscou MJ (2014) Nonhost resistance to rust pathogens – a continuation of continua. Front Plant Sci 5. http://doi.org/10.3389/fpls.2014.00664/abstract

Beyer SF, Beesley A, Rohmann PFW, Schultheiss H, Conrath U, Langenbach CJG (2019) The Arabidopsis non-host defence-associated coumarin scopoletin protects soybean from Asian soybean rust. Plant J 99(3):397–413. https://doi.org/10.1111/tpj.14426

Biazzi E, Nazzicari N, Pecetti L, Brummer EC, Palmonari A, Tava A, Annicchiarico, P (2017) Genome-wide association mapping and genomic selection for alfalfa (*Medicago sativa*) forage quality traits. PLoS ONE, 12(1), 1–17. https://doi.org/10.1371/journal.pone.0169234

Blancon J, Dutartre D, Tixier MH, Weiss M, Comar A, Praud S, et al (2019) A high-throughput model-assisted method for phenotyping maize green leaf area index dynamics using unmanned aerial vehicle imagery. Front Plant Sci 10:1–16

Bock CH, Barbedo JGA, Del Ponte EM, Bohnenkamp D, Mahlein AK (2020) From visual estimates to fully automated sensor-based measurements of plant disease severity: status and challenges for improving accuracy. Phytopathol Res 2(1):9. https://doi.org/10.1186/s42483-020-00049-8

Bock CH, Cook AZ, Parker PE, Gottwald TR (2009) Automated image analysis of the severity of Foliar Citrus canker symptoms. Plant Dis 93(6):660–5

Bock CH, Parker PE, Cook AZ, Gottwald TR (2008) Visual rating and the Use of Image Analysis for assessing different symptoms of Citrus Canker on Grapefruit Leaves Plant Dis 92(4):530–41

Bock CH, Poole GH, Parker PE, Gottwald TR (2010) Plant Disease Severity estimated visually, by Digital Photography and Image Analysis, and by Hyperspectral Imaging. CRC Crit Rev Plant Sci 10(2):29

Bonnett D, Li Y, Crossa J, Dreisigacker S, Sorrells M, Jannink JL (2013) Genomic selection to increase breeding efficiency. In M. Reynolds & H. Braun (Eds.), roceedings of the 3rd International Workshop of the Wheat Yield Consortium.

Borges-Martínez JE, Concha DdRM, Gallardo-Velázquez TG, Martínez CJ, Ruiz-Ruiz JC (2021) Anti-Inflammatory Properties of Phenolic Extracts from *Phaseolus vulgaris* and *Pisum sativum* during Germination. Food Biosci 42:101067

Bourdenx B, Bernard A, Domergue F, Pascal S, Léger A, Roby D et al (2011) Overexpression of Arabidopsis ECERIFERUM1 Promotes Wax Very-Long-Chain Alkane Biosynthesis and Influences Plant Response to Biotic and Abiotic Stresses. Plant Physiol 156:29–45. https://doi.org/10.1104/pp.111.172320

Bromfield KR, Melching J (1982) Sources of specific resistance to soybean rust. In: Phytopathology (ed) American Phytopathological Society, St. Paul, Minn pp 706–706.

Bromfield KR (1984) Soybean rust. American Phytopathological Society. St. Paul, Minnesota, USA.

Bromfield KR, Hartwig EE (1980) Resistance to Soybean Rust and Mode of Inheritance. Crop Sci 20(2):254–5. https://doi.org/10.2135/cropsci1980.0011183X002000020026x

Budhlakoti N, Kushwaha AK, Rai A, Chaturvedi KK, Kumar A, Pradhan AK, Kumar U et al (2022) Genomic Selection: A Tool for Accelerating the Efficiency of Mol Breed for Development of Climate-Resilient Crops. Frontiers in Genetics 13. https://doi.org/10.3389/fgene.2022.832153

Burmeister L, Hau B (2009) Control of the bean rust fungus *Uromyces appendiculatus* by means of *Trichoderma harzianum*: leaf disc assays on the antibiotic effect of spore suspensions and culture filtrates. BioControl 54(4):575–85. http://doi.org/10.1007/s10526-008-9202-9

CAB I UK, Laundon GF, Waterston JM. *Uromyces striatus*. Descr Fungi Bact. https://doi.org/10.1079/DFB/20056400059

Caldwell P, McLaren N (2004) Soybean rust research in South Africa. In: VII World soybean research conference - vi international soybean processing and utilization conference - iii congresso brasileiro de soja, proceedings. pp 354–60.

Camagna M, Takemoto D (2018) Hypersensitive response in plants. In: eLS. Wiley, Chichester, pp 1–7. https://doi.org/10.1002/9780470015902.a0020103.pub2

Carpenter MA, Goulden DS, Woods CJ, Thomson SJ, Kenel F, Frew TJ et al (2018) Genomic selection for ascochyta blight resistance in pea. Front Plant Sci 871:1–13. https://doi.org/10.3389/fpls.2018.01878

Casella G, George EI (1992) Explaining the Gibbs Sampler George 46(3):167–174

Castellar C, Jauch F, Moreira RR, da Silva Silveira Duarte H, De Mio LLM (2021) Standard area diagram set for assessment of severity and temporal progress of apple blotch. Eur J Plant Pathol 160(3):599–609

Castleman KR (1996) Digital Image Processing. Prentice-Hall. New Jersey: Pearson

Cerón-Rojas JJ, Crossa J (2022) The Statistical Theory of Linear Selection Indices from Phenotypic to Genomic Selection. Crop Sci 62:537–563

Chanchu T, Yimram T, Chankaew S, Kaga A, Somta P (2022) Mapping QTLs Controlling Soybean Rust Disease Resistance in Chiang Mai 5, an Induced Mutant Cultivar. Genes 14(1):19. https://doi.org/10.3390/genes14010019

Chand R, Srivastava CP, Kushwaha C. Screening technique for pea (*Pisum sativum*) genotypes against rust disease (*Uromyces fabae*). Indian J Agric Sci 74:166–7

Chander S, Ortega-Beltran A, Bandyopadhyay R, Sheoran P, Ige GO, Vasconcelos MW et al (2019) Prospects for Durable Resistance Against an Old Soybean Enemy: A Four-Decade Journey from Rpp1 (Resistance to *Phakopsora pachyrhizi*) to Rpp7. Agronomy 9(7):348. https://doi.org/10.3390/agronomy9070348

Chandrasekaran U, Luo X, Zhou W, Shu K (2020) Multifaceted Signaling Networks Mediated by Abscisic Acid Insensitive 4. Plant Commun 1:100040. https://doi.org/10.1016/j.xplc.2020.100040

Chandrashekara C, Mishra KK, Stanley J, Subbanna ARNS, Hooda KS, Pal RS et al (2022) Management of diseases and insect-pests of French bean in Northwestern Indian Himalayan region using integrated approaches. J Hortic Sci. 17(2). https://doi.org/10.24154/jhs.v17i2.897

Chapu I, Okello DK, Okello RCO, Odong TL, Sarkar S, Balota M (2022) Exploration of alternative approaches to phenotyping of late Leaf spot and groundnut rosette Virus Disease for Groundnut breeding. Front Plant Sci 13:1–17

Chen XM (2005) Epidemiology and control of stripe rust [*Puccinia striiformis* f. sp. *tritici*] on wheat. Can J Plant Pathol 27(3):314–37. http://www.doi.org/10.1080/07060660509507230

Chérel I, Michard E, Platet N, Mouline K, Alcon C, Sentenac H et al (2002) Physical and Functional Interaction of the Arabidopsis K + Channel AKT2 and Phosphatase AtPP2CA. Plant Cell 14:1133–1146. https://doi.org/10.1105/tpc.000943

Chethana KWT, Jayawardena RS, Chen Y-J, Konta S, Tibpromma S, Phukhamsakda C et al (2021) Appressorial interactions with host and their evolution. Fungal Divers 23;110(1):75–107. https://doi.org/10.1007/s13225-021-00487-5

Childs SP, King ZR, Walker DR, Harris DK, Pedley KF, Buck JW et al (2018) Discovery of a seventh Rpp soybean rust resistance locus in soybean accession PI 605823. Theor Appl Genet 131(1):27–41. http://doi.org/10.1007/s00122-017-2983-4

Chung WH, Kakishima M, Tsukiboshi T, Ono Y (2004) Phylogenetic analyses of *Uromyces viciae-fabae* and its varieties on *Vicia*, *Lathyrus*, and *Pisum* in Japan. Mycoscience 45(1):1–8. https://doi.org/10.1007/S10267-003-0144-X

Ciliuti J, Arrivillaga S, Germán S, Stewart S, Rebuffo M, Hernández S (2003) Studies of rust fungi on *Lotus subbiflorus* and *L. uliginosus*. Lotus Newsl 33:18–24

Civantos-Gómez I, Rubio Teso ML, Galeano J, Rubiales D, Iriondo JM, García-Algarra J (2022) Climate change conditions the selection of rust-resistant

candidate wild lentil populations for in situ conservation. Front Plant Sci 13. https://www.doi.org/10.3389/fpls.2022.1010799

Clemente A, Olias R (2017) Beneficial effects of legumes in gut health. Curr Opin Food Sci 14:32–36. https://doi.org/10.1016/j.cofs.2017.01.005

Clemente A, Arques MC, Dalmais M, Le Signor C, Chinoy C, Olias R, Rayner T, Isaac PG et al (2015) Eliminating Anti-Nutritional Plant Food Proteins: The Case of Seed Protease Inhibitors in Pea. PLoS ONE 10:e0134634

Conner RL (1982a) Host Range of *Uromyces viciae-fabae*. Phytopathology 72(6):687. https://doi.org/10.1094/Phyto-72-687

Conner RL (1982b) Inheritance of Rust Resistance in Inbred Lines of *Vicia faba*. Phytopathology 72(12):1555. http://doi.org/10.1094/Phyto-72-1555

Cools HJ, Fraaije BA, Kim SH, Lucas JA (2006) Impact of changes in the target P450 CYP51 enzyme associated with altered triazole-sensitivity in fungal pathogens of cereal crops. Biochem Soc Trans 34(6):1219–22. https://doi.org/10.1042/BST0341219

Cooper B, Campbell KB, Beard HS, Garrett WM, Islam N (2016) Putative Rust Fungal Effector Proteins in Infected Bean and Soybean Leaves. Phytopathology 106(5):491–9. https://doi.org/10.1094/PHYTO-11-15-0310-R

Cooper B, Neelam A, Campbell KB, Lee J, Liu G, Garrett WM et al (2007) Protein Accumulation in the Germinating *Uromyces appendiculatus* Uredospore. Mol Plant-Microbe Interact 20(7):857–66. https://doi.org/10.1094/MPMI-20-7-0857

Corrêa RX, Costa MR, Good-God PI, Ragagnin VA, Faleiro FG, Moreira MA et al (2000) Sequence Characterized Amplified Regions Linked to Rust Resistance Genes in the Common Bean. Crop Sci 40(3):804–7. http://doi.org/10.2135/cropsci2000.403804x

Coyne CJ, Kumar S, von Wettberg EJB, Marques E, Berger JD, Redden RJ et al (2020) Potential and Limits of Exploitation of Crop Wild Relatives for Pea, Lentil, and Chickpea Improvement. Legum Sci 2:e36

Crossa J, de los Campos G, Pérez-Rodríguez P, Gianola D, Burgueño J, Araus JL et al (2010) Prediction of Genetic Values of Quantitative Traits in Plant Breeding Using Pedigree and Molecular Markers. Genetics 186(2):713–724. https://doi.org/10.1534/genetics.110.118521

Crossa J, Pérez-Rodríguez P, Cuevas J, Montesinos-López O, Jarquín D, de los Campos G, Burgueño J et al (2017) Genomic Selection in Plant Breeding: Methods, Models, and Perspectives. Trends in Plant Science 22(11):961–975. https://doi.org/10.1016/j.tplants.2017.08.011

Crosta M, Nazzicari N, Ferrari B, Pecetti L, Russi L, Romani M, Cabassi G et al (2022) Pea Grain Protein Content Across Italian Environments: Genetic Relationship With Grain Yield, and Opportunities for Genome-Enabled Selection for Protein Yield. Front Plant Sci 12. https://doi.org/10.3389/fpls.2021.718713

Crosta M, Romani M, Nazzicari N, Ferrari B, Annicchiarico P (2023) Genomic prediction and allele mining of agronomic and morphological traits in pea (*Pisum sativum*) germplasm collections. Front Plant Sci 14. https://doi.org/10.3389/fpls.2023.1320506

Cruz-Triana A, Rivero-González D, Infante-Martínez D, Echevarría-Hernández A, Martínez-Coca B (2018) Management of phytopathogenic fungi in *Phaseolus vulgaris* L. with the application of *Trichoderma asperellum* Samuels, Lieckfeldt & Nirenberg. Rev Protección Veg 33(3):1–7

Cuevas J, Crossa J, Soberanis V, Pérez-Elizalde S, Pérez-Rodríguez P, de los Campos G, Montesinos-López OA, Burgueño J (2016) Genomic Prediction of Genotype × Environment Interaction Kernel Regression Models. The Plant Genome 9(3). https://doi.org/10.3835/plantgenome2016.03.0024

Cui D, Zhang Q, Li M, Hartman GL, Zhao Y (2010) Image processing methods for quantitatively detecting soybean rust from multispectral images. Biosyst Eng 107(3):186–93

Daetwyler HD, Bansal UK, Bariana HS, Hayden MJ, Hayes BJ (2014) Genomic prediction for rust resistance in diverse wheat landraces. Theor Appl Genet 127(8):1795–1803. https://doi.org/10.1007/s00122-014-2341-8

Darben LM, Yokoyama A, Castanho FM, Lopes-Caitar VS et al (2020) Characterization of genetic diversity and pathogenicity of *Phakopsora pachyrhizi* mono-uredinial isolates collected in Brazil. Eur J Plant Pathol 156(2):355–72. http://doi.org/10.1007/s10658-019-01872-2

Das A, Parihar AK, Saxena D, Singh D, Singha KD, Kushwaha KPS et al (2019) Deciphering genotype-by-Environment interaction for targeting test environments and rust resistant genotypes in field pea (*Pisum sativum* L.). Front Plant Sci 10. https://doi.org/10.3389/fpls.2019.00825

Das S, Raj SK, Sen C (1999) Temporal and spatial epidemic development of groundnut rust (*Puccinia arachidis* Speg.) as a function of altered date of sowing. Trop Agric 76(1):45–50

Dawit W, Andnew Y (2005) The study of fungicides application and sowing date, resistance, and maturity of *Eragrostis tef* for the management of teff rust [*Uromyces eragrostidis*]. Can J Plant Pathol 27(4):521–7. http://doi.org/10.1080/07060660509507253

de Carvalho MC da CG, Costa Nascimento L, Darben LM, Polizel-Podanosqui AM, Lopes-Caitar VS, Qi M et al (2017) Prediction of the in planta *Phakopsora pachyrhizi* secretome and potential effector families. Mol Plant Pathol 18(3):363–77. https://doi.org/10.1111/mpp.12405

de Jesus WC, do Vale FXR, Coelho RR, Hau B, Zambolim L, Costa LC et al (2001) Effects of Angular Leaf Spot and Rust on Yield Loss of *Phaseolus vulgaris*. Phytopathology 91(11):1045–53. https://doi.org/10.1094/PHYTO.2001.91.11.1045

de Koning R, Daryanavard H, Garmyn J, Kiekens R, Toili MEM, Angenon G (2023) Fine-tuning CRISPR/Cas9 gene editing in common bean (*Phaseolus vulgaris* L.) using a hairy root transformation system and in silico prediction models. Front Plant Sci 14. https://doi.org/10.3389/fpls.2023.1233418

Dean R, Van Kan JAL, Pretorius ZA, Hammond-Kosack KE, Di Pietro A, Spanu PD et al (2012) The Top 10 fungal pathogens in molecular plant pathology. Mol Plant Pathol 13(4):414–30. https://doi.org/10.1111/j.1364-3703.2011.00783.x

Dehghani H, Moghaddam M (2004) Genetic Analysis of the Latent Period of Stripe Rust in Wheat Seedlings. J Phytopathol 152:325–330

Del Ponte EM, Cazón LI, Alves KS, Pethybridge SJ, Bock CH (2022) How much do standard area diagrams improve accuracy of visual estimates of the percentage area diseased? A systematic review and meta-analysis. Trop Plant Pathol 47(1):43–57

Del Ponte EM, Pethybridge SJ, Bock CH, Michereff SJ, Machado FJ, Spolti P (2017) Standard Area Diagrams for Aiding Severity Estimation: Scientometrics, Pathosystems, and Methodological Trends in the Last 25 Years. Phytopathology 107(10):1161–74. https://doi.org/10.1094/PHYTO-02-17-0069-FI

DeLacy IH, Basford KE, Cooper M, Bull J, McLaren C (1996) Analysis of Multi-Environment Trials-an Historical Perspective. In Plant Adaptation and Crop Improvement, 1st ed. Cooper M, Hammer GL (eds) Cab International: Wallingford, UK, pp. 104–119.

Desaki Y, Morishima M, Sano Y, Uemura T, Ito A, Nemoto K et al (2023) Cytoplasmic Kinase Network Mediates Defense Response to *Spodoptera litura* in *Arabidopsis*. Plants 12:1747. https://doi.org/10.3390/plants12091747

Deshmukh DB, Marathi B, Sudini HK, Variath MT, Chaudhari S, Manohar SS et al (2020) Combining High Oleic Acid Trait and Resistance to Late Leaf Spot and Rust Diseases in Groundnut (*Arachis hypogaea* L.). Front Genet 11. https://doi.org/10.3389/fgene.2020.00514

Devi B, Gupta SK, Singh G, Prasad P (2020) Efficacy of new generation fungicides against French bean rust caused by *Uromyces appendiculatus*. Phytoparasitica 48(4):535–43. https://doi.org/10.1007/s12600-020-00820-9

Díaz-Lago JE, Stuthman DD, Leonard KJ (2003) Evaluation of components of partial resistance to Oat Crown Rust using Digital Image Analysis. Plant Dis 87(6):667–74

Didinger C, Thompson HJ (2021) Defining Nutritional and Functional Niches of Legumes: A Call for Clarity to Distinguish a Future Role for Pulses in the Dietary Guidelines for Americans. Nutrients 13(4):1100. https://doi.org/10.3390/nu13041100

Diers BW, Specht J, Rainey KM, Cregan P, Song Q, Ramasubramanian V et al (2018) Genetic Architecture of soybean yield and agronomic traits. G3-GENES GENOM GENET 8(10):3367–75

Dikshit HK, Singh A, Singh D, Aski M, Jain N, Hegde VS et al (2016) Tagging and mapping of SSR marker for rust resistance gene in lentil (*Lens culinaris* Medikus subsp. *culinaris*). Indian J Exp Biol 54(6):394-9.

Dissanayake R, Kahrood HV, Dimech AM, Noy DM, Rosewarne GM, Smith KF, et al (2020) Development and application of image-based high-throughput phenotyping methodology for Salt Tolerance in Lentils. Agronomy 10(12):1992

Dreischhoff S, Das IS, Häffner F, Wolf AM, Polle A, Kasper KH (2023) Fast and easy bioassay for the necrotizing fungus *Botrytis cinerea* on poplar leaves. Plant Methods 19(1):32

Dugyala S, Borowicz P, Acevedo M (2015) Rapid protocol for visualization of rust fungi structures using fluorochrome Uvitex 2B. Plant Methods 11(1):19–21. https://doi.org/10.1186/s13007-015-0096-0

Duplessis S, Lorrain C, Petre B, Figueroa M, Dodds PN, Aime MC (2021) Host Adaptation and Virulence in Heteroecious Rust Fungi. Annu Rev Phytopathol 59(1):403–22. https://www.doi.org/10.1146/annurev-phyto-020620-121149

Eddelbuettel D, Francois R (2011) Rcpp. Seamless R and C + + integration. J Stat Soft 40(8):1–18.

Edema R, Adipala E (1995) Relationships between brown and false rusts and cowpea yields. Crop Prot 14(5):395–8. https://doi.org/10.1016/0261-2194(95)00021-D

El-Fawy MM, Ahmed MMS, Abo-Elyousr KAM (2021) Resistance enhancement of faba bean plants to rust disease by some compounds and plant extracts. Arch Phytopathol Plant Prot 54(19–20):2067–84. https://doi.org/10.1080/03235408.2021.1970464

El-Fawy MM, El-Sharkawy RMI, Abo-Elyousr KAM, Ahmed MMS (2022) Bioefficacy of pumpkin (*Cucurbita pepo* L.), sage (*Salvia officinalis* L.), and sesame (*Sesamum indicum* L.) essential oils as defense inducers of faba bean against rust disease. J Plant Dis Prot 130:587–98. https://doi.org/10.1007/s41348-022-00662-z

El-Hasan A, Walker F, Klaiber I, Schöne J, Pfannstiel J, Voegele RT (2022) New Approaches to Manage Asian Soybean Rust (*Phakopsora pachyrhizi*) Using *Trichoderma* spp. or Their Antifungal Secondary Metabolites. Metabolites 12(6):507. https://doi.org/10.3390/metabo12060507

Elliott K, Berry JC, Kim H, Bart RS (2022) A comparison of ImageJ and machine learning based image analysis methods to measure cassava bacterial blight disease severity. Plant Methods 18(1):86

Emeran AA, Roman B, Sillero JC, Satovic Z, Rubiales D (2008) Genetic variation among and within *Uromyces* species infecting legumes. J Phytopathol 156(7–8):419–24. https://doi.org/10.1111/j.1439-0434.2007.01382.x

Emeran AA, Sillero JC, Fernández-Aparicio M, Rubiales D (2011) Chemical control of faba bean rust (*Uromyces viciae-fabae*). Crop Prot 30(7):907–12. https://doi.org/10.1016/j.cropro.2011.02.004

Emeran AA, Sillero JC, Niks RE, Rubiales D (2005) Infection structures of host-specialized isolates of *Uromyces viciae-fabae* and of other species of *Uromyces* infecting leguminous crops. Plant Dis 89(1):17–22. https://doi.org/10.1094/PD-89-0017

Emeran AA, Sillero JC, Rubiales D (2001) Physiological specialisation of *Uromyces viciae-fabae*. In: 4th European Conference: Grain Legumes Towards the sustainable production of healthy food, feed and novel products. Cracow, Poland; pp 263

EPPO Standards Pea. EPPO Bulletin. Available online: https://www.eppo.int/RESOURCES/eppo_standards/pp2_gpp. (accessed on 14 May 2022)

Eshetu G, Bimrew Y, Shifa H (2018) Association of Chocolate Spot and Faba Bean Rust Epidemics with Climate Change Resilient Cultural Practices in Bale Highlands, Ethiopia. Adv Agric 2018:1–13. https://doi.org/10.1155/2018/6042495

Etheridge JV, Bateman GL (1999) Fungicidal control of foliar diseases of white lupin (*Lupinus albus*). Crop Prot 18(5):349–54. https://doi.org/10.1016/S0261-2194(99)00031-9

Fahlgren N, Feldman M, Gehan MA, Wilson MS, Shyu C, Bryant DW, et al. A versatile phenotyping system and analytics platform reveals diverse temporal responses to Water availability in Setaria. Mol Plant. 2015;8(10):1520–35.

Fambrini M, Usai G, Vangelisti A, Mascagni F, Pugliesi C (2020) The plastic genome: The impact of transposable elements on gene functionality and genomic structural variations. genesis 58. https://doi.org/10.1002/dvg.23399

FAOSTAT. Available online: http://www.fao.org/faostat (accessed on 4 February 2022)

Fernández-Aparicio M, Rubiales D, Flores F, Hauggaard-Nielsen H (2006) Effects of sowing density, nitrogen availability and crop mixtures on faba bean rust (*Uromyces viciae-fabae*) infection. In: International Workshop on faba bean breeding and agronomy. pp 143–7

Fikru M, Are AK, Agrawal SK, Kemal SA, Gill RK, Singh S et al (2014) Identification of molecular markers associated with rust (*Uromyces viciae-fabae* Pers.) resistance genes in lentil (*Lens culinaris* subsp. *culinaris*). Can J Plant Prot 2(2):27–36

Fois M, Malinowska M, Schubiger FX, Asp T (2021) Genomic Prediction and Genotype-by-Environment Interaction Analysis of Crown and Stem Rust in Ryegrasses in European Multi-Site Trials. Agronomy 11(6):1119. https://doi.org/10.3390/agronomy11061119

Fondevilla S, Rubiales D (2012) Powdery mildew control in pea. A review. Agron Sustain Dev 32(2):401–409. https://doi.org/10.1007/s13593-011-0033-1

Fondevilla S, Chattopadhyay C, Khare N, Rubiales D (2013) *Erysiphe Trifolii* Is Able to Overcome Er1 and Er3, but Not Er2, Resistance Genes in Pea. Eur J Plant Pathol 136:557–563

Fontana DC, de Paula S, Torres AG, de Souza VHM, Pascholati SF, Schmidt D et al (2021) Endophytic Fungi: Biological Control and Induced Resistance to Phytopathogens and Abiotic Stresses. Pathogens 10(5):570. https://doi.org/10.3390/pathogens10050570

Franceschi VT, Alves KS, Mazaro SM, Godoy C V, Duarte HSS, Del Ponte EM (2020) A new standard area diagram set for assessment of severity of soybean rust improves accuracy of estimates and optimizes resource use. Plant Pathol 69(3):495–505. https://doi.org/10.1111/ppa.13148

Gallego-Sánchez LM, Canales FJ, Montilla-Bascón G, Prats E. RUST: a robust, user-friendly Script Tool for Rapid Measurement of Rust Disease on cereal Leaves. Plants. 2020;9(9):1182

Gao X, Tang Y, Shi Q, Wei Y, Wang X, Shan W et al (2023) Vacuolar processing enzyme positively modulates plant resistance and cell death in response to *Phytophthora parasitica* infection. J Integr Agric 22:1424–1433. https://doi.org/10.1016/j.jia.2022.08.124

Garcia A, Calvo ÉS, de Souza Kiihl RA, Harada A, Hiromoto DM, Vieira LGE (2008) Molecular mapping of soybean rust (*Phakopsora pachyrhizi*) resistance genes: discovery of a novel locus and alleles. Theor Appl Genet 117(4):545–53. http://doi.org/10.1007/s00122-008-0798-z

Gautam AK, Avasthi S, Verma RK, Sushma, Niranjan M, Devadatha B et al (2022a) A Global Overview of Diversity and Phylogeny of the Rust Genus *Uromyces*. J Fungi 8(6):633. https://doi.org/10.3390/jof8060633

Gautam AK, Payal, Avasthi S, Verma R (2022b) Biology, disease development, distribution and control of rust pathogen *Uromyces viciae-fabae*. Plant Pathol Quar 12(1):60–76. https://doi.org/10.5943/ppq/12/1/5

Gay J (1971) Apparent new race of cowpea rust on *Vigna*. Plant Dis reporter 55(5):384

Gehan MA, Fahlgren N, Abbasi A, Berry JC, Callen ST, Chavez L et al (2017) PlantCV v2: image analysis software for high-throughput plant phenotyping. PeerJ 5:e4088

Georgieva N (2018) Suitability of vetch (*Vicia sativa* and *V. villosa* Roth) cultivars for organic farming conditions. Pakistan J Bot 50(1):161–7

Gill HS, Halder J, Zhang J, Brar NK, Rai TS, Hall C, Bernardo A, Amand PS, Bai G et al (2021) Multi-Trait Multi-Environment Genomic Prediction of Agronomic Traits in Advanced Breeding Lines of Winter Wheat. Front Plant Sci 12. https://doi.org/10.3389/fpls.2021.709545

Gireesh C, Sundaram RM, Anantha SM, Pandey MK, Madhav MS, Rathod S et al (2021) Nested Association Mapping (NAM) populations: Present Status and future prospects in the Genomics era. CRC Crit Rev Plant Sci 40(1):49–67

Gitelson AA, Stark R, Grits U, Rundquist D, Kaufman Y, Derry D (2002) Vegetation and soil lines in visible spectral space: a concept and technique for remote estimation of vegetation fraction. Int J Remote Sens 23(13):2537–62

Glaab J, Kaiser WM (1999) Increased nitrate reductase activity in leaf tissue after application of the fungicide Kresoxim-methyl. Planta 207(3):442–8. http://doi.org/10.1007/s004250050503

Goellner K, Loehrer M, Langenbach C, Conrath U, Koch E, Schaffrath U (2010) *Phakopsora pachyrhizi*, the causal agent of Asian soybean rust. Mol Plant Pathol 11(2):169–77. https:// doi.org /10.1111/j.1364-3703.2009.00589.x

Golisz A, Krzyszton M, Stepien M, Dolata J, Piotrowska J, Szweykowska-Kulinska Z et al (2021) Arabidopsis Spliceosome Factor SmD3 Modulates Immunity to *Pseudomonas syringae* Infection. Front Plant Sci 12. https://doi.org/10.3389/fpls.2021.765003

González-Barrios P, Díaz-García L, Gutiérrez L (2019) Mega-Environmental Design: Using Genotype × Environment Interaction to Optimize Resources for Cultivar Testing. Crop Sci 59(5):1899–1915. https://doi.org/10.2135/cropsci2018.11.0692

Gou M, Shi Z, Zhu Y, Bao Z, Wang G, Hua J (2012) The F-box protein CPR1/CPR30 negatively regulates R protein SNC1 accumulation. Plant J 69:411–420. https://doi.org/10.1111/j.1365-313X.2011.04799.x

Graham PH, Vance CP (2003) Legumes: Importance and Constraints to Greater Use. Plant Physiol 131(3):872–7. https://doi.org/10.1104/pp.017004

Grasso V, Palermo S, Sierotzki H, Garibaldi A, Gisi U (2006a) Cytochrome b gene structure and consequences for resistance to Qo inhibitor fungicides in plant pathogens. Pest Manag Sci 62(6):465–72. https://doi.org/10.1002/ps.1236

Grasso V, Sierotzki H, Garibaldi A, Gisi U (2006b) Relatedness Among Agronomically Important Rusts Based on Mitochondrial Cytochrome b Gene and Ribosomal ITS Sequences. J Phytopathol 154(2):110–8. https://doi.org/10.1111/j.1439-0434.2006.01070.x

Gu J, Sun J, Liu N, Sun X, Liu C, Wu L et al (2020) A novel cysteine-rich receptor-like kinase gene, TaCRK2, contributes to leaf rust resistance in wheat. Mol Plant Pathol 21:732–746. https://doi.org/10.1111/mpp.12929

Gungaabayar A, Jha A, Warkentin T, Knight D, Penner G, Biligetu B (2023) Forage yield and biological nitrogen fixation of pea–cereal intercrops for hay production. Agron J 115(2):607–19. https://doi.org/10.1002/agj2.21270

Guo A, Huang W, Dong Y, Ye H, Ma H, Liu B et al (2021) Wheat yellow rust detection using UAV-Based Hyperspectral Technology. Remote Sens 13(1):123

Guo Z, Luo C, Dong Y, Dong K, Zhu J, Ma L (2021) Effect of nitrogen regulation on the epidemic characteristics of intercropping faba bean rust disease primarily depends on the canopy microclimate and nitrogen nutrition. Field Crop Res 274:108339. https://doi.org/10.1016/j.fcr.2021.108339

Guo Z, Luo C, Dong Y, Dong K, Zhu J, Ma L (2021) Effect of nitrogen regulation on the epidemic characteristics of intercropping faba bean rust disease primarily depends on the canopy microclimate and nitrogen nutrition. Field Crops Res 274:108339. https://doi.org/10.1016/j.fcr.2021.108339

Guo Z, Tucker DM, Basten CJ, Gandhi H, Ersoz E, Guo B, Xu Z et al (2014) The impact of population structure on genomic prediction in stratified populations. Theor Appl Genet 127(3):749–762. https://doi.org/10.1007/s00122-013-2255-x

Gupta M, Dubey S, Jain D, Chandran D (2021) The *Medicago truncatula* Sugar Transport Protein 13 and Its Lr67res-Like Variant Confer Powdery Mildew Resistance in Legumes via Defense Modulation. Plant Cell Physiol 62(4):650–67. https://doi.org/10.1093/pcp/pcab021

Habier D, Fernando RL, Dekkers JCM (2007) The Impact of Genetic Relationship Information on Genome-Assisted Breeding Values. Genetics 177(4):2389–2397. https://doi.org/10.1534/genetics.107.081190

Habier D, Fernando, RL, Kizilkaya K, Garrick DJ (2011) Extension of the bayesian alphabet for genomic selection. BMC Bioinformatics 12(1):186. https://doi.org/10.1186/1471-2105-12-186

Haley SD, Afanador LK, Miklas PN, Stavely JR, Kelly JD (1994) Heterogeneous inbred populations are useful as sources of near-isogenic lines for RAPD marker localization. Theor Appl Genet 88(3–4):337–42. http://doi.org/10.1007/BF00223642

Haley SD, Miklas PN, Stavely JR, Byrum J, Kelly JD (1993) Identification of RAPD markers linked to a major rust resistance gene block in common bean. Theor Appl Genet 86(4):505–12. http://doi.org/10.1007/BF00838567

Hartwig EE (1986) Identification of a Fourth Major Gene Conferring Resistance to Soybean Rust. Crop Sci 26(6):1135–6. https://doi.org/10.2135/cropsci1986.0011183X002600060010x

Hayes BJ, Visscher PM, Goddard ME (2009) Increased accuracy of artificial selection by using the realized relationship matrix. Genetics Research 91(1):47–60. https://doi.org/10.1017/S0016672308009981

He F, Wang C, Sun H, Tian S, Zhao G, Liu C et al (2023) Simultaneous editing of three homoeologues of TaCIPK14 confers broad-spectrum resistance to stripe rust in wheat. Plant Biotechnol J 21(2):354–68. https://doi.org/10.1111/pbi.13956

Heath MC (1994) Genetics and cytology of age-related resistance in North American cultivars of cowpea (*Vigna unguiculata*) to the cowpea rust fungus (*Uromyces vignae*). Can J Bot 72(5):575–81. http://doi.org/10.1139/b94-076

Heffner EL, Jannink J, Sorrells ME (2011) Genomic Selection Accuracy using Multifamily Prediction Models in a Wheat Breeding Program. The Plant Genome 4(1). https://doi.org/10.3835/plantgenome2010.12.0029

Heineck GC, McNish IG, Jungers JM, Gilbert E, Watkins E (2019) Using R-Based image analysis to quantify rusts on perennial ryegrass. Plant Phenome J 2(1):1–10.

Helfer S (2013) Rust fungi and global change. New Phytol 201(3):770–80. https://doi.org /10.1111/nph.12570

Herskowitz Y, Bunimovich-Mendrazitsky S, Lazebnik T (2023) Mathematical model of coffee tree's rust control using snails as biological agents. Biosystems 229:104916. https://doi.org/10.1016/j.biosystems.2023.104916

Hester J, Vaughan D, bench (2023) High Precision Timing of R Expressions. https://cran.r-project.org/package=bench.

Hickey LT, Hafeez A, Robinson H, Jackson SA, Leal-Bertioli SCM, Tester M et al (2019) Breeding crops to feed 10 billion. Nat Biotechnol 37(7):744–54. https://doi.org/10.1038/s41587-019-0152-9

Hillocks R, Bennett C, Mponda O (2012) Bambara nut: A review of utilisation, market potential and crop improvement. African Crop Sci J 20(1):1–16.

Hoch HC, Staples RC, Whitehead B, Comeau J, Wolf ED. Signaling for Growth Orientation and Cell Differentiation by Surface Topography in *Uromyces*. Science 235(4796):1659–62. https://doi.org/10.1126/science.235.4796.1659

Howe GT, Saruul P, Davis J, Chen THH (2000) Quantitative genetics of bud phenology, frost damage, and winter survival in an F2 family of hybrid poplars. Theor Appl Genet 101(4):632–42. https://doi.org/10.1007/s001220051525

Howles PA, Gebbie LK, Collings DA, Varsani A, Broad RC, Ohms S et al (2016) A temperature-sensitive allele of a putative mRNA splicing helicase down-regulates many cell wall genes and causes radial swelling in *Arabidopsis thaliana*. Plant Mol Biol 91:1–13. https://doi.org/10.1007/s11103-016-0428-0

Huang M, Liu X, Zhou Y, Summers RM, Zhang Z (2019) BLINK: A package for the next level of genome-wide association studies with both individuals and markers in the millions. Gigascience 8:1–12. https://doi.org/10.1093/gigascience/giy154

Hurtado-Gonzales OP, Gilio TAS, Pastor-Corrales MA (2017a) Resistant Reaction of Andean Common Bean Lamdrace G19833, Reference Genome, to 13 Races of *Uromyces appendiculatus* Suggests Broad Spectrum Rust Resistance. Annu Rep Bean Improv Coop 60:3–5.

Hurtado-Gonzales OP, Valentini G, Gilio TAS, Martins AM, Song Q, Pastor-Corrales MA (2017b) Fine Mapping of Ur-3, a Historically Important Rust Resistance Locus in Common Bean. G3-GENES GENOM GENET 7(2):557–69. https://doi.org/10.1534/g3.116.036061

Huyghe C (1997) White lupin (*Lupinus albus* L.). Field Crop Res 53(1–3):147–60. https://doi.org/10.1016/S0378-4290(97)00028-2

Hyten DL, Hartman GL, Nelson RL, Frederick RD, Concibido VC, Narvel JM et al (2007) Map Location of the Rpp1 Locus That Confers Resistance to Soybean Rust in Soybean. Crop Sci 47(2):837–8. https://doi.org/10.2135/cropsci2006.07.0484

Hyun MK, Zaitlen NA, Wade CM, Kirby A, Heckerman D, Daly MJ, Eskin E (2008) Efficient control of population structure in model organism association mapping. Genetics 178(3):1709–23. https://doi.org/10.1534/genetics.107.080101

Idrissi O, Sakr B, Dahan R, Houasli C, Nsarellah N, Udupa SM et al (2012) Registration of 'Chakkouf' Lentil in Morocco. J Plant Regist 6(3):268–72. https://doi.org/10.3198/jpr2011.07.0384crc

Ijaz U, Adhikari K, Kimber R, Trethowan R, Bariana H, Bansal U (2021a) Pathogenic Specialization in *Uromyces viciae-fabae* in Australia and Rust Resistance in Faba Bean. Plant Dis 105(3):636–42. https://doi.org/10.1094/PDIS-06-20-1325-RE

Ijaz U, Ayliffe M, Adhikari K, Bariana H, Bansal U (2020) Australian *Uromyces viciae-fabae*: Host and nonhost interaction among cultivated grain legumes. Plant Pathol 69(7):1227–36. https://doi.org/10.1111/ppa.13222

Ijaz U, Sudheesh S, Kaur S, Sadeque A, Bariana H, Bansal U et al (2021b) Mapping of two new rust resistance genes uvf-2 and uvf-3 in faba bean. Agronomy 11(7):1–13. https://doi.org/10.3390/agronomy11071370

Ishiga Y, Rao Uppalapati S, Gill US, Huhman D, Tang Y, Mysore KS (2015) Transcriptomic and metabolomic analyses identify a role for chlorophyll catabolism and phytoalexin during *Medicago* nonhost resistance against Asian soybean rust. Sci Rep 5:13061. https://doi.org/10.1038/srep13061

Jain S, Weeden NF, Porter LD, Eigenbrode SD, McPhee K (2013) Finding Linked Markers to En for Efficient Selection of Pea Enation Mosaic Virus Resistance in Pea. Crop Sci 53(6):2392–2399. https://doi.org/10.2135/cropsci2013.04.0211

Jakada BH, Fakher B, Yao L-A, Wang X, Aslam M, Qin Y (2023) Ectopic Expression of Pineapple Actin-Related Protein 6 (AcARP6) Regulates Flowering and Stress Responses in Arabidopsis. J Plant Growth Regul 42:6461–6473. https://doi.org/10.1007/s00344-022-10874-0

Jakupović M, Heintz M, Reichmann P, Mendgen K, Hahn M (2006) Microarray analysis of expressed sequence tags from haustoria of the rust fungus *Uromyces fabae*. Fungal Genet Biol 43(1):8–19. https://doi.org/10.1016/j.fgb.2005.09.001

Jarquín D, Crossa J, Lacaze X, Du Cheyron P, Daucourt J, Lorgeou J, Piraux, F et al (2014) A reaction norm model for genomic selection using high-dimensional

genomic and environmental data. Theor Appl Genet 127(3):595–607. https://doi.org/10.1007/s00122-013-2243-1

Jayakodi M, Golicz AA, Kreplak J, Fechete LI, Angra D, Bednář P et al (2023) The giant diploid faba genome unlocks variation in a global protein crop. Nature 615(7953):652–9. https://doi.org/10.1038/s41586-023-05791-5

Jeger MJ, Viljanen-Rollinson SLH (2001) The use of the area under the disease-progress curve (AUDPC) to assess quantitative disease resistance in crop cultivars. Theor Appl Genet 102(1):32–40. https://doi.org/10.1007/s001220051615

Jeger MJ, Viljanen-Rollinson SLH (2001) The use of the area under the disease-progress curve (AUDPC) to assess quantitative disease resistance in crop cultivars. Theor Appl Genet 102(1):32–40

Jha AB, Gali KK, Alam Z, Lachagari VBR, Warkentin TD (2021) Potential application of genomic technologies in breeding for fungal and oomycete disease resistance in pea. Agronomy 11(6):1–22. https://doi.org/10.3390/agronomy11061260

Jha AB, Warkentin TD (2020) Biofortification of Pulse Crops: Status and Future Perspectives. Plants 9(1):73. https://doi.org/10.3390/plants9010073

Ji J, Zhang C, Sun Z, Wang L, Duanmu D, Fan Q (2019) Genome Editing in Cowpea *Vigna unguiculata* Using CRISPR-Cas9. Int J Mol Sci 20(10):2471. https://doi.org/10.3390/ijms20102471

Jiang GL (2013) Molecular Markers and Marker-Assisted Breeding in Plants. InTech (ed) Plant Breeding from Laboratories to Fields. http://doi.org/10.5772/52583

Johnson E, Miklas PN, Stavely JR, Martinez-Cruzado JC (1995) Coupling- and repulsion-phase RAPDs for marker-assisted selection of PI 181996 rust resistance in common bean. Theor Appl Genet 90(5):659–64. http://doi.org/10.1007/BF00222130

Juliana P, Singh RP, Singh PK, Crossa J, Huerta-Espino J, Lan C, Bhavani S et al (2017) Genomic and pedigree-based prediction for leaf, stem, and stripe rust resistance in wheat. Theor Appl Genet 130(7):1415–1430. https://doi.org/10.1007/s00122-017-2897-1

Juliatti FC, Azevedo LAS de, Juliatti FC (2017) Strategies of Chemical Protection for Controlling Soybean Rust. Soybean - The Basis of Yield, Biomass and Productivity. InTech. http://dx.doi.org/10.5772/67454

Juroszek P, von Tiedemann A (2011) Potential strategies and future requirements for plant disease management under a changing climate. Plant Pathol 60(1):100–12. https://doi.org/10.1111/j.1365-3059.2010.02410.x

Kamel AM, Metwally K, Sabry M, Albalawi DA, Abbas ZK, Darwish DBE et al (2023) The Expression of *Triticum aestivum* Cysteine-Rich Receptor-like Protein Kinase

Genes during Leaf Rust Fungal Infection. Plants 12:2932. https://doi.org/10.3390/plants12162932

Kandasamy MK, McKinney EC, Meagher RB (2008) ACTIN-RELATED PROTEIN8 Encodes an F-Box Protein Localized to the Nucleolus in Arabidopsis. Plant Cell Physiol 49:858–863. https://doi.org/10.1093/pcp/pcn053

Kant A, Sharma SK, Sharma R, Sharma RK, Mohapatra T (2004) Identification of RAPD and AFLP markers linked with rust resistance gene in lentil. Crop Improv 31(1):1–10

Kassambara A, Mundt F (2020) factoextra: Extract and Visualize the Results of Multivariate Data Analyses. R Packag. version 1.0.7. https://cran.r-project.org/package=factoextra

Kaur G, Toora PK, Tuan PA, McCartney CA, Izydorczyk MS, Badea A et al (2023) Genome-wide association and targeted transcriptomic analyses reveal loci and candidate genes regulating preharvest sprouting in barley. Theor Appl Genet 136:202. https://doi.org/10.1007/s00122-023-04449-0

Kawashima CG, Guimarães GA, Nogueira SR, MacLean D, Cook DR, Steuernagel B et al (2016) A pigeonpea gene confers resistance to Asian soybean rust in soybean. Nat Biotechnol 34(6):661–5. https://doi.org/10.1038/nbt.3554

Keller B, Manzanares C, Jara C, Lobaton JD, Studer B, Raatz B (2015) Fine-mapping of a major QTL controlling angular leaf spot resistance in common bean (*Phaseolus vulgaris* L.). Theor Appl Genet 128(5):813–26. http://doi.org/10.1007/s00122-015-2472-6

Kelly JD, Gepts P, Miklas PN, Coyne DP (2003) Tagging and mapping of genes and QTL and molecular marker-assisted selection for traits of economic importance in bean and cowpea. Field Crop Res 82(2–3):135–54. https://doi.org/10.1016/S0378-4290(03)00034-0

Kemen E, Kemen AC, Rafiqi M, Hempel U, Mendgen K, Hahn M et al (2005) Identification of a Protein from Rust Fungi Transferred from Haustoria into Infected Plant Cells. Mol Plant-Microbe Interact 18(11):1130–9. https://doi.org/10.1094/MPMI-18-1130

Khalil M, Ramadan A, EL-Sayed S, El-Taher A (2023) Effectiveness of natural antioxidants on physiological, anatomical changes and Controlling Downy, Powdery Mildew and Rust Diseases in pea plants. Asian J Plant Sci 22(1):25–36.

Kiani T, Mehboob F, Hyder MZ, Zainy Z, Xu L, Huang L et al (2021) Control of stripe rust of wheat using indigenous endophytic bacteria at seedling and adult plant stage. Sci Rep 11(1):14473. https://doi.org/10.1038/s41598-021-93939-6

Kiba A, Nakano M, Vincent-Pope P, Takahashi H, Sawasaki T, Endo Y et al (2012) A novel Sec14 phospholipid transfer protein from *Nicotiana benthamiana* is up-regulated in response to *Ralstonia solanacearum* infection, pathogen associated molecular patterns and effector molecules and involved in plant immunity. J Plant Physiol 169:1017–22. https://doi.org/10.1016/j.jplph.2012.04.002

King ZR, Harris DK, Pedley KF, Song Q, Wang D, Wen Z et al (2016) A novel *Phakopsora pachyrhizi* resistance allele (Rpp) contributed by PI 567068A. Theor Appl Genet 24;129(3):517–34. http://doi.org/10.1007/s00122-015-2645-3

Köhle H, Grossmann K, Retzlaff G, Akers A (1997) Physiological effects of the new fungicide JuwelReg on yield in cereals. Gesunde Pflanzen 49(8): 267-271

Kosterin OE, Bogdanova VS, Galieva ER (2019) Reciprocal compatibility within the genus *Pisum* L. as studied in F1 hybrids: 2. Crosses involving *P. fulvum* Sibth. et Smith. Genet Resour Crop Evol 66:383–99

Kottek M, Grieser J, Beck C, Rudolf B, Rubel F (2006) World map of the Köppen-Geiger climate classification updated. Meteorologische Zeitschrift 15(3):259–63. https://doi.org/10.1127/0941-2948/2006/0130

Kreplak J, Madoui MA, Cápal P, Novák P, Labadie K, Aubert G et al (2019) A reference genome for pea provides insight into legume genome evolution. Nat Genet 51(9):1411–22. https://doi.org/10.1038/s41588-019-0480-1

Kuhn M, Vaughan D, Hvitfeldt E (2023) yardstick: Tidy Characterizations of Model Performance. https://cran.r-project.org/package=yardstick.

Kuo HI, Dai HY, Wu YP, Tseng YC (2021) Peanut Germplasm Evaluation for Agronomic Traits and Disease Resistance under a Two-Season Cropping System in Taiwan. Agriculture 11(12):1277. https://doi.org/10.3390/agriculture11121277

Kushwaha C, Chand R, Singh AK, Kumar M, Srivastava CP (2018) Differential Induction of β-1,3-Glucanase Gene in Expression of Partial Resistance to Rust (*Uromyces fabae* (Pers.) de Bary) in Pea (*Pisum sativum* L.). Russ J Plant Physiol 65(5):697–701. https://doi.org/10.1134/S1021443718050114

Kushwaha C, Chand R, Singh AK, Rai R, Srivastava CP, Singh BD et al (2016) Lignification and early abortive fungal colonies as indicators of partial resistance to rust in pea. Trop Plant Pathol 41(2):91–7. http://doi.org/10.1007/s40858-016-0071-y

Lado B, Barrios PG, Quincke M, Silva P, Gutiérrez L (2016) Modeling Genotype × Environment Interaction for Genomic Selection with Unbalanced Data from a Wheat Breeding Program. Crop Sci 56(5):2165–79. https://doi.org/10.2135/cropsci2015.04.0207

Leitão ST, Rubiales D, Vaz Patto MC (2023) Identification of novel sources of partial and incomplete hypersensitive resistance to rust and associated genomic regions in common bean. BMC Plant Biol 23(1):610. https://doi.org/10.1186/s12870-023-04619-8

Lemos NG, de Lucca e Braccini A, Abdelnoor RV, de Oliveira MCN, Suenaga K, Yamanaka N (2011) Characterization of genes Rpp2, Rpp4, and Rpp5 for resistance to soybean rust. Euphytica 182(1):53. https://doi.org/10.1007/s10681-011-0465-3

Leprévost T, Boutet G, Lesné A, Rivière JP, Vetel P, Glory I et al (2023) Advanced backcross QTL analysis and comparative mapping with RIL QTL studies and GWAS provide an overview of QTL and marker haplotype diversity for resistance to Aphanomyces root rot in pea (*Pisum sativum*). Front Plant Sci 14. https://doi.org/10.3389/fpls.2023.1189289.

Letessier MP, Svoboda KP, Walters DR (2001) Antifungal Activity of the Essential Oil of Hyssop (*Hyssopus officinalis*). J Phytopathol 149(11–12):673–8. https://doi.org/10.1046/j.1439-0434.2001.00692.x

Lewandowska M, Keyl A, Feussner I (2020) Wax biosynthesis in response to danger: its regulation upon abiotic and biotic stress. New Phytol 227:698–713. https://doi.org/10.1111/nph.16571

Li B, Zeng Y, Jiang L (2022) COPII vesicles in plant autophagy and endomembrane trafficking. FEBS Lett 596:2314–2323. https://doi.org/10.1002/1873-3468.14362

Li C, Sun B, Li Y, Liu C, Wu X, Zhang D et al (2016) Numerous genetic loci identified for drought tolerance in the maize nested association mapping populations. BMC Genomics 8(1):17

Li G, Liu R, Xu R, Varshney RK, Ding H, Li M et al (2023) Development of an Agrobacterium-mediated CRISPR/Cas9 system in pea (*Pisum sativum* L.). Crop J 11(1):132–9. https://doi.org/10.1016/j.cj.2022.04.011

Li G, Liu Y, Ehlers JD, Zhu Z, Wu X, Wang B et al (2007) Identification of an AFLP Fragment Linked to Rust Resistance in Asparagus Bean and Its Conversion to a SCAR Marker. HortScience 42(5):1153–6. https://doi.org/10.21273/HORTSCI.42.5.1153

Li Q, Wang B, Yu J, Dou D (2021) Pathogen-informed breeding for crop disease resistance. J Integr Plant Biol 63(2):305–11

Liebenberg MM, Pretorius ZA (2011) Pathogenic Diversity in and Sources of Resistance to *Uromyces appendiculatus* in Southern Africa. J Phytopathol 159(4):287–97. https://doi.org/10.1111/j.1439-0434.2010.01763.x

Lilin-Yin (2023) CMplot: Circle Manhattan Plot. CRAN. https://cran.r-project.org/package=CMplot

Lim SM, Yoon M-Y, Choi GJ, Choi YH, Jang KS, Shin TS et al (2017) Diffusible and Volatile Antifungal Compounds Produced by an Antagonistic *Bacillus velezensis* G341 against Various Phytopathogenic Fungi. Plant Pathol J 33(5):488–98. https:// doi.org/10.5423/PPJ.OA.04.2017.0073

Lin L (1989) A concordance correlation coefficient to evaluate reproducibility. Biometrics 45(1):255–68.

Lin CS, Binns MR (1988) A Superiority Measure of Cultivar Performance for Cultivar × Location Data. Can J Plant Sci 68:193–8

Lin Z, Shi F, Hayes BJ, Daetwyler HD (2017) Mitigation of inbreeding while preserving genetic gain in genomic breeding programs for outbred plants. Theor Appl Genet 130(5):969–80. https://doi.org/10.1007/s00122-017-2863-y

Link T, Lohaus G, Heiser I, Mendgen K, Hahn M, Voegele RT (2005) Characterization of a novel NADP+-dependent D-arabitol dehydrogenase from the plant pathogen *Uromyces fabae*. Biochem J 389(2):289–95. https://doi.org/10.1042/BJ20050301

Link TI, Seibel C, Voegele RT (2014a) Early insights into the genome sequence of *Uromyces fabae*. Front Plant Sci 5. http://doi.org/10.3389/fpls.2014.00587/abstract

Link TI (2020) Testing reference genes for transcript profiling in *Uromyces appendiculatus* during urediospore infection of common bean. PLoS One 15(8):0237273. https://doi.org/10.1371/journal.pone.0237273

Link TI, Lang P, Scheffler BE, Duke M V., Graham MA, Cooper B et al (2014b) The haustorial transcriptomes of *Uromyces appendiculatus* and *Phakopsora pachyrhizi* and their candidate effector families. Mol Plant Pathol 15(4):379–93. https://doi.org/doi/10.1111/mpp.12099

Link TI, Voegele RT (2008) Secreted proteins of *Uromyces fabae*: similarities and stage specificity. Mol Plant Pathol 9(1):59–66. https://doi.org/10.1111/j.1364-3703.2007.00448.x

Liu M, Li S, Swaminathan S, Sahu BB, Leandro LF, Cardinal AJ et al (2016) Identification of a soybean rust resistance gene in PI 567104B. Theor Appl Genet 129(5):863–77. http://doi.org/10.1007/s00122-015-2651-5

Lopes FS, Pozza EA, Porto ACM, da Silva CM, Miguel LA, Pereira WA (2022) Development and validation of a diagrammatic scale for white mold incidence in tobacco leaf discs. Australas Plant Pathol 51(1):31–8

Lopez-Cruz M, Crossa J, Bonnett D, Dreisigacker S, Poland J, Jannink JL, Singh R et al (2015) Increased Prediction Accuracy in Wheat Breeding Trials Using a Marker × Environment Interaction Genomic Selection Model. G3-GENES GENOM GENET, 5(4):569–82. https://doi.org/10.1534/g3.114.016097

Luo C, Lv J, Guo Z, Dong Y (2022) Intercropping of Faba Bean with Wheat Under Different Nitrogen Levels Reduces Faba Bean Rust and Consequent Yield Loss. Plant Dis 106(9):2370–9. https://doi.org/10.1094/PDIS-11-21-2451-RE

Luo C, Lv J, Guo Z, Dong Y (2022) Intercropping of Faba Bean with Wheat under different Nitrogen levels reduces Faba Bean Rust and Consequent Yield loss. Plant Dis 106(9):2370–9

Madrid E, Rubiales D, Moral A, Moreno MT, Millán T, Gil J et al (2008) Mechanism and molecular markers associated with rust resistance in a chickpea interspecific cross (*Cicer arietinum* × *Cicer reticulatum*). Eur J Plant Pathol 121(1):43–53. http://doi.org/10.1007/s10658-007-9240-7

Maldonado-Bonilla LD, Eschen-Lippold L, Gago-Zachert S, Tabassum N, Bauer N, Scheel D et al (2014). The Arabidopsis Tandem Zinc Finger 9 Protein Binds RNA and Mediates Pathogen-Associated Molecular Pattern-Triggered Immune Responses. Plant Cell Physiol 55:412–425. https://doi.org/10.1093/pcp/pct175

Manjula K, Kishore GK, Podile AR (2004) Whole cells of *Bacillus subtilis* AF 1 proved more effective than cell-free and chitinase-based formulations in biological control of citrus fruit rot and groundnut rust. Can J Microbiol 50(9):737–44. http://doi.org/10.1139/w04-058

Mapuranga J, Zhang N, Zhang L, Chang J, Yang W (2022) Infection Strategies and Pathogenicity of Biotrophic Plant Fungal Pathogens. Front Microbiol 2:13. https://www.doi.org/10.3389/fmicb.2022.799396/full

Martins DC, Rubiales D, Vaz Patto MC (2022) Association Mapping of *Lathyrus sativus* Disease Response to *Uromyces pisi* Reveals Novel Loci Underlying Partial Resistance. Front Plant Sci 13:1–13. https://doi.org/10.3389/fpls.2022.842545

Martins LB, Balint-Kurti P, Reberg-Horton SC (2022) Genome-wide association study for morphological traits and resistance to *Peryonella pinodes* in the USDA pea single plant plus collection. G3-GENES GENOM GENET 25:129

Mattos A do P, Tolentino Júnior JB, Itako AT (2020) Determination of the severity of Septoria leaf spot in tomato by using digital images. Australas Plant Pathol 49(4):329–56

McDonald SC, Buck J, Li Z (2022) Automated, image-based disease measurement for phenotyping resistance to soybean frogeye leaf spot. Plant Methods 18(1):103

McEwen J, Yeoman DP (1989) Effects of row spacing and the control of pests and pathogens on four cultivars of spring-sown field beans (*Vicia faba*). J Agric Sci 113(3):365–71. https://doi.org/10.1017/S0021859600070064

McLean R, Byth D (1980) Inheritance of resistance to rust (*Phakopsora pachyrhizi*) in soybeans. Aust J Agric Res 31(5):951. https://doi.org/10.1071/AR9800951

Meira D, Panho MC, Beche E, Woyann LG, Madella LA, Milioli AS et al (2022) Gene pyramiding combinations confer resistance of Asian soybean rust. Crop Sci 62(2):792–801. https://doi.org/10.1002/csc2.20700

Mendgen K (1978) Attachment of bean rust cell wall material to host and non-host plant tissue. Arch Microbiol 119(2):113–7. http://doi.org/10.1007/BF00964261

Meuwissen THE, Hayes BJ, Goddard ME (2001) Prediction of total genetic value using genome-wide dense marker maps. Genetics 157(4):1819–29. https://doi.org/10.1093/genetics/157.4.1819

Mienie CMS, Liebenberg MM, Pretorius ZA, Miklas PN (2005) SCAR markers linked to the common bean rust resistance gene Ur-13. Theor Appl Genet 111(5):972–9. http://doi.org/10.1007/s00122-005-0037-9

Miklas PN, Stavely JR, Kelly JD (1993) Identification and potential use of a molecular marker for rust resistance in common bean. Theor Appl Genet 85(6–7):745–9. http://doi.org/10.1007/BF00225014

Miller MD, Schmitz Carley CA, Figueroa RA, Feldman MJ, Haagenson D, Shannon LM (2023) TubAR: an R Package for quantifying tuber shape and skin traits from images. Am J Potato Res 100:52–62

Milus EA, Kristensen K, Hovmøller MS (2009) Evidence for increased aggressiveness in a recent widespread strain of *Puccinia striiformis* f. sp. *tritici* Causing Stripe Rust of Wheat. Phytopathol 99(1):89–94

Mitchell DC, Webster A, Garrison B (2022) Terminology Matters: Advancing Science to Define an Optimal Pulse Intake. Nutrients 14(3):655. https://doi.org/10.3390/nu14030655

Miyamoto T, Uemura T, Nemoto K, Daito M, Nozawa A, Sawasaki T et al (2019) Tyrosine Kinase-Dependent Defense Responses Against Herbivory in Arabidopsis. Front Plant Sci 10. https://doi.org/10.3389/fpls.2019.00776

Mmbaga MT, Steadman JR, Roberts JJ (1994) Interaction of bean leaf pubescence with rust urediniospore deposition and subsequent infection density. Ann Appl Biol 125(2):243–54. https://doi.org/10.1111/j.1744-7348.1994.tb04966.x

Modesto JC, Fenille RC, Habermann G (2005) Fungicides effects on the control of leaf bean rust caused by *Uromyces appendiculatus* under field conditions. Arq Inst Biol 72(2):247–50. https://doi.org/10.1590/1808-1657v72p2472005

Modesto LR, Welter LJ, Steiner DRM, Stefen D, Dias AH, Dalbo MA, et al (2022) Phenotyping strategies for *Elsinöe ampelina* symptoms in grapevine (*Vitis* spp). J Phytopathol 170(10):746–52

Mondal S, Badigannavar AM (2015) Peanut rust (*Puccinia arachidis* Speg.) disease: its background and recent accomplishments towards disease resistance breeding. Protoplasma 252(6):1409–20. http://doi.org/10.1007/s00709-015-0783-8

Mondal S, Badigannavar AM (2018) Mapping of a dominant rust resistance gene revealed two R genes around the major Rust QTL in cultivated peanut (*Arachis hypogaea* L.). Theor Appl Genet 131(8):1671–81. http://doi.org/10.1007/s00122-018-3106-6

Mondal S, Badigannavar AM, D'Souza SF (2012) Molecular tagging of a rust resistance gene in cultivated groundnut (*Arachis hypogaea* L.) introgressed from *Arachis cardenasii*. Mol Breed 29(2):467–76. http://doi.org/10.1007/s11032-011-9564-z

Mondal S, Badigannavar AM, Murty GSS (2008) RAPD markers linked to a rust resistance gene in cultivated groundnut (*Arachis hypogaea* L.). Euphytica 159(1–2):233–9. https://doi.org/10.1007/s10681-007-9482-7

Mondal S, Hande P, Badigannavar AM (2014) Identification of Transposable Element Markers for a Rust (*Puccinia arachidis* Speg.) Resistance Gene in Cultivated Peanut. J Phytopathol 162(7–8):548–52. https://doi.org/10.1111/jph.12220

Montejo-Domínguez L de MA, McClean PE, Steadman J, McCoy S, Markell S, Osorno JM (2022) Bean rust resistance in the Guatemalan climbing bean germplasm collection. Legum Sci 4(4). https://doi.org/10.1002/leg3.149

More PE, Deokar CD, Game BC (2018) Effect of temperature on germination and survival of *Uromyces viciae-fabae* (Pers.) de Bary. J Agrometeorol 20(2):144–8. https://doi.org/10.54386/jam.v20i2.527

More PE, Deokar CD, Ilhe BM (2020) Effect of leaf wetness and soil temperatures on pea rust development caused by *Uromyces viciae-fabae* (Pers.) de Bary. J Agrometeorol 2(2):207–11. https://doi.org/10.54386/jam.v22i2.170

More PE, Deokar CD, Bhalerao VK (2019) Effect of Meteorological Factors on Rust Severity of Pea at Rahuri, Maharashtra. J Agrometeorol 21:110–11

Moricca S, Ragazzi A, Assante G (2005) Biological control of rust fungi by *Cladosporium tenuissimum*. In: Rust diseases of willow and poplar. UK, CABI Publishing, pp 213–29 http://www.doi.org/10.1079/9780851999999.0213

Motohka T, Nasahara KN, Oguma H, Tsuchida S (2010) Applicability of Green-Red Vegetation Index for remote sensing of vegetation phenology. Remote Sens 2(10):2369–87

Mundt CC (2014) Durable resistance: A key to sustainable management of pathogens and pests. Infect Genet Evol 27:446–55

Nasini G, Arnone A, Assante G, Bava A, Moricca S, Ragazzi A (2004) Secondary mould metabolites of *Cladosporium tenuissimum*, a hyperparasite of rust fungi. Phytochemistry 65(14):2107–11. https://doi.org/10.1016/j.phytochem.2004.03.013

Nazzicari N, Biscarini F (2022) Stacked kinship CNN vs. GBLUP for genomic predictions of additive and complex continuous phenotypes. Sci Rep 12(1):19889. https://doi.org/10.1038/s41598-022-24405-0

Nazzicari N, Biscarini F, Cozzi P, Brummer EC, Annicchiarico P (2016) Marker imputation efficiency for genotyping-by-sequencing data in rice (*Oryza sativa*) and alfalfa (*Medicago sativa*). Mol Breed 36(6):1–16. https://doi.org/10.1007/s11032-016-0490-y

Negussie T, Pretorius ZA (2012) Lentil rust: Present status and future prospects. Crop Prot 32:119–28. https://doi.org/10.1016/j.cropro.2011.11.004

Negussie T, Pretorius ZA, Bender CM (2005a) Components of rust resistance in lentil. Euphytica 142(1–2):55–64. https://doi.org/10.1007/s10681-005-0511-0

Negussie TG, Bender CM, Van Wyk PWJ Pretorius ZA (2012). Hypersensitivity of rust resistance in lentil. South African J Plant Soil 29:25–29. https://doi.org/10.1080/02571862.2012.688377

Negussie T, Pretorius ZA, Bender CM (2005b) Effect of Some Environmental Factors on In Vitro Germination of Urediniospores and Infection of Lentils by Rust. J Phytopathol 153:43–7

Newcombe G (2004) PATHOLOGY | Rust Diseases. In: Encyclopedia of Forest Sciences, Elsevier, pp 785–92.

Niks RE, Rubiales D (2002) Potentially durable resistance mechanisms in plants to specialised fungal pathogens. Euphytica 124:201–216. https://doi.org/10.1023/A:1015634617334

Nunkumar A, Caldwell PM, Pretorius ZA (2008) Alternative hosts of asian soybean rust (*Phakopsora pachyrhizi*) in South Africa. South African J Plant Soil 25(1):62–3. https://doi.org/10.1080/02571862.2008.10639896

Nyang au E, Nyangeri J, Makatiani J (2016) Identification of Bean Rust (*Uromyces appendiculatus*) Races on Isolates Collected from Nyamira County and Narok South Sub County, Kenya. Annu Res Rev Biol 10;9(3):1–7. https://www.doi.org/10.9734/ARRB/2016/23305

Oakey H, Cullis B, Thompson R, Comadran J, Halpin C, Waugh R (2016) Genomic Selection in Multi-environment Crop Trials. G3-GENES GENOM GENET 6(5):1313-26. https://doi.org/10.1534/g3.116.027524

Oliver RP (2014) A reassessment of the risk of rust fungi developing resistance to fungicides. Pest Manag Sci 70(11):1641–5. https://doi.org/10.1002/ps.3767

Olivoto T (2022) Lights, camera, pliman! An R package for plant image analysis. Methods Ecol Evol 13(4):789–98. https://doi.org/10.1111/2041-210X.13803

Olivoto T, Andrade SMP, Del Ponte E (2022) Measuring plant disease severity in R: introducing and evaluating the pliman package. Trop Plant Pathol 47:95–104. https://doi.org/10.1007/s40858-021-00487-5

Olivoto T, Lúcio ADC (2020) Metan: An R Package for Multi-Environment Trial Analysis. Methods Ecol Evol 11:783–9

Olivoto T, Nardino M (2021) MGIDI: Toward an Effective Multivariate Selection in Biological Experiments. Bioinformatics 37:1383–9

Olle M, Sooväli P (2020) The severity of diseases of faba bean depending on sowing rate and variety. Acta Agric Scand Sect B — Soil Plant Sci 70(7):572–7. https://www.doi.org/10.1080/09064710.2020.1814402

Osorno JM, Vander Wal AJ, Posch J, Simons K, Grafton KF, Pasche JS et al (2021) A new black bean with resistance to bean rust: Registration of 'ND Twilight'. J Plant Regist 15(1):28–36. https://doi.org/10.1002/plr2.20094

Osuna-Caballero S, Olivoto T, Jiménez-Vaquero MA, Rubiales D, Rispail N (2023) RGB image-based method for phenotyping rust disease progress in pea leaves using R. Plant Methods 19:86. https://doi.org/10.1186/s13007-023-01069-z

Osuna-Caballero S, Olivoto T, Rubiales T, Jiménez-Vaquero MA, Rispail N (2023) Script and images for "RGB image-based method for phenotyping rust disease progress in pea leaves using R". Zenodo. https://doi.org/10.5281/zenodo.7991462

Osuna-Caballero S, Rispail N, Barilli E, Rubiales D (2022) Identification and Characterization of Novel Sources of Resistance to Rust Caused by *Uromyces pisi* in *Pisum* spp. Plants 11(17):2268. https://doi.org/10.3390/plants11172268

Osuna-Caballero S, Rubiales D, Rispail N (2024) Genome-Wide association study uncovers pea candidate genes and pathways involved in rust resistance. Theor Appl Genet *Under Review*

Otsu N (1979) A threshold selection method from Gray-Level Histograms. IEEE Trans Syst Man Cybern. 9(1):62–6

Oxenham SK, Svoboda KP, Walters DR (2005) Antifungal Activity of the Essential Oil of Basil (*Ocimum basilicum*). J Phytopathol 153(3):174–80. https://doi.org/10.1111/j.1439-0434.2005.00952.x

Padilla-Roji I, Ruiz-Jiménez L, Bakhat N, Vielba-Fernández A, Pérez-García A, Fernández-Ortuño D (2023) RNAi Technology: A New Path for the Research and Management of Obligate Biotrophic Phytopathogenic Fungi. Int J Mol Sci 24(10):9082. https://doi.org/10.3390/ijms24109082

Pan Q, Cui B, Deng F, Quan J, Loake GJ, Shan W (2016) RTP 1 encodes a novel endoplasmic reticulum (ER)-localized protein in Arabidopsis and negatively regulates resistance against biotrophic pathogens. New Phytol 209:1641–54. https://doi.org/10.1111/nph.13707.

Pariaud B, Goyeau H, Halkett F, Robert C, Lannou C (2012) Variation in Aggressiveness Is Detected among *Puccinia triticina* Isolates of the Same Pathotype and Clonal Lineage in the Adult Plant Stage. Eur J Plant Pathol 134:733–43

Park SO, Coyne DP, Bokosi JM, Steadman JR (1999) Molecular markers linked to genes for specific rust resistance and indeterminate growth habit in common bean. Euphytica 105(2):133–41. https://doi.org/10.1023/A:1003477714349

Park SO, Coyne DP, Steadman JR, Crosby KM, Brick MA (2004) RAPD and SCAR Markers Linked to the Ur-6 Andean Gene Controlling Specific Rust Resistance in Common Bean. Crop Sci 44(5):1799–807. https://doi.org/10.2135/cropsci2004.1799

Park SO, Coyne DP, Steadman JR, Skroch PW (2003) Mapping of the Ur-7 Gene for Specific Resistance to Rust in Common Bean. Crop Sci 43(4):1470–6. https://doi.org/10.2135/cropsci2003.1470

Park T, Casella G (2008) The Bayesian Lasso. Journal of the American Statistical Association, 103(482):681–6. https://doi.org/10.1198/016214508000000337

Parlevliet JE (1979) Components of Resistance that Reduce the Rate of Epidemic Development. Annu Rev Phytopathol 17(1):203–22. https://doi.org/10.1146/annurev.py.17.090179.001223

Pastor-Corrales MA (2004a) Review of coevolution studies between pathogens and their common bean hosts: implication for the development of disease-resistant beans. Annu Rep Bean Improv Coop 47:67-68

Pastor-Corrales MA, Aime MC (2004b) Differential cultivars and molecular markers segregate isolates of *Uromyces appendiculatus* into two distinct groups that correspond to the gene pools of their common bean hosts. Phytopathology 94(6):82

Pastor-Corrales MA, Kelly JD, Steadman JR, Lindgren DT, Stavely JR, Coyne DP (2007) Registration of Six Great Northern Bean Germplasm Lines with Enhanced Resistance to Rust and Bean Common Mosaic and Necrosis Potyviruses. J Plant Regist 1(1):77–9. https://doi.org/10.3198/jpr2005.12.0517crg

Pau G, Fuchs F, Sklyar O, Boutros M, Huber W (2010) EBImage-an R package for image processing with applications to cellular phenotypes. Bioinformatics 2010;26(7):979–81

Paul C, Bowen CR, Bandyopadhyay R, Tefera H, Adeleke R, Sikora E et al (2010) Registration of Three Soybean Germplasm Lines Resistant to *Phakopsora pachyrhizi* (Soybean Rust). J Plant Regist 4(3):244–8. https://doi.org/10.3198/jpr2009.07.0413crg

Pavicic M, Overmyer K, Rehman A, ur Jones P, Jacobson D, Himanen K (2021) Image-based methods to score Fungal Pathogen Symptom Progression and Severity in Excised Arabidopsis Leaves. Plants 10(1):158

Pecetti L, Annicchiarico P, Crosta M, Notario T, Ferrari B, Nazzicari N (2023) White Lupin Drought Tolerance: Genetic Variation, Trait Genetic Architecture, and Genome-Enabled Prediction. Int J Mol Sci 24(3):2351. https://doi.org/10.3390/ijms24032351

Pereira WEL, de Andrade SMP, Del Ponte EM, Esteves MB, Canale MC, Takita MA et al (2020) Severity assessment in the *Nicotiana tabacum-Xylella fastidiosa* subsp. *pauca* pathosystem: design and interlaboratory validation of a standard area diagram set. Trop Plant Pathol 45:710–22

Petrovski S, Wang Q (2016) QQperm: Permutation Based QQ Plot and Inflation Factor Estimation. R Packag. version 1.0.1. https://cran.r-project.org/package=QQperm

Pfunder M, Roy BA (2000) Pollinator-mediated interactions between a pathogenic fungus, *Uromyces pisi* (*Pucciniaceae*), and its host plant, *Euphorbia cyparissias* (*Euphorbiaceae*). Am J Bot 87(1):48–55. https://doi.org/10.2307/2656684

Pierz LD, Heslinga DR, Buell CR, Haus MJ (2023) An image-based technique for automated root disease severity assessment using PlantCV. Appl Plant Sci 11:e11507

Pigliucci M, Murren CJ, Schlichting CD (2006) Phenotypic plasticity and evolution by genetic assimilation. J Exp Biol 209:2362-7

Pilet-Nayel ML, Moury B, Caffier V, Montarry J, Kerlan MC, Fournet S et al (2017) Quantitative Resistance to Plant Pathogens in Pyramiding Strategies for Durable Crop Protection. Front Plant Sci 8. http://doi.org/10.3389/fpls.2017.01838

Porta-Puglia A, Bernier CC, Jellis GJ, Kaiser WJ, Reddy MV (1993) Screening techniques and sources of resistance to foliar diseases caused by fungi and bacteria in cool season food legumes. Euphytica 73(1–2):11–25. https://doi.org/10.1007/BF00027178

Pottinger SE, Bak A, Margets A, Helm M, Tang L, Casteel C et al (2020) Optimizing the PBS1 Decoy System to Confer Resistance to Potyvirus Infection in Arabidopsis and Soybean. Mol Plant-Microbe Interact 33:932–944. https://doi.org/10.1094/MPMI-07-19-0190-R

Prats E, Llamas MJ, Jorrin J, Rubiales D (2007) Constitutive Coumarin Accumulation on Sunflower Leaf Surface Prevents Rust Germ Tube Growth and Appressorium Differentiation. Crop Sci 47(3):1119–24. http://doi.org/10.2135/cropsci2006.07.0482

Précigout PA, Claessen D, Makowski D, Robert C (2020) Does the Latent Period of Leaf Fungal Pathogens Reflect Their Trophic Type? A Meta-Analysis of Biotrophs, Hemibiotrophs, and Necrotrophs. Phytopathology 110:345–61

Prunier JG, Colyn M, Legendre X, Nimon KF, Flamand MC (2015) Multicollinearity in Spatial Genetics: Separating the Wheat from the Chaff Using Commonality Analyses. Mol Ecol 24:263–83

Puthoff DP, Neelam A, Ehrenfried ML, Scheffler BE, Ballard L, Song Q et al (2008) Analysis of Expressed Sequence Tags from *Uromyces appendiculatus* Hyphae and Haustoria and Their Comparison to Sequences from Other Rust Fungi. Phytopathology 98(10):1126–35. https://doi.org/10.1094/PHYTO-98-10-1126

Qi M, Mei Y, Grayczyk JP, Darben LM, Rieker MEG, Seitz JM et al (2019) Candidate Effectors from *Uromyces appendiculatus*, the Causal Agent of Rust on Common Bean, Can Be Discriminated Based on Suppression of Immune Responses. Front Plant Sci 10. https://doi.org/10.3389/fpls.2019.01182

R Core Team (2021). R: A Language and Environment for Statistical Computing. R Found. Stat Comput Vienna. https://www.r-project.org/.

Ragagnin VA, De Souza TLPO, Sanglard DA, Arruda KMA, Costa MR, Alzate-Marin AL et al (2009) Development and agronomic performance of common bean lines simultaneously resistant to anthracnose, angular leaf spot and rust. Plant Breed 128(2):156–63. https://doi.org/10.1111/j.1439-0523.2008.01549.x

Rai R, Singh AK, Chand R, Srivastava CP, Joshi AK, Singh BD (2016) Genomic regions controlling components of resistance for pea rust caused by *Uromyces fabae* (Pers.) de Bary. J Plant Biochem Biotechnol 25(2):133–41. http://doi.org/10.1007/s13562-015-0318-6

Rai R, Singh AK, Singh BD, Joshi AK, Chand R, Srivastava CP (2011) Molecular mapping for resistance to pea rust caused by *Uromyces fabae* (Pers.) de Bary. Theor Appl Genet 123(5):803–13. https://doi.org/10.1007/s00122-011-1628-2

Ramakrishnan P, Manivannan N, Mothilal A, Mahaingam L, Prabhu R, Gopikrishnan P (2020) Marker assisted introgression of QTL region to improve late leaf spot and rust resistance in elite and popular variety of groundnut (*Arachis hypogaea* L.) cv TMV 2. Australas Plant Pathol 49(5):505–13. https://doi.org/10.1007/s13313-020-00721-9

Ranocha P, Denancé N, Vanholme R, Freydier A, Martinez Y, Hoffmann L et al (2010) Walls are thin 1 (WAT1), an Arabidopsis homolog of *Medicago truncatula* NODULIN21, is a tonoplast-localized protein required for secondary wall formation in fibers. Plant J 63:469–483. https://doi.org/10.1111/j.1365-313X.2010.04256.x

Rasha ES, Mohamed SK (2021) Strobilurins: New group of fungicides. J Plant Sci Phytopathol 5(2):63–4. https://doi.org/ 10.29328/journal.jpsp.1001062

Rashid KY (1984) Evaluation of Resistance in *Vicia faba* to Two Isolates of the Rust Fungus *Uromyces viciae-fabae* from Manitoba. Plant Dis 68(1):16. http://www.doi.org/10.1094/PD-68-16

Rashid KY, Bernier CC (1986) The genetics of resistance in *Vicia faba* to two races of *Uromyces viciae-fabae* from Manitoba. Can J Plant Pathol 8(3):317–22. http://doi.org/10.1080/07060668609501806

Rashid KY, Bernier CC (1991) The effect of rust on yield of faba bean cultivars and slow-rusting populations. Can J Plant Sci 71(4):967–72. https://doi.org/10.4141/cjps91-139

Rathod V, Hamid R, Tomar RS, Patel R, Padhiyar S, Kheni J et al (2020) Comparative RNA-Seq profiling of a resistant and susceptible peanut (*Arachis hypogaea*) genotypes in response to leaf rust infection caused by *Puccinia arachidis*. 3 Biotech 10(6):284. https://doi.org/10.1007/s13205-020-02270-w

Renau-Morata B, Molina RV, Carrillo L, Cebolla-Cornejo J, Sánchez-Perales M, Pollmann S et al (2017) Ectopic Expression of CDF3 Genes in Tomato Enhances Biomass Production and Yield under Salinity Stress Conditions. Front Plant Sci 8. https://doi.org/10.3389/fpls.2017.00660

Renzi JP, Coyne CJ, Berger J, von Wettberg E, Nelson M, Ureta S et al (2022) How Could the Use of Crop Wild Relatives in Breeding Increase the Adaptation of Crops to Marginal Environments? Front Plant Sci 13. https://doi.org/10.3389/fpls.2022.886162/full

Resende MFR, Muñoz P, Acosta JJ, Peter GF, Davis JM, Grattapaglia D, Resende, M et al (2012) Accelerating the domestication of trees using genomic selection: accuracy of prediction models across ages and environments. New Phytologist 193(3):617–24. https://doi.org/10.1111/j.1469-8137.2011.03895.x

Rheinheimer J (2019) Succinate Dehydrogenase Inhibitors. In: Jeschke P, Witschel M, Krämer W. Schirmer U (eds) Modern Crop Protection Compounds. 3rd edn. Wiley, New York, pp 230-257. https://doi.org/10.1002/9783527699261

Rispail N, Wohor OZ, Osuna-Caballero S, Barilli E, Rubiales D (2023) Genetic diversity and population structure of a wide *Pisum* spp. core collection. Int J Mol Sci 24(3):2470. https://doi.org/10.3390/ijms24032470

Rocha JR do AS de C, Machado JC, Carneiro PCS (2018) Multitrait index based on factor analysis and ideotype-design: proposal and application on elephant grass breeding for bioenergy. GCB Bioenergy 10(1):52–60. https://doi.org/10.1111/gcbb.12443

Roorkiwal M, Rathore A, Das RR, Singh MK, Jain A, Srinivasan S, Gaur PM et al (2016). Genome-Enabled Prediction Models for Yield Related Traits in Chickpea. Front Plant Sci 7. https://doi.org/10.3389/fpls.2016.01666

Rosewarne GM, Herrera-Foessel SA, Singh RP, Huerta-Espino J, Lan CX, He ZH (2013) Quantitative trait loci of stripe rust resistance in wheat. Theor Appl Genet 126:2427–49

Rubiales D, Barilli E, Rispail N (2023) Breeding for Biotic Stress Resistance in Pea. Agriculture 13(9):1825. https://doi.org/10.3390/agriculture13091825

Rubiales D, Carver TL (2000) Defence reactions of *Hordeum chilense* accessions to three formae speciales of cereal powdery mildew fungi. Can J Bot 78(12):1561–70.

Rubiales D, Castillejo MA, Madrid E, Barilli E, Rispail N (2011) Legume breeding for rust resistance: Lessons to learn from the model *Medicago truncatula*. Euphytica 180(1):89–98. https://doi.org/10.1007/s10681-011-0367-4

Rubiales D, Fondevilla S, Chen W, Gentzbittel L, Higgins TJV, Castillejo MA et al (2015) Achievements and Challenges in Legume Breeding for Pest and Disease Resistance. CRC Crit Rev Plant Sci 34:195–236. https://doi.org/10.1080/07352689.2014.898445

Rubiales D, González-Bernal MJ, Warkentin T, Bueckert R, Vaz Patto MC, McPhee K, McGee R, Smýkal P (2019) CH20 - Advances in breeding of peas. In: Hochmuth G (Ed), Achieving sustainable cultivation of vegetables, Burleig Dodds Science Publishing Limited, Cambridge, UK, http://dx.doi.org/10.19103/AS.2019.0045.28

Rubiales D, Khazaei H (2022) Advances in disease and pest resistance in faba bean. Theor Appl Genet 135:3735–56. https://doi.org/10.1007/s00122-021-04022-7

Rubiales D, Moral A (2004) Prehaustorial Resistance against Alfalfa Rust (*Uromyces striatus*) in *Medicago truncatula*. Eur J Plant Pathol 110(3):239–43. http://doi.org/10.1023/B:EJPP.0000019792.19573.64

Rubiales D, Niks RE (1995) Characterization of Lr34, a Major Gene Conferring Nonhypersensitive Resistance to Wheat Leaf Rust. Plant Dis 79(12):1208. http://doi.org/10.1094/PD-79-1208

Rubiales D, Rojas-Molina MM, Sillero JC (2013b) Identification of pre- and posthaustorial resistance to rust (Uromyces viciae-fabae) in lentil (Lens culinaris) germplasm. Plant Breed 132(6):676–80. https://doi.org/10.1111/pbr.12096

Rubiales D, Sillero JC, Emeran AA (2013a) Response of vetches (*Vicia* spp.) to specialized forms of *Uromyces vicia-fabae* and to *Uromyces pisi*. Crop Prot 46:38–43. https://doi.org/10.1016/j.cropro.2012.12.011

Rubiales D, Annicchiarico P, Vaz Patto MC, Julier B (2021) Legume Breeding for the Agroecological Transition of Global Agri-Food Systems: A European Perspective. Front Plant Sci 12. https://doi.org/10.3389/fpls.2021.782574

Rubio J, Moreno MT, Moral A, Rubiales D, Gil J (2006) Registration of RIL58-ILC72/Cr5, a Chickpea Germplasm Line with Rust and Ascochyta Blight Resistance. Crop Sci 46(5):2331–2. https://doi.org/10.2135/cropsci2006.02.0107

Rubio J, Rubiales D (2021) Resistance to rusts and broomrape in one-flowered vetch (*Vicia articulata*). Euphytica 217(1):1–7. https://doi.org/10.1007/s10681-020-02741-4

Rutkoski JE, Heffner EL, Sorrells ME (2011) Genomic selection for durable stem rust resistance in wheat. Euphytica 179(1):161–73. https://doi.org/10.1007/s10681-010-0301-1

Saha GC, Sarker A, Chen W, Vandemark GJ, Muehlbauer FJ (2010) Identification of markers associated with genes for rust resistance in *Lens culinaris* Medik. Euphytica 21;175(2):261–5. https://doi.org/10.1007/s10681-010-0187-y

Sakr B, Sarker A, El Hassan H, Kadah N, Karim BA, Erskine W (2004) Registration of 'Bichette' Lentil. Crop Sci 44(2):686–7. https://doi.org/10.2135/cropsci2004.686a

Sampaio AM, Araújo S de S, Rubiales D, Vaz Patto MC (2020) Fusarium Wilt Management in Legume Crops. Agronomy 10(8):1073. https://doi.org/10.3390/agronomy10081073

Sandlin CM, Steadman JR, Araya CM, Coyne DP (1999) Isolates of *Uromyces appendiculatus* with Specific Virulence to Landraces of *Phaseolus vulgaris* of

Andean Origin. Plant Dis 83(2):108–13. https://doi.org/10.1094/PDIS.1999.83.2.108

Santos C, Almeida NF, Alves ML, Horres R, Krezdorn N, Leitão ST et al (2018) First genetic linkage map of *Lathyrus cicera* based on RNA sequencing-derived markers: Key tool for genetic mapping of disease resistance. Hortic Res 5(1):45. https://doi.org/10.1038/s41438-018-0047-9

Santos C, Martins DC, González-Bernal MJ, Rubiales D, Vaz Patto MC (2022) Integrating Phenotypic and Gene Expression Linkage Mapping to Dissect Rust Resistance in Chickling Pea. Front Plant Sci 13. https://doi.org/10.3389/fpls.2022.837613

Schmutz J, McClean PE, Mamidi S, Wu GA, Cannon SB, Grimwood J et al (2014) A reference genome for common bean and genome-wide analysis of dual domestications. Nat Genet 46(7):707–13. https://doi.org/10.1038/ng.3008

Schneider CA, Rasband WS, Eliceiri KW (2012) NIH Image to ImageJ: 25 years of image analysis. Nat Methods 9(7):671–5

Searle SR, Casella G, McCulloch CE (2006) Variance Components. Wiley Series in Probability and Statistics. https://doi.org/10.1002/9780470316856

Shang X, Cao Y, Ma L (2017) Alternative Splicing in Plant Genes: A Means of Regulating the Environmental Fitness of Plants. Int J Mol Sci 18:432. https://doi.org/10.3390/ijms18020432

Shtaya MJY, Emeran AA, Fernández-Aparicio M, Qaoud HA, Abdallah J, Rubiales D (2021) Effects of crop mixtures on rust development on faba bean grown in Mediterranean climates. Crop Prot 146:105686. https://doi.org/10.1016/j.cropro.2021.105686

Si B, Wang H, Bai J, Zhang Y, Cao Y (2022) Evaluating the Utility of *Simplicillium lanosoniveum*, a Hyperparasitic Fungus of *Puccinia graminis* f. sp. *tritici*, as a Biological Control Agent against Wheat Stem Rust. Pathogens 12(1):22. https://doi.org/10.3390/pathogens12010022

Sierotzki H, Scalliet G (2013) A Review of Current Knowledge of Resistance Aspects for the Next-Generation Succinate Dehydrogenase Inhibitor Fungicides. Phytopathology 103(9):880–7. https://doi.org/10.1094/PHYTO-01-13-0009-RVW

Sillero JC, Fondevilla S, Davidson J, Vaz Patto MC, Warkentin TD, Thomas J et al (2006) Screening techniques and sources of resistance to rusts and mildews in grain legumes. Euphytica 147(1–2):255–72. https://doi.org/10.1007/s10681-006-6544-1

Sillero JC, Moreno MT, Rubiales D (2000) Characterization of new sources of resistance to *Uromyces viciae-fabae* in a germplasm collection of *Vicia faba*. Plant Pathol 49(3):389–95. https://doi.org/10.1046/j.1365-3059.2000.00459.x

Sillero JC, Moreno-Alías I, Rubiales D (2012) Identification and characterization of resistance to rust (*Uromyces ciceris-arietini* (Grognot) Jacz. & Boyd) in a germplasm collection of *Cicer* spp. Euphytica 188(2):229–38. https://doi.org/10.1007/s10681-012-0709-x

Sillero JC, Rubiales D (2002) Histological characterization of resistance to *Uromyces viciae-fabae* in faba bean. Phytopathology 92(3):294–9. https://doi.org/10.1094/PHYTO.2002.92.3.294

Sillero JC, Villegas-Fernández AM, Thomas J, Rojas-Molina MM, Emeran AA, Fernández-Aparicio M et al (2010) Faba bean breeding for disease resistance. Field Crop Res 115(3):297–307. https://doi.org/10.1016/j.fcr.2009.09.012

Simko I, Jimenez-Berni JA, Sirault XRR (2017) Phenomic Approaches and Tools for Phytopathologists. Phytopathology 107(1):6–17. https://doi.org/10.1094/PHYTO-02-16-0082-RVW

Simko I, Piepho HP (2012) The Area under the Disease Progress Stairs: calculation, advantage, and application. Phytopathology 102(4):381–9

Singh AK, Kushwaha C, Shikha K, Chand R, Mishra GP, Dikshit HK et al (2023) Rust (*Uromyces viciae-fabae* Pers. de Bary) of Pea (*Pisum sativum* L.): Present Status and Future Resistance Breeding Opportunities. Genes 14(2):374. https://doi.org/10.3390/genes14020374

Singh AK, Singh VK, Chand R, Kushwaha C, Srivastava CP (2015) Evaluation of slow rusting components in pea. J Plant Pathol 97(1):87–92.

Singh D, Kumar A, Singh AK (2014) Influence of planting time, planting geometry, intercropping and row direction on rust (*Uromyces viciae fabae*) pers. de Bary of field pea (*Pisum sativum* L.). Legum Res 37(5):542–6. https://doi.org/10.5958/0976-0571.2014.00673.0

Singh J, Sirari A, Singh H, Kumar A, Jaidka M, Mandahal KS et al (2021) Identifying and validating SSR markers linked with rust resistance in lentil (Lens culinaris). Plant Breed 140(3):477–85. https://doi.org/10.1111/pbr.12917

Singh AK, Rai R, Singh BD, Chand R, Srivastava CP (2015) Validation of SSR Markers Associated with Rust (*Uromyces fabae*) Resistance in Pea (*Pisum sativum* L.). Physiol Mol Biol Plants 21, 243–7

Singh D, Tripathi H, Singh A (2012) Influence of Environmental Factors on Development of Field Pea Rust Caused by *Uromyces viciae-fabae*. J Plant Dis Sci 7:13–7

Singh RP, Hodson DP, Huerta-Espino J. Jin Y, Bhavani S, Njau P, Herrera-Foessel S et al (2011) The emergence of Ug99 races of the stem rust fungus is a threat to world wheat production. Annu Rev Phytopathol 49:465–81

Singh RP, Hodson DP, Huerta-Espino J, Jin Y, Njau P, Wanyera R, Herrera-Foessel SA, Ward RW (2008) Will Stem Rust Destroy the World's Wheat Crop? Adv Agron 98:271–309

Skoufogianni E, Giannoulis K, Bartzialis D, Danalatos N (2019) Relations between crop rotation with pea and soil structure. Bulg J Agric Sci 25 1205–1210

Smith HF (1936) A discriminant function for plant selection. Ann Eugen 7:240–50

Sokhi SS, Singh SJ, Munshi GD (1984) Parameters of rating pea varieties/lines against rust. Indian Phytopathol 37(2):252–5

Souza TLPO, Ragagnin VA, Dessaune SN, Sanglard DA, Carneiro JES, Moreira MA et al (2014) DNA marker-assisted selection to pyramid rust resistance genes in "carioca" seeded common bean lines. Euphytica 199(3):303–16. https://doi.org/10.1007/s10681-014-1126-0

Stakman EC, Stewart DM, Loegering WQ (1962) Identification of physiologic races of Puccinia graminis var. tritici. US Dep Agric Agric Res Serv 54

Stalker HT (2017) Utilizing Wild Species for Peanut Improvement. Crop Sci 57(3):1102–20. https://doi.org/10.2135/cropsci2016.09.0824

Stavely JR (1989) New Pathogenic Variability in *Uromyces appendiculatus* in North America. Plant Dis 73:428

Stonebloom S, Ebert B, Xiong G, Pattathil S, Birdseye D, Lao J et al (2016) A DUF-246 family glycosyltransferase-like gene affects male fertility and the biosynthesis of pectic arabinogalactans. BMC Plant Biol 16:90. https://doi.org/10.1186/s12870-016-0780-x

Storey JD Tibshirani R (2003) Statistical significance for genomewide studies. Proc Natl Acad Sci USA 100:9440–5. https://doi.org/10.1073/pnas.1530509100

Storey JD, Bass AJ (2022) qvalue: Q-value estimation for false discovery rate control. R Packag. version 2.30.0. http://github.com/jdstorey/qvalue

Stuteville DL, Graves WL, Dixon LJ, Castlebury LA, Minnis AM (2010*) Uromyces ciceris-arietini*, the Cause of Chickpea Rust: New Hosts in the *Trifolieae*, *Fabaceae*. Plant Dis 94(3):293–7. https://doi.org/10.1094/PDIS-94-3-0293

Subrahmanyam P, McDonald D, Waliyar F, Reddy LJ, Nigam SN, Gibbons RW et al (1995) Screening methods and sources of resistance to rust and late leaf spot of groundnut. ICARDA Inf Bull 47

Subrahmanyam, P, McDonald D, Reddy LJ, Nigam SN, Smith DH (1993) Origin and Utilization of Rust Resistance in Groundnut. In: Jacobs, T., Parlevliet, J.E. (eds) Durability of Disease Resistance. Current Plant Science and Biotechnology in Agriculture, vol 18. Springer, Dordrecht. https://doi.org/10.1007/978-94-011-2004-3_12

Suffert F, Thompson RN (2018) Some Reasons Why the Latent Period Should Not Always Be Considered Constant over the Course of a Plant Disease Epidemic. Plant Pathol 67:1831–40

Sugha SK, Banyal DK, Rana SK (2008) Management of pea (*Pisum sativum*) rust (*Uromyces fabae*) with fungicides. Indian J Agric Sci 78(3):269–71

Susmitha P, Kumar P, Yadav P, Sahoo S, Kaur G, Pandey MK et al (2023) Genome-wide association study as a powerful tool for dissecting competitive traits in legumes. Front Plant Sci 14. https://doi.org/10.3389/fpls.2023.1123631

Swisher-Grimm K D, Porter LD (2021) KASP Markers Reveal Established and Novel Sources of Resistance to Pea Seedborne Mosaic Virus in Pea Genetic Resources. Plant Dis 105(9):2503–8. https://doi.org/10.1094/PDIS-09-20-1917-RE

Tabassum N, Eschen-Lippold L, Athmer B, Baruah M, Brode M, Maldonado-Bonilla LD et al (2020) Phosphorylation-dependent control of an RNA granule-localized protein that fine-tunes defence gene expression at a post-transcriptional level. Plant J 101:1023–39. https://doi.org/10.1111/tpj.14573

Talhinhas P, Carvalho R, Figueira R, Ramos AP (2019) An annotated checklist of rust fungi (*Pucciniales*) occurring in Portugal. Sydowia 71:65–84

Tang D, Ade J, Frye CA, Innes RW (2006) A mutation in the GTP hydrolysis site of Arabidopsis dynamin-related protein 1E confers enhanced cell death in response to powdery mildew infection. Plant J 47:75–84. https://doi.org/10.1111/j.1365-313X.2006.02769.x

Tayeh N, Aubert G, Pilet-Nayel ML, Lejeune-Hénaut I, Warkentin TD, Burstin J (2015) Genomic tools in pea breeding programs: Status and perspectives. Front Plant Sci 6. https://doi.org/10.3389/fpls.2015.01037

Tayeh N, Klein A, Le Paslier MC, Jacquin F, Houtin H, Rond C, Chabert-Martinello M, Magnin-Robert JB, Marget P, Auber G, Burstin J (2015) Genomic prediction in pea: Effect of marker density and training population size and composition on prediction accuracy. Front Plant Sci 6:1–11. https://doi.org/10.3389/fpls.2015.00941

Thibivilliers S, Cooper B, Campbell K, Scheffler B, Boerma R, Boovaraghan B et al (2007) Phaseolus vulgaris-*Uromyces appendiculatus* pathosystem as a model for

Asian soybean rust. In: Phytopathology: American Phytopathological Society, St. Paul, Minnesota p S114–S114

Thibivilliers S, Joshi T, Campbell KB, Scheffler B, Xu D, Cooper B et al (2009) Generation of *Phaseolus vulgaris* ESTs and investigation of their regulation upon *Uromyces appendiculatus* infection. BMC Plant Biol 9(1):46. https://doi.org/10.1186/1471-2229-9-46

Tibbs Cortes L, Zhang Z, Yu J (2021) Status and prospects of genome-wide association studies in plants. Plant Genome 14. https://doi.org/10.1002/tpg2.20077

Todd A, Donofrio N, Sripathi V, McClean P, Lee R, Pastor-Corrales M et al (2017) Marker-Assisted Molecular Profiling, Deletion Mutant Analysis, and RNA-Seq Reveal a Disease Resistance Cluster Associated with *Uromyces appendiculatus* Infection in Common Bean *Phaseolus vulgaris* L. Int J Mol Sci 18(6):1109. https://doi.org/10.3390/ijms18061109

Toker C (2004) Estimates of broad-sense heritability for seed yield and yield criteria in faba bean (*Vicia faba* L.). Hereditas 140:222–5

Tolhurst DJ, Gaynor RC, Gardunia B, Hickey JM, Gorjanc G (2022) Genomic selection using random regressions on known and latent environmental covariates. Theor Appl Genet 135(10):3393–3415. https://doi.org/10.1007/s00122-022-04186-w

Toome-Heller M (2016) Latest Developments in the Research of Rust Fungi and Their Allies (*Pucciniomycotina*). In: Li D-W (ed) Biology of Microfungi, Springer International Publishing, pp. 147–68.

Tucker CJ (1979) Red and photographic infrared linear combinations for monitoring vegetation. Remote Sens Environ 8(2):127–50

Tulbek MC, Lam RSH, Wang YC, Asavajaru P, Lam A (2016) Pea: A Sustainable Vegetable Protein Crop. Elsevier Inc pp. 145–164. https://doi.org/10.1016/B978-0-12-802778-3.00009-3

Uddin MN, Ellison FW, O'Brien L, Latter BDH (1994) The performance of pure lines derived from heterotic bread wheat hybrids. Aust J Agric Res, 45(3), 591–600. https://doi.org/10.1071/AR9940591

Vale F, Fernandes-Filho E, Liberato J (2003) QUANT: a software for plant disease severity assessment. In: Proceedings of the 8th International Congress of Plant Pathology. Christchurch, New Zealand: Horticulture Australia p. 10

Valentini G, Gonçalves-Vidigal MC, Hurtado-Gonzales OP, de Lima Castro SA, Cregan PB, Song Q et al (2017) High-resolution mapping reveals linkage between genes in common bean cultivar Ouro Negro conferring resistance to the rust,

anthracnose, and angular leaf spot diseases. Theor Appl Genet 130(8):1705–22. http://doi.org/10.1007/s00122-017-2920-6

van de Wouw M, Kik C, van Hintum T, van Treuren R, Visser B (2010) Genetic erosion in crops: concept, research results and challenges. Plant Genet Resour, 8(1), 1–15. https://doi.org/10.1017/S1479262109990062

Vance CP, Graham PH, Allan DL (2000) Biological Nitrogen Fixation: Phosphorus - A Critical Future Need?. In: Pedrosa FO, Hungria M, Yates G, Newton WE (eds) Nitrogen Fixation: From Molecules to Crop Productivity. Current Plant Science and Biotechnology in Agriculture, vol 38. Springer, Dordrecht. https://doi.org/10.1007/0-306-47615-0_291

Varman PV (1999) A foliar disease resistant line developed through interspecific hybridization in groundnut (*Arachis hypogaea*). Indian J Agric Sci 69(1).

Varshney RK, Pandey MK, Janila P, Nigam SN, Sudini H, Gowda MVC et al (2014) Marker-assisted introgression of a QTL region to improve rust resistance in three elite and popular varieties of peanut (*Arachis hypogaea* L.). Theor Appl Genet 127(8):1771–81. https://doi.org/10.1007/s00122-014-2338-3

Vaz Patto MC, Fernández-Aparicio M, Moral A, Rubiales D (2009a) Pre and posthaustorial resistance to rusts in *Lathyrus cicera* L. Euphytica 165(1):27–34. https://doi.org/10.1007/s10681-008-9737-y

Vaz Patto MC, Rubiales D (2009b) Identification and characterization of partial resistance to rust in a germplasm collection of Lathyrus sativus L. Plant Breed 128(5):495–500. https://doi.org/10.1111/j.1439-0523.2008.01601.x

Vaz Patto MC, Rubiales D (2014) Unveiling common responses of *Medicago truncatula* to appropriate and inappropriate rust species. Front Plant Sci 5. http://doi.org/10.3389/fpls.2014.00618

Venkidasamy B, Selvaraj D, Nile AS, Ramalingam S, Kai G, Nile SH (2019) Indian pulses: A review on nutritional, functional and biochemical properties with future perspectives. Trends Food Sci Technol 88:228–42. https://doi.org/10.1016/j.tifs.2019.03.012

Vieira A, Talhinhas P, Loureiro A, Thürich J, Duplessis S, Fernandez D et al (2012) Expression profiling of genes involved in the biotrophic colonisation of *Coffea arabica* leaves by *Hemileia vastatrix*. Eur J Plant Pathol 133(1):261–77. http://doi.org/10.1007/s10658-011-9864-5

Vijayalakshmi S, Yadav K, Kushwaha C, Sarode SB, Srivastava CP, Chand R et al (2005) Identification of RAPD markers linked to the rust (*Uromyces fabae*) resistance gene in pea (*Pisum sativum*). Euphytica 144(3):265–74. https://doi.org/10.1007/s10681-005-6823-2

Villegas-Fernández ÁM, Amarna AA, Moral J, Rubiales D (2023) Crop diversification to Control Rust in Faba Bean caused by *Uromyces viciae-fabae*. J Fungi 9(3):344.

Voegele RT (2006) *Uromyces fabae*: development, metabolism, and interactions with its host *Vicia faba*. FEMS Microbiol Lett 259(2):165–73. https://doi.org/10.1111/j.1574-6968.2006.00248.x

Voegele RT, Hahn M, Lohaus G, Link T, Heiser I, Mendgen K (2005) Possible Roles for Mannitol and Mannitol Dehydrogenase in the Biotrophic Plant Pathogen *Uromyces fabae*. Plant Physiol 137(1):190–8. https://doi.org/10.1104/pp.104.051839

Voegele RT, Mendgen K (2003) Rust haustoria: nutrient uptake and beyond. New Phytol 159(1):93–100. https://doi.org/10.1046/j.1469-8137.2003.00761.x

Voegele RT, Schmid A (2011) RT real-time PCR-based quantification of *Uromyces fabae* in planta. FEMS Microbiol Lett 322(2):131–7. https://doi.org/10.1111/j.1574-6968.2011.02343.x

Vuong TD, Walker DR, Nguyen BT, Nguyen TT, Dinh HX, Hyten DL et al (2016) Molecular Characterization of Resistance to Soybean Rust (*Phakopsora pachyrhizi* Syd. & Syd.) in Soybean Cultivar DT 2000 (PI 635999). PLoS One 11(12):0164493. https://doi.org/10.1371/journal.pone.0164493

Waliyar F, Bosc J, Bonkoungou S (1993) sources of resistance to foliar diseases of groundnut and their stability in West-Africa. Oléagineux 48(6):283–7

Wang J, Wang Y, Liu X, Xu Y, Ma Q (2016) Microtubule Polymerization Functions in Hypersensitive Response and Accumulation of H2O2 in Wheat Induced by the Stripe Rust. Biomed Res Int 2016. https://doi.org/10.1155/2016/7830768

Wang J, Zhang Z (2021) GAPIT Version 3: Boosting Power and Accuracy for Genomic Association and Prediction. Genom Proteom Bioinform 19:629–640. https://doi.org/10.1016/j.gpb.2021.08.005

Wang R, Li X, Sun M, Xue C, Korban SS, Wu J (2023) Genomic insights into domestication and genetic improvement of fruit crops. Plant Physiology 192(4):2604–27. https://doi.org/10.1093/plphys/kiad273

Wang X, Xu Y, Hu Z, Xu C (2018) Genomic selection methods for crop improvement: Current status and prospects. Crop Journal 6(4):330–40. https://doi.org/10.1016/j.cj.2018.03.001

Ward BP, Brown-Guedira G, Tyagi P, Kolb FL, Van Sanford DA, Sneller CH, Griffey CA (2019) Multienvironment and Multitrait Genomic Selection Models in Unbalanced Early-Generation Wheat Yield Trials. Crop Sci 59(2):491–507. https://doi.org/10.2135/cropsci2018.03.0189

Watanabe K, Guo W, Arai K, Takanashi H, Kajiya-Kanegae H, Kobayashi M et al (2017) High-throughput phenotyping of Sorghum Plant Height using an unmanned aerial vehicle and its application to genomic prediction modeling. Front Plant Sci 8:421

Wickham H, Averick M, Bryan J, Chang W, McGowan L, François R et al (2019) Welcome to the Tidyverse. J Open Source Softw 4(43):1686

Wickham H (2016) Ggplot2: Elegant Graphics for Data Analysis; Springer: New York, NY, USA

Wirsel SGR, Voegele RT, Mendgen KW (2001) Differential Regulation of Gene Expression in the Obligate Biotrophic Interaction of *Uromyces fabae* with Its Host *Vicia faba*. Mol Plant-Microbe Interact 14(11):1319–26. https://doi.org/10.1094/MPMI.2001.14.11.1319

Wu X, Li G, Wang B, Hu Y, Wu X, Wang Y et al (2018b) Fine mapping Ruv2, a new rust resistance gene in cowpea (*Vigna unguiculata*), to a 193-kb region enriched with NBS-type genes. Theor Appl Genet 131(12):2709–18. http://doi.org/10.1007/s00122-018-3185-4

Wu X, Wang B, Wu X, Lu Z, Li G, Xu P (2018a) SNP marker-based genetic mapping of rust resistance gene in the vegetable cowpea landrace ZN016. Legum Res 41(2):222–5. https://doi.org/10.18805/LR-387

Wu X, Wang B, Xin Y, Wang Y, Tian S, Wang J et al (2022) Unravelling the Genetic Architecture of Rust Resistance in the Common Bean (*Phaseolus vulgaris* L.) by Combining QTL-Seq and GWAS Analysis. Plants 11(7):953. https://doi.org/10.3390/plants11070953

Wynn WK (1975) Appressorium Formation over Stomates by the Bean Rust Fungus: Response to a Surface Contact Stimulus. Phytopathology 66(2):136. http://doi.org/10.1094/Phyto-66-136.

Wynn WK, Staples RC (1981) Tropisms of fungi in host recognition. R.C. Stapl. Plant disease control: resistance and susceptibility. Wiley-Interscience New York, pp 45–69

Xiong H, Chen Y, Pan Y-B, Wang J, Lu W, Shi A (2023) A genome-wide association study and genomic prediction for *Phakopsora pachyrhizi* resistance in soybean. Front Plant Sci 14. https://doi.org/10.3389/fpls.2023.1179357

Yadav S, Chattopadhyay D (2023) Lignin: the Building Block of Defense Responses to Stress in Plants. J Plant Growth Regul 42(10):6652–66. https://doi.org/10.1007/s00344-023-10926-z

Yamanaka N, Hossain MM (2019) Pyramiding three rust-resistance genes confers a high level of resistance in soybean (*Glycine max*). Plant Breed 138(6):686–95. https://doi.org/10.1111/pbr.12720

Yamanaka N, Morishita M, Mori T, Lemos NG, Hossain MM, Akamatsu H et al (2015) Multiple Rpp-gene pyramiding confers resistance to Asian soybean rust isolates that are virulent on each of the pyramided genes. Trop Plant Pathol 40(5):283–90. http://doi.org/10.1007/s40858-015-0038-4

Yamaoka Y, Fujiwara Y, Kakishima M, Katsuya K, Yamada K, Hagiwara H (2002) Pathogenic Races of *Phakopsora pachyrhizi* on Soybean and Wild Host Plants Collected in Japan. J Gen Plant Pathol 68(1):52–6. http://doi.org/10.1007/PL00013053

Yamaoka Y, Yamanaka N, Akamatsu H, Suenaga K (2014) Pathogenic races of soybean rust *Phakopsora pachyrhizi* collected in Tsukuba and vicinity in Ibaraki, Japan. J Gen Plant Pathol 80(2):184–8. http://doi.org/10.1007/s10327-014-0507-5

Yang K-W, Chapman S, Carpenter N, Hammer G, McLean G, Zheng B et al (2021) Integrating crop growth models with remote sensing for predicting biomass yield of sorghum. in silico Plants 3(1):1–19

Yang T, Liu R, Luo Y, Hu S, Wang D, Wang C et al (2022) Improved pea reference genome and pan-genome highlight genomic features and evolutionary characteristics. Nat Genet 54(10):1553–63. https://doi.org/10.1038/s41588-022-01172-2

Yin L, Liu S, Sun W, Ke X, Zuo Y (2023) Genome-wide identification of glutamate receptor genes in adzuki bean and the roles of these genes in light and rust fungal response. Gene 879:147593. https://doi.org/10.1016/j.gene.2023.147593

Yol E, Upadhyaya HD, Uzun B (2016) Identification of rust resistance in groundnut using a validated SSR marker. Euphytica 210(3):405–11. https://doi.org/10.1007/s10681-016-1705-3

Yop GS, Gair LHV, da Silva VS, Machado ACZ, Santiago DC, Tomaz JP (2023) Abscisic Acid Is Involved in the Resistance Response of *Arabidopsis thaliana* Against *Meloidogyne paranaensis*. Plant Dis 107:2778–3. https://doi.org/10.1094/PDIS-07-22-1726-RE

Yu N, Kim M, King ZR, Harris DK, Buck JW, Li Z et al (2015) Fine mapping of the Asian soybean rust resistance gene Rpp2 from soybean PI 230970. Theor Appl Genet 128(3):387–96. https://doi.org/10.1007/s00122-014-2438-0

Yuen G, Steadman J, Lindgren D, Schaff D, Jochum C (2001) Bean rust biological control using bacterial agents. Crop Prot 20(5):395–402. https://doi.org/10.1016/S0261-2194(00)00154-X

Yusnawan E, Inayati A (2018) Antifungal Activity of Crude Extracts of *Ageratum conyzoides*, *Cyperus rotundus*, and *Amaranthus spinosus* Against Rust Disease. AGRIVITA J Agric Sci 40(3). http://doi.org/10.17503/agrivita.v40i0.1889

Zargar SM, Raatz B, Sonah H, MuslimaNazir, Bhat JA, Dar ZA et al (2015) Recent advances in molecular marker techniques: Insight into QTL mapping, GWAS and genomic selection in plants. J Crop Sci Biotechnol 18(5):293–308. http://doi.org/10.1007/s12892-015-0037-5

Zeiders KE (1985) First Report of Rust Caused by *Uromyces* Species on Birdsfoot Trefoil in the United States. Plant Dis. 69:727. https://doi.org/10.1094/PD-69-727a.

Zeng Y, Liang Z, Liu Z, Li B, Cui Y, Gao C et al (2023) Recent advances in plant endomembrane research and new microscopical techniques. New Phytol 240:41–60. https://doi.org/10.1111/nph.19134

Zhang C, Dong Y, Tang L, Zheng Y, Makowski D, Yu Y et al (2019) Intercropping cereals with faba bean reduces plant disease incidence regardless of fertilizer input; a meta-analysis. Eur J Plant Pathol 154(4):931–42. http://doi.org/10.1007/s10658-019-01711-4

Zhang H, Wang C, Cheng Y, Wang X, Li F, Han Q et al (2011) Histological and molecular studies of the non-host interaction between wheat and *Uromyces fabae*. Planta 234(5):979–91. http://doi.org/10.1007/s00425-011-1453-5

Zhang J, Pu R, Huang W, Yuan L, Luo J, Wang J (2012) Using in-situ hyperspectral data for detecting and discriminating yellow rust disease from nutrient stresses. Field Crop Res 134:165–74

Zhang J, Qin Q, Nan X, Guo Z, Liu Y, Jadoon S et al (2020) Role of Protein Phosphatase1 Regulatory Subunit3 in Mediating the Abscisic Acid Response. Plant Physiol 184:1317–1332. https://doi.org/10.1104/pp.20.01018

Zhang J, Yuan L, Pu R, Loraamm R, Yang G, Wang J (2014) Comparison between wavelet spectral features and conventional spectral features in detecting yellow rust for winter wheat. Comput Electron Agric 100:79–87

Zhang A, Wang H, Beyene Y, Semagn K, Liu Y, Cao S, Cui Z, Ruan Y, Burgueño J, San Vicente F et al (2017). Effect of Trait Heritability, Training Population Size and Marker Density on Genomic Prediction Accuracy Estimation in 22 bi-parental Tropical Maize Populations. Front Plant Sci 8. https://doi.org/10.3389/fpls.2017.01916

Zhao J, Wang M, Chen X, Kang Z (2016) Role of Alternate Hosts in Epidemiology and Pathogen Variation of Cereal Rusts. Annu Rev Phytopathol 54(1):207–28. https://www.doi.org/10.1146/annurev-phyto-080615-095851

Zhou L, He H, Liu R, Han Q, Shou H, Liu B (2014) Overexpression of GmAKT2potassium channel enhances resistance to soybean mosaic virus. BMC Plant Biol 14:154. https://doi.org/10.1186/1471-2229-14-154

Zhou Y, Li S, Qian Q, Zeng D, Zhang M, Guo L et al (2009) BC10, a DUF266-containing and Golgi-located type II membrane protein, is required for cell-wall biosynthesis in rice (*Oryza sativa* L.). Plant J 57:446–462. https://doi.org/10.1111/j.1365-313X.2008.03703.x